



**BRITISH
COLUMBIA**

Ministry of Employment and Investment
Energy and Minerals Division
Geological Survey Branch

EARLY JURASSIC ROSSLAND GROUP Southern British Columbia

Part I - Stratigraphy and Tectonics

By Trygve Höy, P.Eng. and Kathryn P.E. Dunne, P.Geo.

BULLETIN 102

Canadian Cataloguing in Publication Data

Høy, Trygve, 1945-
Early Jurassic Rossland Group Southern British Columbia

(Bulletin ; 102)

Issued by Geological Survey Branch
Includes bibliographical references: p.
ISBN 0-7726-3215-4

1. Geology, Stratigraphic - Jurassic. 2. Geology, Structural - British Columbia - Salmo Region. 3. Geochemistry - British Columbia - Salmo Region. 4. Geology, Economic - British Columbia - Salmo Region. I. Dunne, Kathryn, P.E., 1963- II. British Columbia. Ministry of Employment and Investment. III. British Columbia. Geological Survey Branch. IV. Series: Bulletin (British Columbia. Ministry of Employment and Investment) ; 102.

QE.187.H69 1997

551.7'66'0971162

C97-960096-0

SUMMARY

The Rossland Group comprises a succession of mafic volcanic rocks and associated clastic rocks of Early Jurassic age. It extends in an arcuate belt south from Nelson to Salmo and west to the Rossland-Trail area in southeastern British Columbia (Figures 1-2, 2-3). It includes a basal succession of fine to coarse-grained clastic rocks of the Archibald Formation, volcanic and epiclastic rocks of the Elise Formation, and overlying clastic rocks of the Hall Formation.

Based on structural position and lithologic similarities, the basal unit of the Rossland Group, the Archibald Formation, is correlated with the upper part of the Ymir Group and, in part, with the Late Triassic Slokan Group. South and southwest of Salmo, the Rossland Group is in fault contact with the Lower Cambrian Laib Group and Paleozoic metasedimentary rocks of Unit Cs, both part of the Kootenay terrane. In the Rossland area, the Group unconformably overlies Pennsylvanian-Permian sedimentary rocks of the Mount Roberts Formation (Little, 1982b) of the Harper Ranch subterrane of Quesnellia.

The Rossland Group records Early Jurassic arc volcanism on the eastern margin of Quesnellia. Early tectonism associated with arc development involved extension with uplift and erosion in the west and deposition of coarse clastics of the Archibald Formation in a deepening structural basin to the east. This basin fill comprised dominantly sedimentary debris eroded from the Mount Roberts Formation basement, as well as numerous intrusive clasts possibly derived from Triassic or Permian subvolcanic intrusions exposed farther west.

Volcanism began in Late Sinemurian time with deposition of Elise Formation submarine shoshonitic flows in eastern exposures and mafic tuffs in the Fruitvale area east of Rossland. The mafic, primitive character of this early Elise volcanism, dominated by augite phyric flows and tuffs, suggests minimal contamination by continental crustal rocks. As the volcanic arc evolved, it became dominated by stratovolcanoes; these were largely subaerial with only subaqueous deposition of debris flows and tuffs on their distal flanks. As well, plagioclase phyric volcanism began to dominate in the upper Elise Formation, with deposition of thick accumulations of crystal tuffs.

Petrochemistry and U-Pb isotopic data indicates that these tuffs were contaminated by continental crustal rocks, suggesting that they may have formed on the distal, thin edge of the North American craton.

The overlying Hall Formation comprises marine clastic rocks that were deposited in a structural basin on an eroded Elise paleosurface. The disconformity between the Elise and the Hall formations, the inferred hiatus from Late Sinemurian to early Toarcian time, and the lack of any volcanism in the Hall indicates that it records essentially post-arc deposition in a marine basin.

The Rossland Group is intruded by a variety of igneous rocks. The Eagle Creek plutonic complex, the Rossland monzodiorite and a number of stocks of dominantly monzogabbro composition are assumed to be comagmatic with Lower Jurassic volcanic rocks of the Elise Formation. Silver King intrusions, located south of Nelson, are a suite of Toarcian to early Middle Jurassic synkinematic? leucodiorites. Middle Jurassic intrusions, including the Nelson batholith and Bonnington pluton, the Trail pluton and numerous other stocks are common throughout the Nelson-Trail-Rossland area. Early Cretaceous intrusions, such as the Wallack Creek and Hidden Creek stocks, occur along the eastern margin of Rossland exposures near Salmo. Tertiary intrusions include Middle Eocene Coryell syenites and numerous mafic to felsic dikes of Paleocene and Middle Eocene age.

A variety of deposit types occur in rocks of the Rossland Group. The most important are gold-copper veins and minor associated skarn mineralization related to intrusion of the Rossland monzodiorite in the Rossland camp. Copper-gold porphyry deposits have been explored recently southwest of Salmo and within and along the margins of the Early Jurassic? Eagle Creek plutonic complex west of Nelson. The potential for VMS discoveries continues to attract interest to the Elise Formation. Molybdenite skarn-breccia deposits on Red Mountain just north of the Rossland gold camp and molybdenite-copper porphyries south of Nelson are related to Middle Jurassic plutons. Numerous base and precious metal vein deposits have been the focus of exploration and development throughout the Rossland Group, but particularly in the Silver King and Ymir camps south of Nelson.

TABLE OF CONTENTS

SUMMARY	1	- interpretation.....	46
Table of contents.....	3	Rossland area.....	46
List of figures.....	4	- interpretation.....	50
List of tables.....	6	Elise Formation: depositional environment	
List of plates.....	6	summary.....	50
Appendices.....	7		
CHAPTER 1 - INTRODUCTION	8	ELISE FORMATION: GEOCHEMISTRY	53
Introduction.....	8	Introduction.....	53
Acknowledgements.....	8	Major element data.....	53
		- classification.....	55
CHAPTER 2 - REGIONAL GEOLOGY	11	Trace element data.....	55
Introduction.....	11	Rare earth element data.....	57
Ancestral North America.....	11	Tectonic setting.....	57
Kootenay Terrane.....	13	Summary and discussion.....	58
Lardeau Group; Laib Formation.....	13		
Milford Group.....	15	CHAPTER 5 - HALL FORMATION	59
Slide Mountain Terrane.....	15	Introduction.....	59
Quesnellia.....	15	Age.....	59
Mount Roberts Formation.....	16	Description.....	59
Mesozoic arc rocks.....	16	Depositional environment.....	64
Post-accretionary volcanic and sedimentary			
rocks.....	17	CHAPTER 6 - PLUTONIC ROCKS	65
Sophie Mountain Formation.....	17	Introduction.....	65
Marron Formation.....	17	Early Jurassic (Sinemurian) plutons.....	65
Plutonic rocks.....	17	Eagle Creek plutonic complex.....	65
		- petrography.....	65
CHAPTER 3 - ROSSLAND GROUP:		- mineral prospects.....	68
ARCHIBALD FORMATION	19	Rossland monzonite.....	69
Rossland Group: nomenclature.....	19	- petrography.....	70
Archibald Formation.....	19	- age.....	70
Age.....	19	Rossland sill.....	71
Description.....	21	Monzogabbro intrusions.....	73
Mount Kelly area.....	22	- petrography.....	73
Mount Verde area.....	24	Petrographic summary: Early Jurassic	
Fruitvale area.....	24	plutons.....	74
Patterson area.....	25	Geochemistry: Early Jurassic plutons.....	74
Facies trends and interpretation.....	25	- introduction.....	74
		- elimination of "altered" data.....	74
CHAPTER 4 - ELISE FORMATION:		- alkalinity.....	74
DESCRIPTION	29	- nomenclature.....	74
Introduction.....	29	- aluminous character.....	77
Age.....	29	- fractional crystallization trends.....	78
Fossil data.....	29	- tectonic implications.....	78
U-Pb dating.....	29	Early - Middle Jurassic plutons.....	82
Description.....	31	Description.....	82
Highway 6 section, south of Nelson.....	31	Petrography.....	82
- interpretation.....	35	Geochemistry.....	83
Copper Mountain - Mount Conner area...	36	Age and tectonic implications.....	84
- interpretation.....	37	Mineral prospects.....	84
Cabin Peak area.....	37	Middle Jurassic plutons.....	84
- interpretation.....	39	Cretaceous plutons.....	89
Erie Lake area.....	41	Cenozoic plutons.....	89
Mount Kelly area.....	42	Summary.....	89
- interpretation: Mount Kelly			
and Erie Lakes sections.....	44		
Fruitvale area.....	44		

CHAPTER 7 - TECTONIC SYNTHESIS	91
Tectonic summary	91
Early Paleozoic	91
Late Paleozoic	91
Early Triassic	93
Middle and Late Triassic	93
Early Jurassic (Sinemurian)	93
Early Jurassic (Toarcian)	93
Middle Jurassic	94
Late Cretaceous	94
Tertiary	94
 SELECTED BIBLIOGRAPHY	95
 APPENDICES	105
 FIGURES	
1-1. Regional location map	9
1-2. Map of physiographic features, Nelson-Rossland map-area (82F/SW), and locations of published geological maps	10
2-1. Tectonic synthesis map, southern British Columbia, showing regional correlation chart (after Wheeler and McFeeley, 1991)	12
2-2. Stratigraphic correlation chart	13
2-3. Geology of the Nelson-Rossland map-area, southeastern British Columbia (82F/SW); (after Andrew <i>et al.</i> , 1991; Little, 1985 and included references)	14
3-1. Map showing the distribution of the Archibald Formation, fossil locations and location of sections	20
3-2. Detailed sections of the Archibald Formation in the Fruitvale, Mount Kelly and Mount Verde areas	22
3-3. Composite stratigraphic sections of the Archibald Formation	23
3-4. Geological map of the Patterson area showing the distribution of the Mount Roberts Formation and unconformably overlying Archibald and Elise Formations	26
3-5. Paleocurrent directions of turbidites and debris flows of the Archibald Formation in the Fruitvale, Mount Kelly and Archibald Creek areas (<i>from</i> Fitzpatrick, 1985)	27
3-6. Schematic diagram illustrating the tectonic evolution of the Archibald Formation in Early Jurassic time	8
4-1. Map showing the distribution of the Elise Formation	30
4-2. U-Pb concordia diagram of zircon data, Sample 129-7, Elise Formation; see Table 4-1 for data and text for discussion	31
4-3. U-Pb concordia diagram of zircon data, Sample 19-4, Elise Formation; see Table 4-1 for data and text for discussion	31
4-4a. Geological map of the Elise Formation, Highway 6 section, south of Nelson (<i>from</i> Andrew and Höy, 1988)	
4-4b. Vertical cross-section, Highway 6 area	33
4-5. Stratigraphic section of the Elise Formation, Highway 6 section, determined from data shown in cross-section of Figure 4-4	34
4-6. Geological map of the Cabin Peak - Midday Peak area, showing the distribution of the Elise Formation (<i>from</i> Höy and Andrew, 1989b).	38
4-7a. Stratigraphic section of the Elise Formation, Cabin Peak - Midday Peak area.	
4-7b. Detail of Cabin Peak section; <i>see</i> 4-7a for position	39
4-8. Composite stratigraphic section, Elise Formation, Erie Creek area	41
4-9. Geological map of the Mount Kelly area (<i>from</i> Höy and Andrew, 1990b)	42
4-10. Stratigraphic section of the Elise Formation, Mount Kelly area	44
4-11. Stratigraphic sections of the Elise Formation in the Beaver Creek - Champion Lakes area	45
4-12. Geological map of the Rossland Area, Rossland-Trail map-sheet (82F/4); (<i>after</i> Höy and Andrew, 1991b; Fyles, 1984; Little, 1982b and Drysdale, 1915)	47
4-13. Composite stratigraphic section of the Elise Formation, Rossland map-area	48
4-14. Composite stratigraphic sections of the Elise Formation, Nelson - Trail area	50
4-15. Schematic model for evolution of the Elise Formation in (a) Early Elise time and (b) Late Elise time	51

4-16 Plots of (a) SiO ₂ versus MgO, (b) SiO ₂ versus Al ₂ O ₃ and (c) SiO ₂ versus P ₂ O ₅ , Elise Formation, Rossland Group (after Harker, 1909).....	53	6-1. Regional geology, distribution of intrusions and location of U-Pb and K-Ar samples (this study) in the Nelson-Trail map-area (082F/SW).....	66
4-17. A plot of Na ₂ O + K ₂ O versus SiO ₂ , Elise Formation, Rossland Group (after Cox <i>et al.</i> 1979)	54	6-2. Quartz-alkali feldspar-plagioclase diagram of Early Jurassic intrusions in the Trail map-area (plot after Streckeisen, 1973)	68
4-18. A plot of K ₂ O versus Na ₂ O, Elise Formation, Rossland Group (after Middlemost, 1975).....	54	6-3. Plot of U-Pb zircon data, sample H88-Rsmn, Rossland monzonite	72
4-19. An AFM plot, Elise Formation, Rossland Group (after Irving and Barager, 1971).....	54	6-4. A plot of wt. % K ₂ O versus wt. % SiO ₂ of samples of intrusive rocks, showing the effects of alteration associated with mineralization on their compositions	75
4-20a. A plot of Ba (ppm) versus K ₂ O (weight percent), Elise Formation, Rossland Group; (after Green, 1980).		6-5. A plot of wt. % K ₂ O versus wt. % SiO ₂ of "unaltered" or "least altered" Trail map-area intrusive rocks.....	75
4-20b. A plot of Ni versus Cr, Elise Formation, Rossland Group.....	54	6-6. A Q-P plot of least altered Early Jurassic plutons (after Debon and Le Fort, 1983).....	77
4-21. Elise Formation incompatible element abundances normalized to primordial mantle values; (after Sun, 1980)	56	6-7. A plot of Shand's index: Al ₂ O ₃ /(Na ₂ O + K ₂ O) versus Al ₂ O ₃ /(CaO + Na ₂ O + K ₂ O) of least altered Early Jurassic plutons, (after Shand, 1951).....	79
4-22. A plot of Ba versus La, Elise Formation, Rossland Group.....	56	6-8. A plot of Shand's index: A = Al - (K + Na + 2Ca) versus B = Fe + Mg + Ti of Debon and Le Fort (1983) of least altered Early Jurassic plutons, illustrating their dominantly metaluminous character	79
4-23. A plot of Th/Yb versus Ta/Yb, Elise Formation, Rossland Group (after Pearce, 1983).....	56	6-9. A Pearce element ratio plot of P/Y versus Nb/Y to test for cogeneration of least altered Early Jurassic plutons	80
4-24. Elise Formation MORB-normalized trace element patterns, Rossland Group (after Pearce, 1983)	56	6-10. Plots of MgO versus SiO ₂ and CaO versus SiO ₂ of Early Jurassic plutons to illustrate fractionation trends	80
4-25. A plot of Ti-Y-Zr, Elise Formation, Rossland Group (after Pearce and Cann, 1973)	56	6-11. A Pearce element ratio plot of Al ₂ O ₃ /Y versus SiO ₂ /Y of least altered Early Jurassic plutons	81
4-26. A plot of K ₂ O versus SiO ₂ , Elise Formation, Rossland Group (after Basaltic volcanism study project, 1981, summarized in Wilson, 1989).....	57	6-12. A Pearce element ratio plot of Na + K/Y versus Al/Y of least altered Early Jurassic plutons to illustrate the effects of fractional crystallization of alkali feldspars.....	81
4-27. Relative volumes of basalt (B), basaltic andesite (BA), andesite (A), dacite (D) and rhyolite (R) in the Elise Formation compared with volumes in the Andes continental arc and the southwest Pacific island arcs; data from this study (Elise Formation) and Ewart (1982)	58	6-13. A tectonic discrimination plot of Nb versus Y of Early Jurassic plutons illustrating their volcanic arc or syn-collisional setting (after Pearce <i>et al.</i> , 1984)	81
5-1. Map showing distribution of the Hall Formation	60	6-14. A tectonic discrimination plot of Rb versus Y + Nb of Early Jurassic plutons illustrating their volcanic arc setting (after Pearce <i>et al.</i> , 1984).....	81
5-2. Composite stratigraphic sections of the Hall Formation in the core of the Hall Creek syncline, Keystone Mountain, Stewart Creek and Hall Creek areas (from Andrew and Höy, 1991).....	61		
5-3. Correlation of the Hall Formation showing main lithologic and thickness changes (from Andrew and Höy, 1991)	62		

6-15. Alkali-silica plot of samples of Silver King intrusions, and comparison with other Early Jurassic plutons	83	3-3: Matrix-supported conglomerate with limestone and siltstone clasts (0.5-10 cm diameter), Archibald Formation, Beaver Creek area.....	24
6-16a. Plot of U-Pb zircon data, sample H88R47-2, Silver King intrusion.		3-4: Limestone breccia of Archibald Formation, Patterson area.....	24
6-16b. Plot of U-Pb zircon data, sample H88R60-4, Silver King intrusion.....	86	4-1: Coarse-grained augite phyric flow breccia of Unit Je1; note large augite phenocrysts in both matrix and fragments	35
6-17a. Plot of U-Pb zircon data, sample H88R70-1, Silver King intrusion.		4-2: Massive and brecciated flows of Unit Je1, Highway 6, 2 km west of Apex Creek. Note: thin mud selvages between flows	35
6-17b. Plot of U-Pb zircon data, sample H88R-Lectus, Silver King intrusion.....	87	4-3: Boulder conglomerate near the base of Unit Je1, Elise Formation.....	35
6-18. Plot of U-Pb zircon data, sample H89R256-5B.....	89	4-4: Reverse grading in a crystal tuff surge layer; note lithic fragments, laminated layers and contorted bedding; Cabin Peak section (Figure 4-7b).....	40
7-1. Schematic diagram showing the tectonic evolution of the Rossland-Nelson area, southern British Columbia in (a) Late Triassic and (b) Early Jurassic time.....	92	4-5: Well-bedded, mafic to intermediate lapilli crystal and fine tuff, Cabin Peak area. Note numerous structures, including graded and laminated beds, scours, channels and crosslaminations indicative of base-surge deposition; Cabin Peak section (Figure 4-7b).....	40
TABLES		4-6: Base surge deposits, interlayered with highly contorted, possible air fall deposits; note mafic crystal content, grading, scouring and vague laminations in surge layers; Cabin Peak section (Figure 4-7b).....	40
4-1. U-Pb data of zircons, samples H86R129-7 and H87R19-4, Elise Formation; data plotted in figures 4-2 and 4-3	32	4-7: Planar bedded surge deposits with associated highly deformed, penecontemporaneous slumping of ash beds; Cabin Peak section (Figure 4-7b).....	40
4-2. Lithological units, Elise Formation.....	34	4-8: Amygdaloidal pillow basalt, Unit Je1, Elise Formation, southeast of Mount Kelly	43
6-1. Petrographic comparison of typical Lower Jurassic intrusions in the Rossland Group, Nelson-Rossland area, southeastern British Columbia	67	4-9: Lahars, with a variety of rounded boulders and cobbles in a calcareous grit matrix, on ridge southeast of Mount Kelly	43
6-2. U-Pb zircon data, sample H88-Rsmn, Rossland monzonite	71	4-10: Coarse, fragmental debris flows of the Elise Formation along Highway 3 just west of Montrose. A variety of fragments include augite porphyry of the Elise, metasediments and limestone of the Mount Roberts Formation, and feldspar porphyries.....	46
6-3. CIPW normative calculations for Rossland-Nelson area least altered intrusions	76		
6-4. Summary of geochemical nomenclature for Rossland-Nelson area plutonic rocks.....	78		
6-5. U-Pb zircon data, Silver King intrusions.....	85		
6-6. U-Pb zircon data, sample H89R256-5B	88		
PLATES			
3-1: Thick-bedded, graded turbidite wacke with sharp basal contacts and basal scours, Archibald Formation, west of Salmo	24		
3-2: Crossbedding in thick-bedded, graded turbidite wacke, siltstone and silty argillite, Archibald Formation, east of Mount Kelly	24		

4-11: Massive crystal and lapilli tuff, deposited on scoured tuffaceous muds that locally contain prominent flame structures, west of Baldy Mountain, south of Rosslund 49

4-12: Detail of lapilli tuff (Plate 4-11); note variety of lithic clasts, but abundant small augite phyric fragments 49

5-1: Rip-up structures, laminated beds in interbedded siltstone and sandstone, Hall Formation, Stewart Creek area 63

5-2: Pebble conglomerate of the middle part of the Hall Formation with 5-10 cm subangular, flattened mudstone fragments, south of Hall Creek 63

6-1: Microcline crystal, 640 microns, in gabbro phase of the pseudodiorite (f.o.v = 1.48 mm) .. 69

6-2: Coarse-grained augite crystals are pervasively rimmed and replaced by chlorite in coarse-grained clinopyroxene phase of the pseudodiorite (field of view = 1.48 mm) 69

6-3: Symplectite texture: ilmenite or magnetite and clinopyroxene intimately intergrown in a vermicular fashion in a coarse-grained clinopyroxenite phase of the pseudodiorite (field of view = 1.48 mm) 69

6-4: Augite rimmed by hornblende in the Rosslund sill (field of view = 1.48 mm) 72

6-5: Symplectite texture of magnetite?-clinopyroxene mantled by biotite in the Rosslund sill (field of view = 370 microns) 72

6-6: Hornblende, chlorite and epidote in "gabbro" from the Nelson area (f.o.v. = 1.48 mm) 73

6-7: Intensely sausseritized plagioclase phenocrysts with inner zones replaced by clusters of sericite needles in a fine-grained matrix of feldspar and secondary quartz, Silver King intrusion (field of view = 1.48 mm)..... 82

6-8: Cataclastic fabric in the Silver King intrusion; platy minerals rotated into parallelism and rounded feldspar boudins in a protomylonite (field of view = 1.48 mm) 82

APPENDICES..... 105

1. Major, trace and minor element data, Elise Formation 105

2. Minor, trace and rare earth element data, Elise Formation 111

3. Major and trace element data, Nelson-Rosslund area intrusions 114

4. Location of samples..... 120

CHAPTER 1- INTRODUCTION

INTRODUCTION

The Rossland Group occurs in southeastern British Columbia (Figure 1-1) along the eastern edge of Quesnellia. It comprises intermediate to mafic volcanic rocks and associated coarse to fine clastic rocks of Lower Jurassic age. It hosts a variety of deposit types, including the vein deposits of the Rossland camp that produced 84 000 kilograms of gold and 105 000 kilograms of silver between 1894 and 1941. In 1995, the Iron Colt returned to limited production. Deposits in the Nelson area have produced 16 750 kilograms of gold and 190 000 kilograms of silver, primarily from vein deposits in the Ymir camp. Exploration in the Rossland Group continues to be active, directed primarily towards alkali gold-copper porphyry deposits, such as the Katie, gold-rich veins within the Rossland camp, gold-copper skarns and shear-related mineralization.

Exposures of the Rossland Group are within the Selkirk Mountains south and southwest of Nelson and the Monashee Mountains in the Rossland area. Relief is moderate, with valley floors of the Salmo River and Beaver Creek at approximately 800 metres and higher mountains just southwest of Nelson rising to more than 2400 metres. Access to most of the area is provided by Highways 3 and 6 that extend east from Rossland - Trail to Salmo and north to Nelson. Numerous logging roads follow major drainages and valleys throughout the area.

Previous geological work has included reconnaissance mapping and more detailed mapping of mineral camps by both the Geological Survey of Canada and the British Columbia Ministry of Energy, Mines and Petroleum Resources. Thesis studies of Rossland Group rocks are limited; the most comprehensive include a study of the Rossland Group in the Beaver Valley area (Fitzpatrick, 1985) and a geochemical study of Elise volcanic rocks (Beddoe-Stephens, 1977).

The purpose of the present study is to develop a better understanding of the nature, timing and controls of mineralization in the Rossland Group, particularly the intrusion-related gold-copper veins in the Rossland camp (Höy and Dunne, in preparation). Fieldwork began in 1987, with detailed mapping south of Nelson which defined the stratigraphy of the Elise Formation. It continued with regional 1:50 000 mapping from 1988 to

1990 and release of Open File maps and reports in Geological Fieldwork that outlined the geology of the Rossland Group from Nelson to Rossland (Figure 1-2). This mapping has been summarized in a 1:100 000 compilation map (Andrew *et al.*, 1991). More recently, work in the Rossland camp (1995-1996) concentrated on vein morphology, alteration and geochemistry, and relationships between the veins and molybdenite breccia deposits.

This paper describes the stratigraphy of the Rossland Group, its paleotectonic setting and associated intrusions. It summarizes the structure of the area and presents a tectonic model for the Group. Mineral deposits and Early Jurassic volcanic arc metallogeny will be the focus of a subsequent paper (Höy and Dunne, in preparation).

ACKNOWLEDGEMENTS

We would like to thank the many persons that have been involved in this project. Their continued help and support are much appreciated. Able field assistance was provided by M. Fournier, C. Lund, M. Holmes, D. Lindsay, H. Blyth, J. Drobe, E. Höy and H. Karam. We would also like to thank companies for their support and for permission to publish some of their data.

Discussions with numerous geologists and prospectors helped develop many of the ideas and interpretations in this paper. Some of these include C. Ash, B. Bourden, E. Denny, J. Denny, J. Einarsen, F. Ferri, W. Howard, O. Janout, J. Jenks, D. Lefebure, K. Murray, G. Nixon, G. Ray, R. Robeck, R. St. Lambert, P. Simony, D. Wehrle and P. Wilton.

Much of the drafting was done by M. Fournier, A. Pettipas and V. Koyanagi. U-Pb age dating and discussion, are due to the efforts of J. Gabites of The University of British Columbia. R. Lett is thanked for expediting samples for chemical analyses and R. Player, for thin and polish section preparations.

This paper has not benefitted from peer review or formal editing. We would, however, like to thank D. Lefebure, B. Grant and J. Newell for editing early Fieldwork articles that formed the basis for parts of this manuscript.

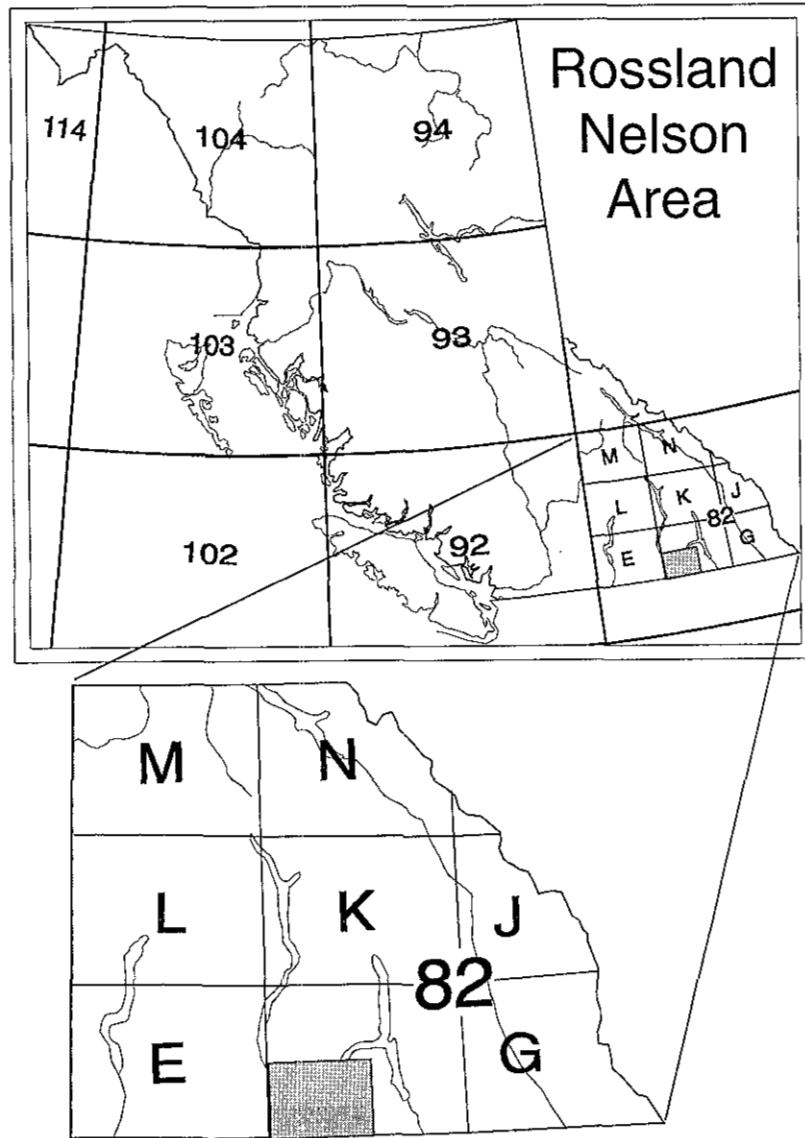


Figure 1-1. Regional location map.

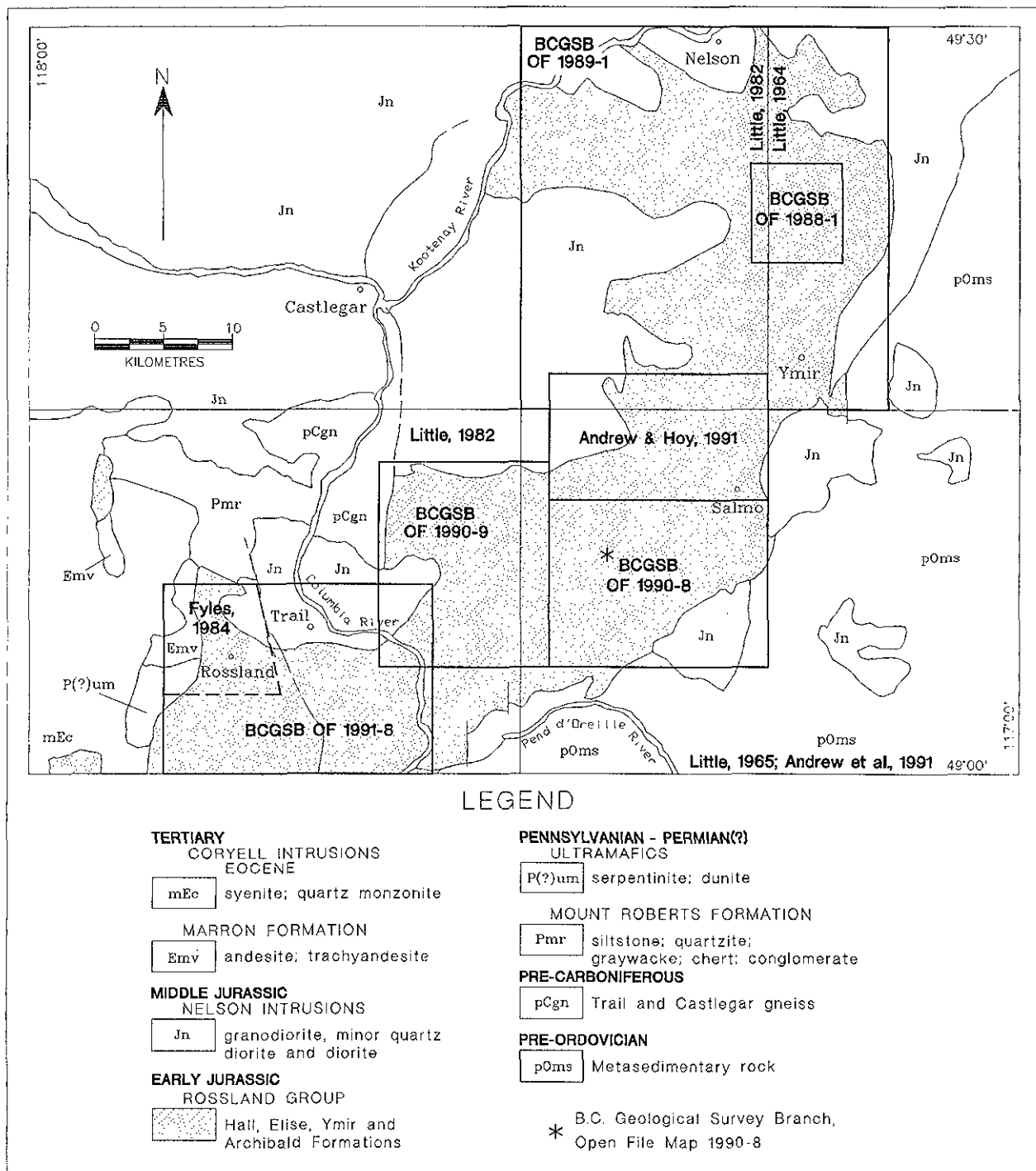


Figure 1-2: Map of physiographic features, Nelson-Rossland map-area (82F/SW), and location of published geological maps.

CHAPTER 2 - REGIONAL GEOLOGY

INTRODUCTION

The Rossland Group is in the southern Omineca Crystalline Belt, an uplifted zone of variably metamorphosed and deformed Proterozoic to Tertiary rocks that straddles the boundary between accreted terranes and ancestral North America. The belt includes a series of structural culminations, typically cored by Paleoproterozoic crystalline rocks, and flanked in the intervening depressions by rocks similar to those in the Foreland Belt to the east. These rocks are structurally overlain by accreted rocks of the Slide Mountain and Quesnell terranes.

The Omineca Crystalline Belt comprises an imbricated succession of thrust sheets that were transported eastward in Mesozoic time. This tectonism was accompanied by intrusion of granitic bodies and localization of a variety of structurally controlled vein deposits. In early Tertiary time, regional extension resulted in local uplift of core complexes as cover rocks were displaced along low angle normal faults. This extension was associated with widespread mafic volcanism, intrusion of alkalic rocks and, locally, vein and shear-hosted mineralization.

The Rossland Group is traditionally regarded as the most eastern belt of volcanic rocks within Quesnellia, a terrane that comprises dominantly arc volcanics and associated sediments that were accreted to North America in Middle Jurassic time. These rocks tectonically overlie pericratonic rocks of the Kootenay Terrane or miogeoclinal Proterozoic to lower Paleozoic rocks that were deposited on the western ancestral margin of North America. The tectonic boundary between Quesnellia and pericratonic or cratonic rocks is locally marked by mafic volcanic rocks and associated ultramafics of the Slide Mountain Terrane, interpreted to record deposition in a marginal basin or back-arc setting (Nelson, 1993) that separated Quesnellia from North America. Overlap assemblages, rocks deposited after collision of accreted rocks with North America, include (in the Rossland-Nelson area) the Cretaceous Sophie Mountain Formation and Eocene Marron Formation.

The following sections describe briefly the stratigraphic successions of terranes in the Rossland-Nelson area, emphasizing their ties to the Rossland Group.

ANCESTRAL NORTH AMERICA

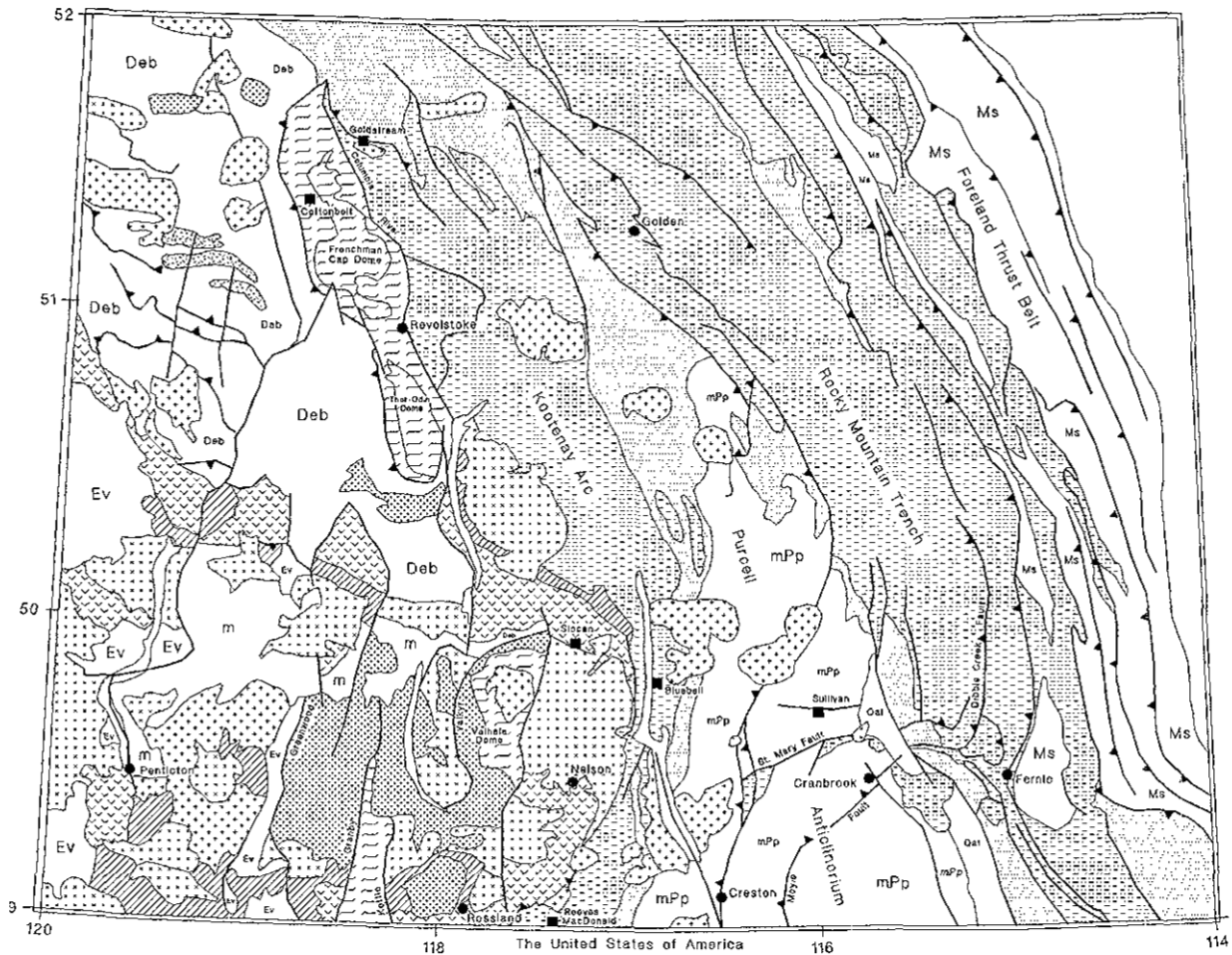
Rocks of the North American Terrane were deposited on the western rifted margin of North

America from Mesoproterozoic through Mesozoic time. They are structurally separated from Rossland Group rocks by the Waneta fault (Fyles and Hewlett, 1959), interpreted to be a west-dipping structure that emplaced both Quesnellia and Slide Mountain onto the continental margin. Within the Nelson-Trail map-area, these rocks include the Neoproterozoic Windermere succession and overlying Hamill Group and Badshot (Reeves) Formation (Figures 2-1, 2-2).

The Windermere Supergroup (Walker, 1926) unconformably overlies the Mesoproterozoic Purcell Supergroup, exposed in the Purcell anticlinorium in the Purcell Mountains farther east. The **Purcell Supergroup** comprises a thick succession of basinal marine clastic rocks and overlying shallow marine to locally subaerial fine-grained clastics, carbonates and minor basaltic lavas in the core of the Purcell anticlinorium east of the Nelson-Trail map-area. The **Windermere Supergroup** comprises a basal conglomeratic unit, the Toby Formation, typically overlain by a succession of coarse immature clastic rocks, minor carbonate and locally, intraformational conglomerate. A mafic volcanic unit near the base of the Windermere, the Irene volcanics, has been dated at *ca.* 762 Ma (Devlin *et al.*, 1988). The upper part of the Windermere is more calcareous with a number of prominent carbonate successions. Abrupt facies changes, coarse-grained lithologies and associated volcanism within the Windermere document a period of rifting that preceded continental separation (Lis and Price, 1976; Ross *et al.*, 1995)

Late Proterozoic to early Paleozoic miogeoclinal rocks were deposited along the rifted western margin of North America. This sedimentary prism thickens rapidly west of a hinge that marks a transition from platformal carbonate rocks to more clastic and argillaceous basinal facies. Western exposures of this miogeoclinal prism include the Hamill Group and an overlying platformal carbonate unit, the Badshot Formation.

In the Trail map-area, the **Hamill Group** (Figures 2-2, 2-3) comprises massive white quartzites, argillaceous quartzites, and minor argillites and phyllitic rocks of the Quartzite Range and Reno formations. These rocks record the transition from a rift to a post-rift environment as continental separation occurred and early Paleozoic miogeoclinal sedimentation began (Devlin and Bond, 1987). They comprise dominantly fluvial deposits in the southwest and marine facies farther north, inferring northerly transport of sediments from an uplifted southern source area. Upper Hamill rocks are interpreted to be shallow marine indicating widespread erosion and bevelling of



	Slide Mtn	Quesnellia	Kootenay	North America	Intrusive
Cenozoic				Ev volcanic	Eocene (Paleocene)
Mesozoic		Rosland Group Nicola Group (Slocan, Kaslo)	m metamorphic	Ms sedimentary	Middle Cretaceous Middle Jurassic
Paleozoic	Anarchist, Harper Ranch Mt. Roberts (Kaslo)		Dob Eagle Bay Arc Lardeau meta-sedimentary	sedimentary	
Proterozoic				upper Windermere middle mPp Purcell	

Figure 2-1. Tectonic synthesis map, southern British Columbia, showing regional correlation chart (after Wheeler and McFeely, 1991).

the uplifted source terrain (Devlin and Bond, *op. cit.*; Warren, 1996)

The Lower Cambrian **Badshot Formation** is an extensive platformal limestone and dolomite unit, up to several hundred metres thick, that hosts the Kootenay Arc lead-zinc massive sulphide deposits, including the Reeves MacDonald, HB and Jersey deposits in the correlative **Reeves member** south of Salmo (Fyles and Hewlett, 1959).

KOOTENAY TERRANE

The Kootenay Terrane overlies Proterozoic and Paleozoic North American rocks. To the west and south, Kootenay Terrane rocks underlie the accreted rocks of Quesnellia and Slide Mountain.

The Kootenay Terrane comprises intensely deformed, variably metamorphosed clastic sediments, subordinate volcanics and limestones ranging in age from Proterozoic to Triassic. The terrane is referred to as pericratonic as some of the lower Paleozoic rocks appear to be in stratigraphic contact with North American rocks (Fyles and Eastwood, 1962). Smith and

Gehrels (1992) have proposed, however, that the Paleozoic Lardeau Group is an inverted succession that tectonically overlies North American rocks. This is not supported in the Illecillewaet synclinorium east of Revelstoke where a normal stratigraphic contact has been demonstrated between the Lardeau and underlying successions (Colpron and Price, 1992; 1995).

Major rock packages in the Kootenay Terrane include the Lower Paleozoic Lardeau Group, the Eagle Bay Assemblage in the Kamloops area, eastern assemblages of the Late Paleozoic Milford Group, and equivalent rocks in the highly metamorphosed Shuswap complex to the west.

LARDEAU GROUP; LAIB FORMATION

The Lardeau Group is exposed in the Kootenay Arc from north of Revelstoke to southeast of Nelson (Figure 2-1). The lower part of the Lardeau correlates with the Laib Formation in the Nelson-Trail map area (Figure 2-2), with the Reeves member of the Laib equivalent to the Badshot Formation of the continental margin sequence.

AGE		ROSSLAND - TRAIL AREA	NELSON - SALMO AREA	SLOCAN AREA	
CRETACEOUS		MT. SOPHIE			
JURASSIC	Upper				
	Middle				
	LOWER	Toarcian	HALL	HALL	
		Pliensbachian	ELISE	ELISE	
		Sinemurian	ARCHIBALD		
Hettangian			YMIR		
TRIASSIC			SLOCAN		
PERMIAN		MOUNT ROBERTS	KASLO		
CARBONIFEROUS			MILFORD		
DEVONIAN		TRAIL GNEISS			
SILURIAN					
ORDOVICIAN		CS	Active Neway Reeves	LARDEAU	
CAMBRIAN			LAIB	BADSHOT	
PROTEROZOIC			HAMILL	HAMILL	
			WINDERMERE		

Figure 2-2. Stratigraphic correlation chart.

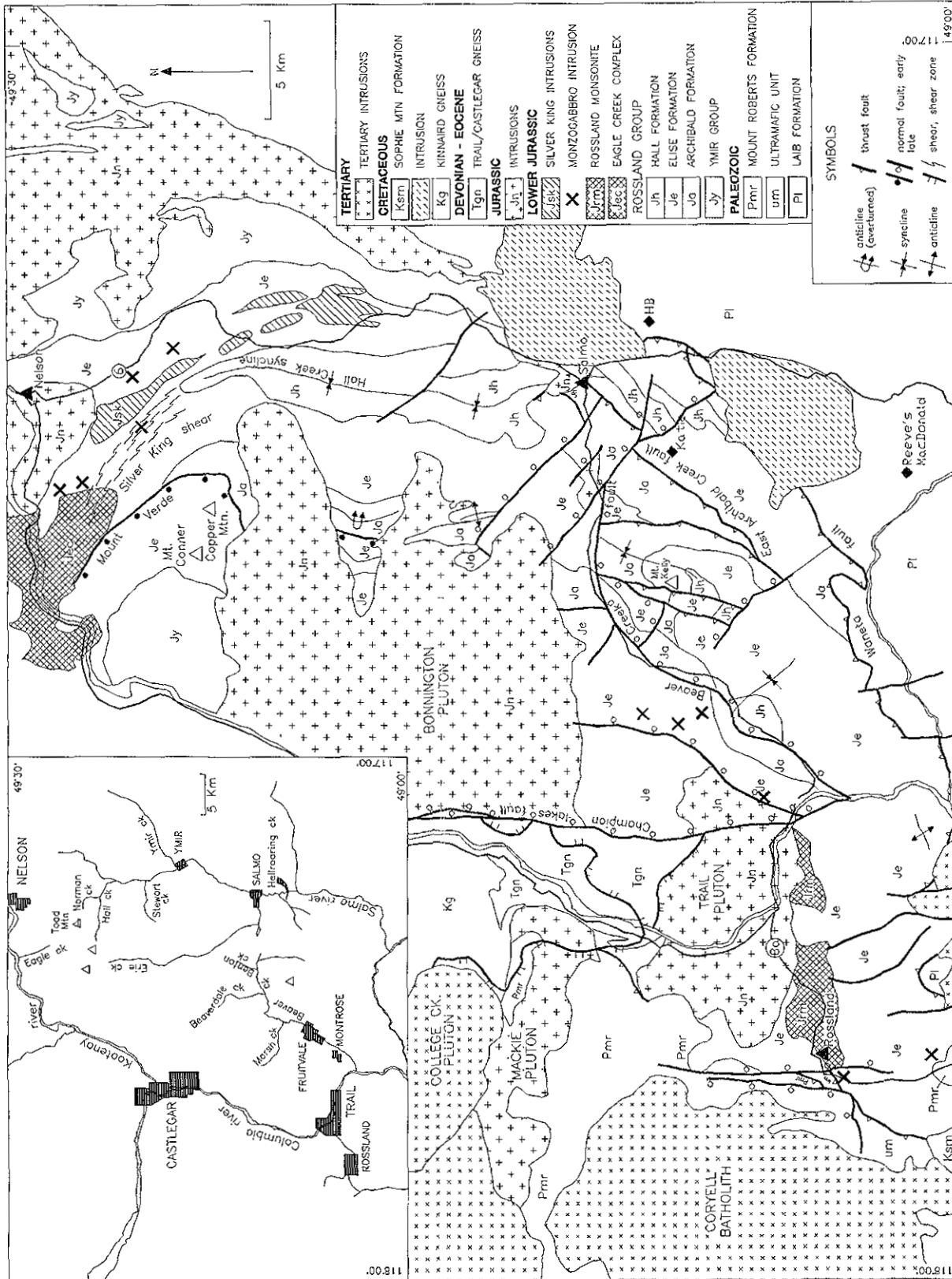


Figure 2-3. Geology of the Nelson-Rossland map-area, southeastern British Columbia (82F/SW); (after Andrew *et al.*, 1991; Little, 1985 and included references).

The Lardeau Group comprises a thick sequence of phyllite, calcareous phyllite, marble, basalt and minor quartzite of the basal Index Formation, overlain by black siliceous argillite, grey quartzite, and black siliceous argillite of the Triune, Ajax and Sharon Creek formations respectively (Fyles and Eastwood, 1962). A prominent basaltic succession, the Jowett Formation, overlies the Sharon Creek Formation and a thick accumulation of coarse clastic wackes and grits of the Broadview Formation comprises the top of the Lardeau. Only the lower part of the Lardeau, the Index Formation, is exposed in the Nelson-Trail map area (Figure 2-3). It is metamorphosed and deformed, comprising micaceous schist, amphibolite, calcsilicate gneiss, with some marble and quartzitic layers (LeClair, 1986; Einersen, 1994).

The Laib Formation (Little, 1950) comprises a thick assemblage of phyllite, micaceous quartzite and limestone that conformably overlies the Reno Formation of the upper Hamill (Fyles and Hewlett, 1959). The upper part has not been subdivided; it grades up into the Middle Cambrian Nelway Formation. The lower part includes the Truman, Reeves and Emerald members, correlative respectively with the Mohican, Badshot and Index formations farther north.

MILFORD GROUP

Mississippian to Pennsylvanian Milford Group rocks unconformably overlie Lardeau Group rocks in the central Kootenay Arc. In general, they comprise a basal limestone succession overlain by argillite, metasandstone, and volcanic units with a number of prominent conglomeratic horizons.

Klepacki (1985) and Klepacki and Wheeler (1985) have subdivided the Milford into three stratigraphic assemblages, the Davis, Keen and McHardy. The Davis and Keen unconformably overlie Lardeau Group rocks and, hence, are included in the Kootenay Terrane. The McHardy assemblage, in fault contact with the Keen assemblage and conformably overlain by Kaslo Group rocks, is included with the Slide Mountain Terrane. All three assemblages contain Mississippian limestone near the base, include siliciclastic rocks consisting of bedded cherty argillite, chert or quartz-pebble conglomerate, and slate or mica phyllite, and contain pyroxene pillow lava, breccias or tuffaceous greenstone (Roback, 1993).

Klepacki (1985) infers deposition in a rift environment developed, in part, on deformed Lardeau Group rocks above continental crust and, in part, on back-arc oceanic crust.

SLIDE MOUNTAIN TERRANE

The Slide Mountain Terrane comprises dominantly oceanic volcanic and minor sedimentary rocks of Mississippian to Permian age. In southern British Columbia, it includes tholeiitic pillow basalts and breccia, serpentinite, siliceous argillite and volcanic-

derived sediments of the Permian to Carboniferous Kaslo Group, underlying McHardy assemblage of the Milford Group (Klepacki and Wheeler, 1985; Roback *et al.*, 1994) and correlative Fennel Formation in the Kamloops area (Schiarizza and Preto, 1987).

Slide Mountain rocks are dominated by depleted ocean ridge basalts. They may record the remnants of a wide ocean basin (Harms, 1986); however, their stratigraphic ties with Kootenay Terrane rocks (Klepacki and Wheeler, 1985; Roback *et al.*, 1994) suggest a marginal basin or possibly back arc setting (Nelson, 1993; Roback *et al.*, *op. cit.*; Ferri, 1997).

QUESNELLIA

Oceanic rocks of the Slide Mountain Terrane are flanked on the west by upper Paleozoic volcanoclastic and minor volcanic rocks of parts of the Okanagan and Harper Ranch subterrane (Monger *et al.*, 1991). These are overlain by Upper Triassic volcanic rocks of the Nicola Group or Lower Jurassic Rossland Group rocks. These successions of dominantly arc volcanics of Triassic-Jurassic age, and underlying Paleozoic rocks, comprise Quesnellia in southern British Columbia.

The Okanagan subterrane is characterized by rocks of oceanic affinity, including the Knob Hill, Chapperton and Kobau Groups of the Greenwood area. It may also include ultramafic rocks exposed in fault slices in the Rossland camp area, although these have been included in the Mount Roberts Formation by Little (1982b) or in the Slide Mountain Terrane by Ash *et al.* (in press). This latter correlation implies that oceanic Slide Mountain rocks separate Paleozoic and Mesozoic rocks of eastern Quesnellia (Rossland Group and underlying Mount Roberts Formation) from more western exposures of Quesnellia near Greenwood. This may be due to an eastward migration of the axis of the arc volcanism by Early Jurassic time, with deposition of Rossland Group rocks on a telescoped basement comprising imbricated Slide Mountain and Harper Ranch successions (see Chapter 7).

The ultramafic rocks of the Rossland area comprise two obducted fragments of lower oceanic plutonic rocks (Ash *et al.*, 1992; Ash *et al.*, in press). The larger of these, the Record Ridge ultramafic, is composed of variably serpentinized and locally carbonatized ultramafics, including dunite, pyroxene-bearing dunite, olivine wehrlite and wehrlite. Disseminated chrome spinel is present in all ultramafic rocks, locally increasing to over 30 percent within dunite. Platinum group element abundances of massive chromite clearly show that these rocks are ophiolitic and not Alaskan-type (Ash *et al.*, *op. cit.*).

The Nicola Group (Preto, 1977; 1979; Mortimer, 1986, 1987; Souther, 1991) comprises a western, typical arc succession of calcalkaline, mafic to felsic volcanic and volcanoclastic rocks. A possible back arc basin to the east is dominated by mafic to intermediate feldspar and feldspar-augite porphyry volcanoclastic rocks.

Farther east, the eastern facies of the Nicola comprises alkaline, augite phyric flows and related volcanoclastic rocks. Volcanic rocks of the Early Jurassic Rossland Group, the Elise Formation, are a younger, eastern alkaline volcanic arc succession in Quesnellia.

MOUNT ROBERTS FORMATION

The Mount Roberts Formation is the dominant formation in eastern exposures of the Harper Ranch subterrane. It comprises a succession of siliceous clastic rocks, carbonate, greywacke and minor greenstone of Pennsylvanian to Permian age (Little, 1982a,b). In the Rossland area, the formation is exposed near Patterson at the United States border and on the eastern slopes of

Mount Roberts, and near Granite and OK Mountains. Exposures on the west slopes of Red Mountain, including those that host a molybdenite breccia complex, were also included in the Mount Roberts Formation (Little, 1982b; Höy and Andrew, 1991a,b); however, they are now believed to be part of the Elise Formation as mapped by Fyles (1984), with a gradational stratigraphic contact with underlying volcanics.

Two conodont collections, one from the Patterson area and a second from the eastern slopes of OK Mountain, were identified by M.J. Orchard of the Geological Survey of Canada and confirm a late Carboniferous to Permian age for exposures of the Mount Roberts Formation in the Rossland area:

(1) **Field number:** BCHA-306-7a **GSC Loc. No.:** C-154324

Locality: east slope of OK Mountain, west of Rossland

NTS 82F/04; Lat./Long.: 49.0750° N; 117.8431° W

Description: brown impure dolomite layer mixed with limestone

Identification: conodont taxa: *Neogondolella* sp. indet.

Age and comments: Late Carboniferous-Permian; no older than Bashkirian (Early Pennsylvanian).

(2) **Field number:** BCHA-269-9 **GSC Loc. No.:** C-154329

Locality: northeast of Patterson

NTS 82F/04; Lat./Long.: 49.0097° N; 117.8236° W

Description: white limestone carbonate boulders in base of Archibald Formation

Identification: conodont taxa: *Idiognathodus?* sp. indet.

ramiform specimens

Age and comments: Late (?) Carboniferous; although host unit is mapped as basal Archibald Formation, limestone boulders containing fossils are derived from the immediately unconformably underlying Mount Roberts Formation.

Patterson area exposures consist of massive to thinly laminated, fine-grained, dark grey to black argillite, pale grey-green silty chert, siliceous siltstone and massive to brecciated fossiliferous limestone and dolomite. They are unconformably overlain by a conglomerate at the base of the Rossland Group. In the Rossland area, silt scours, graded beds and bedding-cleavage intersections indicate that the formation faces west. Thicker bedded, graded siltstone and sandstone beds, referred to as the sandstone member by Fyles (1984), are locally interbedded with thin, impure dolomite and limestone lenses. These occur directly beneath unconformably overlying volcanic breccia of the Elise Formation.

In northern Washington, Roback and Walker (1995) includes lithologically similar Early Triassic rocks in the Mount Roberts Formation, thus extending the stratigraphic range of this formation. Based on petrographic and U-Pb geochronological studies, these rocks are interpreted to have been deposited adjacent to an active magmatic arc. As suggested by Simony (1979) and supported by Roback and Walker (*op. cit.*), basement to the Mount Roberts Formation may be the Trail Gneiss (Figure 2-2).

MESOZOIC ARC ROCKS

Mesozoic arc rocks of Quesnellia unconformably overlie the upper Paleozoic rocks of the Okanagan and Harper Ranch subterrane. The late Triassic Nicola Group has been subdivided into three north-trending belts separated by major faults (Preto, 1977; 1979). The Western belt comprises calcalkaline to intermediate flows, breccias and volcanoclastic sediments; ignimbrites and subaerial facies indicate local emergence. The Central belt comprises dominantly pyroxene and plagioclase-rich andesitic and basaltic flows, breccias, conglomerates and lahars (Lefebvre, 1976). Eastern facies are similar to the Central belt but contain more sedimentary and epiclastic deposits. The Nicola Group formed as an oceanic island arc above an east-dipping subduction zone (Preto, 1979; Mortimer, 1987). Western calcalkaline facies may represent the active volcanic arc while the more alkaline eastern facies and associated sediments, a rifted back-arc basin.

The Rossland Group, the focus of this study, represents a younger and more eastern axis of Jurassic arc volcanism. It records volcanism that developed, in

part, above North American crustal rocks. It is separated from Nicola Group rocks by Middle Jurassic thrust faults that expose ophiolitic ultramafic rocks, by Eocene extensional faults, by exposures of North American crustal rocks in the cores of domal structures, and by numerous plutonic bodies including the Eocene Coryell batholith.

POST-ACCRETIONARY VOLCANIC AND SEDIMENTARY ROCKS

Post-accretionary rocks refer to those that formed after the allochthonous terranes of Quesnellia and Slide Mountain had docked against the western edge of North America. In the Nelson-Trail map-area, they include coarse conglomerates of the Late Cretaceous Sophie Mountain Formation and andesitic flows and tuffs of the Eocene Marron Formation.

SOPHIE MOUNTAIN FORMATION

The Sophie Mountain Formation, first referred to as the Sophie Mountain conglomerate (Bruce, 1917), comprises a number of isolated patches of conglomeratic rock in the Grouse Ridge and Mount Sophie areas south of Rossland (Little, 1960; Höy and Andrew, 1991b). The largest of these, the Mount Sophie occurrence, overlies the Elise Formation in the east and the inferred thrust fault that places oceanic ultramafic rocks on to the Rossland Group. It is intruded on the west by the Eocene Coryell batholith. The Grouse Ridge occurrence unconformably overlies Elise Formation rocks in the north and unit Cs of the Kootenay Terrane to the south. Small exposures are also recognized on the ridge north of Lake Mountain (Høy and Andrew, 1991b) and in Hudu Creek 2 kilometres from its confluence with Beaver Creek (Andrew *et al.*, 1990a; b). The basal contact in the small occurrence north of Lake Mountain is a shallow north-dipping unconformity with Sophie Mountain resting unconformably on more steeply north-dipping lapilli tuff of the Elise Formation.

The age of the Sophie Mountain Formation, based on plant fossils, is Late Cretaceous (Little, 1960). The Grouse Ridge occurrence is cut by Middle Eocene Sheppard dikes (Høy and Andrew, 1991b) and Little (1960) describes Coryell syenite cutting the formation.

The formation comprises poorly sorted, heterolithic conglomerate with thin interbeds of argillite and argillaceous siltstone. The conglomerate consists dominantly of rounded clasts of quartzite and other sedimentary units; in the Grouse ridge area, clasts of highly altered granitic rock are also recognized. Clasts derived from the underlying Elise Formation are rare or absent.

MARRON FORMATION

The Middle Eocene Marron Formation (Bostock, 1940; Little, 1960; Church, 1973) is exposed on the

eastern slopes of OK Mountain and Mount Roberts just west of Rossland (Figure 2-3). The formation comprises grey, green and, locally, mauve andesitic flows and minor lapilli tuff, tuffaceous sandstone and tuffaceous conglomerate. It is in fault contact with the Elise Formation near Rossland (Fyles, 1984) but unconformably overlies the Elise farther southeast (Figure 2-3). It is intruded by Eocene Coryell intrusions.

PLUTONIC ROCKS

Plutonic rocks occur extensively throughout southeastern British Columbia (Woodsworth *et al.*, 1992). The oldest are synrift mafic sills and anorogenic granites that intrude the Mesoproterozoic Purcell Supergroup. Paleozoic intrusive bodies include a number of alkalic stocks, including carbonatites, as well as some granitic bodies. Alkalic ultramafic diatremes, explored for their diamond potential, occur in several areas in the Rocky Mountains (Pell, 1987; 1994). Both intrusive and extrusive carbonatites occur along the flanks of "gneiss domes" in the Monashee Complex, and carbonatites are associated with the Ice River Complex, a late Devonian alkaline ultramafic intrusive complex south of Field. The carbonatites contain high values of rare earth elements, strontium and niobium. A number of folded and foliated granitic bodies in the Kootenay Terrane, including the Mount Fowler batholith and Clachnacudainn gneiss, have been interpreted as Paleozoic (Okulitch *et al.*, 1975).

Two suites of Early Jurassic plutons are recognized in the Nelson-Trail area. The Silver King intrusions (Figure 2-3) are a suite of medium to high-K calcalkaline feldspar porphyries located south of Nelson (Dunne and Höy, 1992; Chapter 6). Contact relationships, internal structures and geochemistry suggest that they are a pre to syntectonic suite, probably related to the collision of Quesnellia with North America (Dunne and Höy, *op. cit.*).

A number of mafic, high-K alkalic plutonic complexes within the Rossland Group are interpreted to be volcanic arc granitoids, comagmatic with the Elise Formation. These include the Rossland monzodiorite, the Eagle Creek complex, a number of dikes and sills at the Katie prospect, and a number of small mafic plugs scattered throughout the Rossland-Nelson area (Dunne and Höy, *op. cit.*). Many of these are clearly associated with copper-gold mineralization, including gold skarns, porphyry deposits, and the copper-gold rich massive pyrrhotite veins of the Rossland camp.

Large plutons of Middle Jurassic age are common in the Intermontane and Omineca Belts, and less common in the Foreland Belt. Typically, these plutons are complex, with early alkaline followed by calcalkaline plutonism and finally, two mica granite intrusions. They include the Kuskanax, Nelson, Bonnington and Trail plutons (Figure 2-3), the Galena Bay stock, the Similkameen batholith, the Okanagan intrusions and a number of small stocks in the northern Selkirk

Mountains. Many have vein gold-silver deposits within them, as well as a variety of mineralized veins or skarns along their margins; the Slocan, Ainsworth, Ymir and Nelson mining camps all occur along the edges of the Nelson batholith, inferring a genetic link. Beaudoin *et al.* (1992) have argued, however, that the Slocan camp is related to Eocene extensional tectonics.

Middle Cretaceous granitic rocks also form an extensive plutonic suite in the Omineca belt of southeastern British Columbia. In contrast with the Middle Jurassic plutons, these are clearly discordant, postdating regional metamorphism and Jurassic deformation. The larger plutons include the Bayonne Batholith and the White Creek stock. Mid-Cretaceous plutons are typically highly evolved S-type leucogranites and granodiorites. Many are associated with tungsten and minor copper, lead and zinc mineralization (Ray and Webster, 1997); the Invincible, Dodger, Emerald and

Feeney mines near Salmo are skarn deposits along the contact of a small middle Cretaceous stock with Lower Cambrian limestone. Recently, exploration in the vicinity of the Emerald deposit has been directed towards gold-bismuth mineralization.

Cenozoic plutonic rocks are locally important, particularly west of Rossland. Most, including the Coryell suite, are Eocene in age. They were intruded during regional Eocene extension, commonly along major shear zones, and are often associated with mafic volcanism (Marron Formation) and intrusion of many northerly trending mafic dykes. The Ladybird suite includes S-type quartz monzonite of Paleocene to Early Eocene age. The Coryell suite consists of high-level batholiths and stocks of porphyritic syenite and lesser granite, diorite and monzonite. They are an important source of dimension stone.

CHAPTER 3 - ROSSLAND GROUP: ARCHIBALD FORMATION

ROSSLAND GROUP: NOMENCLATURE

The Rossland Volcanic Group (McConnell and Brock, 1904) was initially defined to include sediments of the Archibald Formation, exposed in Archibald Creek, and overlying volcanic rocks. Volcanic rocks near Mount Kelly (formerly Beaver Mountain) were originally regarded as younger than the Rossland Group and assigned to the Beaver Mountain Group, a term that was retained by Little (1950) and Mulligan (1952).

Daly (1912) assigned the sediments now recognized to be part of the Archibald Formation to the Beaver Mountain Group and redefined the Rossland Volcanic Group as the Rossland Volcanic Formation (Figure 2-2). However, fossil evidence has indicated that rocks of the Beaver Mountain are actually Rossland Group (Frebald, 1959; Frebald and Little, 1962) and hence the term, Beaver Mountain, has been discarded (Little, 1982a; b).

The Rossland Group has been redefined by Frebald and Little (1962) to include clastic rocks of the Archibald Formation, dominantly volcanic rocks of the Elise Formation and dominantly fine-grained clastic rocks of the overlying Hall Formation. It has been further redefined to include the Ymir Group (Little, 1960) as "there can be little doubt that the upper part at least of the Ymir Group is equivalent to the Archibald" (Little, 1982b, p.15).

ARCHIBALD FORMATION

The Archibald Formation is named for thick exposures of sedimentary rock along Archibald Creek, southwest of Salmo (Frebald and Little, 1962). The formation occurs on the west limb of the Hall Creek syncline southwest of Nelson, in the limbs of the Mt. Kelly syncline west of Salmo and in the hangingwall of the East Archibald Creek fault just to the east (Figure 3-1). It thins to the west where it is exposed as a west-facing homoclinal panel on the slopes northwest of Montrose and Fruitvale. Farther west at Patterson, a thin

vener of conglomerate between the Mount Roberts Formation and overlying tuffs of the Elise Formation are included in the Archibald Formation. These rocks were previously included in the basal part of the Elise (Little, 1982b); however, their stratigraphic position and sedimentary nature allow correlation with the Archibald (Høy *et al.*, 1992). Farther north at Rossland, the Archibald Formation is missing and volcanic rocks of the Elise Formation unconformably overlie the Mount Roberts Formation.

The Archibald correlates with the Ymir Group on the east limb of the Hall Creek syncline and may correlate with the upper part of the Slocan Group exposed north of Nelson (Little, 1962). The base of the Archibald (and Rossland Group) is only exposed at Patterson where it unconformably overlies dominantly fine-grained siliceous rocks, argillite, carbonate and minor greenstone of the Pennsylvanian to Permian Mount Roberts Formation.

AGE

The age of the upper part of the Archibald Formation is well established. It contains numerous fossils of early Sinemurian as well as, locally, late Sinemurian age in the Salmo area (Frebald and Little, 1962; Frebald and Tipper, 1970). Frebald and Little (*op. cit.*) suggested that two poorly or incompletely preserved ammonites within the Archibald may be Hettangian. However, Tipper (1984) argued that these fossils are more comparable with Sinemurian genera.

A number of new fossil localities were discovered in the upper Archibald during regional mapping in this project and were submitted to H.W. Tipper of the Geological Survey of Canada for identification. These are listed below and located on Figure 3-1. Although many were not identifiable or their age determinable, two confirm a Sinemurian age for the upper part of the Archibald Formation.

(1) **Field number:** BCHA-196-27 **GSC Loc. No.:** C-154312

Locality: 1/2 kilometre north of Montrose;

NTS 82F/04E; UTM zone 11, 456700 E, 5436825 N.

Identification: wood fragments

Age and comments: sample from near top of Archibald Formation in shallow-water environment; age not determinable.

(2) **Field number:** BCHA-197-2 **GSC Loc. No.:** C-154313

Locality: 1 kilometre north of Beaver Falls, west of Beaver Creek; NTS 82F/04E; UTM zone 11, 458000 E, 5438050 N.

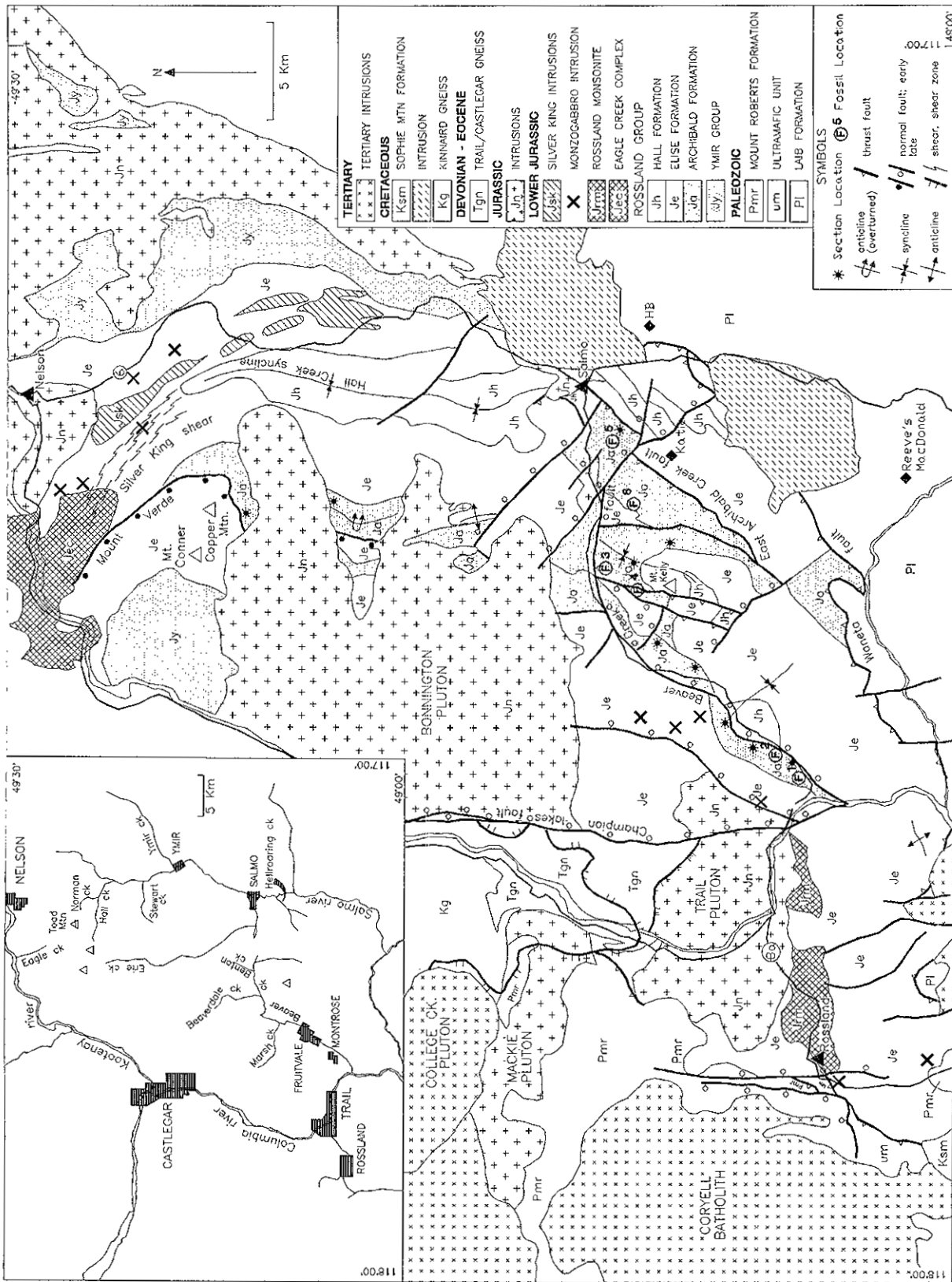


Figure 3-1. Map showing the distribution of the Archibald Formation, fossil locations and location of sections; (after Andrew *et al.*, 1991; Little, 1985 and included references).

Identifications: rhynchonellid brachiopods
bivalves - *Weyla?* and others
coleoids?

Age and comments: sample from upper Archibald, similar stratigraphic position as 196-27; a definitive age is not possible; early Jurassic is possible.

(3) **Field number:** BCHA-204-12 **GSC Loc. No.:** C-154314

Locality: 1/4 kilometre east of Query Creek, 1/2 kilometre south of Highway 3B; NTS 82F/03W; UTM zone 11, 468600 E, 5447470 N.

Identifications: ammonites - echioceratids?
wood fragments
bivalves

Age and comments: sample is from upper Archibald, a few hundred metres below Elise Formation contact; Sinemurian age; closely resembles *Paltechioceras* but is not identifiable confidently; if ammonites are echioceratids, the age would be Late Sinemurian.

(4) **Field number:** BCHA-207-4 **GSC Loc. No.** C-154317

Locality: 2 kilometres north of Mt. Kelly, between Hammond and Doubtful Creeks; NTS 82F/03W; UTM zone 11, 467300 E, 5445900 N.

Identifications: bivalve - not determinable

Age and comments: Age unknown.

(5) **Field number:** BCHA-208-18 **GSC Loc. No.:** C-154318

Locality: One kilometre east of Gilliam Creek; one kilometre south of Erie Creek; NTS 82F/03W; UTM zone 11, 477050 E, 5446950 N.

Identifications: *Arnioceras* aff. *A. miserabile*
Arnioceras cf. *A. arnouldi* (spelling)

Age and comments: Early Sinemurian; Mid-early Sinemurian.

(6) **Field number:** BCHA-218-6 **GSC Loc. No.:** C-154319

Locality: 2 kilometres south of Beaver Creek; 1/4 kilometre east of Archibald Creek; NTS 82F/03W; UTM zone 11, 471850 E, 5445700 N.

Identifications: *Paltechioceras* sp.
Plesechioceras sp.

Age and comments: Sample from near top of Archibald Formation; Late Sinemurian.

(7) **Field No.:** BCHA-226-3 **GSC Loc. No.:** C-154320

Locality: Headwaters of Bell Creek; 1 1/2 kilometres west of Mt. Kelly; NTS 82F/03W; UTM zone 11, 466600 E; 5444300 N.

Identifications: bivalve - *Weyla?* sp., possibly *Weyla acutiplicata*

Age and comments: Sample is from upper Archibald, a few hundred metres below Elise Formation contact; Early Jurassic? if suggested identification is correct.

(8) **Field No.:** BCHA-229-1 **GSC Loc. No.** C-154321

Locality: 2 kilometres east-northeast of Mt. Kelly on branch of Mt. Kelly access road. NTS 82F/03W; UTM zone 11, 471750 E; 5445000 N.

Identifications: fragment of bivalve

Age and comments: Sample from upper Archibald, close to Elise Formation contact; age not determinable.

DESCRIPTION

The Archibald Formation generally comprises a succession of interbedded siltstones, sandstones and argillites with prominent sections of interbedded conglomerate. Its total exposed thickness varies from a few tens of metres of conglomerate near Patterson to an

estimated 2550 metres of finer grained clastic rocks near Gilliam Creek where the base is not exposed.

The contact with the overlying Elise Formation is abrupt to locally gradational. In eastern exposures it is mapped where fine-grained interbedded siltstones and argillites give way to massive augite porphyry flows. In

the Patterson area, the contact is placed where conglomerates with argillaceous matrix are replaced by tuffaceous conglomerates that contain lithic volcanic clasts and a green tuffaceous matrix. At Fruitvale, siltstones and sandstones with rare tuffaceous conglomerate lenses are included in the Archibald as these correlate with massive siltstone units farther east. Little (1982a) included these units in the Elise Formation, placing the Archibald-Elise contact at the base of the first volcanic unit.

Stratigraphic sections of the Archibald Formation are located on Figure 3-1 and shown in Figure 3-2. These are not measured sections; they are scaled and described from structural cross-sections. A correlation chart (Figure 3-3) illustrates the prominent lateral facies changes, with dominantly fine-grained facies in eastern and northeastern exposures and much coarser grained facies, including conglomerates, prominent in western (Beaver Falls) exposures.

MOUNT KELLY AREA

The Mount Kelly, Archibald Creek West and Gilliam Creek sections are the most complete (Figure 3-3). The basal parts of these sections comprise argillite and minor siltstone. The exposed basal part of the Mount Kelly section is estimated to be 600 metres thick. However, this section occurs within the core of the Mount Kelly syncline and therefore the true thickness may be less. It comprises dark grey to black, rusty-weathering argillite and silty argillite. It is generally massive to thinly laminated and contains occasional thin tan to grey siltstone layers that are commonly scoured at their base, suggestive of turbidite deposition. A thin conglomerate unit within this basal Archibald, referred to as the Benton Creek member by Fitzpatrick (1985), consists of polymict conglomerate, with sedimentary (dominantly limestone and siltstone), feldspar porphyry and rare volcanic clasts in a sandy matrix.

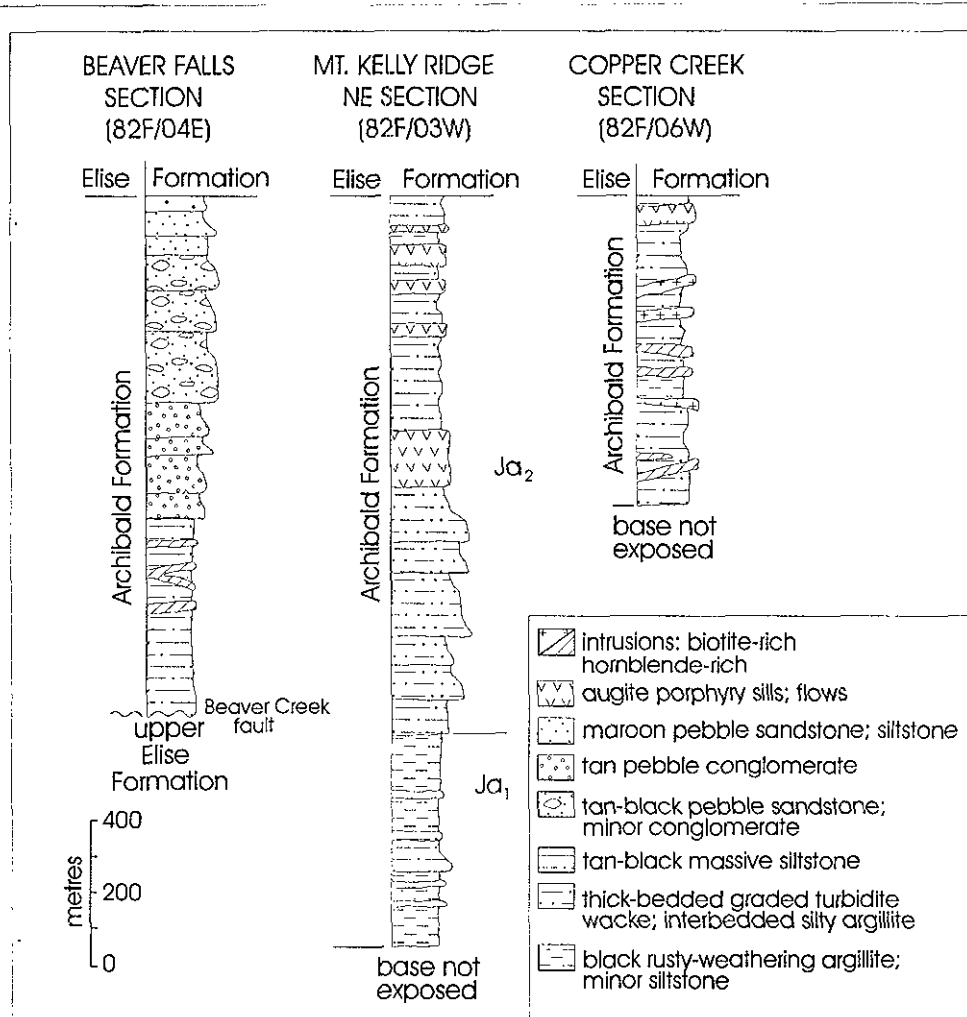


Figure 3-2 Detailed sections of the Archibald Formation in the Fruitvale (Beaver Falls), Mount Kelly and Mount Verde (Copper Creek) areas.

The basal Archibald is overlain by up to 1500 metres of interbedded wacke, siltstone and silty argillite of Unit Ja2. In the Mount Kelly section (Figure 3-2), the basal part of Ja2 comprises thick-bedded wacke interlayered with thinner bedded interlaminated siltstone and argillite. Wacke and rare arenite beds are up to one metre thick and may contain small lithic fragments. They are commonly graded, locally scour underlying units and contain flame structures indicative of turbidite deposition. In general, the abundance and thickness of individual wacke beds decrease upsection within Unit Ja2.

The upper part of Ja2 is typically thinner bedded and finer grained. It comprises thin to medium-bedded siltstone and wacke beds with minor grey, laminated

siltstone-argillite interbeds. The siltstone units are commonly graded, occasionally crossbedded and locally contain rip-up clasts (Plates 3-1, 3-2). Silty argillite beds may contain ripples, cross-laminations and slump structures. These bed forms are typical of the Bouma turbidite sequence (Bouma, 1962; Walker, 1979) with coarse, commonly graded siltstone-wacke at the base (A interval), overlain by laminated siltstone (B interval) and finally, convoluted laminae (C interval).

East of Archibald Creek, a west-facing panel of Unit Ja2 contains a prominent graded tuff unit with large feldspar phyric clasts at the base and crystal tuff at the top. Massive amygdaloidal augite porphyry sills (or possibly flow units) occur in the upper Archibald in the Mount Kelly section (Figure 3-2).

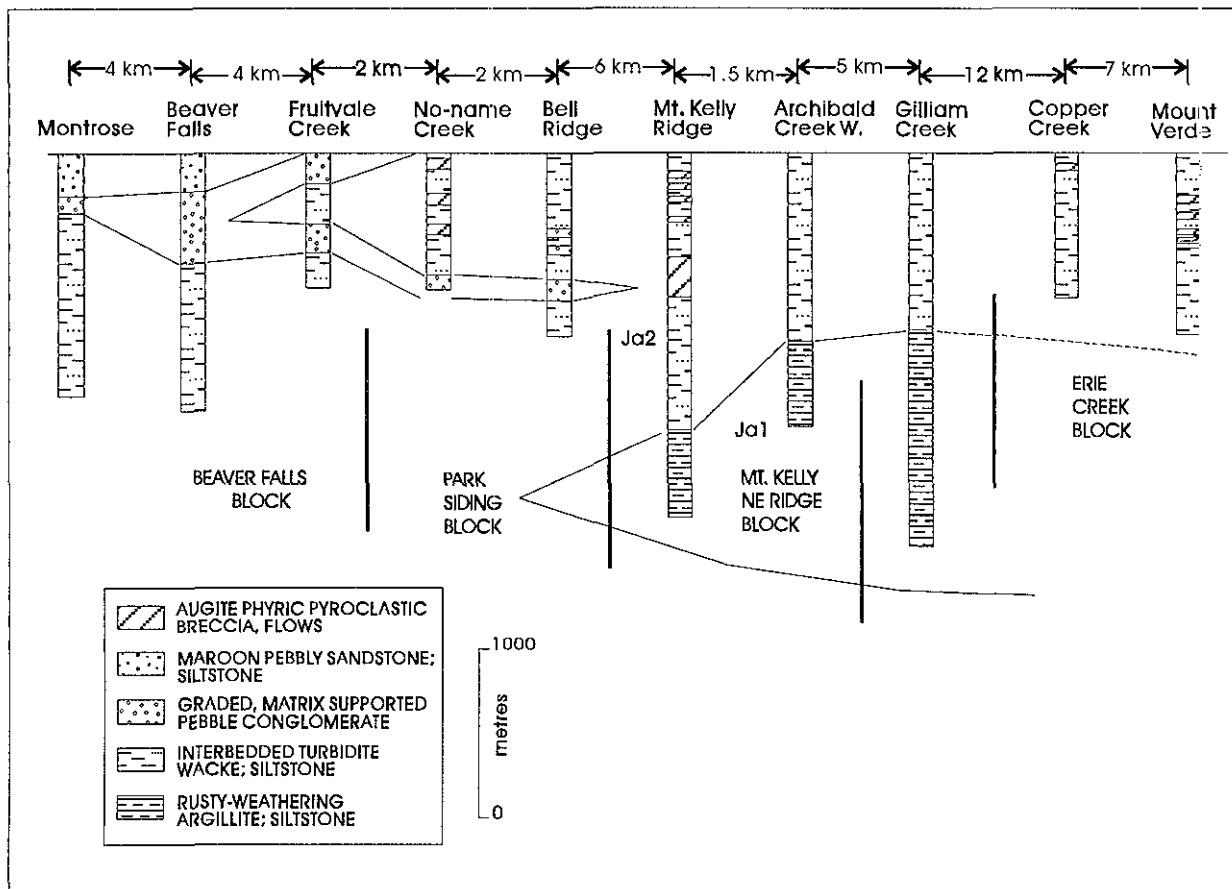


Figure 3-3. Composite stratigraphic sections of the Archibald Formation.

MOUNT VERDE AREA

Farther north in the Mount Verde and Copper Mountain area, only the upper part of the Archibald Formation is exposed (Figure 3-3). It generally comprises a fining-upward succession of interbedded siltstones, sandstones and argillites. The lower part of the section is characterized by over 200 metres of interbedded tan siltstone and impure grey sandstone-wacke in beds 3 to 4 centimetres thick. These are overlain by a finer grained sequence of rusty-weathering, tan siltstones intercalated with grey to black silty argillite and minor black graphitic argillite. A few thin (2 to 10 metres) mafic flows or sills occur with increasing abundance near the top of the section in Erie Creek southwest of Mount Verde and the Red Mountain area to the north. This succession of interbedded

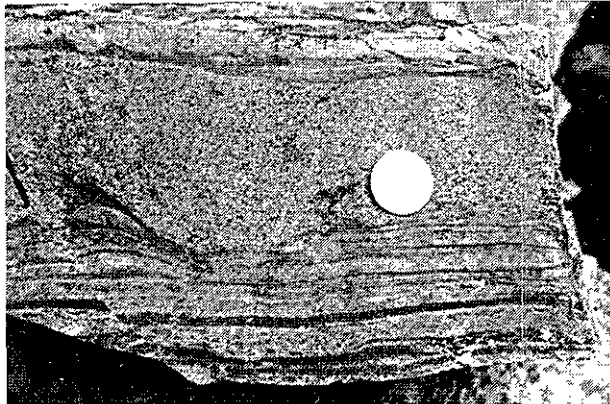


Plate 3-1: Thick-bedded, graded turbidite wacke with sharp basal contacts and basal scours, Archibald Formation, west of Salmo.



Plate 3-2: Crossbedding in thick-bedded, graded turbidite wacke, siltstone and silty argillite, Archibald Formation, east of Mount Kelly.

volcanic and sedimentary units correlates with a similar succession at the top of the Ymir Group. The Mount Verde section is generally thinner bedded and finer grained than the correlative upper part of the Mount Kelly section.

FRUITVALE AREA

West of Mount Kelly in the Fruitvale area, the upper part of the Archibald Formation is coarser grained and locally contains facies indicative of shallow water to subaerial exposure. The Beaver Falls section (Figure 3-2) comprises approximately 540 metres of massive, thick to medium-bedded siltstone at the base, overlain by 300 metres of chaotic matrix-supported conglomerate, pebble sandstone and siltstone. The siltstone beds are commonly graded with flame structures at their base, suggestive of turbidite deposition. Numerous plagioclase porphyry sills, a few metres thick, with prominent baked contacts occur within the succession. They are assumed to be of Eocene age.



Plate 3-3: Matrix-supported conglomerate with limestone and siltstone clasts (0.5-10 cm), Archibald Formation, Beaver Creek area.

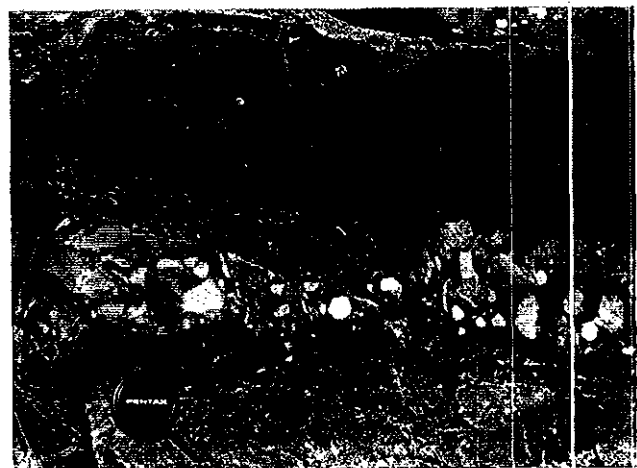


Plate 3-4: Limestone breccia of Archibald Formation, Patterson area.

The upper conglomeratic section comprises a number of fining upward sequences, 2 to 3 metres thick, with pebble conglomerate at the base and lithic-rich sandstone at the top. The conglomerate is dominated by siltstone clasts, but includes some plagioclase porphyry intrusive clasts and approximately 10 percent limestone clasts (Plate 3-3); fossils in the limestone clasts have been identified as Permian, indicating that they are derived from the Mount Roberts Formation (Little, 1982b).

Massive, poorly sorted conglomerate units near the top of the Archibald contain large rounded to subangular clasts in a mixed lithic sandstone-siltstone matrix. Locally, the conglomerate and interlayered sandstone is red to brown-coloured. A thin (3 to 4 cm) brecciated limestone bed within the conglomerate is irregularly laminated, suggestive of algal mat formation; it also contains thin oolitic layers. The contact with the overlying Elise Formation is placed beneath the first conglomeratic unit with a pronounced green-coloured tuffaceous matrix. This basal Elise conglomerate contains abundant clasts of intrusive plagioclase porphyry.

The coarse conglomeratic facies in the upper part of the Archibald Formation in the Fruitvale area are alluvial fan and locally fluvial deposits. Poorly sorted heterolithic conglomerates with abundant limestone clasts are interpreted to be debris flows. The maroon facies and associated limestone units suggest shallow-water deposition.

PATTERSON AREA

The Archibald Formation at Patterson at the United States border south of Rossland comprises a veneer of conglomerates up to several hundred metres thick that lies unconformably on the Mount Roberts Formation. These conglomerates were previously included in the basal part of the Elise (Little, 1982b); however, their stratigraphic position at the base of the Rossland Group, their sedimentary nature and their inferred paleotectonic setting allow correlation with the Archibald Formation.

The Mount Roberts paleosurface was irregular, resulting in isolated patches of Archibald in depressions in the surface and small outcrops of Mount Roberts on paleohighs (Figure 3-4). Most commonly, a limestone of the Mount Roberts Formation lies near the paleosurface.

The Archibald Formation here is typically a heterolithic pebble conglomerate with subrounded to subangular clasts of grey-green siliceous siltstone, argillaceous siltstone, limestone, and minor chert, quartzite and plagioclase porphyry in an argillaceous or granular sandy matrix. Locally, a coarse limestone breccia derived from the underlying Mount Roberts Formation is at the base of the Archibald (Plate 3-4). The argillaceous matrix is commonly tinged purple, suggesting subaerial exposure. Bedding, clast-sorting or winnowing, grading or other features indicative of fluvial environments are lacking. These sedimentary

conglomerates are distinct from tuffaceous conglomerates in the immediately overlying Elise Formation as they contain virtually no volcanic clasts nor a tuffaceous matrix.

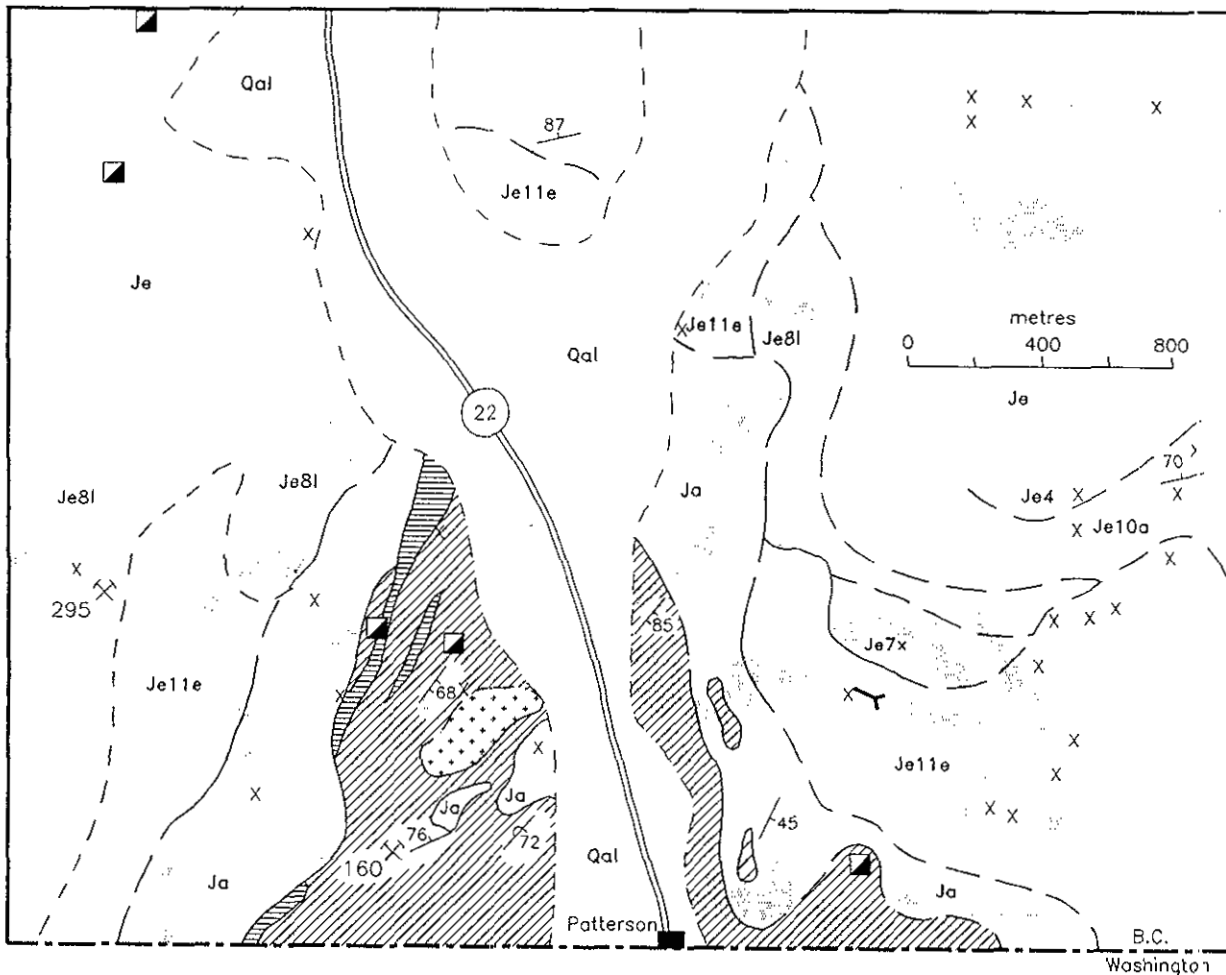
FACIES TRENDS AND INTERPRETATION

Archibald Formation sections, summarized in Figure 3-3, show pronounced and systematic facies changes. Alluvial fan conglomerates and coarse sandstone facies dominate the upper part of the Archibald Formation in the western exposures near Fruitvale and Montrose. Farther east in the Mount Kelly and Archibald Creek areas, the upper Archibald, Unit Ja2, comprises mainly coarse to medium-grained turbidites. To the northeast in the Nelson area, finer grained, more distal turbidite deposits predominate and southeast of Nelson, correlative Ymir Group rocks are predominantly argillites with thin-bedded, fine-grained distal turbidites.

These facies changes indicate that the Archibald was deposited in a large submarine fan with a source area to the west. The coarse clastic facies of the Fruitvale area are laterally discontinuous subaqueous debris flows; fining-upward cycles may record fluvial deposition and maroon facies and oolitic and algal limestone, shallow-water and intermittent subaerial exposure. These give way to the east to thick sequences of A-E turbidites near Mount Kelly and finally, deep-water pelagic sediments with more distal turbidites in the Nelson area. An inferred eastward transport direction of turbidites is supported by paleocurrent measurements which show dominantly east to northeast current direction (Fitzpatrick, 1985; Figure 3-5).

Debris flows, associated rapid facies changes and locally subaerial deposition in the Fruitvale area suggest deposition near a faulted basin margin. To the west, near Rossland, the Archibald Formation is missing and the Elise Formation sits unconformably on Mount Roberts Formation; at Patterson only a thin veneer of conglomerate of the Archibald Formation separates the Elise and Mount Roberts formations. These changes indicate that the Archibald records deposition on a tectonic high in the Rossland-Patterson area and in a fault-bounded structural basin located to the east. Periodic uplift of the western block triggered debris flows along the eastern faulted margin and provided a source for clasts of Mount Roberts Formation in conglomerates of the Archibald and for the apron of turbidite deposits to the east.

The inferred evolution of the Archibald Formation and the correlative Ymir Group southeast of Nelson is summarized in Figure 3-6. The argillite succession in the lower Archibald was deposited as predominantly deep-water pelagic muds, with thin carbonates in the Ymir (McAllister, 1951) and only minor input of distal or low-energy turbidites, in a marine basin that stretched from Archibald Creek to Ymir and perhaps



LEGEND

- | | | | |
|-------------------------------|----------------------------|---|----------------------------|
| QUATERNARY | | | SYMBOLS |
| Qal alluvium | Je7l basaltic lapilli tuff | bedding: tops known overturned, unknown | past producer minifile no. |
| JURASSIC | Je7x basaltic crystal tuff | | pit |
| diorite | Je4 mafic flows | | adit |
| ROSSLAND GROUP | | | outcrop |
| Je ELISE FORMATION | Ja ARCHIBALD FORMATION | | |
| Je11e tuffaceous conglomerate | | PENNSYLVANIAN - PERMIAN | |
| Je10a siltstone, argillite | | MOUNT ROBERTS FORMATION | |
| Je8l andesitic lapilli tuff | | carbonate | |

Figure 3-4. Geological map of the Patterson area showing the distribution of the Mount Roberts Formation and unconformably overlying Archibald and Elise Formations.

northward to include part of the Slocan Group (Figure 3-6a). The source of these turbidites is not known; it is possible that they had an eastern source. The initiation of growth faulting near the southwestern basin margin produced coarse clastic facies in the Fruitvale area and proximal turbidites in the Mount Kelly area. These

early Jurassic growth faults are located between the basin margin near Fruitvale and the uplifted tectonic high near Rosslund (Figure 3-6b) Final shallow water to locally subaerial deposition in the Fruitvale area produced more oxidized facies immediately prior to deposition of Elise pyroclastic breccia (Figure 3-6c).

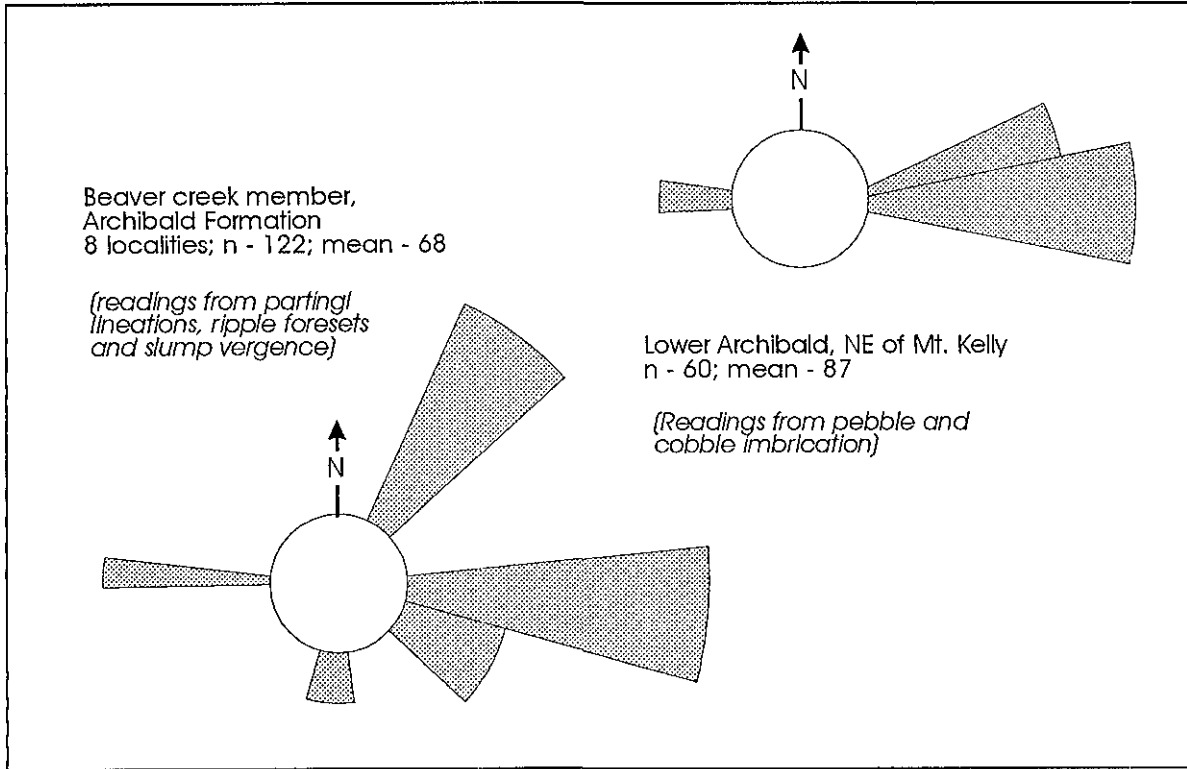


Figure 3-5. Paleocurrent directions of turbidites and debris flows of the Archibald Formation in the Fruitvale, Mount Kelly and Archibald Creek areas (from Fitzpatrick, 1985).

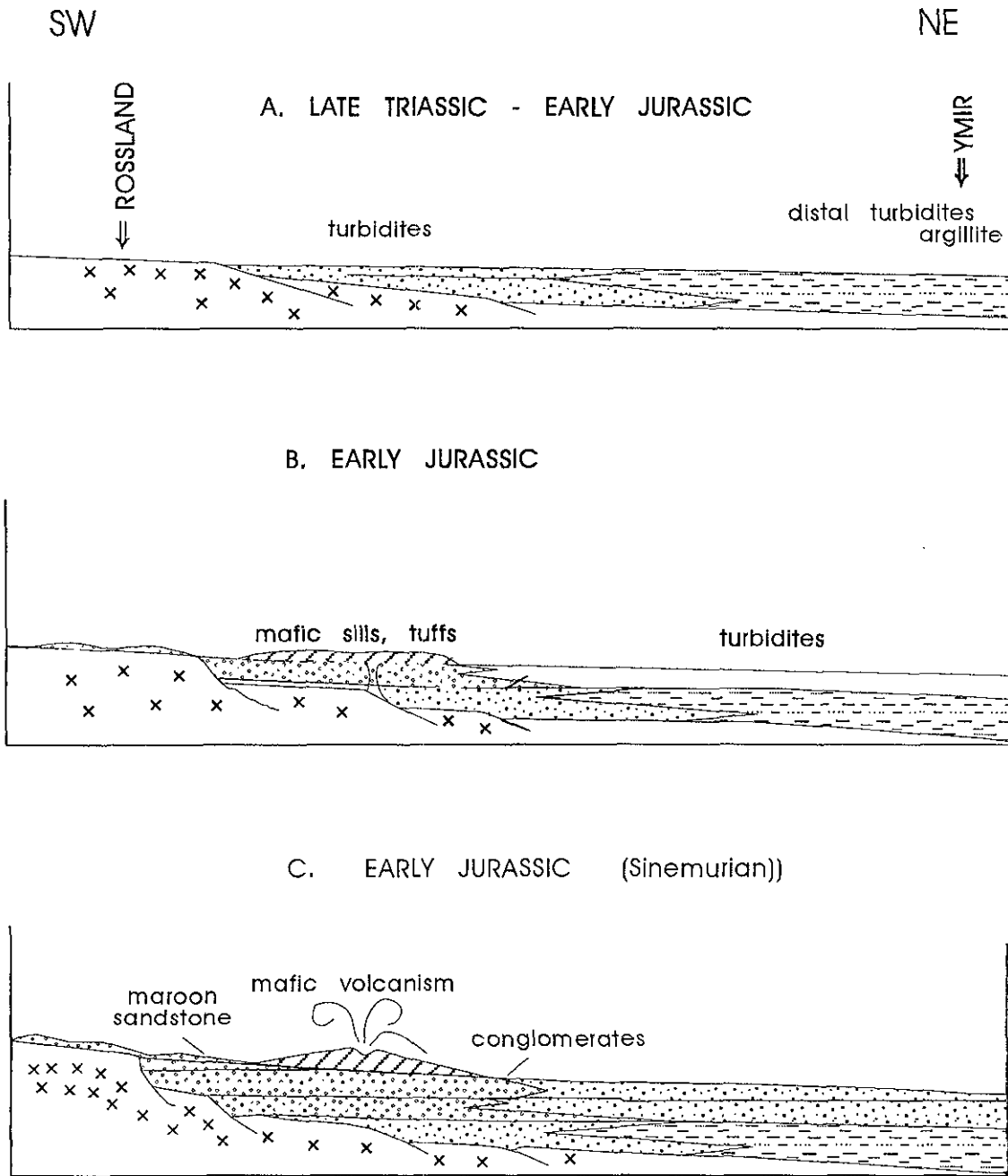


Figure 3-6. Schematic diagram illustrating the tectonic evolution of the Archibald Formation, Early Jurassic time.

CHAPTER 4 - ELISE FORMATION: DESCRIPTION

INTRODUCTION

The Elise Formation was named by Little (1950) to include the thick succession of Lower Jurassic volcanic rocks that are exposed on the western slopes of Mount Elise south southeast of Nelson (Figure 4-1). The name was retained by McAllister (1951) in the Ymir area and by Mulligan (1952) in the Bonnington area but renamed the Rossland Formation by Little (1960). In subsequent reports, however, these volcanic rocks have been called the Elise Formation (Frebald and Little, 1962; Little, 1962; Little, 1982a;b).

The Elise Formation comprises up to 5000 metres of dominantly mafic volcanic rocks, including mafic flows, thick sequences of pyroclastic rocks, some epiclastic rocks and locally interlayered fine to medium grained sedimentary rocks. It is exposed in the limbs of the Hall Creek syncline from Nelson to Salmo, extends west to underlie a large part of the block-faulted area between Salmo and Montrose, and comprises an essentially north-dipping homoclinal succession from the Washington border to Rossland (Figure 4-1). South of the border, Elise volcanic rocks have been traced discontinuously westward from the Colville Quadrangle (Joseph, 1990) to the Republic Quadrangle (Stoffel, 1990). The Elise Formation is also exposed in isolated roof pendants in Nelson age intrusions northwest of the Nelson-Trail map-area; for example, the dominant host rocks of both the Willa Cu-Mo deposit near Silverton (Wong and Spence, 1996) and the Tillicum gold skarn near Burton (Ray and Spence, 1986) are Elise volcanic rocks.

The Elise Formation is generally in sharp to gradational, conformable contact with underlying sedimentary rocks of the Archibald Formation. However, as described above, it rests unconformably on Mount Roberts Formation on the slopes of OK Mountain just west of the town of Rossland. In eastern exposures, it is overlain conformably by sedimentary rocks of the Hall Formation. However, in the Rossland area, the Hall Formation is missing and conglomerates of the Early Cretaceous Mount Sophie Formation unconformably overlie Elise volcanic rocks (Little, 1982a; Höy and Andrew, 1991b).

AGE

FOSSIL DATA

The age of the Elise Formation is constrained by Late Sinemurian fossils in the underlying Archibald Formation and early Toarcian fossils in the Hall

Formation. As well, a number of ammonites of Sinemurian age have been discovered in interbedded siltstones and argillites in the lower few hundred metres of the Elise Formation in the Maude Creek area south of Rossland and the Waneta and Fruitvale areas to the east (Little, 1982b). One locality (F6; 1.5 km due east of Fruitvale; Little, *op. cit.*) is interpreted to be within upper Elise rocks (Andrew *et al.*, 1990b) suggesting that the entire Elise was deposited in a relatively short time span, in Late Sinemurian time.

However, in the Ymir area, marine beds that were interpreted to be at the top of the type Elise succession contain fossils of lower Toarcian age (Frebald and Little, 1962). It is suggested that these beds are within the Hall Formation (Høy and Andrew, 1989b) thereby restricting the age of the Elise. This implies a hiatus between volcanism of the Elise and deposition of the Hall Formation, a hiatus that may be recognized locally by conglomerates at the base of the Hall along Salmo River between Hall Creek and Stewart Creek.

Diagnostic fossils have not been recognized in Rossland Group rocks in the United States (Stoffel, 1990; Joseph, 1990).

U-Pb DATING

A number of attempts have been made to determine the radiometric age of the Elise Formation. In the Sackit Canyon, Republic Quadrangle, Washington, granitic boulders in metaconglomerate at the base of the Rossland Group have yielded a U-Pb zircon age of 196 ± 1 Ma (Roback, 1993), providing a maximum age for the formation (Stoffel, 1990). In this study, a tuff unit, epiclastic sediments within the formation, and the Rossland monzonite, interpreted to be comagmatic with the volcanic rocks have been dated. The analytical work was done at UBC by J. Gabites (pers. comm., 1996).

Zircons from both the epiclastic and tuff units were separated using standard heavy-mineral separation techniques. Fractions were selected using conventional size (nylon mesh sieve) and magnetic (Frantz isodynamic separator) separations, followed by hand-picking to virtually 100 per cent purity. Sample dissolution and chemistry were carried out using a procedure modified from Kroch (1973) and mass spectrometric analysis was done using a VG Isomass 54R solid-source mass spectrometer in single collector mode (Faraday cup). Precisions for $^{207}\text{Pb}/^{206}\text{Pb}$ and $^{208}\text{Pb}/^{206}\text{Pb}$ were better than 0.1 per cent and for $^{204}\text{Pb}/^{207}\text{Pb}$, better than 0.5 per cent.

A massive feldspar crystal tuff, unit Je8x, in the Copper Mountain area southwest of Nelson (locality 1; Figure 4-1) yielded four zircon fractions. U-Pb data,

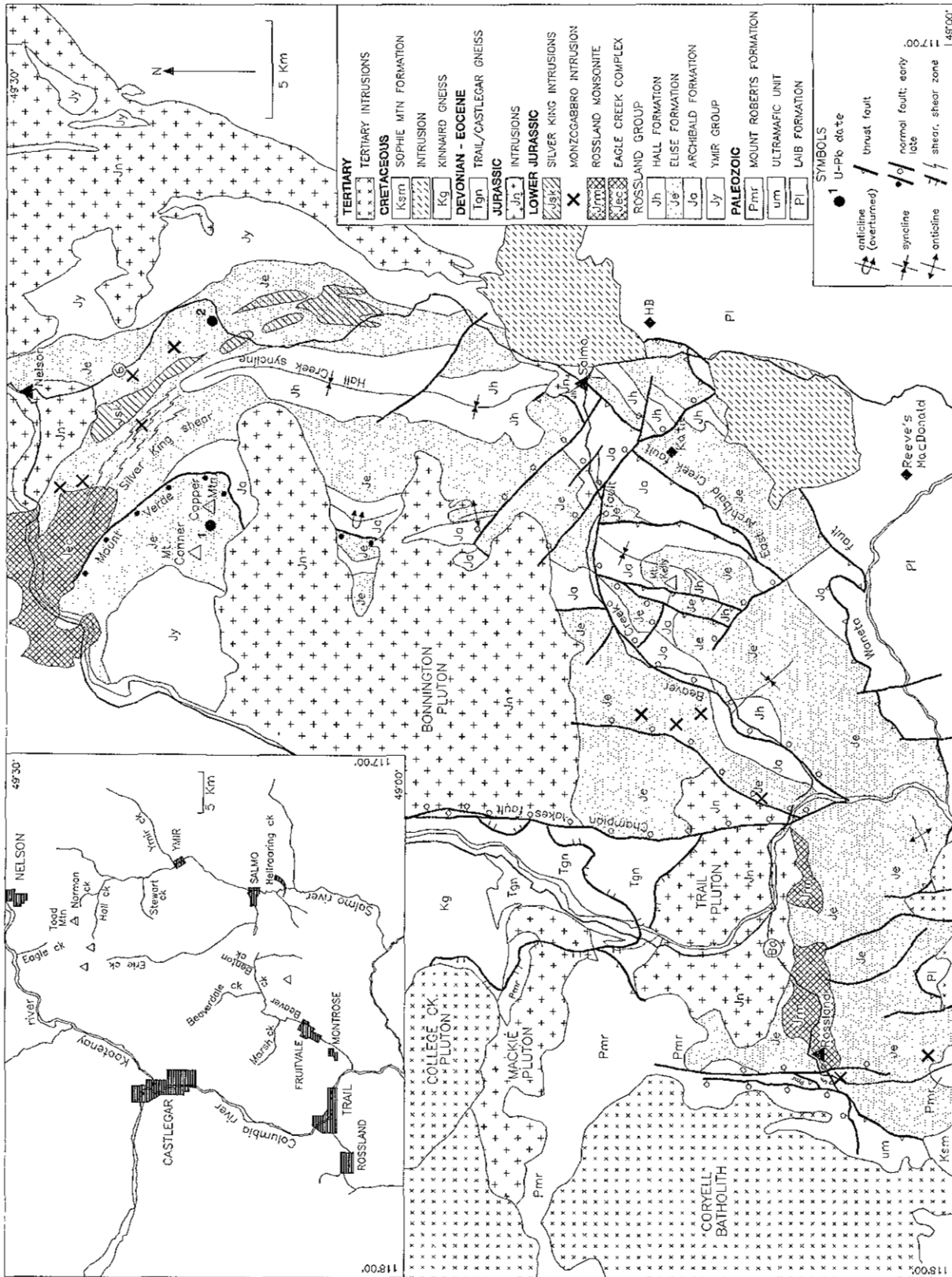


Figure 4-1 Map showing the distribution of the Elise Formation and locations of sections described in text; (after Andrew *et al.*, 1991; Little, 1985 and included references).

shown in Table 4-1 and plotted on Figure 4-2 were fitted to a straight line and extrapolated to the concordia. The lower intercept date of 197.1 ± 0.5 Ma confirms an early Sinemurian age for tuffs in the middle part of the Elise Formation. The upper intercept indicates inherited zircon of average age 2.28 Ga.

The upper intercept age implies that Elise volcanics were deposited above North American (or equivalent) crustal rocks. This contrasts with Late Triassic Nicola arc volcanics to the west that do not record Precambrian inheritance, and constrains models for generation of volcanic arcs in Quesnellia (see Chapter 7).

A second sample, a composite bulk sample of Unit Je10 was collected from a Highway 6 roadcut approximately 1.7 kilometres west of the junction with the Apex Creek road (locality 2; Figure 4-1). Je10 is a sequence of grit, sandstone and siltstone of predominantly volcanic or subvolcanic intrusive provenance. Sample 19-4 from near the top of the succession comprises mixed pyroclastic? and epiclastic fragments with average clast size of less than 1

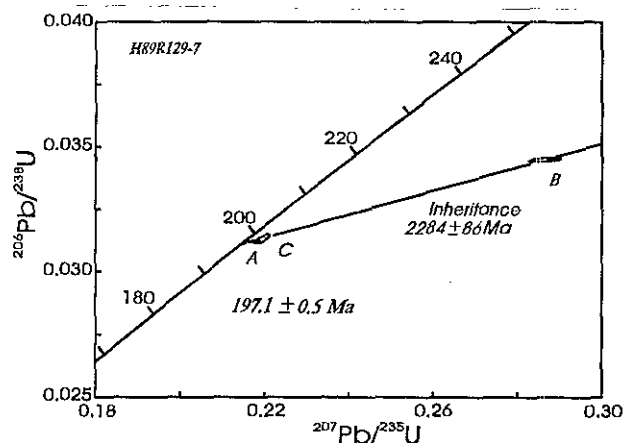


Figure 4-2: U-Pb concordia diagram of zircon data, Sample 129-7, Elise Formation; see Table 4-1 for data and text for discussion.

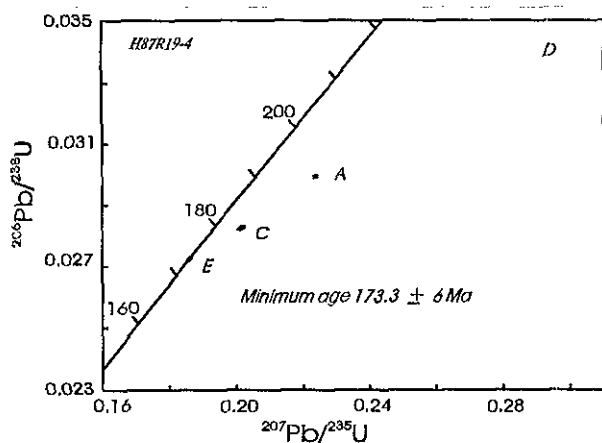


Figure 4-3: U-Pb concordia diagram of zircon data, Sample 19-4, Elise Formation; see Table 4-1 for data and text for discussion.

millimetre. To the north, Je10 becomes coarser grained and is eventually replaced by tuffaceous conglomerate of Unit Je11 that contains abundant subrounded boulders and cobbles of intrusive feldspar porphyry. The tuffaceous siltstone-grit was dated in order to determine the age of a presumed subvolcanic intrusion that had been eroded and supplied detritus to units Je10 and Je11 and hence would constrain the maximum age of the Elise Formation.

Separated zircons were clear, colourless to pink, doubly terminated prisms. No cores or zoning were visible in the picked crystals, but approximately 20 per cent of the population contained cloudy cores or clear inclusions. Most grains were subhedral to euhedral prisms; the coarse magnetic fraction was mainly broken crystals. As described above, U-Pb data (Table 4-1) were plotted on a concordia diagram (Figure 4-3). Errors on individual dates and on calculated intercept ages are quoted at the 2σ level (95 per cent confidence interval).

The data of sample 19-4 is difficult to interpret. Analyses of five fractions show both lead loss and inheritance. A minimum age for the sample is given by the only concordant fraction E, which consists of abraded tips of large, non-magnetic crystals. This age is $173.1 \pm 6/-0.2$ Ma based on the $^{207}\text{Pb}/^{206}\text{Pb}$ and $^{206}\text{Pb}/^{238}\text{U}$ ages. It is considerably younger than the Sinemurian age of the Elise, constrained by fossil data. The inherited components in the zircons appear to be of various ages, and because the rock is epiclastic and the zircons may be detrital, a regression of the data is not appropriate.

DESCRIPTION

The Elise Formation changes in both character and thickness from the Nelson area in the north to the Rossland area in the southwest. In the Nelson area, it includes a prominent basal succession of mafic flows, overlain by dominantly mafic to intermediate pyroclastic rocks, whereas in the Rossland area, the basal succession is missing and pyroclastic flow deposits predominate. In the following sections, lithologic units of the Elise Formation (summarized in Table 4-2) are described, composite stratigraphic sections constructed in a number of different areas, and a model for Elise volcanism presented.

HIGHWAY 6 SECTION, SOUTH OF NELSON

A complete section of the Elise Formation is exposed in the east limb of the Hall Creek syncline along Highway 6 south of Nelson (Figure 4-4a). The composite Elise section, illustrated in Figure 4-5, is derived from the cross-section in Figure 4-4b. It has been subdivided into a lower and an upper division. The lower Elise lies with apparent conformity on sedimentary rocks of the Ymir Group; a few argillite beds persist through the lower part of the lower Elise. It is a sequence of dominantly mafic flows and flow

Table 4-1: U-Pb data of zircons, samples 129-7 and 19-4, Elise Formation; data plotted in figures 4-2 and 4-3

Fraction: ^{1,2}	wt	U ³	Pb ³	208Pb	Pb	206Pb	Isotopic Ratios ($\pm 1\sigma$)			Isotopic Dates (Ma, $\pm 2\sigma$)	
	mg	ppm	ppm	% ⁴	pg ⁵	204Pb	206Pb/238U	207Pb/235U	207Pb/206Pb	206Pb/238U	207Pb/206Pb
6											
H87R19-4 Elise Formation, tuffaceous sandstone											
a N2,-c+d	8.6	313	9	4.5	1601	3040	0.02994 (.08)	0.2237 (.13)	0.05418 (.09)	190.2 \pm 0.3	378.6 \pm 4.0
b M2,-c+d abr	0.90	1446	32	11.4	447	3832	0.02139 (.23)	0.1716 (.24)	0.05820 (.05)	136.4 \pm 0.6	537.1 \pm 2.1
c M2,-c+d abr	0.3	252	7	4.0	86	1535	0.02824 (.13)	0.2016 (.23)	0.05178 (.17)	179.6 \pm 0.5	275.7 \pm 8.0
d M1.5,-d+e	1.30	394	13	6.1	451	2336	0.03355 (.13)	0.2990 (.18)	0.06463 (.09)	212.7 \pm 0.5	762.4 \pm 3.8
e N2,+d tips abr	0.068	266	7	3.2	11	2752	0.02723 (.13)	0.1860 (.20)	0.04953 (.14)	173.2 \pm 0.4	173.1 \pm 6.3
H89R129-7											
a N2,+a abr	0.129	146	5	9.0	31	1150	0.03121 (.07)	0.2176 (.30)	0.05057 (.27)	198.1 \pm 0.3	222 \pm 13
b N2,-a+d abr	0.115	113	4	9.6	73	390	0.03450 (.11)	0.2866 (.64)	0.06026 (.59)	218.6 \pm 0.5	613 \pm 26
c M2,+d abr	0.098	129	4	9.4	22	1100	0.03130 (.26)	0.2196 (.38)	0.05088 (.26)	198.7 \pm 1.0	235 \pm 12
d M2,-d abr	0.039	195	5	10.3	30	417	0.02565 (.16)	0.1892 (.59)	0.05351 (.54)	163.2 \pm 1.0	350 \pm 25

Notes: Analyses and interpretation by J.E. Gabites, 1989 - 1996, in the geochronology laboratory, Department of Geological Sciences, U.B.C..

1. IUGS conventional decay constants (Steiger and Jäger, 1977) are: $^{238}\text{U}\lambda=1.55125\times 10^{-10}\text{a}^{-1}$, $^{235}\text{U}\lambda=9.8485\times 10^{-10}\text{a}^{-1}$, $^{238}\text{U}/^{235}\text{U}=137.88$ atom ratio.
2. Zircon fractions are labelled according to magnetic susceptibility and size. NM = non-magnetic at given amperes on magnetic separator, M = magnetic. Side slope is given in degrees. The - indicates zircons are smaller than, + larger than the stated mesh (μ). Abr = air abraded.
3. U and Pb concentrations in mineral are corrected for blank U and Pb. Isotopic composition of Pb blank is 206:207:208:204 = 17.299:15.22:35.673:1.00, based on ongoing analyses of total procedural blanks of 37 ± 1 pg (Pb) and 6 ± 0.5 pg (U) during the time of this study. Include sample weight error of ± 0.001 mg in concentration uncertainty.
4. Total Common Pb in analysis
5. Radiogenic Pb
6. Initial common Pb is assumed to be Stacey and Kramers (1975) model Pb at the $^{207}\text{Pb}/^{206}\text{Pb}$ age for each fraction.

Size fractions are: a 149, b 134, c 104, d 74, e 44 μm . n = needles
Magnetic fractions : N2 = NM2a/1°, M2 = M2a/1°, M1.5 = M1.5a/3°

Locations: H87R19-4 - 49°23'46"N; 117°13'25"W
H87R129-7 - 49°23'25"N; 117°23'15"W

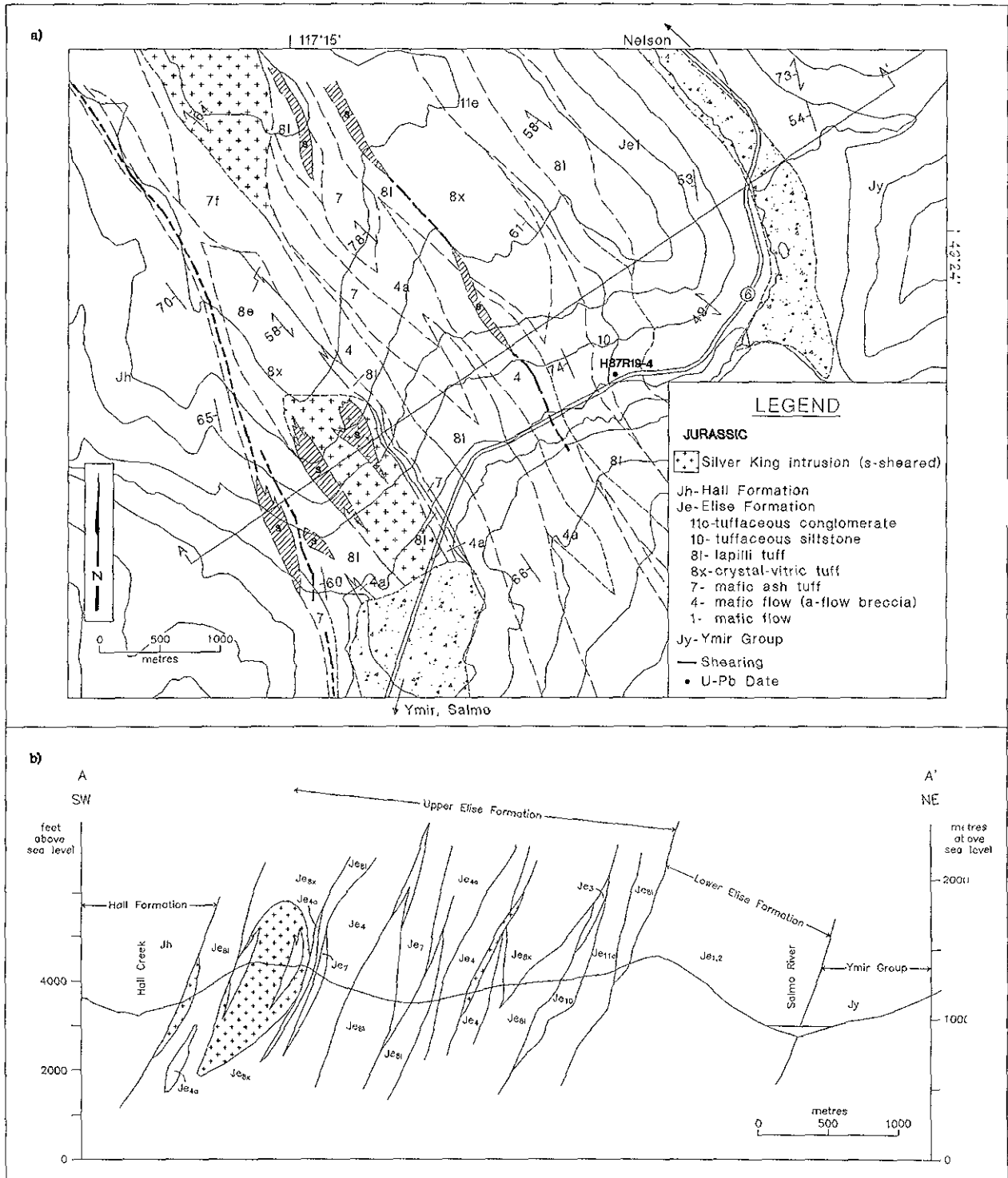


Figure 4-4. (a) Geological map of the Elise Formation, Highway 6 section, south of Nelson (from Andrew and Höy, 1988).
 (b) Vertical cross-section, Highway 6 area.

breccias (Unit Je1), minor lahars and tuffs up to 1 kilometre thick.

A coarse-grained augite porphyry flow breccia is the dominant lithology of Unit Je1 in the lower Elise. It comprises monolithic fragments in flows typically 0.5 to 1 metre thick. Such textures are indicative of fragmentation by mechanical friction or gaseous explosion during lava flow. Size, shape and abundance of clasts are highly variable. Most often, flow breccias are matrix supported with subrounded clasts ranging from 2 to 10 centimetres in diameter. The clasts are similar in composition to the matrix and hence the autoclastic nature of the unit is often difficult to see. Clasts and matrix are essentially augite porphyry, with euhedral to subhedral augite or augite pseudomorphs up to 1 cm in diameter in a finer grained matrix of secondary plagioclase, biotite, chlorite, epidote and carbonate (Plate 4-1). Microphenocrysts of titaniferous magnetite have also been identified in thin section (Beddoe-Stephens and Lambert, 1981). Due to regional greenschist facies metamorphism, the augites are largely replaced by an assemblage of actinolite, biotite, epidote and chlorite.

Massive augite porphyry flows, with little evidence of brecciation, are not common. They are dark green, simple or compound flows, typically 0.5 to 1 metre thick, and rarely pillowed. Thin mud selvages are

conspicuous between some flows (Plate 4-2). The flows are characterized by 20 to 40 percent augite phenocrysts and virtually no plagioclase phenocrysts. Way-up structures include occasional amygdaloidal pillows and flow-top breccias.

The upper Elise in the Highway 6 section is a sequence of mafic to intermediate flows, tuffs and minor epiclastic deposits up to 2500 metres thick (Figure 4-5). A number of cyclical sequences of pyroclastic rocks that typically grade upward from lapilli tuff to crystal tuff or fine tuff are common. Augite porphyry flows and flow breccias are a minor constituent.

The dominant lithology of the upper Elise in the Highway 6 section is a plagioclase-augite lapilli tuff of andesitic to shoshonitic composition (Unit Je8l). It is typified by 5 to 20 per cent subrounded cognate pyroclasts ranging from 2 millimetres to 6 centimetres in diameter. The clasts contain 10 to 20 per cent euhedral plagioclase laths (An₆₀₋₈₀), 1 to 2 mm length, and less than 5 per cent subhedral augite crystals, 2 to 5 mm in diameter. Clasts are generally darker than their matrix due to the preferential alteration of the fine-grained matrix to calcite, epidote and secondary plagioclase.

Crystal tuffs (Je8x) are commonly a lateral or vertical facies of the lapilli tuffs and are similar in

Table 4-2: Lithological Units, Elise Formation, Rossland Group

Lower Elise flow units	
Je1	augite plagioclase phyric flows, flow breccias
Lower and upper Elise (Midday Peak)	
Je2	mafic lapilli tuff, pyroclastic breccia, with augite plagioclase bearing clasts
Je3	mafic to intermediate lapilli, crystal and fine tuff, commonly well bedded, locally crossbedded (surge deposits)
Upper Elise flow units	
Je4	augite - plagioclase mafic flows, flow breccia
Je5	plagioclase - amphibole andesite flow
Je6	rhyolite, dacite
Pyroclastic units	
Je7	mafic tuff, fine tuff
Je8	andesitic lapilli tuff, minor mafic tuff
	Je8l - lapilli tuff
	Je8x - crystal-vitric tuff
Epiclastic units	
Je10	tuffaceous siltstone, sandstone
	Je10a - argillaceous siltstone
Je11	tuffaceous conglomerate
	Je11c - intermediate to felsic volcanic and intrusive clasts
	Je11b - mixed mafic to felsic clasts
	Je11a - predominantly mafic clasts

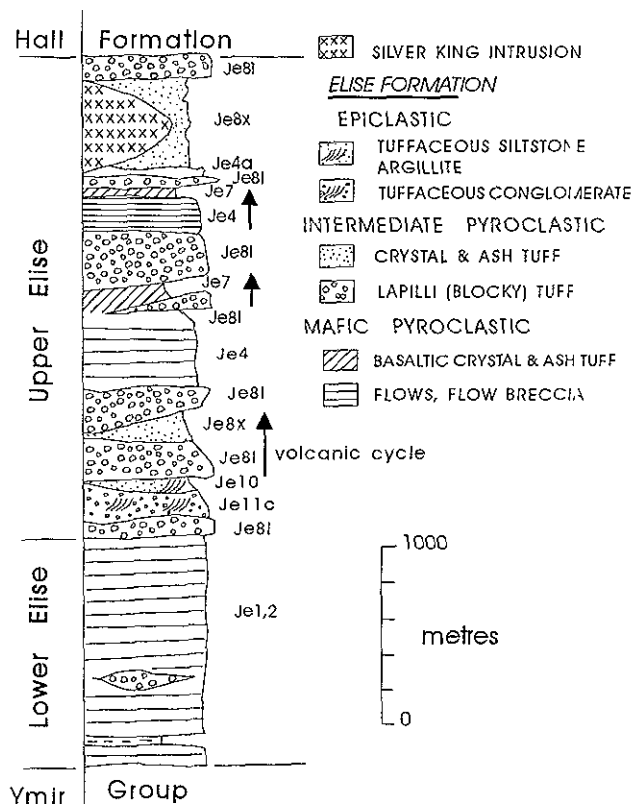


Figure 4-5. Stratigraphic section of the Elise Formation, Highway 6 section, determined from data shown in cross-section of Figure 4-4.

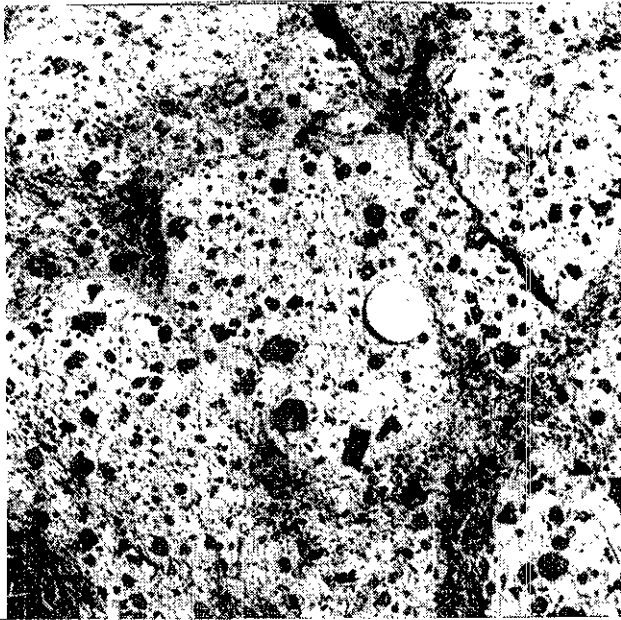


Plate 4-1: Coarse-grained augite phyric flow breccia of Unit Je1; note large augite phenocrysts in both matrix and fragments.



Plate 4-2: Massive and brecciated flows of Unit Je1, Highway 6, 2 km west of Apex Creek; note thin mud selvages between flows.

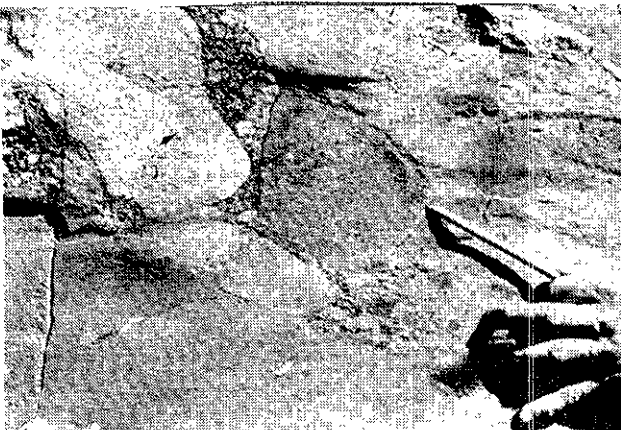


Plate 4-3: Boulder conglomerate near the base of Unit Je11.

composition. They are characterized by up to 20 per cent plagioclase and typically only a few per cent augite. Widely scattered 1 to 2 centimetre volcanic clasts of dominantly intermediate composition are common throughout. Je8x is generally massive; only rarely is layering noted. However, a penetrative foliation, conspicuous in most outcrops, may mask many primary features.

Fine mafic tuff (Je7) occurs in dark green, fine-grained layers commonly associated with augite porphyry units. Several per cent broken, commonly sausseritized plagioclase phenocrysts, less than 1 mm in diameter, and rare quartz crystals are the only primary textures preserved in the tuff. A penetrative foliation is defined by aligned biotite. In thin section, the groundmass is entirely altered, composed of epidote, secondary plagioclase and minor calcite.

Tuffaceous siltstone of Unit Je10 comprises mixed pyroclastic and epiclastic fragments with average clast size less than 1 millimetre. Pale green volcanic siltstone is interbedded with coarser tuffaceous plagioclase-rich beds that contain small lithic fragments. The siltstone is thinly bedded and finely laminated with, locally, isolated clasts within it. It contains well-defined graded beds, basal scours, crossbeds and channels. Zircons from a bulk sample of Je10 were dated in an effort to determine the minimum age of the Elise (see U-Pb dating, above).

The tuffaceous conglomerate unit (Je11), near the base of the upper Elise, comprises an interbedded sequence of conglomerate, grit, sandstone and siltstone. It underlies tuffaceous siltstone of Unit Je10 and hence forms the basal part of a thick, fining-upward succession. It comprises a series of fining-upward clastic cycles, generally a few to several tens of metres thick, that are coarser near the base of the succession and finer at the top. Hence, cycles near the base grade from coarse conglomerates (Plate 4-3) to grits whereas those at the top typically grade upward from sandstone to siltstone. As in unit Je10, crossbeds, scours and channels are common throughout the unit.

The most abundant clasts in Je11 are subrounded boulders and cobbles of feldspar porphyry; some are similar in texture and mineralogy to the Silver King intrusive porphyry suite. Other clasts include chert fragments, less commonly mafic volcanic fragments and rarely small fragments that appear to be felsic volcanics with fiamme textures. The sources of the chert and felsic volcanic(?) clasts have not been recognized within the Elise Formation.

INTERPRETATION

The absence of pyroclastic features in the basaltic lava flows at the base of the Elise Formation suggests eruption along a fissure in relatively deep-water environment. The high phenocryst content may decrease viscosity and perhaps promote auto-brecciation. Local transition to pillow lavas could reflect a decrease in discharge rates (Cas and Wright,

1987, p. 74). Lahars, locally associated with thin calcareous argillites within the basal Elise, suggest both intermittent volcanism and local steepening of seafloor resulting in debris flows.

A change from massive flows to pyroclastic deposits suggests a decrease in water depth. Subaqueous mafic pyroclastic deposits are restricted to shallow water, probably less than a few hundred metres (McBirney, 1963). Subaqueous deposition is indicated by interlayered subaqueous epiclastic deposits in the lower part of the upper Elise.

Interpretation of pyroclastic deposits in deformed belts is often difficult. Distinction between fall deposits and pyroclastic flow deposits is based largely on evidence of hot emplacement of flow deposits. This distinction is difficult to make in the Nelson area due to regional metamorphism and tectonic flattening and elongation of clasts. Despite these limitations, we suggest that a considerable portion of the upper Elise, particularly Unit Je8l, was deposited as subaerial pyroclastic flow deposits.

Unit Je8l has many features typical of a block- and ash-flow deposit, a common pyroclastic flow deposit type:

- it comprises large non-vesicular cognate lithic blocks;
- it is typically massive and unsorted with an ash matrix;
- it is monolithologic; and,
- layering is uncommon.

However, it is possible that Unit Je8l is dominantly remobilized pyroclastic debris and should therefore be described more simply as a volcanoclastic debris flow deposit.

Although pyroclastic flow deposits generally record subaerial deposition, a model for subaqueous pyroclastic flow deposition has been proposed by Fiske and Matsuda (1964). They describe depositional sequences, with coarse pyroclastic flow deposits overlain by doubly-graded turbidites and finally capped by fine ash deposited from suspension. Massive, foliated sequences of fine-grained mafic crystal tuff, with widely scattered small lithic clasts (Unit Je8x), that occur with the block- and ash-flow deposits may record repeated deposition from turbidity currents. However, they lack many features typical of turbidite deposition, and are therefore also interpreted to be dominantly pyroclastic flow deposits.

Unit Je7 is a mafic ash deposit. The pervasive alteration of the matrix suggests a vitric tuff protolith with abundant crystals throughout. Lack of highly vesiculated pumice or scoria in associated deposits and inferred subaerial to shallow marine environment suggests formation by phreatomagmatic explosions (compare Heiken, 1972 and Self and Sparks, 1978)

Epiclastic deposits record periods of erosion, transportation and deposition. Units Je10 and Je11 are fine to coarse-grained clastic rocks that were eroded from a paleohigh that may have been subaerially exposed, and included both volcanic rocks and denuded

intrusive rocks. This debris was shed southward, initially and proximally as debris flows and coarse, possibly fluvial, sedimentation in alluvial fans (Unit Je11), followed by dominantly shallow-water (?) turbidite deposits of Unit Je10.

COPPER MOUNTAIN - MOUNT CONNER AREA

The Elise Formation is exposed in the hanging wall of the Mount Verde fault in the Copper Mountain - Mount Conner area southwest of Nelson (Figure 4-1). Interpretation of the succession is complicated by lack of bedding, structures that include broad open folds and locally a penetrative foliation, and numerous small intrusive plugs and dikes with associated alteration. The succession is similar to the upper Elise, dominated by pyroclastic breccia. However, it is in contact with underlying Ymir Group to the west and may, therefore, be correlative in part with the lower Elise.

On the ridges south and east of Copper Mountain (Figure 4-1), the Elise comprises featureless, homogenous crystal tuff, with dominantly plagioclase and rare augite in a fine-grained pale green to grey, altered groundmass; locally, small clasts of feldspar porphyry are scattered throughout. Massive, poorly-sorted blocky tephra and lapilli tuff, with clasts of plagioclase porphyry, also occur here. Locally, these have a pinkish hue on fresh surfaces and weather to a grey or greenish-grey colour. A heterolithic tuffaceous conglomerate, with subrounded clasts of plagioclase porphyry, pale green siltstone, chert and minor augite porphyry, is exposed farther east. Here, the section is cut by a number of small granodiorite(?) intrusions, similar to a larger stock on Red Mountain farther east. The upper part of the section, exposed in the vicinity of Copper Mountain, comprises blocky tephra that grades upward through lapilli tuff into fine to medium-grained, graded beds, 10 to 15 centimetres thick.

On the ridge between Copper Mountain and Mount Conner, interpreted to be lower in the Elise section, volcanic breccias are interlayered with volcanic sandstones. These are assumed to be pyroclastic deposits; they are commonly altered, with pervasive epidotization or preferential epidotization of fragments, and locally skarned to a garnet-diopside-epidote assemblage. A north-trending swarm of dikes, similar in composition and mineralogy to the Silver King feldspar porphyries, cuts the ridge approximately one kilometre east of Mount Conner.

In less altered exposures, the volcanic breccias comprise dominantly closely-packed clasts of plagioclase porphyry, locally up to 1 metre in diameter, in a granular matrix. They commonly form a graded sequence with smaller clasts up-section, and are overlain by thick sequences of crystal-lithic tuff. The tuff is massive, pale grey-green, with white euhedral to subhedral plagioclase crystals set in a dark tuffaceous matrix. It superficially resembles an intrusive feldspar porphyry, but contains small lithic fragments and

broken feldspar crystals throughout. It has been dated at 197.1 ± 0.5 Ma (see U-Pb dating, page 29). Locally, accretionary lapilli are associated with a pyroclastic breccia.

Near the west end of the section in the Mount Conner area, occasional lenses of tuffaceous conglomerate with clasts of feldspar porphyry, mudstone, chert and mafic volcanic rock, are interbedded with tuffaceous siltstone. The siltstones are well-bedded, but contact metamorphism and alteration by the Mount Conner stock has obliterated many primary features. Farther down-section (?) to the west, the regional metamorphic grade increases rapidly, and biotite phyllites and schists predominate with some relict fragmental textures indicating interbedded tuffaceous conglomerate or tuff-breccia.

INTERPRETATION

The Elise in the Copper Mountain - Mount Conner area is distinct from the Elise on the east side of the Hall Creek syncline. It contains primarily pyroclastic breccia of intermediate composition and virtually no mafic volcanic component.

The monolithologic pyroclastic breccias are interpreted to be dominantly block- and ash-flow deposits. They commonly grade upward or are interlayered with thick sequences of crystal-lithic tuff. On Copper Mountain, these tuffs are overlain by well-bedded water-lain tuffaceous sandstone, possibly ash turbidite deposits, which suggests that at least part of the succession is subaqueous. However, the extensive thickness and apparent lateral continuity of the coarse volcanoclastic deposits suggests either subaerial or only shallow-water conditions.

Alternatively, these deposits may be essentially subaerial pyroclastic deposits, either air-fall or pyroclastic flow, that have been transported into water and redeposited by epiclastic processes.

Heterolithic tuffaceous conglomerates are epiclastic debris flows; they are associated with shallow-water (?) tuffaceous sandstone and siltstone and may indicate intermittent volcanism.

In summary, the Elise in the Copper Mountain - Mount Conner area is dominated by pyroclastic breccia. Shallow marine to locally subaerial conditions are inferred. The pyroclastic breccias may include both shallow-water to locally subaerial pyroclastic flow deposits and pyroclastic debris redeposited as epiclastic deposits. Due to structural complexity, an estimate of the thickness of the Elise Formation is not possible here.

CABIN PEAK AREA

A relatively complete Elise section is exposed from the ridge east of Erie Creek, across Cabin and Midday peaks to Barrett Creek (Figure 4-6). However, as in the Copper Mountain area, folds complicate the section and exposures become less abundant in the upper Elise on

the slopes of Barrett Creek. The total estimated thickness is 2000 metres (Figure 4-7a).

The base of the Elise is abrupt, placed above the last prominent argillite succession of the Archibald Formation. Hence, prominent tuffaceous conglomerates that are stratigraphically lower are included in the upper Archibald. The basal Elise comprises a succession of interlayered, on a scale of tens of metres, massive to well-bedded water-lain sandy tuffs and coarse mafic volcanic breccias. The volcanic breccias comprise clasts of mafic augite porphyry and minor augite-plagioclase porphyry in a fine to coarse crystal matrix.

The crystal-lithic tuffs are medium to dark green, commonly well-bedded, with abundant augite crystals throughout. Locally, they are graded with thin tuffaceous siltstone tops. A few massive augite porphyry flows also occur in the basal part of the Elise.

On the ridge trending northwest of Cabin peak and on the slopes to the southwest, the Elise succession generally youngs to the southeast despite a number of open syncline-anticline pairs that occur there (see cross-section, Figure 4-6). It comprises sections with beds of dominantly planar bedded to locally massive, fine to coarse-grained green augite-rich fine ash tuff, up to a few tens of metre thick, interbedded with lapilli tuff or massive flows.

A detailed measured section of a fine ash tuff sequence, located southwest of Cabin Peak, is illustrated in Figure 4-7b. Vaguely laminated beds, typically up to a metre thick, comprise augite crystals and fine-grained lithic fragments. Grading is common in some beds, and may be either normal (with coarser crystals near the base), reverse, or occasionally both reverse and normal with a coarser central part. These beds typically scour underlying thin beds of fine ash tuff and may contain small rip-up? clasts. The fine ash tuff beds are commonly in sharp contact with the crystal tuff layers. They are typically finely laminated, well-sorted, and contain low-angle cross-stratification (Plates 4-4 to 4-7).

The ash tuff-lapilli tuff successions appear to be aerially restricted or discontinuous; correlative exposures two to three kilometres due south comprise massive augite-rich flows or coarse lapilli tuff. The restricted distribution, bed forms and associated structures, and the associated volcanic facies indicate that they are dominantly surge deposits.

Interlayered lapilli tuff or pyroclastic breccia comprise augite porphyry and less abundant augite-plagioclase clasts in a dark green augite-rich crystal matrix. Massive flows are similar in mineralogy and composition. They are usually a few metres thick with sharp basal contacts; others appear to have gradational contacts with surge deposits.

The upper part of the Elise (Figure 4-7a) is exposed on the ridge east of Cabin Peak and northeast of Midday Peak. Thick accumulations of well-bedded, dominantly crystal surge deposits are interlayered with some augite and augite-plagioclase phytic flows. They are overlain

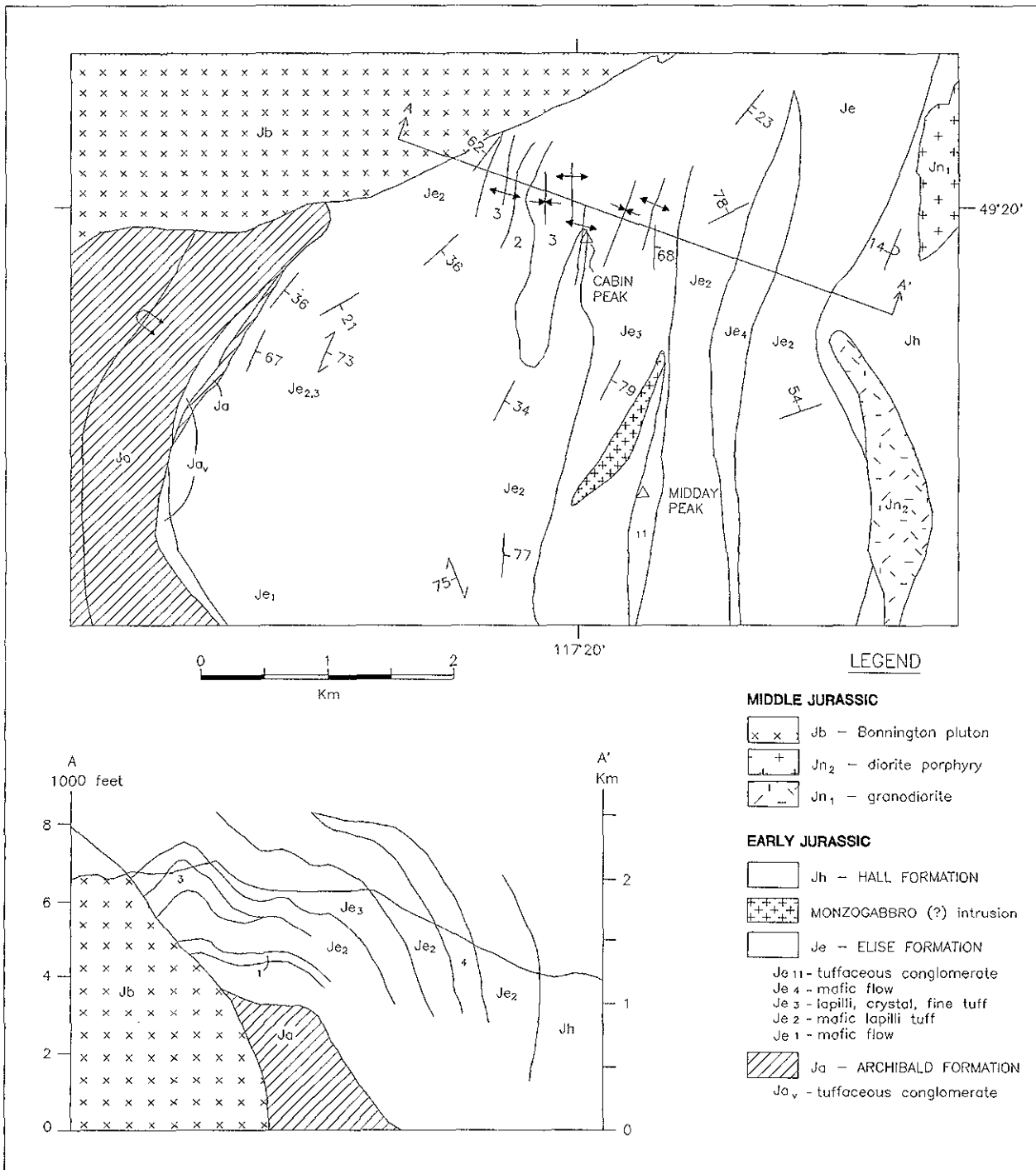


Figure 4-6. Geological map of the Cabin Peak - Midday Peak area, showing the distribution of the Elise Formation (from Höy and Andrew, 1989b).

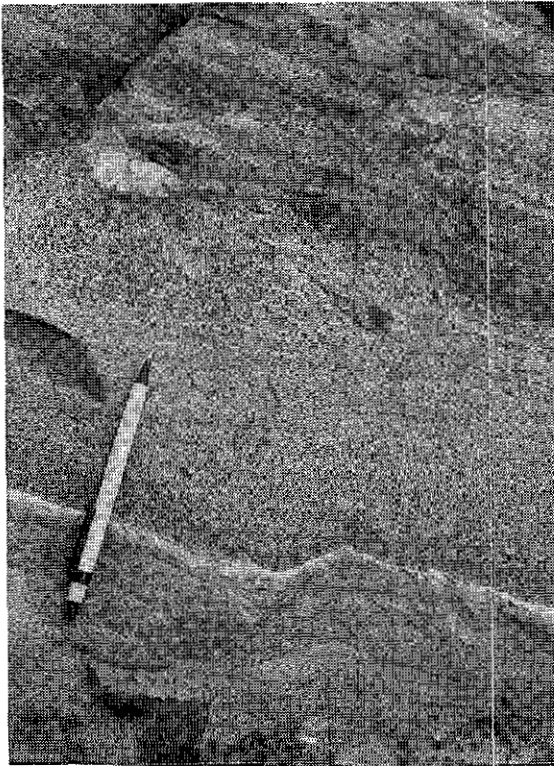


Plate 4-4: Reverse grading in a crystal tuff surge layer; note lithic fragments, laminated layers and contorted bedding; Cabin Peak section (Figure 4-7b).

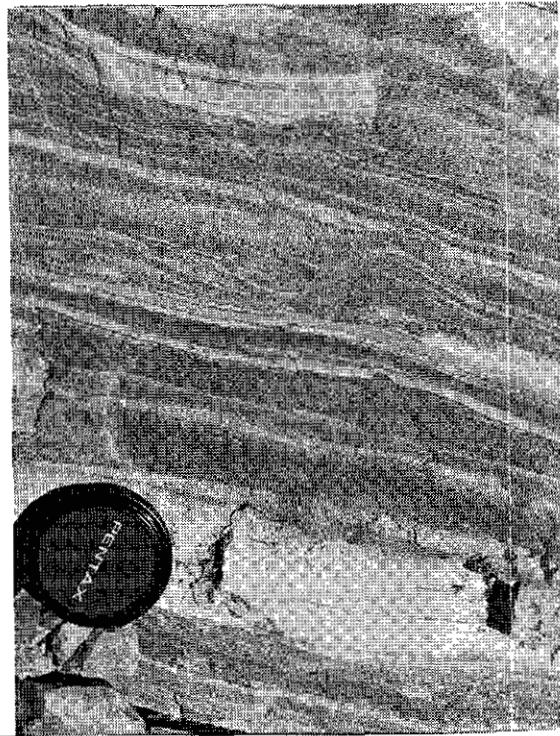


Plate 4-5: Well-bedded, mafic to intermediate lapilli, crystal and fine tuff, Cabin Peak area. Note numerous structures, including graded and laminated beds, scours, channels and crosslaminations indicative of base-surge deposition; Cabin Peak section (Figure 4-7b).

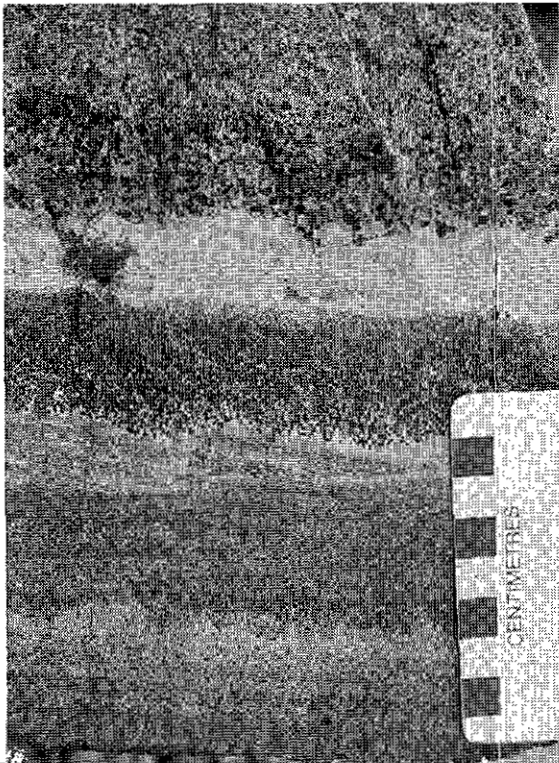


Plate 4-6: Base surge deposits, interlayered with highly contorted, possible air fall deposits; note mafic crystal content, grading, scouring and vague laminations in surge layers; Cabin Peak section (Figure 4-7b).

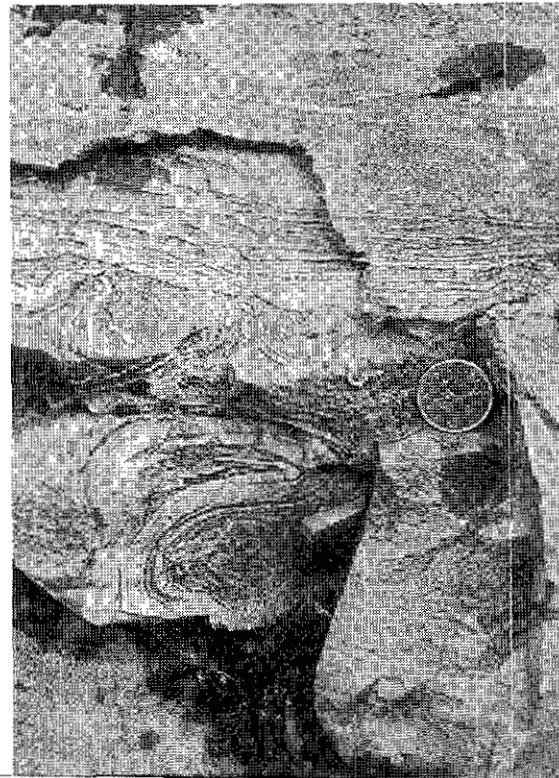


Plate 4-7: Planar bedded surge deposits with associated highly deformed, penecontemporaneous slumping of ash beds; Cabin Peak section (Figure 4-7b).

Surge deposits in the Cabin Peak area comprise beds typically up to a metre thick of vaguely bedded, laminated or crossbedded crystal and lithic tuff. They may comprise sections several tens of metres thick (Figure 4-7b) or are closely interlayered with more massive, thicker bedded, poorly sorted lapilli tuff, interpreted to be block and ash-flows. The close association of surge deposits with pyroclastic flow deposits or ash flows, suggests that they are dominantly ground surge and ash cloud deposits. Thin interlayers of fine tuff may be air-fall deposits.

Farther to the east, and presumed higher in the section, surge deposits are associated with mafic flows. Associated coarse heterolithic breccias are slump deposits suggestive of locally steep topographic gradients. Just west of Midday peak, a plagioclase-augite porphyritic intrusion, the Mammoth intrusion, cuts the layered volcanic succession (Figure 4-6). It is a monzogabbro that is interpreted to be comagmatic with the Elise Formation (Dunne and Höy, 1992).

In summary, the Elise Formation in the Cabin Peak and Midday Peak area includes a variety of generally well-layered volcanic units. Proximal (near-vent) facies in the Midday Peak area include flows, associated surge deposits, epiclastic slump deposits and a subvolcanic intrusion. To the west and lower in the succession, surge and pyroclastic flow deposits predominate, and at the base of the Elise, ash turbidites are interlayered with massive flows. To the south, these units are replaced by massive augite-phyric flows. The variety of volcanic facies, the proximal nature of many of the units, and the associated intrusion and epiclastic facies suggests eruption as a stratovolcano. Early deposits are subaqueous flows associated with ash turbidites, whereas the bulk of the volcanism, centered near Midday and Cabin Peaks, produced subaerial pyroclastic flows and surge deposits.

ERIE LAKE AREA

A composite section of the Elise Formation in the area northeast of Erie Lake is illustrated in Figure 4-8. The section is schematic due to lack of outcrop and structural complexities. However, the total estimated thickness is approximately 5100 metres (Andrew and Höy, 1991).

The basic subdivision of the Elise into a lower mafic flow succession and an upper pyroclastic-epiclastic succession is not everywhere apparent. The basal part of the succession in the Erie Lake area is characterized by rapid lateral facies changes. On the west limb of the Hall Creek syncline north of Beaver Creek, the lower Elise comprises mafic pyroclastic breccia whereas near Ymir, mafic flows predominate. The top of the formation is poorly exposed in the limbs of the Hall Creek syncline. It includes intermediate lapilli and crystal tuff in the limbs of the Hellroaring Creek syncline south of Salmo; elsewhere the top of the formation is faulted out.

In the Erie Creek area, the Elise Formation comprises dominantly mafic lapilli tuff and pyroclastic breccia as well as more intermediate crystal tuff, tuffaceous conglomerate and 500 metres of finely laminated siltstone near the base (Figure 4-8). Little (1960, 1982b) included the siltstone succession in the upper part of the Archibald Formation but it is stratigraphically underlain by several hundred metres of mafic lapilli tuff.

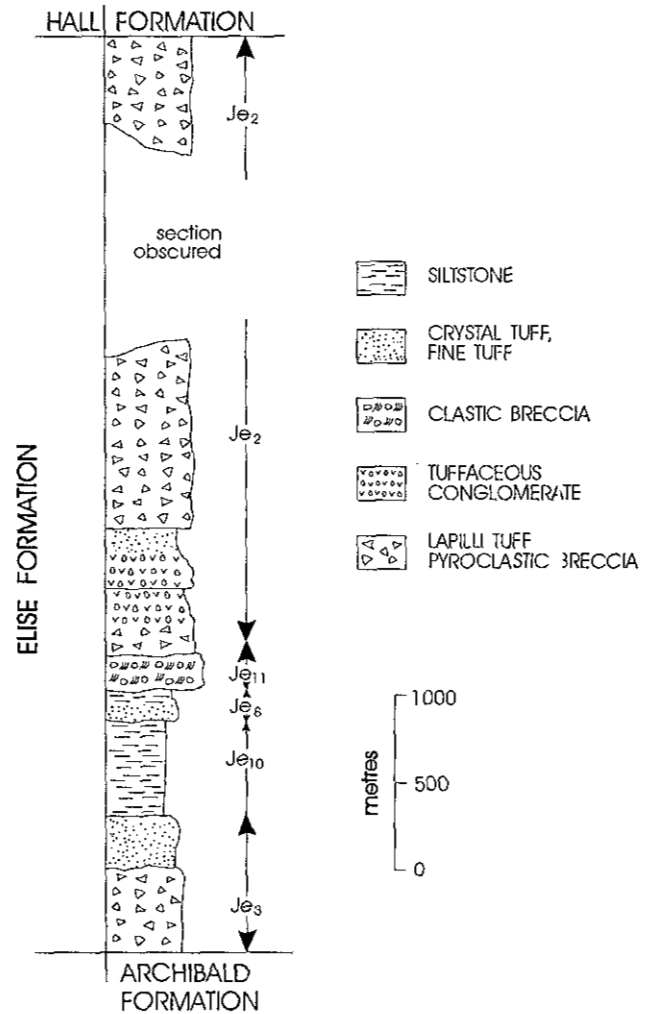


Figure 4-8. Composite stratigraphic section, Elise Formation, Erie Lake area.

MOUNT KELLY AREA

The Elise Formation in the Mount Kelly area (Figure 4-1) comprises a lower section of massive augite-phyric flows and an upper section dominated by lapilli tuff, pyroclastic breccia and epiclastic slump deposits. The lower Elise (Je1) thickens to the south, from approximately 500 metres on the ridge north of Mount Kelly to 700-800 metres, four kilometres south of Mount Kelly (Figure 4-9). The upper Elise is characterized by rapid lateral facies changes, with more mafic lapilli tuff in the north and more intermediate tuff and tuffaceous siltstone in the south. A composite Elise section, from the ridge northwest of Mount Kelly, across the peak and south to the Hall Formation contact is illustrated in Figure 4-10 and described below.

The base of the Elise section comprises a few tens of metres of pyroclastic breccia, with augite-phyric clasts up to eight centimetres across in a lapilli-crystal matrix. It is in sharp contact with interlayered siltstone and silty argillite of the underlying Archibald Formation. It is overlain by massive, locally amygdaloidal augite-phyric flows (Je1). Large pillows

are noted occasionally in the lower Elise (Plate 4-8), and thin rusty-weathering argillaceous siltstone layers (Je10) provide a few bedding attitudes.

The lower Elise is overlain by a thick section of lapilli tuff and pyroclastic breccia (Je2), with some tuffaceous siltstone and conglomerate layers. Augite-phyric clasts with variable but generally minor plagioclase content predominate. A few thin interbeds of rusty-weathering argillaceous siltstone (Je10a) and well-bedded ash turbidite(?) and layers (Je3) occur throughout the lower part of the upper Elise (Figure 4-10).

The top of the Elise section includes mafic lapilli tuff and pyroclastic breccia, numerous sections of massive to coarsely graded tuffaceous conglomerate, and some thin-bedded tuffaceous sandstone or crystal-lapilli tuff; in general, the epiclastic component increases up-section with coarse heterolithic conglomerate near the top. The conglomerate contains rounded cobbles and boulders of dominantly augite-phyric and plagioclase porphyry clasts in a calcareous grit matrix (Plate 4-9). The bedded units are mafic, with abundant augite crystals throughout, and are massive to

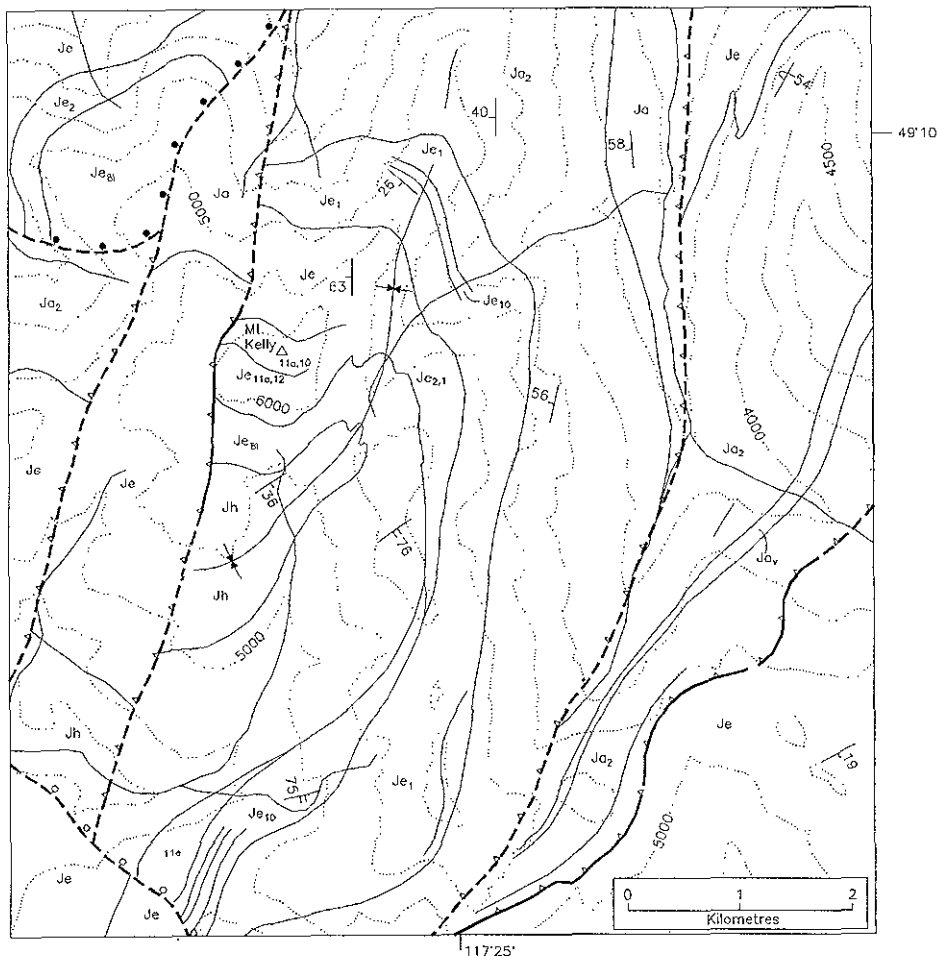


Figure 4-9. Geological map of the Mount Kelly area (from Höy and Andrew, 1990b); Ja - Archibald Formation; Je - Elise Formation; Jh - Hall Formation; for detailed legend, see Figure 4-10.



Plate 4-8: Amygdaloidal pillow basalt, Unit Jc1, Elise Formation, southeast of Mount Kelly.



Plate 4-9: Lahars, with a variety of rounded boulders and cobbles in a calcareous grit matrix, on ridge southeast of Mount Kelly.

well-bedded. Locally, they are graded with small lithic fragments at the base and tuffaceous siltstone at the top. Some beds contain rare large augite-rich clasts. The contact with overlying argillite of the Hall Formation was not observed.

The mafic flows at the base of the Elise thicken to the south to just north of Tillicum Creek. However, they thin rapidly farther south and are represented by a thin sequence of amygdaloidal flows. This has been interpreted as a normal stratigraphic thinning or pinch-out, possibly against a local high in the underlying Archibald Formation (Höy and Andrew, 1990b); alternatively, an unrecognized fault may cut out part of the lower Elise section.

The overlying mafic pyroclastic breccias and lapilli tuffs (Je2) die out to the south. They are replaced by a prominent succession of interbedded rusty-weathering argillaceous siltstone and tuffaceous conglomerate (units Je10a, Je11a; Figure 4-9) that overlies a thin succession of flows.

Coarse lapilli tuff and pyroclastic breccia (Unit Je8l), exposed near the fire lookout on the peak southeast of Mount Kelly, thicken rapidly to the south.

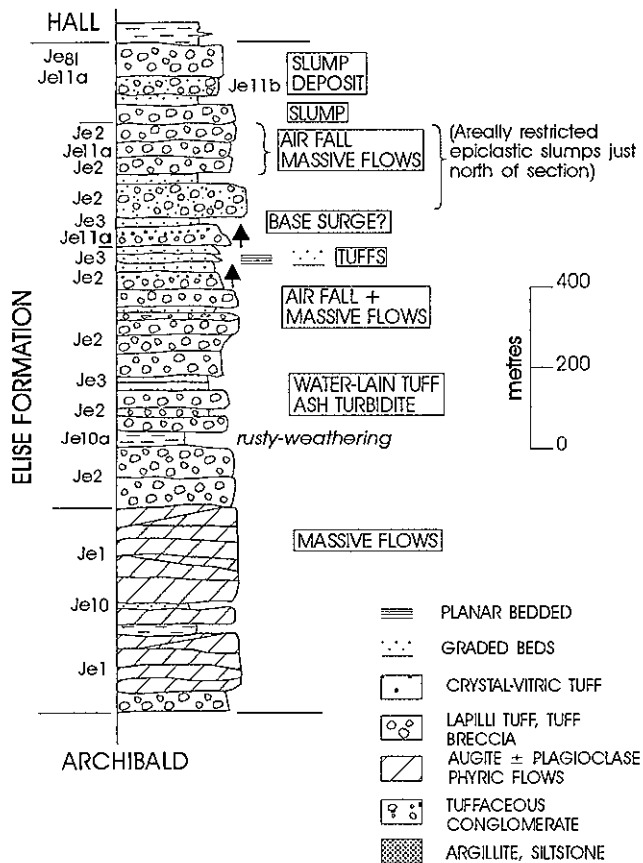


Figure 4-10. Stratigraphic section of the Elise Formation, Mount Kelly area.

The clast size decreases, with lapilli tuff exposed on the ridge to the south, and minor fine to coarse lapilli tuff in the headwaters of Tillicum Creek. Occasional coarse heterolithic tuffaceous conglomerates may be slump debris.

INTERPRETATION: MOUNT KELLY AND ERIE LAKE SECTIONS

The Elise in the Mount Kelly and Erie Lake areas is somewhat similar to the Highway 6 section, with initial effusive mafic volcanism followed by explosive mafic to intermediate volcanism, possibly reflecting a change from deeper to shallow water (and possibly subaerial) conditions.

Coarse lapilli tuff and pyroclastic breccia, in large part fall deposits, intermixed with slump debris and locally bedded crystal tuffs, suggest near-vent environment of a stratovolcano close to Mount Kelly. Interpretation of the bedded tuff units is difficult; it is possible that they are ash turbidites as they are underlain locally by subaqueous pillow basalt.

The thick sequence of heterolithic volcanic breccias to the south include both pyroclastic and epiclastic debris. These are deposited on the flanks of the stratovolcano, as pyroclastic fall (and flow) and volcanoclastic mass-flow deposits. Paleocurrent measurements suggest deposition on a northeast facing slope (Mount Kelly member, Fitzpatrick, 1985). Farther south, contemporaneous epiclastic sediments predominate; they comprise coarse immature detritus interlayered with marine tuffaceous siltstones.

In summary, the Mount Kelly area profiles a longitudinal section through a stratovolcano, with near-vent facies in the north, flank facies farther south and mixed flank facies and an epiclastic apron in the south near Tillicum Creek.

FRUITVALE AREA

In this area, the broad subdivision of the Elise Formation into a lower succession of mafic flows and an upper succession of intermediate to mafic pyroclastic and epiclastic rocks is only locally applicable near the Fruitvale area (Andrew *et al.*, 1990a). Elsewhere, rapid facies changes, or possibly difficulty in correlation across fault blocks, complicate the division into lower and upper members.

Figure 4-11 illustrates a number of Elise sections in the area. Near Barclay Creek, southeast of Fruitvale, the formation can be separated into a lower section of augite porphyry flows and flow breccias approximately 950 metres thick, overlain by 1800 metres of upper Elise, comprising heterolithic tuffaceous conglomerate, a siltstone interval, interbedded mafic lapilli and crystal tuff, and capped by coarse mafic lapilli tuff or blocky tuff.

Near Grif Creek north of Fruitvale, the distinction between a lower and upper Elise is not as evident. The total exposed thickness here is approximately 1400

metres. It comprises dominantly mafic pyroclastic breccia overlain by tuffaceous conglomerate and clastic breccia containing several percent angular siltstone and volcanic clasts (Figure 4-11b). A thin siltstone interval within the section contains Sinemurian ammonites (*Arniotites*; localities F7 and F8; Little, 1982b). In contrast, the Elise Formation in the Park Siding section, 2-3 kilometres to the northeast, is characterized by at least 2750 metres of mafic pyroclastic and effusive rocks interbedded with a thick succession of siltstone (Figure 4-11c). The correlation between the two sections is based on extrapolating the prominent siltstone interval across Marsh Creek (Andrew *et al.*, 1990b).

In the Champion Lakes area, exposures of the Elise Formation are flat-lying to gently folded and comprise flows, flow breccias and clastic breccias that overlie a succession of thinly bedded and finely laminated siltstone of unknown thickness. It is possible that this

siltstone-flow breccia succession correlates with the lithologically similar succession in the Park Siding section, as shown in Figure 4-11. Alternatively, the siltstone succession in the Champion Lakes area may be the upper part of the Archibald Formation, overlain by characteristic mafic flows of the lower Elise (Andrew *et al.*, 1990b).

Lower Elise exposed on Highway 3a just west of Montrose comprises a thick succession of debris flows with prominent clasts of the underlying Mount Roberts Formation, possible eroded Archibald Formation clasts, a variety of plagioclase porphyry clasts, and smaller but common augite-phyric flow clasts (Plate 4-10). These grade northeast into coarse lapilli tuff and tuff breccia with clasts of plagioclase-amphibole porphyry. Farther northeast, this section appears to correlate with the Grif Creek section, dominated in its base by mafic pyroclastic breccia and tuffaceous conglomerate.

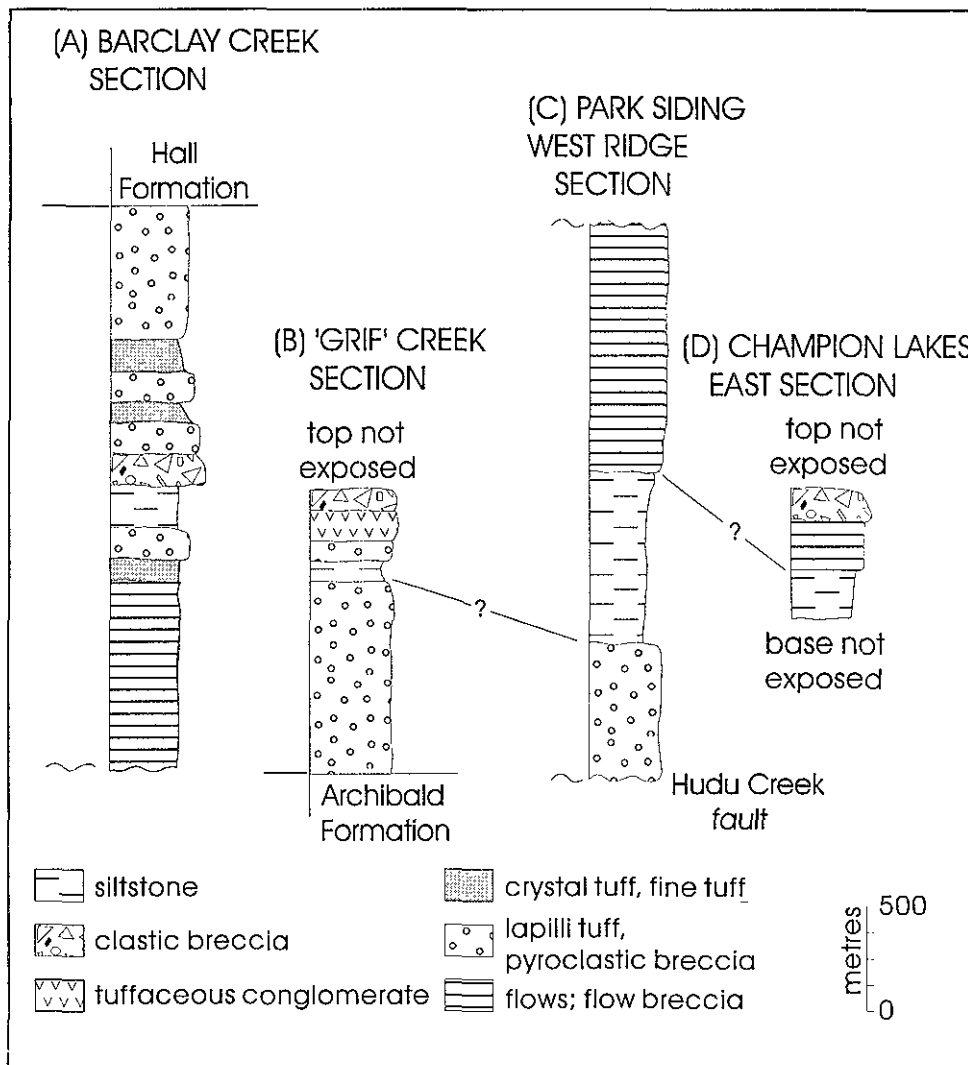


Figure 4-11. Stratigraphic sections of the Elise Formation in the Beaver Creek - Champion Lakes area.



Plate 4-10: Coarse, fragmental debris flows of the Elise Formation along Highway 3 just west of Montrose. A variety of fragments include augite porphyry of the Elise, metasediments and limestone of the Mount Roberts Formation, and feldspar porphyries.

INTERPRETATION

Limited exposures, separated by a number of late normal faults, make it difficult to correlate Elise sections throughout the Fruitvale area and, hence, to construct composite stratigraphic sections. However, it is probable that growth faulting, initiated during deposition of the Archibald Formation, continued in the early Elise. Debris flows in the Highway 3a section just west of Montrose, with clasts of Mount Roberts Formation limestone and siltstone and lower Elise augite porphyry, derived from mafic flows, indicates proximity to an uplifted fault block or tectonic high to the west.

Elsewhere, the lower Elise is more typical with effusive flows (Barclay Creek and Champion Lakes sections) or pyroclastic breccias (Grif Creek and Park Siding). The contrast in these lower Elise sections may be due to water depth, with shallow water conditions prevalent in the area bounded by the Marsh Creek and Beaver Creek faults and deeper water conditions resulting in lava flows to the north and south. This implies that these late faults may be the loci of early structures.

Upper Elise rocks, exposed southeast of Beaver Falls (section A, Figure 4-11), comprise subaqueous debris flows, thin-bedded marine siltstones and overlying mafic pyroclastic breccias. These may record evolution from marine conditions in the distal epiclastic apron of volcanism centered to the northeast near Mount Kelly or to the west in the Rosslund area, to subaerial, more proximal flank deposits with increased growth and elevation of a stratovolcano.

ROSSLAND AREA

The Elise Formation in the Rosslund map area comprises essentially a homoclinal succession that dips north to northwesterly and extends from Patterson in the south to Rosslund in the north (Figure 4-12). Although this succession is offset by numerous north-trending faults, it does not appear to be repeated by thrust faulting (Höy and Andrew, 1991a,b). It is not a complete succession as it is developed on tectonic high, recognized by prominent facies and lithologic changes in the underlying Archibald Formation. To the east, in the Goodeve and Sheppard Creek areas (Figure 4-12), the Elise thickens, due in part to thickening of some units and introduction of others into the succession, but mainly due to inclusion of a more complete lower section.

A composite section of the Elise Formation in the Rosslund area is illustrated in Figure 4-13. It extends from the Archibald Formation at Patterson northward to the Rosslund monzonite.

Tuffaceous conglomerate (Unit Jellie) at the base is in gradational contact with conglomerates of the underlying Archibald Formation. The Archibald-Elise contact is placed where either volcanic clasts are first noticed or the matrix becomes tuffaceous. The tuffaceous conglomerates are dominated by clasts of underlying Mount Roberts Formation, including prominent limestone clasts, in a green tuffaceous matrix. Rare augite porphyry and andesite clasts are also noted. The distribution of the basal tuffaceous conglomerate approximately follows that of the underlying Archibald and Mount Roberts formations

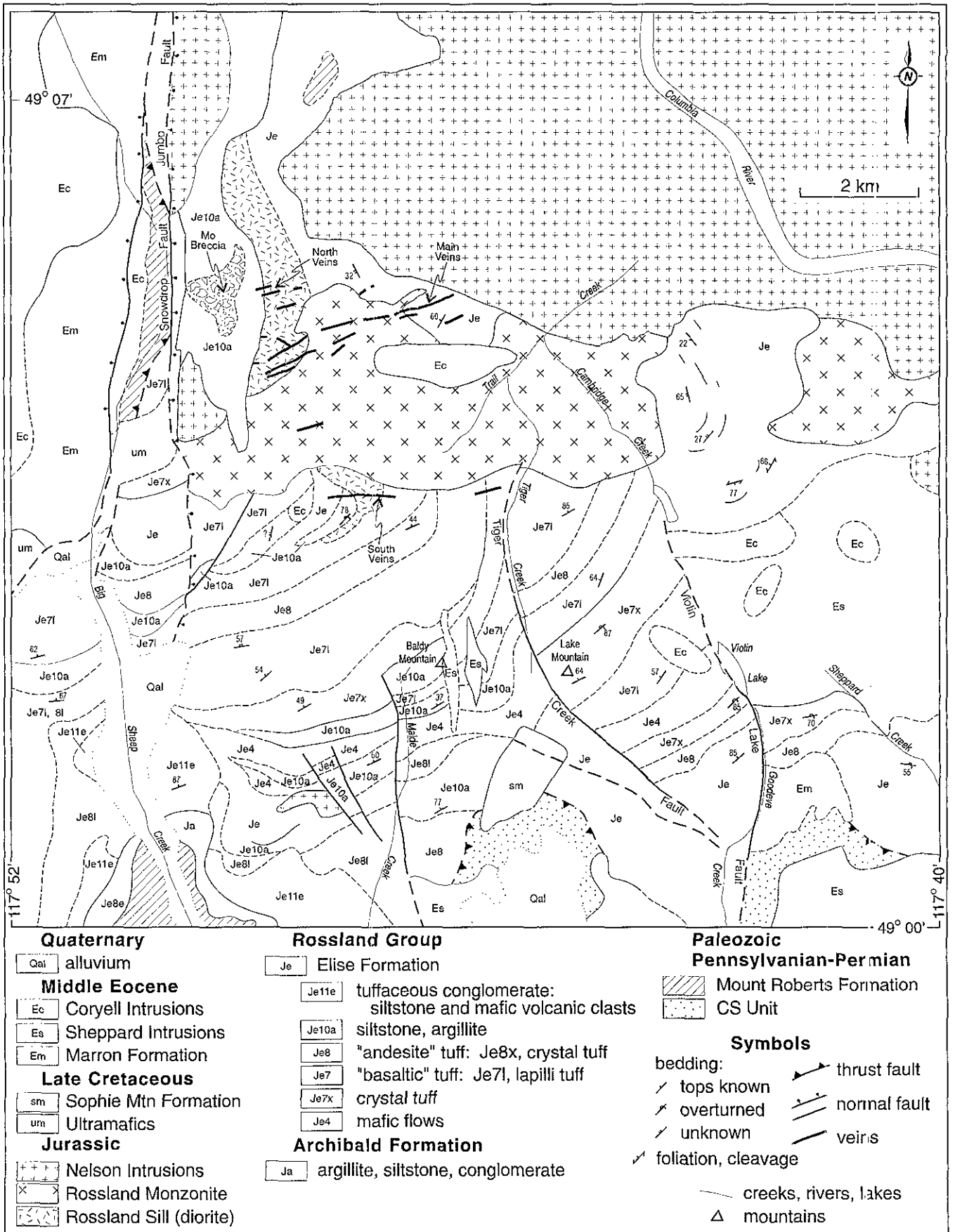


Figure 4-12. Geological map of the Rossland Area, Rossland-Trail map-sheet (82F/4); (after Höy and Andrew, 1991b; Fyles, 1984; Little, 1982b and Drysdale, 1915).

whereas overlying Elise units thin dramatically as they approach the Patterson paleohigh.

Plagioclase-porphphy lapilli tuff (unit Je81) locally overlies the tuffaceous conglomerate. It thickens rapidly just east of Malde Creek. Farther east in the Sheppard Creek area, it is underlain by mafic lapilli tuff and the base of the Elise is not exposed. A sequence of argillaceous siltstone (Unit Je10a) and mafic flows and flow breccias (Unit Je4) overlies the tuffaceous conglomerate. The mafic flows comprise massive augite porphyry, flow breccias and possible minor lapilli tuff; it is the only significant mafic flow succession in the Rosslund area. It appears to pinch out to the west, but can be traced or extrapolated eastward to the Tiger Creek fault. A similar succession of mafic flows east of Tiger Creek may be a faulted repetition of this unit (Figure 4-12). The interbedded siltstones are thin-bedded, typically rusty weathering distal turbidites. Numerous sedimentary structures, including rip-ups, graded beds and load casts provide reliable top indicators. This sedimentary succession also thins westward, and increases in thickness to the east. Just west of the Tiger Creek fault a sequence of mafic lapilli tuffs are interbedded with the upper part of the siltstone succession (Figure 4-12).

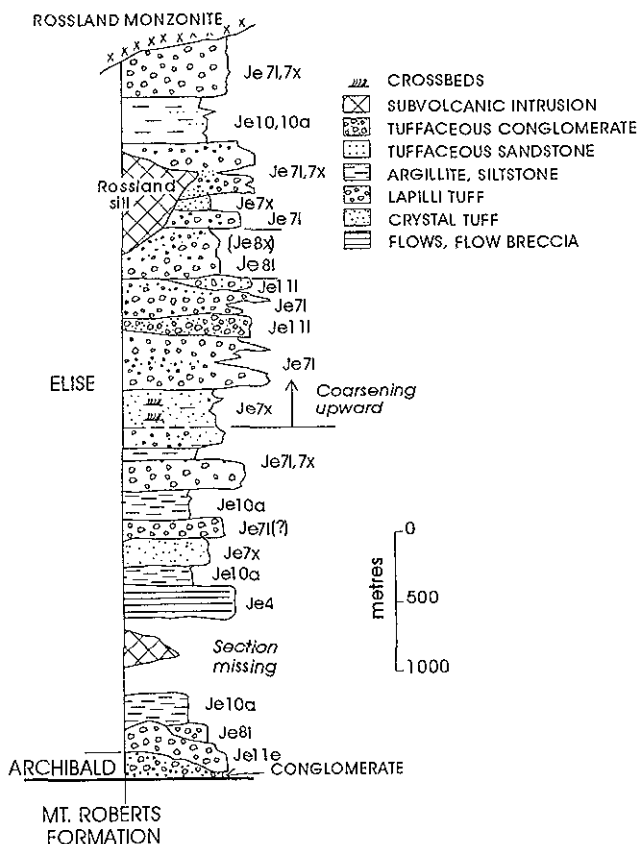


Figure 4-13. Composite stratigraphic section of the Elise Formation, Rosslund map area.

A distinctive succession of dominantly fine mafic tuff beds (Unit Je7x) extends from the western slopes of Tamarac Mountain to the north slopes of Baldy Mountain and in the Lake Mountain and Gooie Creek areas. The succession coarsens upward to interlayered mafic lapilli and crystal tuff and is supplanted to the east by dominantly mafic lapilli tuff (Unit Je71). Unit Je7x is an interbedded succession of brown-weathering, massive to well-bedded mafic argite crystal tuffs, fine lapilli tuffs, and minor coarse lapilli tuff and, at the base, minor argillite and silty argillite. The crystal tuffs commonly contain small, widely scattered augite porphyry lapilli and numerous plagioclase and augite crystals. They are typically well bedded, locally scour underlying units, and include convoluted beds and occasional small rip-up? casts. Minor rusty-weathering silty argillite and argillite occurs near the base of the succession and coarser lapilli tuff layers become more prominent near the top as Unit Je7x grades into Je71.

Unit Je71 (Figure 4-12) is a thick accumulation of dominantly mafic lapilli tuff, but includes pyroclastic breccia and well-bedded mafic crystal tuffs. Clasts in the tuffs are dominantly augite porphyry; however, a variety of other clasts are noted in some layers, including limestone, plagioclase porphyry and green 'siltite' clasts (Plates 4-11, 4-12). A prominent more felsic lapilli tuff (Unit Je8) is recognized within Unit Je71 both east and west of the Tiger Creek fault. It contains fragments of both plagioclase porphyry and augite porphyry. Some plagioclase-rich crystal tuffs are also included in Unit Je8x.

Interbedded argillaceous siltstone and tuffaceous sandstone (units Je10, 10a) occur near the top of the exposed Elise succession, just south of the Rosslund monzonite. These host a number of vein deposits of the South Belt of the Rosslund camp. This siltstone succession may correlate with very rusty weathering siltstone and argillite on the west slopes of Red Mountain that host the Red Mountain molybdenite breccia complex. These latter sediments have been correlated previously with the Mount Roberts Formation (Little, 1960; 1982; Höy and Andrew, 1991a) but, based on gradational contacts with underlying mafic tuffs exposed in drill core on the Gertrude property, are now included in the Elise Formation, as mapped by Fyles (1984).

The top of the Elise is not exposed. On the east slopes of Red Mountain, it is intruded by the Rosslund sill, a porphyritic to inequigranular monzogabbro that hosts a number of the principal orebodies of the Rosslund camp (Fyles, 1984).

In summary, the Elise Formation south of Rosslund comprises dominantly mafic to intermediate lapilli tuffs interlayered with prominent sections of thinner bedded mafic crystal and fine lapilli tuffs. Tuffaceous siltstone and argillaceous siltstone occur locally throughout the succession. Mafic flows are subordinate and tuffaceous conglomerates are essentially restricted to the basal part of the succession. The succession thins to the southwest,

towards exposures of underlying Mount Roberts Formation near Patterson, and is underlain to the east by a thick sequence of lapilli tuffs and augite phyric flows that correlate with lower Elise rocks near Mount Kelly to the east. It is possible that it thins dramatically to the north, where only Mount Roberts Formation and younger intrusive rocks are exposed.

INTERPRETATION

Tuffaceous conglomerates at the base of the Elise Formation in the Rossland-Trail area record deposition on a structural high that is exposed in the Patterson area and on the eastern slopes of Mount Roberts. Virtually the entire basal succession of the Rossland Group, the Archibald Formation, and a considerable part of the lower Elise is missing. Despite this, the Elise in the Rossland area represents one of the thickest successions recognized, in excess of 5000 metres.

Subsidence is indicated in overlying Elise rocks as the coarse conglomeratic facies give way to subaqueous mafic lava flows interbedded with siltstones and silty argillites. These sedimentary units, interpreted to be mainly low energy turbidites, thicken to the east towards a deepening basin.

Layered mafic tuff units of Je7x, with basal scours and convoluted beds, are similar to surge deposits described in the Cabin Peak area. Near the top of the succession, they are interbedded with dominantly mafic lapilli tuffs, interpreted to be largely pyroclastic flow

deposits. These units record deposition in subaerial to possibly very shallow water conditions.

The top of the exposed Elise Formation in the Rossland area comprises argillaceous siltstone and tuffaceous sandstone, indicative of subaqueous environments, overlain by mafic crystal and lapilli tuff. However, water depths are not known and it is possible that they are very shallow water deposits.

In summary, the anomalous thickness of Elise rocks, the dominance of mafic pyroclastic facies, and the association with mafic comagmatic intrusions suggest that the Rossland-Trail area is near a volcanic center. Rapid thinning of units to the west and absence or only minor development of underlying Mount Roberts Formation suggest this volcanism initiated on a tectonic high. However, subaqueous siltstones and argillites that typically occur immediately following coarse pyroclastic deposition, suggest regional subsidence accompanied this explosive volcanism.

ELISE FORMATION - DEPOSITIONAL ENVIRONMENT SUMMARY

Schematic sections of the Elise Formation, from the Highway 6 section south of Nelson, through the Cabin Peak, Erie-Stewart Creek and Mount Kelly areas to the Rossland area, are illustrated in Figure 4-14. The thickness of the Elise varies considerably, from greater than 5000 metres in an incomplete section south of

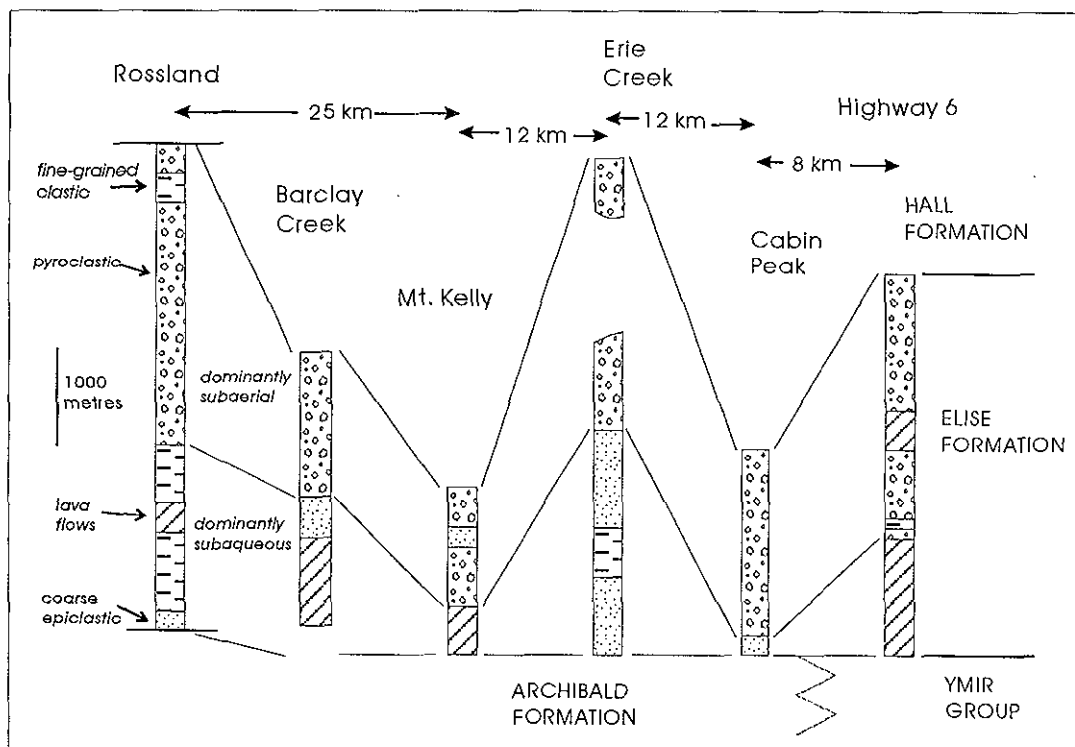


Figure 4-14. Composite stratigraphic sections of the Elise Formation, Nelson-Trail area.

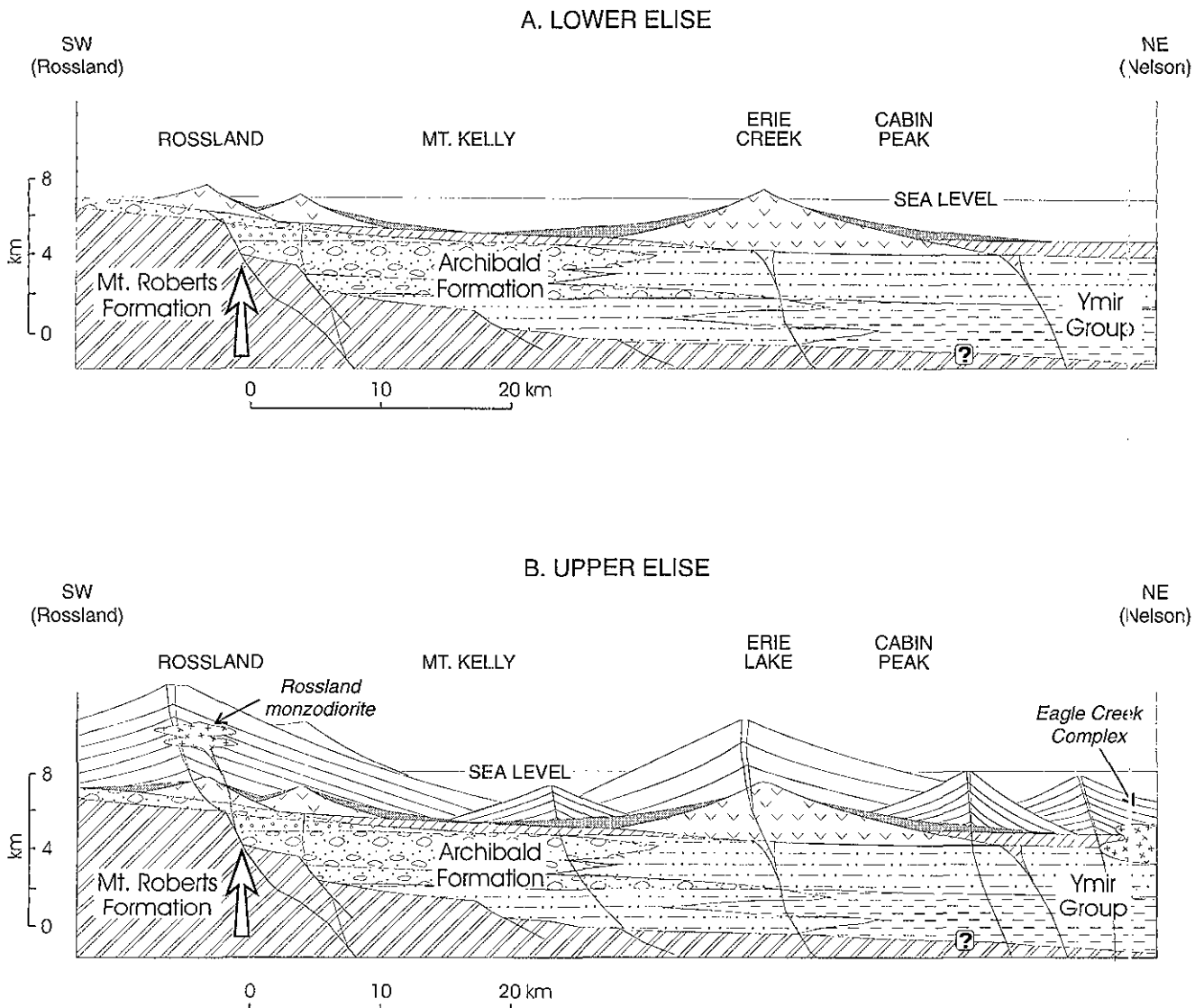


Figure 4-15: Schematic model for evolution of the Elise Formation.

Rosslund to approximately 1800 metres in the Mount Kelly area. It is difficult to correlate individual units suggesting that there are a number of discrete volcanic centers. However, in all areas, subaqueous lava flows, debris flows or turbidites are overlain by dominantly subaerial pyroclastic and associated coarse epiclastic deposits.

A model for deposition of the Elise Formation is shown in Figure 4-15. Initially, effusive basic lava flows dominate in the Nelson area along the eastern margin of exposed Elise volcanism, and in the Mount Kelly area east of Rosslund (Figure 4-15a). The extent of this subaqueous volcanism south of Rosslund is not known. Coarse debris flows with large blocks of augite porphyry as well as debris from underlying Mount Roberts Formation, exposed along Highway 3a just west of Montrose, suggests that at least some lower Elise flows were deposited farther west and subsequently slumped eastward into a structural basin.

North of Erie Lake, a thicker section, rapid facies changes and abundant coarse mafic pyroclastic and epiclastic deposits (Andrew and Höy, 1991), indicate contemporaneous explosive volcanism and slumping, characteristics of deposits on the flanks of a stratovolcano that may have risen several kilometres above its base (Figure 4-15a). The abundance of subaqueous epiclastic deposits, including tuffaceous siltstone turbidites and debris flows, as well as the documented submarine volcanism to the north and west, suggest that the early Erie Lake area stratovolcano was dominantly marine. However, it is possible that much of this subaqueous debris originated in the subaerial or possibly shallow marine parts of the volcano.

Overlying Elise volcanic rocks throughout the entire area are dominated by mafic to intermediate pyroclastic rocks, coarse debris flows, minor lava flows

and, only locally, marine ash turbidites and waterlain sandstone and siltstone. Rapid facies changes, both vertical and lateral, major thickness changes, the abundance of subaerial pyroclastic flow deposits associated with surge deposits, coarse debris facies indicative of high relief, air-fall deposits and minor lava flows are typical of deposits associated with stratovolcanoes. These volcanoes are centered in two areas: the Rosslund area and the Erie-Stewart Creek area (Figure 4-15b). Surge, pyroclastic flow deposits and intrusion of a small mafic plug, the Mammoth intrusion, in the Cabin Peak area indicate a third, smaller volcanic center. Facies and thickness changes in the Mount Kelly area also suggest deposition on the flanks of a stratovolcano with possible proximal volcanoclastic facies in the north, medial flank facies farther south and distal volcanoclastic facies in an epiclastic apron in the Tillicum Creek area. Considering the proximity, large volume and relief of the volcanic complex in the Erie Lake area to the northeast, it is likely that a considerable portion of Elise deposits northeast of Mount Kelly are derived from this northern source.

The Rosslund area has the thickest preserved accumulation of Elise volcanic rocks, also interpreted to have been deposited largely on the flanks of a stratovolcano. Coarse pyroclastic volcanism was typically followed by relative subsidence and quiescence with deposition of subaqueous, but possibly very shallow water tuffaceous siltstones and sandstones. This implies that relative subsidence in western exposures of the Elise Formation was greater than that farther east, possibly due to the large volume of extruded volcanic material and accommodated by reactivation of older growth faults.

ELISE FORMATION: GEOCHEMISTRY

INTRODUCTION

The petrology and geochemistry of the Elise Formation has been studied by Beddoe-Stephens (1977) and Beddoe-Stephens and Lambert (1981). This work suggested that the Elise Formation volcanic rocks are of island arc affinity and that the Rossland Group accumulated in a back-arc sedimentary basin, with a volcanic arc to the west. The source of Rossland Group volcanic rocks was ascribed to the upper mantle with olivine fractionation occurring at crustal levels (Beddoe-Stephens, 1977). Beddoe-Stephens (*op. cit.*, p. 147) suggested that the Elise Formation has similarities with rare shoshonitic or alkalic rocks of young island arcs. He proposed that the conflict between calcalkaline Rossland Group rocks and the apparent island arc stratigraphy and mineralogy of the group could be explained by source heterogeneity of the magmas. He also noted that secondary mineral assemblages and chemistry indicated progressive regional metamorphism varying from prehnite-pumpellyite through greenschist to locally epidote-amphibolite, supported by more recent work by Powell and Ghent (1966). However, at the time of Beddoe-Stephens' work, the internal stratigraphy and facies changes of the Elise Formation were not known, limiting the interpretation of the geochemical data.

Chemical analyses in this study (Appendices 1 and 2) have been used to evaluate magmatic processes, classify rock types, and establish tectonic environments. Interpretations are aided by a clearer understanding of the internal stratigraphy of the Elise Formation, and a better knowledge of the tectonic setting of Mesozoic arc rocks in the Canadian Cordillera.

MAJOR ELEMENT DATA

Major and trace element variation diagrams are often used to test for magmatic processes such as fractional crystallization and to determine the degree of alteration by metasomatic or other secondary processes.

The most common and widely used variation diagrams are Harker diagrams (Harker, 1909) that plot percentages of elements against an index of differentiation, such as SiO_2 or, in basic volcanic suites, MgO or Zr . Suites of rocks related by fractional crystallization processes and unmodified by extensive crustal contamination define coherent linear trends on these diagrams, with inflections marking beginning of crystallization of phenocrysts.

A series of Harker variation diagrams with SiO_2 as the abscissa (Figures 4-16a,b,c) indicate that the Elise volcanic rocks may be related by fractional crystallization of olivine, clinopyroxene, plagioclase and possibly apatite. However, caution must be used in interpretation of these diagrams. Although inflection points on these diagrams can be attributed to the commencement of crystallization of phenocrysts, new

models for fluid processes in magma chambers (Sparkles *et al.*, 1984; Turner and Campbell, 1986; Wilson, 1989) suggest that these phenocrysts may represent crystals generated from a variety of processes including fractional crystallization, magma mixing or partial melting. Scatter on the diagrams can also be due to alteration by metamorphism, metasomatism and/or weathering; crystal or phenocryst accumulation obscuring partial melting trends or high pressure crystal fractionation trends; and/or sampling of more than one cogenetic suite.

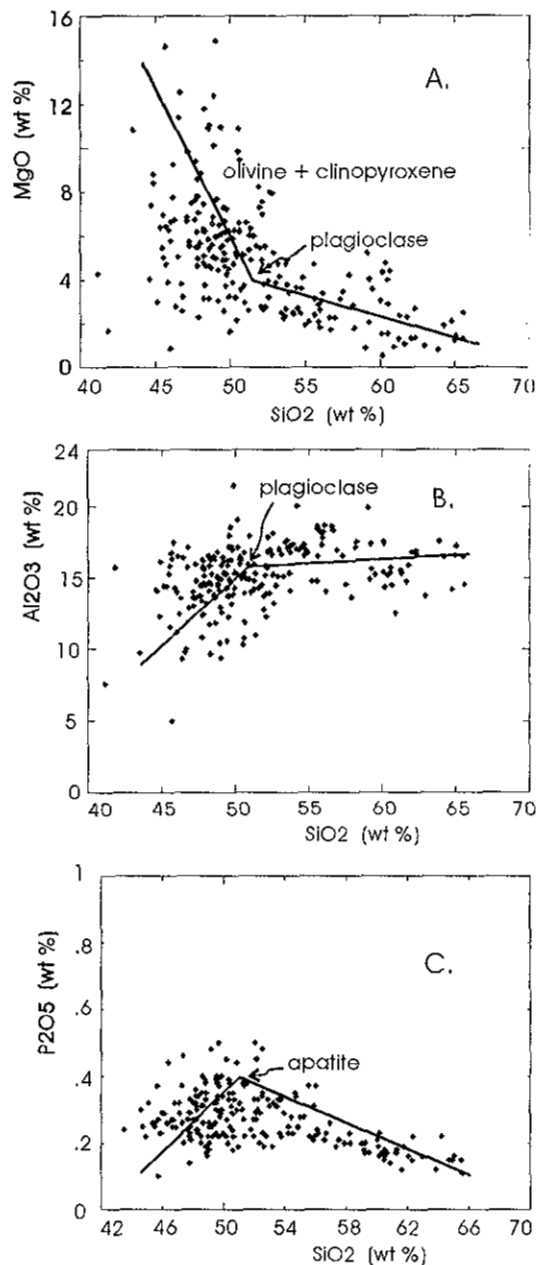


Figure 4-16. Plots of (a) SiO_2 versus MgO , (b) SiO_2 versus Al_2O_3 and (c) SiO_2 versus P_2O_5 , Elise Formation, Rossland Group (after Harker, 1909).

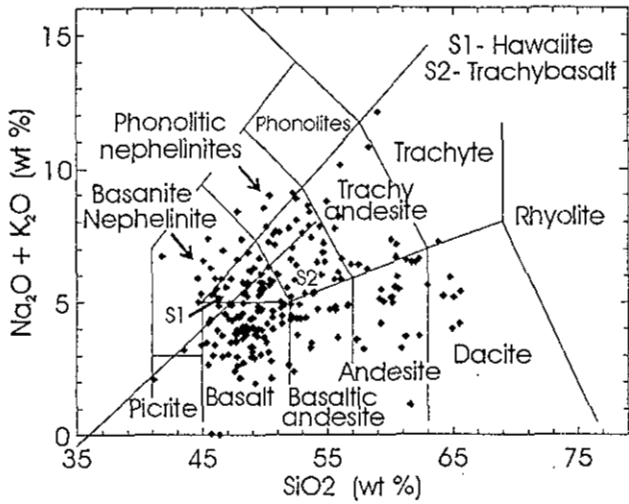


Figure 4-17. A plot of $\text{Na}_2\text{O} + \text{K}_2\text{O}$ versus SiO_2 , Elise Formation (after Cox et al. 1979).

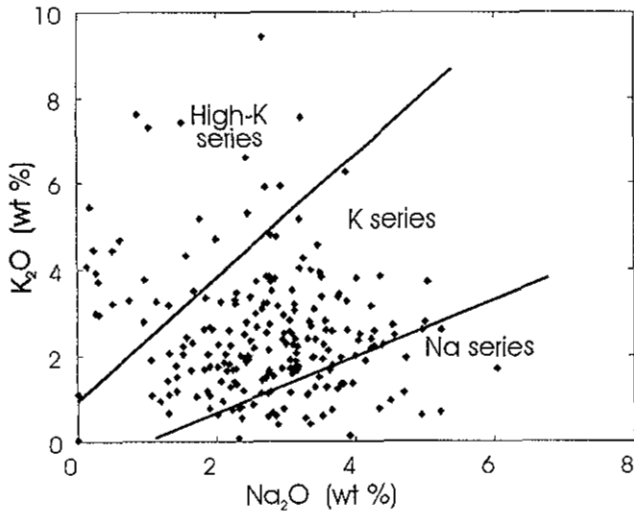


Figure 4-18. A plot of K_2O versus Na_2O , Elise Formation, (after Middlemost, 1975).

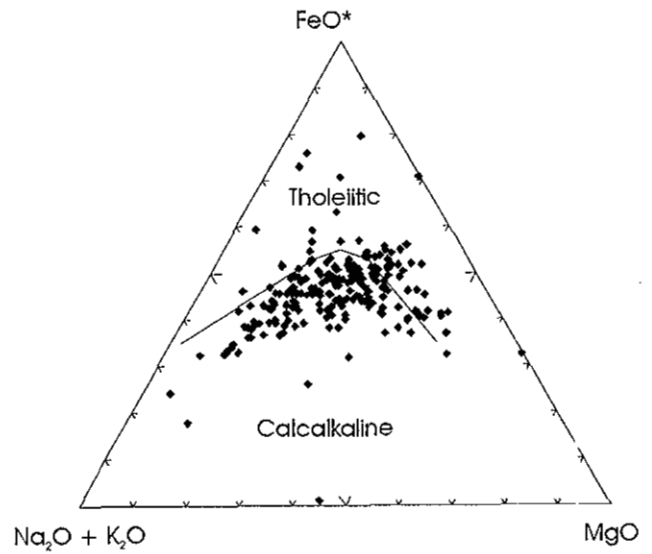


Figure 4-19. An AFM plot, Elise Formation, (after Irving and Barager, 1971).

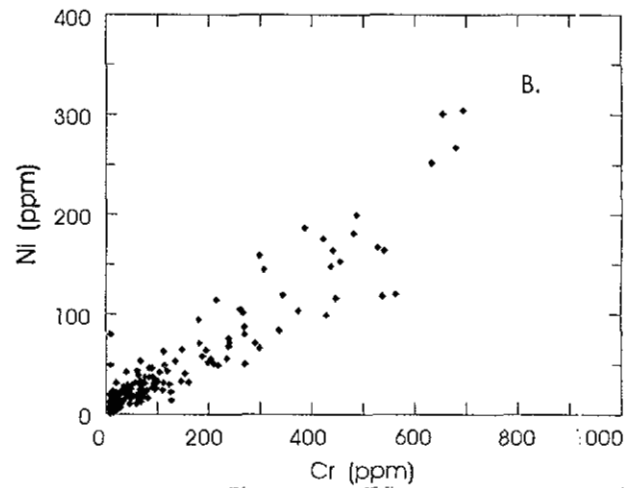
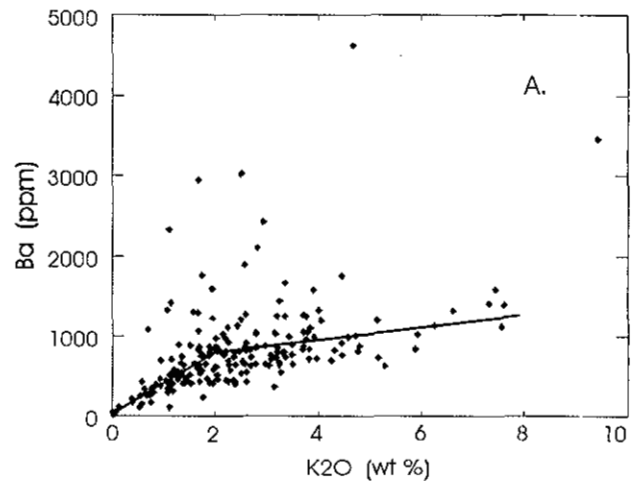


Figure 4-20. Plots of (a) Ba versus K_2O (after Green, 1980) and (b) Ni versus Cr, Elise Formation.

Pearce element ratios (PER) provide a more rigorous approach to determine cogenesis and fractionation trends (Pearce, 1968; Russell and Nicolls, 1988; Russell *et al.*, 1990). PER diagrams were used to test whether rocks from the Elise Formation are cogenetic; *i.e.*, have a common parental magma source and related fractional crystallization trend. The results of this analysis for Elise Formation volcanic rocks are inconclusive; virtually no elements appear conserved. This may be due either to alteration of the volcanics from regional metamorphic or local metasomatic processes, to heterogeneity of rocks sampled (*eg.*, volcanoclastic rocks with multiple clast sources), and/or to varying grain size of the volcanic rocks sampled (*i.e.*, the dominantly porphyritic nature of the volcanic flows). Harker and rock classification diagrams (using major element data) are, therefore, interpreted here with caution.

CLASSIFICATION

Elise volcanic rocks fall into both the alkaline and subalkaline fields and geochemically may be referred to as basalt, basaltic andesite, andesite, dacite, trachyandesite, trachybasalt and hawaiiite (Figure 4-17). The high alkalinity of many of these samples is due mainly to high K_2O content with most samples plotting in the high-potassic to potassic fields (Figure 4-18). The high potassic alkaline basalts and basaltic andesites are called shoshonites.

The subdivision of the subalkaline rocks into calcalkaline and tholeiitic is illustrated on an AFM diagram (Figure 4-19). Most samples show a dominantly calcalkaline trend. The most prominent chemical difference between the more basic end-members of typical tholeiitic and calcalkaline series is in their Al_2O_3 content: calcalkaline basalts and andesites contain 16 to 20 per cent Al_2O_3 whereas tholeiitic basalts contain only 12 to 16 per cent. Elise volcanics have a spread in values from 12 to 18 per cent. This may be due to alteration or metasomatism of the volcanics. The principal rock type of the calcalkaline series is a two-pyroxene andesite with about 60 per cent SiO_2 (Wilson, 1989). Elise volcanic rocks are characterized by substantial andesite but are typically one-pyroxene.

Calcalkaline eruptions tend to be more explosive than tholeiitic eruptions, commonly producing pyroclastic fall and ash flow deposits with minor lava flows (Wilson, 1989). Within the Rosslund Group, these eruptions have produced large stratovolcanoes dominated by pyroclastic deposits but also containing abundant epiclastic debris (*see* previous section). The lavas are porphyritic, with abundant calcic plagioclase phenocrysts, and contain hydrous minerals such as amphibole and biotite, reflecting the more volatile-rich nature of the magmas.

In summary, based on major element chemistry, Elise volcanic rocks have both alkaline and subalkaline

trends. Calcalkaline magma series are restricted to magmatic arcs with the type of volcanism dependent on the stage of evolution of the arc, vertical distance above the Benioff zone and lateral position in the arc (Wilson, 1989). The basaltic to andesitic nature of Elise calcalkaline rocks are suggestive of mature island or continental margin arcs.

TRACE ELEMENT DATA

Trace element data can be used to evaluate magmatic processes such as fractionation and to constrain tectonic environments.

Potassium, barium, rubidium and strontium abundances are high in Elise Formation volcanic rocks (Appendix 1), comparable with those of continental margin arc basalts and andesites, and supporting a transitional to shoshonitic affinity (Beddoe-Stephens, 1977). Correlation of both Ba and Rb with K (*e.g.*, Figure 4-20a) indicates substitution of these elements for potassium in K-feldspar, hornblende and biotite.

Elise volcanic rocks have highly variable Ni and Cr values, typical of both arc volcanism and mid ocean ridge basalts. However, the abundance of Cr values below 250 ppm, in both basalts and andesites (Figure 4-20b), is more typical of arc volcanism.

Titanium and vanadium both correlate negatively with SiO_2 . Positive correlation of Ti with V may be the result of fractionation of Fe-Ti oxides such as ilmenite or titanomagnetite since V readily substitutes for ferric iron.

Elise Formation andesites generally have low TiO_2 and Y content. These concentrations may indicate hydrous and oxidizing conditions with stabilization of amphibole and magnetite. On an SiO_2/Y diagram, Y tends to flatten above 53 per cent SiO_2 which supports the suggestion that it can partition into amphibole (Lambert and Holland, 1974; Beddoe-Stephens, 1977). Yttrium generally behaves as an incompatible element during crystal fractionation, although it can readily partition into garnet.

In summary, Elise volcanic rocks have high concentrations of potassium, barium, rubidium and strontium. This enrichment of incompatible elements of low ionic potential is characteristic of arc volcanics and contrasts with lower values typical of N-MORB (Pearce, 1982). Within oceanic island arcs, this higher abundance is attributed to metasomatism of island-arc mantle source regions by hydrous fluids derived from the subducted oceanic crust (Wilson, 1989). Elise Formation values compare closely with the higher values typical of continental margin arc volcanics; we suggest this is due to the combined effects of an enriched mantle source and to contamination during ascent through crustal rocks of the North American plate. High K/Rb and Fe/Mg ratios also suggest assimilation of crustal rocks.

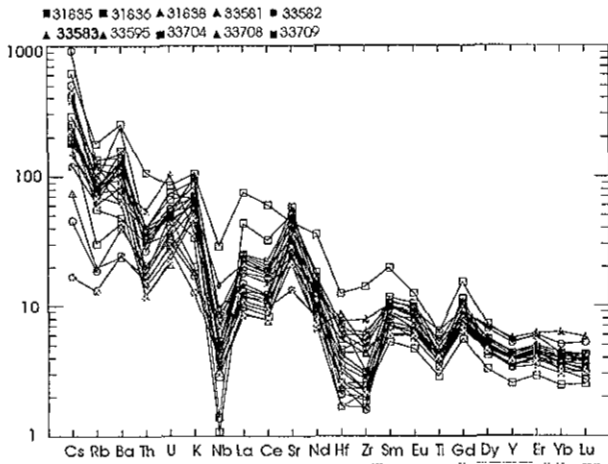


Figure 4-21. Elise Formation incompatible element abundances normalized to primordial mantle values; (after Sun, 1980).

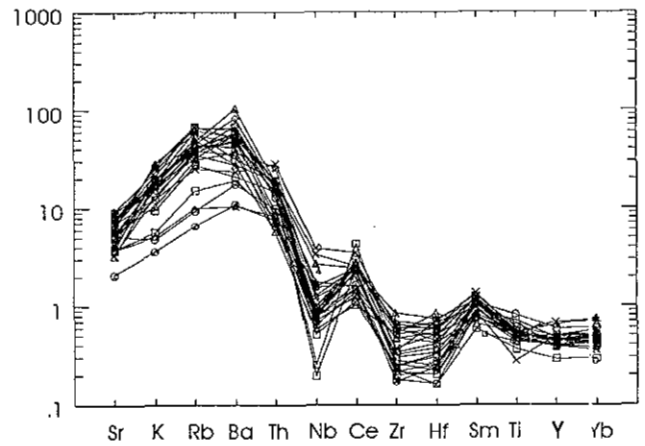


Figure 4-24. Elise Formation MORB-normalized trace element patterns (after Pearce, 1983).

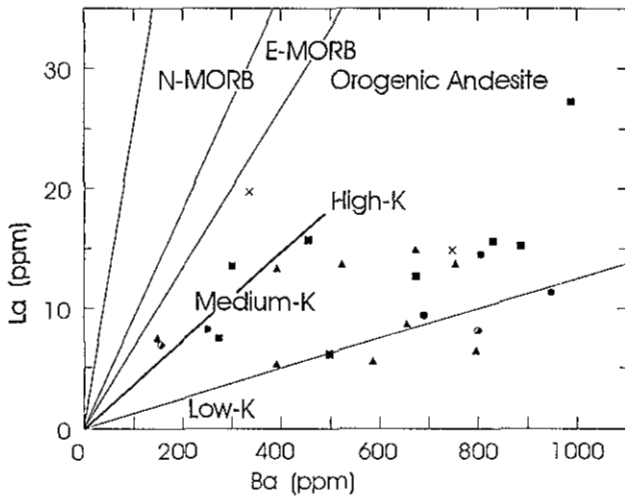


Figure 4-22. A plot of Ba versus La, Elise Formation (after Gill, 1981).

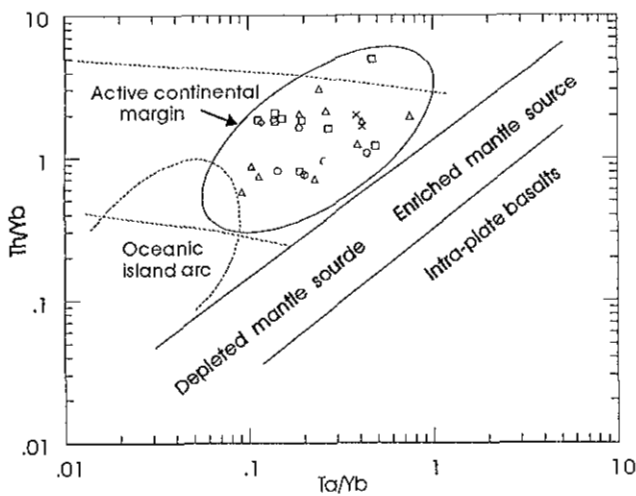


Figure 4-23. A plot of Th/Yb versus Ta/Yb, Elise Formation (after Pearce, 1983).

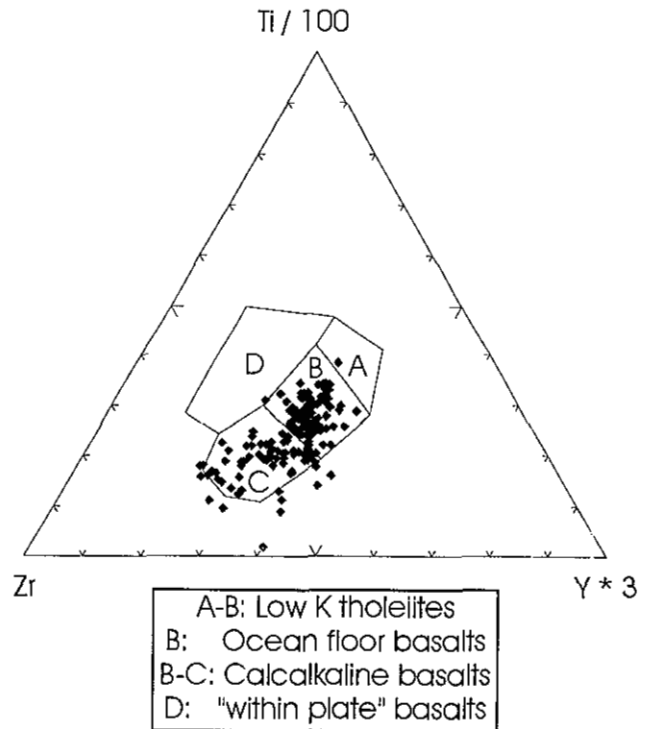


Figure 4-25. A plot of Ti-Y-Zr, Elise Formation (after Pearce and Cann, 1973).

RARE EARTH ELEMENT DATA

Rare earth element (REE) analyses are also important in studies of the petrogenesis of volcanic rocks, and are used for classification and analyses of source magmas and subsequent evolution. Analyses of 26 samples are given in Appendix 2.

Patterns of incompatible trace and rare earth elements can be illustrated on a spiderdiagram, normalized to chondritic abundances (Sun, 1980). A spiderdiagram of Elise volcanic rocks produces a distinctive "spiked" pattern with enrichment of the incompatible elements, Sr, K, Ba and U, and a pronounced trough at Nb (Figure 4-21). This pattern is similar to those of subduction related basalts and contrasts with the relatively smooth shapes of the MORB or oceanic island arc basalts (Thompson *et al.*, 1984; Sun, 1980).

The chondrite normalized REE abundances (Figure 4-21) show only slight light REE enrichment, comparable to calcalkaline arc volcanics and in contrast with depleted light REE patterns of tholeiitic basalts. Two samples with high light REE enrichment (Figure 4-21) are more typical of high-K arc basalts.

High Ba/La ratios, also typical of Elise volcanic rocks (Figure 4-22), are characteristic of island arc and continental margin basalts, and contrast with lower ratios of MORB and intraplate basalt. Hole *et al.* (1984) suggested that this high ratio in the Mariana arc is due to enrichment of Ba from subducted oceanic sediments.

Elise volcanic rocks plot within the active continental margin (ACM) calcalkaline field on a Th/Yb versus Ta/Yb diagram (Figure 4-23). This plot is useful for distinguishing subduction-related components from source mantle components as it largely eliminates variations due to partial melting and fractional crystallization (Pearce, 1983). The ACM field reflects enrichment of Th relative to Ta, probably due to contamination of mantle derived magma by subduction-zone fluids (Wilson, 1989).

Trace and rare earth element concentrations, normalized to typical mid-ocean ridge basalt, can be used to highlight the nature of subduction-zone components. In Figure 4-24 (after Pearce, 1983), Elise Formation element abundances are ordered according to their mobility in an aqueous fluid phase and their relative incompatibility. Because Sr, K, Rb and Ba are concentrated in plagioclase, they are considered relatively mobile and plot on the left of the diagram; the elements Th through to Yb are relatively immobile and plot on the right side of the diagram. As MORB data are the datum in this diagram, they plot as a horizontal line at 1.0.

Oceanic-island arc tholeiitic basalts parallel the MORB pattern from Nb to Yb (the immobile elements) but with a lower rock/MORB ratio. High-K calcalkaline oceanic-island arc basalts have a greater degree of mobile element enrichment than the tholeiites; the immobile elements also define less of a horizontal line. Within-plate basalts are enriched in most incompatible

elements compared to MORB and show rounded MORB-normalized trace element patterns, similar to those of continental basalts.

Rossland Group immobile elements, Ta, Nb, Zr, Hf, Ti, Y and Yb, define a pattern more similar to intraplate or continental basalts than to MORB (Figure 4-24). This may indicate that the mantle source of Rossland Group magmas was either enriched in subcontinental lithosphere or possibly, derived in part from subduction of oceanic island basalts.

TECTONIC SETTING

Major, trace and rare earth element analyses of Elise volcanic rocks suggest formation in a subduction related environment, as an oceanic island arc. However, concentrations of immobile trace elements and REE suggest contamination by continental lithosphere, resulting in element ratios and values that approach those of active continental margin arcs. The paucity of high SiO₂ magmas, such as rhyolite or dacite, would tend to preclude a continental margin setting, with subduction of oceanic lithosphere beneath continental crust.

On a Ti-Y-Zr plot (Pearce and Cann, 1973), Elise basalts fall in the field of calcalkaline basalts (Figure 4-25), typical of oceanic arc volcanics. The high Th/Yb ratios (Figure 4-23), more common in continental margin arcs, may reflect contamination by continental crustal rocks. As well, higher concentrations of K, Sr, Rb, Ba, Zr and U and higher K/Rb and Fe/Mg ratios, characteristic of continental arc volcanics, may be due to the combined effects of derivation from partial melting of an enriched mantle wedge and to crustal contamination during magma ascent. Elise volcanics also have large scatters on a K₂O versus SiO₂ discrimination diagram, in contrast with the positive linear trend in many island-arc volcanic suites (Figure 4-26). This, as well, may reflect assimilation of crustal components during magma ascent (or alteration).

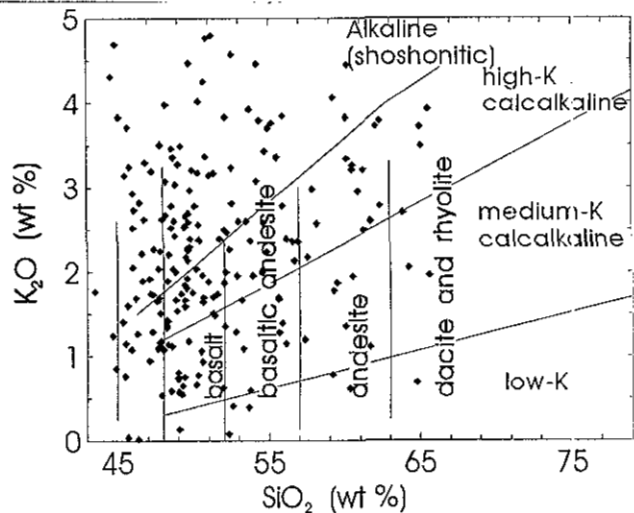


Figure 4-26. A plot of K₂O vs SiO₂, Elise Formation (after Basaltic volcanism study project, 1981, summarized in Wilson, 1989).

In summary, we suggest that the somewhat atypical oceanic arc volcanism recorded in Elise volcanic rocks is due to contamination by continental crustal rocks above the wedge and a subducting oceanic plate. This suggests that they were formed close to the North American continental margin above an extended and thinned continental prism, or possibly above thinned continental crust in an oceanic environment. Supportive isotopic evidence for formation close to the continental margin includes xenocrystic cores in Elise volcanic tuffs with dates similar to those of North American crustal rocks. Earlier, more western facies of the Quesnel arc, including the late Triassic rocks of the Nicola Group, have trace element concentrations more characteristic of oceanic island arc volcanism (Mortimer, 1986; 1987).

SUMMARY AND DISCUSSION

The Elise Formation is dominated by high-K, alkalic and calcalkaline oceanic island arc volcanic rocks. It includes mainly basaltic and shoshonitic phases, less andesite, minor latite and possible rhyolite (see p. 83). This contrasts with higher proportions of more felsic phases in both continental arc rocks of the Andes and island arc rocks of the southwest Pacific (Figure 4-27). Although basaltic rocks predominate in the Elise Formation, these contrast markedly with MORB or back arc basalt compositions.

As described above, the Elise Formation has many lithologic features typical of arc environments. These include early, mafic subaqueous shoshonitic flows, common in the more eastern facies of the Rossland Group south of Nelson, and overlying pyroclastic and epiclastic deposits. The latter comprise thick sequences of pyroclastic flow and air-fall deposits, including strongly porphyritic coarse pyroclastic breccias, block-and-ash flow deposits and fine mafic tuffs, as well as lava flows and debris flows, deposited on flanks of stratovolcanoes.

Basaltic magmas erupted in island arcs are related to variable contributions from two main source components: a parental partial melt of the asthenospheric mantle wedge (Arculus and Powell, 1986) and a metasomatic component, either a hydrous fluid or a partial melt, derived from the subducted oceanic crust and overlying sediment cover. This metasomatic component, a characteristic feature of all subduction-related magmatism, includes the transfer of Sr, K, Rb, Ba, Th + Ce, P and Sm to the mantle wedge by partial melt or fluid-transfer processes associated with the dehydration of the subducted slab (Anderson *et al.*, 1980; Hawkesworth and Powell, 1980; Wilson and Davidson, 1984). It may account, in part, for the relatively high concentrations of these elements in Elise volcanic rocks although other elements, notably Na, would then also be expected to be relatively high.

Hence, high concentrations of some immobile trace elements, as well as REE, similar to those in continental

margin arcs, suggest that Elise Formation magmas were contaminated by a continental crustal component during their ascent. This implies that the Elise Formation was deposited above a thinned continental crust, perhaps marginal to the North American craton. However, these high concentrations may also reflect an enriched mantle wedge magma source. Alldrick (1993) has pointed out that the Jurassic arcs are built on previous Permian and Triassic oceanic arcs, conceivably providing a K-enriched source for younger arc magmas. Partial melting of older arc rocks may be possible in older and more western exposures of the Quesnel arc rocks, such as the Nicola (Smith *et al.*, 1995), which may have been generated at shallower depths.

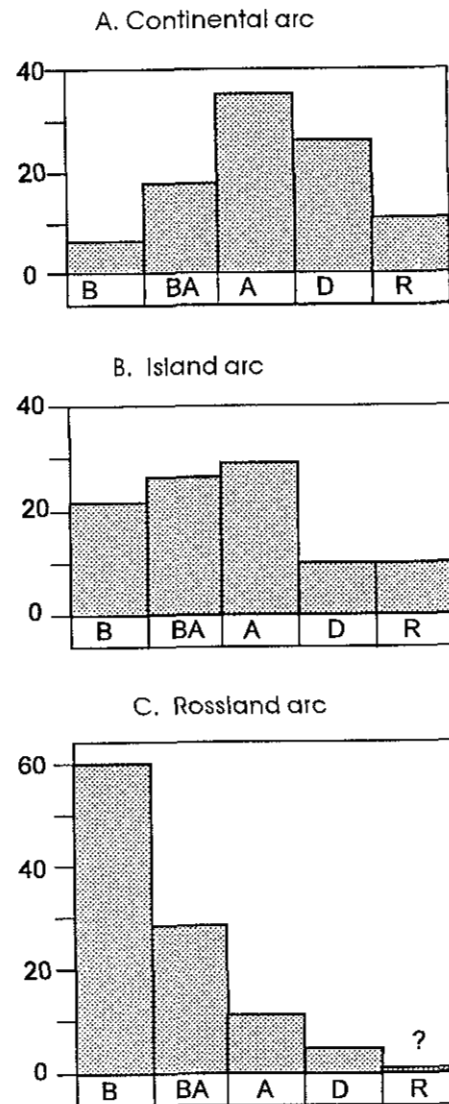


Figure 4-27. Relative volumes of basalt (B), basaltic andesite (BA), andesite (A), dacite (D) and rhyolite (R) in the Elise Formation compared with volumes in the Andes continental arc and southwest Pacific island arcs; data from this study and Ewart (1982).

CHAPTER 5 - HALL FORMATION

INTRODUCTION

The "Hall Series", from which the Hall Formation was named, was defined by Drysdale (1917) to include a series of sedimentary units within the volcanic rocks of the Rossland Group. These are now known to be a sedimentary succession that lies at the top of the Rossland Group. It was renamed the Hall Group by Little (1950) and subsequently referred to as the Hall Formation (Mulligan, 1952). The formation consists of conglomerate, lithic wacke, sandstone, siltstone and argillite with minor intercalated crystal tuffs. It is exposed in the core of the Hall Creek syncline, forming a belt that extends from the headwaters of Noman Creek just east of Toad Mountain in the Nelson area, southward to the town of Salmo. It is also exposed in the core of the tight Hellroaring Creek syncline just south of Salmo and in the core of an open syncline south of Fruitvale (Figure 5-1). It is not exposed in the Rossland area where Lower Cretaceous conglomerates of the Mount Sophie Formation or Eocene volcanic rocks of the Marron Formation unconformably overlie the Elise Formation.

The Hall Formation contains early Toarcian ammonites (Tipper, 1984). A plant fragment and pelecypods were also collected from the formation by Little (1950).

The maximum original thickness of the Hall Formation is not known. All measured or estimated thicknesses are minimum values as the top is not seen. The exposed thicknesses vary from approximately 350 metres near Fruitvale to an estimated 2100 metres in the core of the Hellroaring Creek syncline southwest of Salmo.

AGE

The age of the Hall Formation is restricted by a Sinemurian age for the underlying Elise Formation and a Late Cretaceous age for the overlying Sophie Mountain Formation in the Rossland area.

Early Toarcian macrofossils have been recognized in the Hall Formation in both the Salmo (Frebold and Little, 1962) and Fruitvale (Little, 1982a) areas. A new fossil locality in the Fruitvale area also suggests a Toarcian or younger age (Tipper, personal communication, 1991):

Field number: BCHA-153-8

GSC Loc. No.: C-154311

Locality: one kilometre west of Fruitvale;
NTS 82F/04E; UTM zone 11; 458400
E, 5440000 N

Identification: fragments of bivalves
fragments of true belemnites

Age and comments: age not determinable;
however, belemnites in the Canadian
Cordillera are not older than Toarcian.

A Bajocian age and a younger age have been suggested for two other Hall Formation fossil collections (Little, 1982a). Tipper (1984), however, suggested that one of these fossils, a highly distorted imprint, is similar to late Toarcian *Haugiella* found on the Queen Charlotte Islands. The collection of supposedly younger than Bajocian age (GSC loc. 38942; Frebold and Little, 1962; Tipper, 1984) was re-examined and found to contain fossils with a close resemblance to Early Pliensbachian age genera from Oregon and the Queen Charlotte Islands (Tipper, 1984). However, this locality may be within the upper part of the Elise Formation, rather than the Hall, and is interpreted to stratigraphically underlie Elise rocks that contain Sinemurian fossils (Andrew *et al.*, 1990a;b). Hence, the only reliable fossil age determination for the Hall Formation is early Toarcian.

DESCRIPTION

The Hall Formation in the core of the Hall Creek syncline can be subdivided into three broadly defined members: a lower, rusty black siltstone and argillite succession, coarsening upward into a coarse sandstone and conglomerate succession of the middle Hall, overlain locally, by dominantly carbonaceous siltstone of the upper Hall (Figure 5-2).

In general, the contact of the Hall Formation with the underlying Elise Formation is conformable. However, in the Salmo River valley near Hall Creek, an erosional unconformity with development of basal conglomerates separates the formations. The conglomeratic unit comprises approximately 5 metres of boulder and cobble conglomerate separated by a bedded tuffaceous sandstone and siltstone unit. Clasts within the conglomerate are rounded and comprise dominantly volcanics of the Elise Formation but include feldspar porphyry and feldspar-amphibole porphyry indicating an erosional unconformity that locally has exposed subvolcanic intrusions presumably also from within the

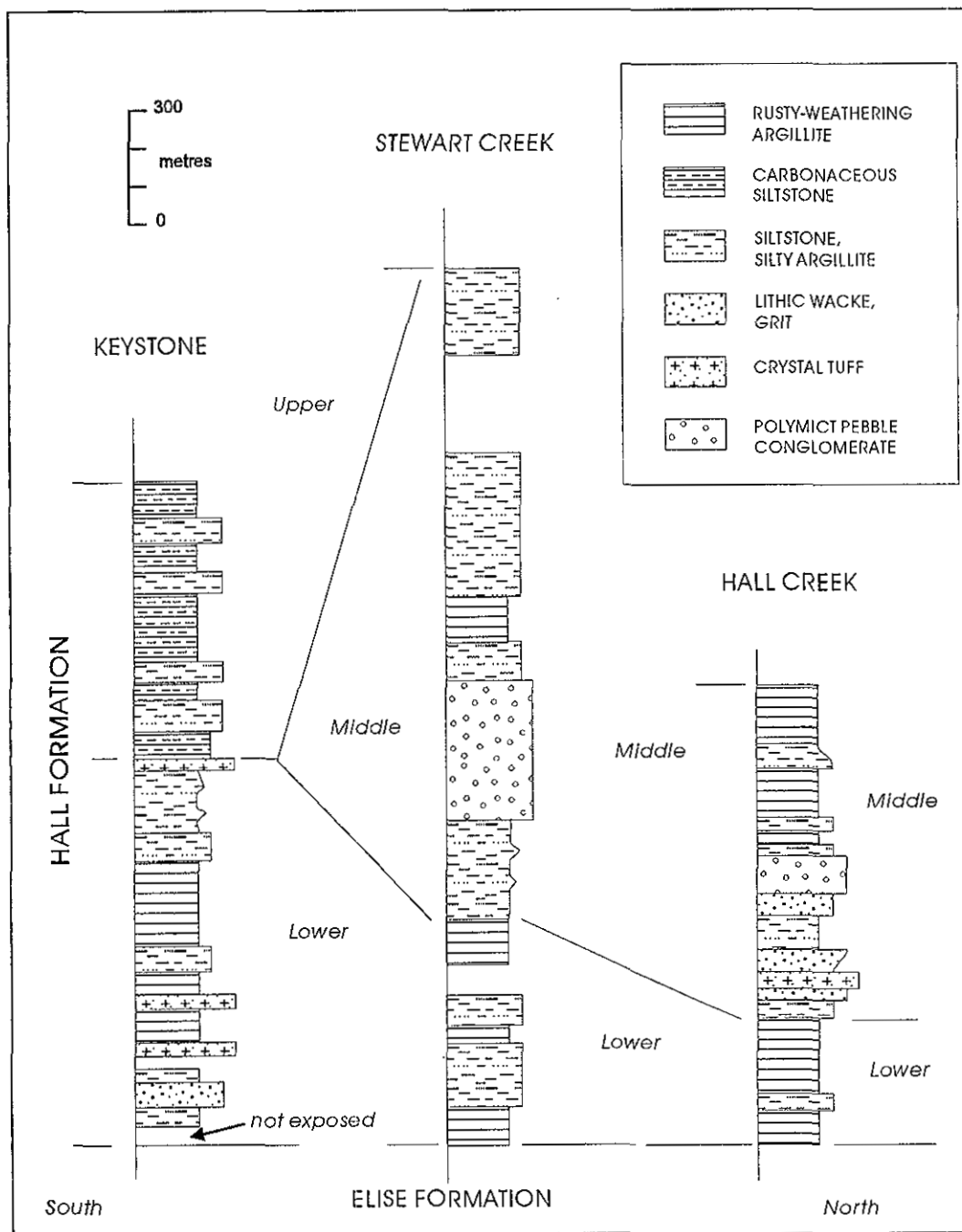


Figure 5-2. Composite stratigraphic sections of the Hall Formation in the core of the Hall Creek syncline, Keystone Mountain, Stewart Creek and Hall Creek areas (from Andrew and Höy, 1991).

Elise Formation. Elsewhere, as in highway cuts just south of Salmo and in Hellroaring Creek, moderate to intense shearing occurs at the contact.

Rocks of the lower Hall are thicker and better exposed in the western and southern sections, particularly in the Hellroaring Creek and Keystone Mountain areas (Figure 5-3). To the north, the lower Hall thins as it is supplanted by coarser facies of the middle Hall (Figure 5-3). Argillites within the lower Hall are rusted due to weathering of disseminated pyrite. Interbedded quartzitic siltstone and argillite, also typical of the lower part of the formation, are well exposed in Hall Creek (Plate 5-1). Although primary small-scale structures such as graded beds are absent or only poorly developed in these rocks, rip-up clasts and flame structures are occasionally seen and can be used for top determinations.

A number of thin volcanic units occur within the lower Hall and the lower part of the middle Hall. They comprise tuffaceous conglomerate, minor crystal tuff, and rare augite pyritic flows (or possibly sills).

The middle member of the Hall Formation varies from a coarse polymict pebble conglomerate to lithic wacke and minor silty argillite. The conglomerate is characterized by elongate, subangular mudstone fragments up to 5 to 10 cm in diameter that are commonly aligned parallel to layering and minor volcanic and intrusive fragments, probably derived from the underlying Elise Formation (Plate 5-2). The lithic wacke contains up to 50 percent quartz, as well as feldspar, ferromagnesium minerals and angular rock fragments (Mulligan, 1952).

The triangular shaped distribution of the Hall Formation near Fruitvale was recognized by Little (1982a) and constitutes the most western recognized Hall exposures (Figure 5-1). The basal part of the exposed succession is similar to the lower Hall farther east. It is overlain by conglomeratic facies interbedded with siltstones and wackes. The conglomerates contain a variety of clasts, including plagioclase porphyry, limestone, andesite? and siltstone, and based on their similarity with conglomerates to the southwest were

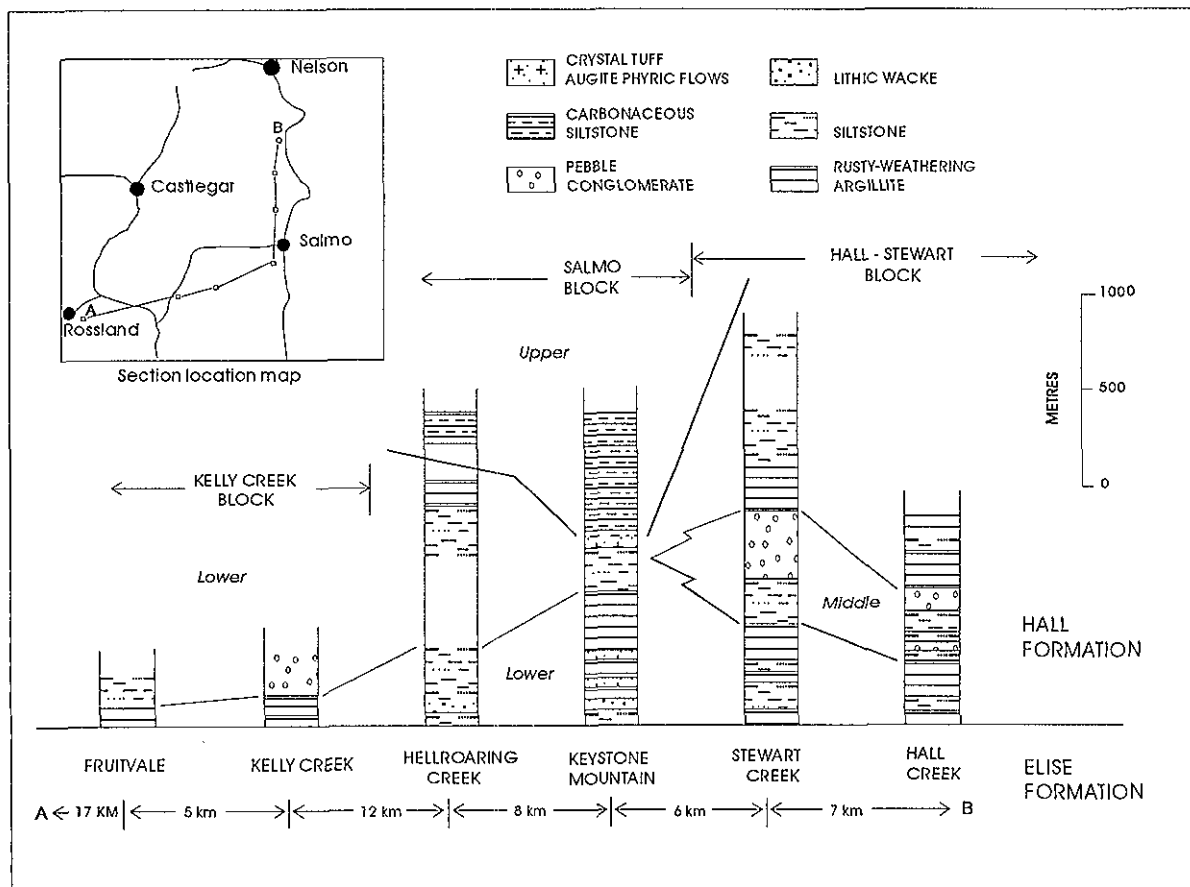


Figure 5-3. Correlation of the Hall Formation showing main lithologic and thickness changes (from Andrew and Höy, 1991).



Plate 5-1: Rip-up structures, laminated beds in interbedded siltstone and sandstone, Hall Formation, Stewart Creek area.



Plate 5-2: Pebble conglomerate of the middle part of the Hall Formation with 5-10 cm subangular, flattened mudstone fragments, south of Hall Creek.

initially mapped as Archibald Formation (Andrew *et al.*, 1990a). However, fossil locality BCHA-153-8 suggests that these conglomerates are Toarcian in age and must therefore belong to the Hall Formation (Andrew *et al.*, 1991). The succession on the slopes immediately north of Fruitvale is similar and has been included in the Hall Formation (Figure 5-1); alternatively, these latter conglomerates could be part of the Archibald Formation necessitating a fault in the Fruitvale Creek valley as shown by Little (*op. cit.*)

The upper part of the Hall is best exposed in the Hall Creek syncline on Keystone Mountain. It comprises dominantly hard, fine-grained carbonaceous siltstone lying above thin-bedded black shale. Bedding is not apparent, but in thin section thin laminae are noted. As well, occasional thin silty layers occur within the upper Hall (Figure 5-2).

Thickness and facies variations in the Hall Formation are summarized in the stratigraphic columns of Figure 5-3. The formation is absent in the Rossland area where Elise rocks are unconformably overlain by either late Cretaceous Sophie Mountain Formation or volcanic rocks of the Eocene Marron Formation. To the east in the Fruitvale area, the Hall Formation forms a wedge of fine-grained clastic rocks that thicken and coarsen eastward. Farther east in the Hall Creek and Stewart Creek areas, conglomerates are more predominant. The fine-grained, carbonaceous unit of the upper Hall appears to be laterally discontinuous, confined to the Keystone Mountain area and the core of the Hellroaring Creek southwest of Salmo.

DEPOSITIONAL ENVIRONMENT

Based on sedimentary rock types and the abundance of marine fossils, the Hall Formation has been interpreted to have been deposited in a littoral to offshore environment (Little, 1950; Mulligan, 1951). It was deposited on an irregular paleosurface, after a hiatus of several million years following volcanism of the Elise Formation. The only reliable fossils in the Hall indicate an early Toarcian age, whereas underlying Elise rocks are Sinemurian in age; there is no conclusive evidence of Pliensbachian deposition of either Elise Formation or Hall Formation. Supportive

evidence for a hiatus between Elise and Hall deposition is the local occurrence of a prominent basal conglomerate in the Hall that contains large and abundant clasts of Elise Formation rocks.

In general, the lower Hall is dominated by argillite with occasional siltstone lenses and minor crystal tuff. The general lack of slump or intraformational conglomerates in the basal Hall, indicative of active fault scarps and possible deepening water conditions, suggests that deposition may be in a shallow marine, possibly lagoonal environment.

Middle Hall rocks are marked by intraformational conglomerates within dominantly immature finer grained clastic rocks. Clasts of the underlying Elise within the conglomerates, locally coarse massive units suggestive of debris flows, and coarsening and thickening of units towards the north and east, suggest growth faulting along basin margin to the north and east. Abundant quartz in some wacke beds suggest a continental (North American) source. Conglomerates in the Fruitvale and Kelly Creek area indicate a faulted source area to the west as well. Some of these conglomerates contain limestone clasts, probably derived from the Permian Mount Roberts Formation, indicating a highland to the west that locally exposed the Mount Roberts as well as the Elise. Graded beds, flame structures and rip-up clasts are indicative of turbidite deposition.

Lack of sedimentary structures or diagnostic fossils in the monotonous, black, carbonaceous argillites of the upper Hall precludes definitive interpretation of the depositional environment. The upper Hall may have been deposited in a shallow, restricted lagoonal environment or may comprise pelagic sediments.

In summary, the Hall Formation was deposited in a marine structural basin on an irregular paleosurface developed after arc volcanism of the Elise Formation. Early Hall sediments may be shallow water lagoonal, followed by coarse clastic deposits derived from fault-bounded marginal highlands to the west and northeast. These deposits are remnants of a Pliensbachian to Lower Bajocian overlap assemblage, including the Ashcroft Formation (McMillan, 1974), that were deposited unconformably on arc rocks throughout Quesnellia.

CHAPTER 6 - PLUTONIC ROCKS

INTRODUCTION

Plutonic rocks occur extensively throughout southeastern British Columbia (Woodsworth *et al.*, 1992). The oldest are mafic sills and granitic bodies that intrude the Mesoproterozoic Purcell Supergroup. The Moyie sills are a thick accumulation of gabbroic sills that record rifting during deposition of the Aldridge Formation at the base of the Purcell Supergroup (Höy, 1993). The Hellroaring Creek stock is a coarse grained, S-type anorogenic granodiorite, dated at 1365 Ma (J. Mortenson, personal communication, 1993) that also intrudes the Aldridge Formation.

Paleozoic intrusive bodies include a number of alkalic stocks, including carbonatites, as well as some granitic bodies. Alkalic ultramafic diatremes, explored for their diamond potential, occur in several areas in the Rocky Mountains (Pell, 1987; 1994). Both intrusive and extrusive carbonatites occur along the flanks of "gneiss domes" in the Monashee Complex, and carbonatites are associated with the Ice River Complex, a late Devonian alkaline ultramafic intrusive complex south of Field. The carbonatites contain high values of rare earth elements, strontium and niobium. A number of folded and foliated granitic bodies in the Kootenay terrane, including the Mount Fowler batholith and Clachnacudainn gneiss, have been interpreted as Paleozoic (Okulitch *et al.*, 1975).

Mesozoic and Tertiary plutonic rocks occur throughout the Rossland-Nelson map-area. Two suites of Early to Middle Jurassic plutons are recognized: volcanic arc granitoids that are interpreted to be comagmatic with the Rossland Group and the synkinematic Silver King intrusions south of Nelson. Middle Jurassic intrusions include the Nelson batholith and the Bonnington pluton and a number of related stocks. Middle Cretaceous granites are clearly post tectonic and numerous Cenozoic intrusions are related to regional Eocene extension.

This chapter describes briefly the plutonic rocks of the Rossland-Trail map-area (Figure 6-1), focusing on those of Early/Middle Jurassic age. It reviews field data, presents new petrographic and geochronological data and discusses metallogeny. The relationships between magmatism and tectonics are dealt with in Chapter 7.

EARLY JURASSIC (SINEMURIAN) PLUTONS

A number of mafic, high-K alkalic plutonic complexes within the Rossland Group are interpreted to be subvolcanic intrusions, comagmatic with the Elise Formation (Dunne and Höy, 1992). These include the

Rosslund monzodiorite, the Eagle Creek complex, the Katie pluton and a number of small mafic plugs scattered throughout the Rossland-Nelson area. Many of these are clearly associated with Au-Cu mineralization, including skarns, porphyry deposits, and the massive chalcopyrite-pyrrhotite veins of the Rossland camp.

EAGLE CREEK PLUTONIC COMPLEX

The Eagle Creek plutonic complex, referred to as 'pseudodiorite' (Mulligan, 1952), straddles the Kootenay River 3 kilometres west of Nelson (Figure 6-1). It is generally a medium to coarse-grained mafic intrusion, in part gneissic; however, it grades into leucocratic hornblende syenite (Mulligan, 1951) and locally incorporates coarse ultramafic phases (Mulligan, 1951, 1952; Little, 1982a,b; Lindsay, 1991). On the basis of extensive petrography and rock geochemistry at the Moochie occurrence, Lindsay (*op. cit.*) describes it as a metadiorite. It is suggested that the term Eagle Creek, originally proposed by Mulligan (1951), be retained.

Contacts of the Eagle Creek plutonic complex with the Rossland Group rocks are generally sharp, locally marked by coarse-grained clinopyroxenites. The southwest part of the complex is cut by the Mount Verde fault, a steep, west-dipping, listric normal fault that records a period of extension just prior to intrusion of the Nelson batholith.

The age of the Eagle Creek plutonic complex is not known. Attempts to separate zircons have been unsuccessful. Two titanite fractions were separated but they yielded inconclusive results (J. Gabites, personal communication, 1997). The Eagle Creek complex is cut by the Middle Jurassic Nelson granodiorite and by the Silver King shear zone, a wide zone of shearing that extends along the margins of the complex and extends into the core of the Hall Creek syncline. This shearing and deformation is interpreted to have occurred *ca* 175 Ma, during intrusion of the Silver King plutonic suite. Its relationship to the surrounding Early Jurassic Rossland Group rocks is less clear. However, based on similarity with the Rossland monzodiorite and its pre-tectonic age, it is possible that the Eagle Creek plutonic complex may be cogenetic with Rossland Group volcanism.

PETROGRAPHY

The Eagle Creek plutonic complex is a composite intrusion with phases varying from equigranular to porphyritic and mafic to ultramafic. The mafic phases contain 10 to 30 per cent plagioclase (An₅₋₈₄) and

minor (one to 15 per cent) microcline (Plate 6-1, Table 6-1). Primary quartz ranges up to 5 per cent. Most mafic minerals are variably altered to chlorite and carbonate; unaltered mafic minerals are rare and include euhedral augite (5-15 per cent), hornblende (3 per cent) and green biotite (10-30 per cent). Apatite occurs frequently as an accessory mineral in the mafic phases. The ultramafic phase contains at least 25 per cent augite, 10 per cent amphibole and abundant alteration of remaining mafic minerals to chlorite.

The complex is variably altered and sheared close to the Silver King shear zone (Figure 6-1). Plagioclase is commonly saussuritized, sericitized and/or partially replaced by chlorite. Muscovite, chlorite and calcite overprint and surround plagioclase and microcline (Lindsay, 1991) and segregated albite and epidote show fine-grained cataclastic textures.

Table 6-1: Petrographic comparison of typical Early Jurassic intrusions in the Rossland Group, Nelson-Rossland area, southeastern British Columbia

	Eagle Creek plutonic complex	Rossland monzonite	Rossland sill	"Gabbro" Nelson area	"Gabbro" Fruitvale area	"Gabbro" Rossland area	Silver King intrusions
plagioclase	10-30	40-60	30-40	15-45	30-45	20-55	30-60
(An content)	5-84	38-48	48-54	50-67	54-69	55	28-60
orthoclase	0	20-25	25	5-24	0-25	0	0
microcline	1-15	1-2	0	0	0	0	0
quartz	1-5	1-2	0	2-5	0	0	1-2
augite	5-15	3-15	10	0	10-20	7-25	0
hornblende	3	0-30	10	0-7	0-5	0	0-3
biotite	10-30	5-15	10	1-25	0	0-1	0
chlorite	2-35	5-25	1	5-20	0-20	10-40	10-15
epidote	2-20	0	0	0-15	0-15	0-10	1-5
sericite	10-20	0	0	0-35	0-35	0	5-60
carbonate	7-25	0	0	0-10	0	0	5-30
apatite	0-1	1	1	0-1	0-1	0-1	0-1
sphene	0	0-1	0	0	0	0	0
opaques	0-10	1-5	1	0-3	0-5	0-7	0-3
matrix	0	0	0	0-25	0-35	0	0-60

Analyses incorporate, in part, work by Beddoe Stephens and Lambert (1981), Fyles (1984), Lindsay (1991) and Mulligan (1951).

Petrographic analysis of samples of the Eagle Creek Plutonic Complex fall within the monzonite, quartz monzonite, quartz monzodiorite, quartz gabbro and diorite/gabbro fields on Streckeisen's (1973) quartz-alkali feldspar-plagioclase diagram (Figure 6-2). Diorite or gabbro are the most common phases in the field and because of regional metamorphism, may be referred to as metadiorite/gabbro.

Ultramafic phases along the margins of the complex are coarse-grained clinopyroxenite. They have similar mineral assemblages to the metadiorite/gabbro (Mulligan, 1951), comprising dominantly augite with lesser green amphibole rimming and replacing the augite, and secondary chlorite (Plate 6-2). Symplectite texture, comprising iron oxide, probably ilmenite, intimately intergrown with clinopyroxene in a vermicular fashion, is seen in the ultramafic phases (Plate 6-3). Minor saussuritized plagioclase is noted in some ultramafic localities (Mulligan, 1951).

Certain phases of the Eagle Creek plutonic complex such as the monzonitic to syenitic rocks and clinopyroxenites suggest affinities to Alaskan-type mafic-ultramafic complexes (Nixon, 1990). However,

silica oversaturated rocks such as the quartz monzonites, diorites and gabbros are more similar to calc-alkaline plutonic suites.

Beddoe-Stephens (1977, p. 178) noted that Ni and Cr concentrations in the Eagle Creek Complex are generally low indicating high degrees of differentiation for these rocks. He suggested that this pluton has a cumulate origin, representing an aggregate of olivine, pyroxene and plagioclase that precipitated from a fairly evolved basalt.

MINERAL PROSPECTS

Several mineral deposits and showings occur within or adjacent to the Eagle Creek plutonic complex. These include copper-gold porphyry showings such as the Toughnut and Moochie occurrences and copper-gold-lead veins. Mineralization at the Toughnut zone includes disseminated chalcopyrite, tetrahedrite and pyrite within potassic altered, carbonate and sericite-rich lower Elise Formation volcanic rocks adjacent to the complex.

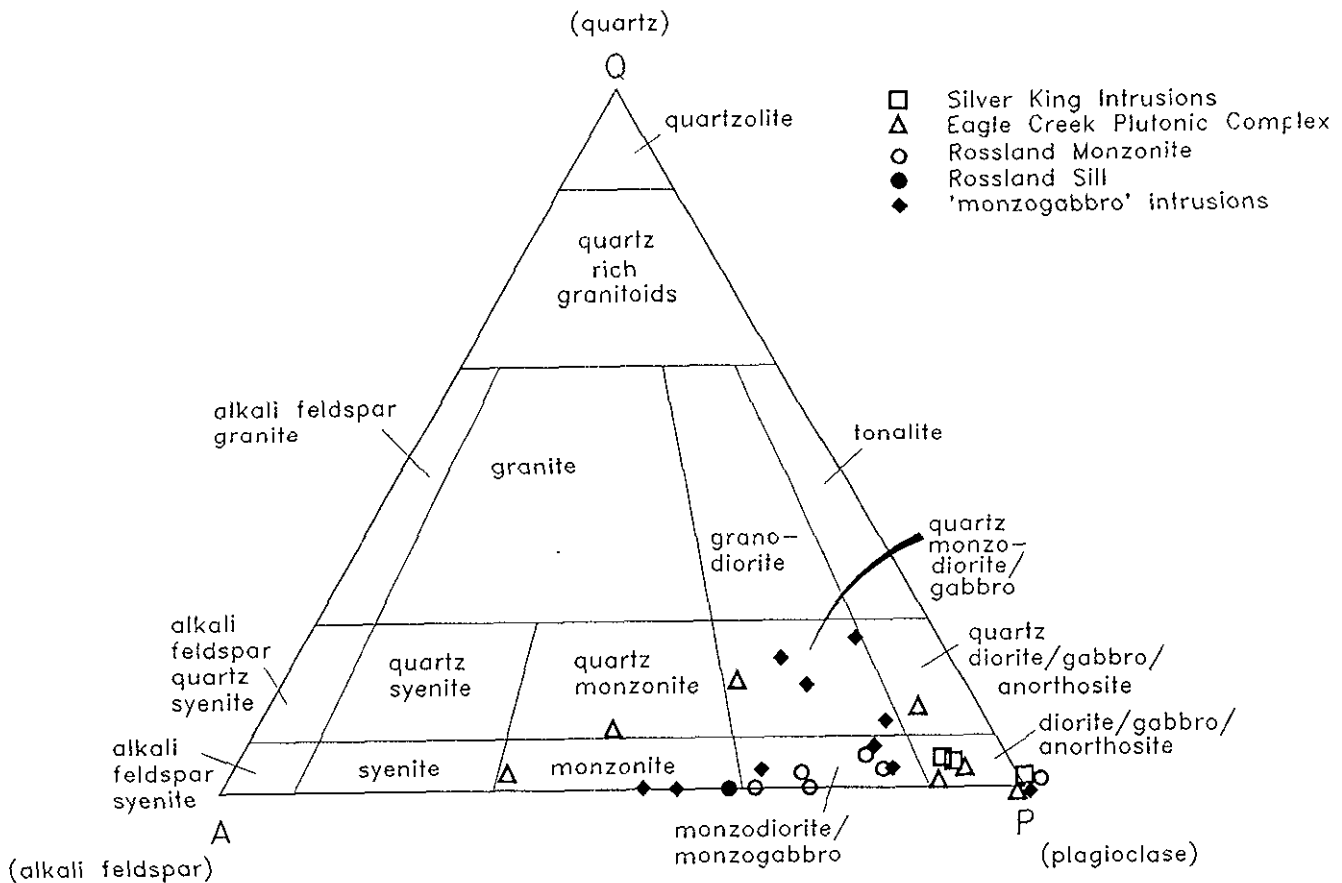


Figure 6-2. Quartz-alkali feldspar-plagioclase diagram of Early Jurassic intrusions in the Trail map-area (plot after Streckeisen, 1973).



Plate 6-1: Microcline crystal, 640 microns, in gabbro phase of the pseudodiorite (view = 1.48mm)



Plate 6-2: Coarse-grained augite crystals are pervasively rimmed and replaced by chlorite in coarse-grained clinopyroxene phase of the pseudodiorite (view = 1.48 mm).

The Moochie occurrence, within the complex, is characterized by disseminated chalcopyrite, magnetite and pyrite within locally potassic altered metadiorite. Magnetite commonly encloses irregular lenses of ilmenite and cataclastic aggregates of chalcopyrite and magnetite are also noted (Lindsay, 1991). The occurrence is locally overprinted by the Silver King shear zone.

The Star and Granite Poorman occurrences are vein deposits within the complex. Quartz veins at the Star deposit carry patches of chalcopyrite, pyrite, malachite and galena. The Granite Poorman mine (Dawson, 1889) is characterised by veins of quartz carrying pyrite, galena, chalcopyrite, sphalerite, minor scheelite and free gold.

ROSSLAND MONZONITE

The Rossland monzonite, centred on the town of Rossland, extends north to Monte Cristo and Colubia-Kootenay mountains and east to the vicinity of Lookout Mountain (Figure 6-1). A small fault slice of Rossland monzonite is found on the northwest slopes of Red

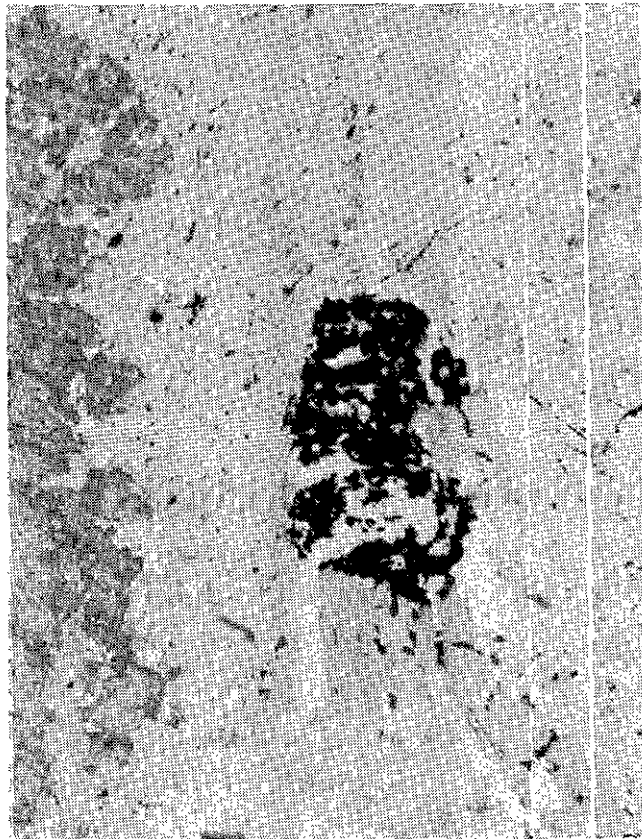


Plate 6-3: Symplectite texture: ilmenite or magnetite and clinopyroxene intimately intergrown in a vermicular fashion in a coarse-grained clinopyroxenite phase of the pseudodiorite (view = 1.48 mm).

Mountain. Contact relationships with the Rosslund Group vary from sharp to locally gradational over several hundreds of metres, obscured by a wide thermal aureole (Fyles, 1984). The Rosslund monzonite and Rosslund mining camp have been studied by many previous workers including Drysdale (1915), Bruce (1917), Gilbert (1948), Little (1960, 1963, 1982b), Fyles (1984) and Höy and Andrew (1991a,b). Veins in the gold camp, and their relationship to the monzonite and structures, as well as the molybdenum breccia deposits will be discussed in a manuscript in preparation.

The Rosslund monzonite hosts a number of different vein deposit types, including the Le Roi, Centre Star and Evening Star mines. Gold-copper-lead-zinc veins hosted by the Elise Formation such as the Bluebird and Mayflower deposits occur mainly south of Rosslund near the southern margin of the stock. Bonanza gold veins, including the Midnight deposit, occur adjacent to ultramafic bodies southwest of Rosslund. Gold-copper skarn mineralization occurs within the Rosslund monzonite adjacent to some of the main and north belt veins.

PETROGRAPHY

The Rosslund monzonite is a composite stock with coarse to fine grained phases, and more mafic to intermediate (feldspar-dominated) phases. Contacts between these phases range from gradational to intrusive with, more commonly, coarse grained or more feldspathic phases being younger (Drysdale, 1915). These phases have not been mapped separately in this study.

One of the more common phases of the Rosslund monzonite is a dark, coarse-grained inequigranular intrusion. It comprises 40 to 60 per cent euhedral to subhedral andesine (An_{38-48}), with rare labradorite (An_{62-68}) in the Crown Point area, and 10 to 25 per cent orthoclase. Primary mafic minerals are only partially preserved, typically as ragged grains. Augite is replaced by hornblende in some areas but, more commonly, biotite replaces both hornblende and augite. Remnant augite comprises 3 to 15 per cent anhedral, often poikilitic crystals mantled by biotite and chlorite. Magnetite and apatite are ubiquitous accessory minerals; sphene is rare. Quartz, if present, ranges from 1 to 2 per cent as late, resorbed crystals which may indicate a subvolcanic origin for the intrusion (Table 6-1). This mineralogy indicates that this phase is dominantly a monzodiorite (Figure 6-2). It can grade to a dark greenish black phase comprised dominantly of pyroxene and hornblende with abundant biotite. Other phases include monzonite and, at the Centre Star deposit, a large biotite clinopyroxenite xenolith (?) several metres across.

Diorite porphyry dikes, referred to as diorite porphyrite by Drysdale (1915) and Gilbert (1948), are common in underground workings in the area of the

main veins. Their similar orientation and close spatial association with the veins indicated a genetic link (Drysdale, *op. cit.*). Drysdale suggested that these were phases of the Middle Jurassic Trail pluton, whereas Gilbert (*op. cit.*) concluded that they grade into the Rosslund monzonite, and may be an early dike phase and marginal contact phase. This interpretation is supported by Fyles (1984) who also noted similar hornblende porphyry phases in the margins of the Rosslund monzonite, and intense alteration of these dikes in contrast to dikes known to be related to the Trail pluton.

Metamorphic studies by Fyles (1984) define a wide thermal aureole around the intrusion. The northern margin, near Columbia-Kootenay Mountain, and the southern margin, south of Rosslund, have a zone of well-indurated biotite hornfels, 300 to 500 metres wide and locally bleached, silicified and containing pyroxene and garnet (Fyles, *op. cit.*). Alteration of mafic minerals in the monzonite to ragged hornblende, biotite and chlorite may be due in part to superimposed regional metamorphism.

AGE

The Rosslund monzonite is interpreted to be a subvolcanic intrusion, cogenetic with the Early Jurassic Elise Formation. It is cut by phases of the Middle Jurassic (*ca.* 165 Ma) Trail pluton.

Petrographic evidence suggestive of subvolcanic intrusion include the common porphyritic textures and the resorbed mineral grains. Intense, hydrothermal alteration throughout the stock, with pervasive alteration of pyroxene and abundant hornblende and biotite, suggest shallow intrusion into a relatively wet host succession. Diffuse, irregular contacts with Elise host rocks and a similar chemistry (see below) also suggest that the Rosslund monzonite is related to the Elise Formation.

A number of K-Ar dates of biotite give ages ranging from 48.1 to 92.3 Ma; these dates reflect metamorphic Tertiary overprinting (Fyles, 1984). U-Pb data of separated zircons from the Rosslund monzonite are given in Table 6-2 and plotted on Figure 6-3. Fraction A plots on the concordia at 194.4 Ma; other fractions cluster near the concordia at *ca.* 165 Ma. Based in part on the subvolcanic nature of the Rosslund monzonite, we interpret the older date to be the age of crystallization, supporting syn-Elise intrusion. The *ca.* 165 Ma fractions are similar to the age of the Nelson intrusions, including the Trail pluton, that cut the Rosslund monzonite. They may reflect resetting associated with Pb loss during circulation of Nelson-age magmatic fluids, an interpretation supported by molybdenite mineralization in the vicinity of the Rosslund monzonite that is inferred to be related to Nelson intrusions (Fyles, 1984; Höy *et al.*, 1992). However, J. Gabites and J. Mortenson (personal communication, 1996) suggest that these data support a Middle Jurassic age for the Rosslund monzonite.

Additional dating may be required to determine the age of the Rosslund monzonite with more certainty.

Other intrusions of Sinemurian age in southeastern British Columbia include a small massive to foliated diorite on the southwest side of the Valhalla complex, dated at 193 ± 1 Ma (Parrish, 1992) and the Lexington porphyry in the Greenwood camp, dated at *ca.* 200 Ma (Church, 1992). The Lexington porphyry has been explored recently for its copper-gold porphyry potential (Seraphin *et al.*, 1995).

ROSSLAND SILL

The Rosslund sill is exposed on the eastern slope of Red Mountain near Rosslund. It has similar mineral assemblages to the Rosslund monzonite and to some of the mafic phases of the Elise Formation. The sill is fragmental in part, with blocks up to a metre wide with

the same composition as the matrix (Fyles, 1984). Its upper contact with hornfelsed siltstones of the Elise Formation, observed in drill core at the Gertrude prospect, appears to be gradational, with a number of thin sills interlayered with siltstone. It is generally concordant, but in detail is locally transgressive (Fyles, *op. cit.*).

The Rosslund sill is inequigranular to porphyritic with 30 to 40 per cent euhedral, sausseritized, oscillatory zoned calcic andesine to sodic labradorite (An 48-54) and 25 per cent orthoclase. Mafic minerals (30 per cent) comprise nearly equal proportions of augite, a blue-green amphibole and biotite. The blue-green amphibole is probably secondary hornblende and may be described as uralite. The augite is oscillatory zoned and is often rimmed with hornblende (Plate 6-4). Accessory apatite in the sill has distinct mineral cores.

Table 6-2: U-Pb zircon data, sample H88R-rsm, Rosslund monzonite.

Fraction: ^{1,2}	wt	U ³	Pb ³	²⁰⁸ Pb	Pb	²⁰⁶ Pb	Isotopic Ratios ($\pm 1\sigma$)			Isotopic Dates (Ma, $\pm 2\sigma$)	
	mg	ppm	ppm	% ⁴	pg ⁵	²⁰⁴ Pb	²⁰⁶ Pb/ ²³⁸ U	²⁰⁷ Pb/ ²³⁵ U	²⁰⁷ Pb/ ²⁰⁶ Pb	²⁰⁶ Pb/ ²³⁸ U	²⁰⁷ Pb/ ²⁰⁶ Pb
						6					
H88R-rsm	Rosslund monzonite										
a N2,+a abr	0.200	364	12	19.1	166	826	0.03062 (.23)	0.2113 (.50)	0.05005 (.41)	194.4 \pm 0.9	197 \pm 19
b N2,+d abr	0.400	464	13	19.2	152	1986	0.02568 (.08)	0.1751 (.15)	0.04945 (.09)	163.4 \pm 0.2	169.1 \pm 4.4
c M2,+d abr	0.400	592	17	19.2	309	1253	0.02590 (.15)	0.1766 (.37)	0.04947 (.28)	164.8 \pm 0.4	170 \pm 13
d M1.5,-d abr	0.600	741	22	18.6	603	1196	0.02634 (.27)	0.1797 (.44)	0.04946 (.29)	167.6 \pm 0.9	169.9 \pm 14
e M1.5,-d abr	0.179	773	22	18.7	105	2176	0.02605 (.10)	0.1805 (.16)	0.05025 (.10)	165.8 \pm 0.3	206.6 \pm 4.7
f N2,+d abr	0.065	762	23	19.7	44	1862	0.02625 (.06)	0.1798 (.13)	0.04967 (.10)	167.0 \pm 0.2	179.6 \pm 4.9

Notes: Analyses by J.E. Gabites, 1989 - 96, in the Geochronology Laboratory, Department of Geological Sciences, The University of British Columbia.

IUGS conventional decay constants (Steiger and Jäger, 1977) are: $^{238}\text{U}\lambda=1.55125\times 10^{-10}\text{a}^{-1}$, $^{235}\text{U}\lambda=9.8485\times 10^{-10}\text{a}^{-1}$, $^{238}\text{U}/^{235}\text{U}=137.88$ atom ratio.

1. Column one gives the label used in the figures.
2. Zircon fractions are labelled according to magnetic susceptibility and size. NM = non-magnetic at given amperes on magnetic separator, M = magnetic. Side slope is given in degrees. The - indicates zircons are smaller than, + larger than the stated mesh (μ). Abr = air abraded.
3. U and Pb concentrations in mineral are corrected for blank U and Pb. Isotopic composition of Pb blank is $206:207:208:204 = 17.299:15.22:35.673:1.00$, based on ongoing analyses of total procedural blanks of 37 ± 1 pg (Pb) and 6 ± 0.5 pg (U) during the time of this study. Include sample weight error of ± 0.001 mg in concentration uncertainty.
4. Total common Pb in analysis
5. Radiogenic Pb
6. Initial common Pb is assumed to be Stacey and Kramers (1975) model Pb at the $^{207}\text{Pb}/^{206}\text{Pb}$ age for each fraction.

Size fractions are: a 149, b 134, c 104, d 74, e $44\mu\text{m}$. n = needles
 Magnetic fractions : N2 = NM2a/1°, M2 = M2a/1°, M1.5 = M1.5a/3°

Location: $117^{\circ}47'66''\text{W}$; $49^{\circ}05'\text{N}$

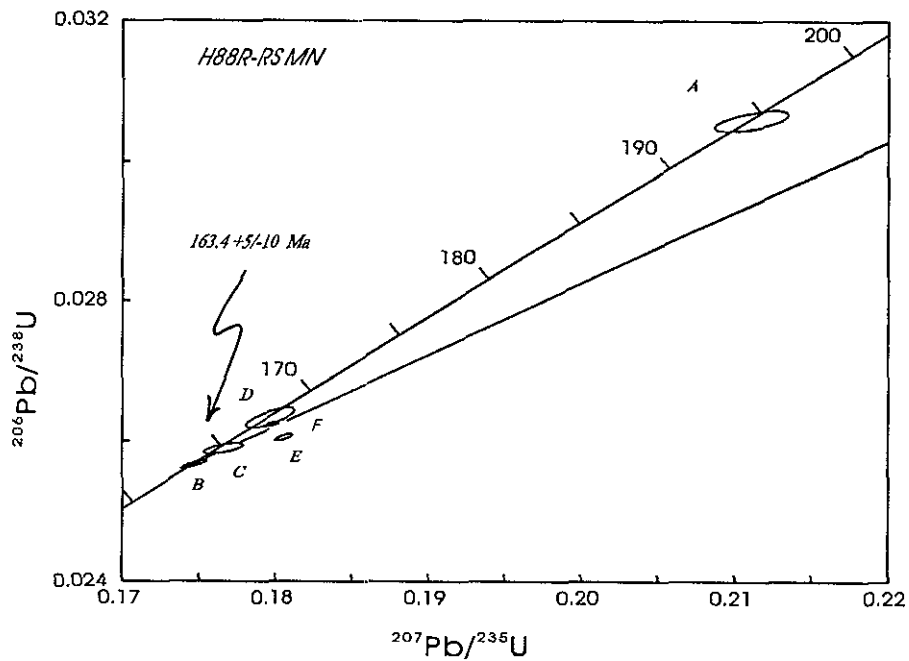


Figure 6-3. Plot of U-Pb zircon data, sample H88-Rsmn, Rossland monzonite.



Plate 6-4: Augite rimmed by hornblende in the Rossland sill (view = 1.48 mm).



Plate 6-5: Symplectite texture of magnetite-clinopyroxene mantled by biotite in the Rossland sill (view = 370 microns).

Symplectite textures of magnetite or ilmenite and clinopyroxene are common in the Rossland sill (Plate 6-5). On Monte Cristo Mountain, opaque oxide has symplectite textures and is mantled by biotite.

MONZOGABBRO INTRUSIONS

A number of monzogabbro/gabbro sills or small stocks occur throughout the exposures of the Elise Formation and are interpreted to be high-level syn-Rossland Group intrusions. They are typically tabular, lensoid or sill-like, several tens of metres thick and can often be traced for several kilometres. Others are subrounded, discordant plutons. They are fine to medium grained and often porphyritic with 30 to 40 per cent plagioclase phenocrysts in dark green-grey matrix. They are petrographically distinct from the Eagle Creek plutonic complex, Rossland monzonite and Silver King intrusions. Monzogabbro stocks can occur anywhere within the Elise Formation but tend to be mainly in the upper part. Their locations are shown on Figure 6-1.

Examples in the Nelson map-area include the Shaft, Mammoth and Katie intrusions. Shaft is a tabular, locally brecciated complex up to 50 metres in width and 5 kilometres in strike length. This monzogabbro intrusion has pervasive propylitic alteration that hosts disseminated chalcopyrite, pyrite and magnetite (Andrew and Höy, 1989).

PETROGRAPHY

Monzogabbros in the Nelson area have the widest diversity of mineral assemblages. Most are found intruding both upper and lower Elise Formation rocks within 5 kilometres south and west of Nelson, in the plateau areas east of Toad Mountain and in the vicinity of Morning Mountain. They are characterized by 15 to 45 per cent labradorite (An 50-67), rarely saussuritized, a significant orthoclase component (5 to 25 per cent), and minor quartz (2 to 10 per cent). Primary mafic minerals are rarely seen (Plate 6-6), as they are commonly altered to hornblende, biotite, chlorite and epidote. Often, these intrusions have a fine-grained matrix of feldspar and chlorite with up to 1 per cent apatite and 1 per cent magnetite and pyrite. The Nelson area intrusions fall within the monzonite, (quartz) monzogabbro and quartz gabbro fields on Streckeisen's (1973) quartz-alkali feldspar-plagioclase diagram (Figure 6-2).

The Shaft intrusion, exposed 3 kilometres south of Nelson (Figure 6-1), is a fine to medium-grained, locally porphyritic monzogabbro. It is brecciated and locally sheared. It contains 30 to 45 per cent labradorite (An 50-64), 5 to 10 per cent orthoclase and 2 to 3 per cent quartz. It ranges in composition from quartz gabbro to quartz monzogabbro and monzogabbro. The feldspars are variably saussuritized and sericitized (10 to 25 per cent). Biotite, chlorite and epidote have totally replaced all mafic minerals. Apatite and sphene are present as

accessory minerals. Opaques include chalcopyrite, pyrite and magnetite. Hematite and malachite are common oxide minerals.

A number of monzogabbro intrusions north and east of Fruitvale are quartz-poor but have diverse feldspar compositions. They are characterized by 30 to 45 per cent plagioclase (dominantly labradorite: An 54-69), rarely concentrically zoned or saussuritized, and varying orthoclase content (0 to 25 per cent); quartz is generally absent. Augite is usually preserved but variably altered to hornblende and chlorite. These monzogabbros may have a fine-grained matrix of feldspar, biotite and chlorite. Accessory apatite is rarely seen. Up to five per cent opaque minerals, mainly pyrite, are present. The Fruitvale area monzogabbros plot within the monzonite, monzogabbro and gabbro fields (Figure 6-2).

Monzogabbros in the Rossland area are quartz-poor and alkali-feldspar poor. Most are found in the Elise Formation south of Rossland on Tamarac Mountain or Deer Park Hill. They are characterized by 20 to 55 per cent euhedral labradorite and bytownite (An 58-88), typically saussuritized, minor orthoclase and no quartz. Augite is still preserved but variably altered to biotite and chlorite. Apatite is rare and up to seven per cent



Plate 6-6: Hornblende, chlorite and epidote in "gabbro" from the Nelson area (view = 1.48 mm)

opaque minerals, mainly pyrite, occur in the matrix. These monzogabbros are mainly within the gabbro field on Figure 6-2.

PETROGRAPHY SUMMARY: EARLY JURASSIC PLUTONS

Mineral assemblages and alteration patterns of Early Jurassic plutons support a model of magmatic crystallization in high-level subvolcanic magma chambers. Island arc intrusions are commonly porphyritic and characterized by assemblages indicative of high volatile content. High calcium content of plagioclase phenocrysts, locally producing gabbros, is evidence of high water content, as is the crystallization of microcline as opposed to orthoclase and the occurrence of granophyric intergrowths (Parsons, 1978). Calcic augite reflects high water fugacities, supported by the ubiquitous, probably deuteric alteration to hornblende.

The differentiated nature of high-level arc intrusions and their high volatile content promotes scavenging and concentration of metals, accounting for the numerous deposits associated with these intrusions. In particular, copper and gold, abundant in associated mafic arc volcanics, tend to concentrate as vein, porphyry and skarn deposits within and along the margins of Early Jurassic plutons in the Rossland Group.

GEOCHEMISTRY: EARLY JURASSIC PLUTONS

INTRODUCTION

There are few geochemical studies on coarse-grained igneous rocks (*e.g.* Hanson, 1978; Debon and Le Fort, 1983; Pearce *et al.*, 1984; Maniar and Piccoli, 1989). Most variation and discriminant diagrams are constructed using aphyric basalt flows. The main reason for the apparent paucity in coarse-grained igneous rock discrimination diagrams is their more complicated petrogenetic histories and, hence, difficulties in interpretation.

Geochemical discrimination diagrams for "granite" or "granitoid" rocks make up the majority of studies on plutonic rocks. Granitoids are usually defined as >60 weight per cent SiO₂ and/or >2 modal per cent quartz. Geochemical signatures of granites can be obscured by crystal accumulation, involvement of continental crust, redistribution and loss of elements by volatile fluxing and crystallization of trace element-rich minor phases (Pearce *et al.*, 1984). However, granites are often less susceptible to alteration than their fine-grained mafic counterparts allowing cautious use of mobile elements in understanding their petrogenesis and tectonic setting.

ELIMINATION OF "ALTERED" DATA

Figure 6-4 is a plot of weight per cent K₂O versus weight per cent SiO₂ for all plutonic rocks analyzed from the Nelson-Rossland area (Appendix 3). Labeled samples are from intrusions associated with mineral occurrences. High K₂O values suggest that the Silver King, Star and Shaft prospect samples have undergone some degree of alkali metasomatism, a similar conclusion reached for Elise volcanic rocks near these deposits, whereas the Kena, Second Relief and Ymir occurrence samples have lower K₂O contents (<5 wt. % K₂O) and are interpreted to be in the range of unaltered samples.

Geochemical samples proximal to mineral occurrences in the Rossland-Nelson area are not included in most figures. It is difficult to eliminate potentially altered plutonic rock samples more rigorously since methods like Beswick and Soucie (1978) apply only to fine-grained igneous rocks.

ALKALINITY

Analyses of samples proximal to mineral occurrences have been removed from the K₂O versus SiO₂ plot of Figure 6-5 (*cf.*, Figure 6-4). These "least altered" samples are used in all subsequent variation diagrams and plots of alkalinity, rock name, and tectonic discrimination. The Eagle Creek, Rossland and monzogabbro intrusions have very high-K or alkaline characteristics with restricted SiO₂ contents (< 60 wt.%). In contrast, the Silver King and Nelson intrusions have medium to high-K calcalkaline characteristics, spanning the compositional range from gabbro to granite.

On a total alkalis versus silica diagram (Irving and Baragar, 1971), the Eagle Creek complex and monzogabbro intrusions define an alkaline trend (A), the Rossland intrusions, a boundary trend (B), and the Silver King and Nelson intrusions, a calcalkaline trend (C); (*see* Figure 6-15). These trends may reflect crystallization of plutons in progressively more differentiated magma chambers.

NOMENCLATURE

CIPW normative calculations are given for least altered samples in Table 6-3. Rocks of the Eagle Creek plutonic complex are dominantly silica undersaturated whereas other Early Jurassic intrusions are mainly silica oversaturated.

Chemical data can be graphically portrayed to classify intrusions; two classifications are considered, one by Debon and Le Fort (1983) and the other by Le Maitre (1989).

Debon and Le Fort devised a chemical-mineralogical classification of common plutonic rocks based on a quartz-plagioclase-orthoclase diagram of La Roche *et al.* (1980). Their superimposed grid (Figure 6-6) allows classification of silica-saturated and silica

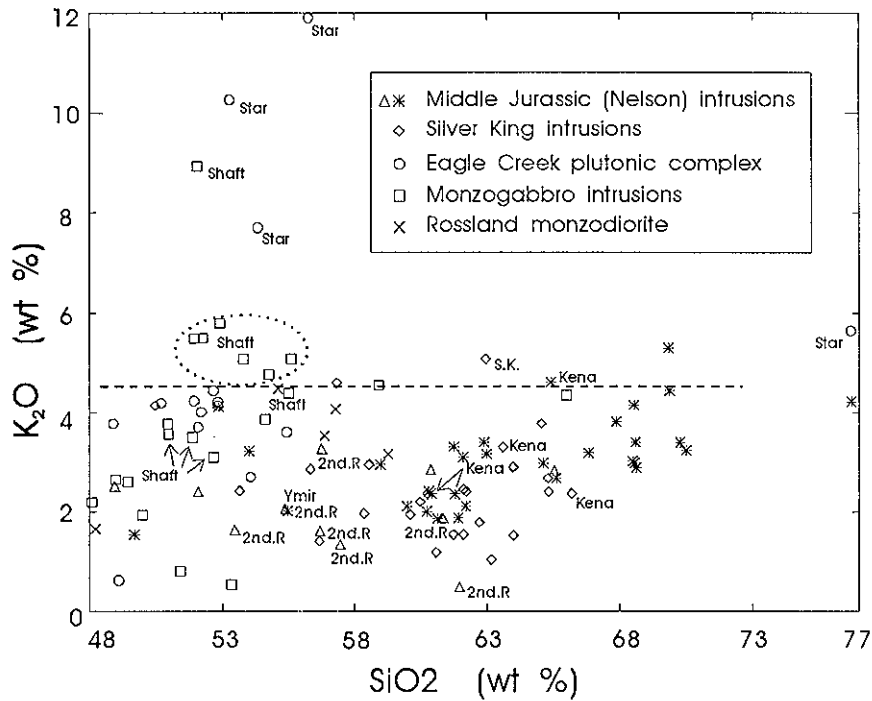


Figure 6-4. A plot of wt. % K_2O versus wt. % SiO_2 of samples of Trail area intrusive rocks, showing the effects of alteration associated with mineralization on their compositions.

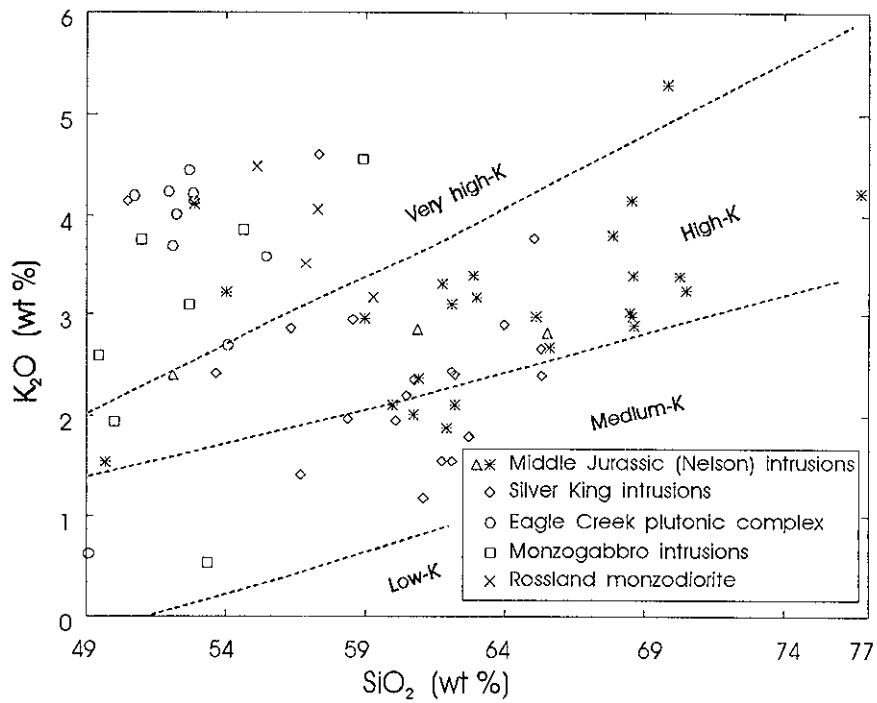


Figure 6-5. A plot of wt. % K_2O versus wt. % SiO_2 of "unaltered" or "least altered" Trail map-area intrusive rocks.

Table 6-3: CIPW normative calculations for Rossland-Nelson least altered intrusions
(Ol - olivine; Hy - hypersthene; Qz - quartz; Ne - nepheline)

Sample	Normative Minerals	Saturation	Sample	Normative Minerals	Saturation
Eagle Creek complex:			6-11	Qz,Hy	over
73-3	Ol,Hy	sat	16-3	Qz,Hy	over
75-1	Ol,Hy	sat	23-2	Qz,Hy	over
75-2	Ol,Ne	under	27-7	Qz,Hy	over
75-4	Qz,Hy	over	33-15	Qz,Hy	over
L5-15	Ol,Ne	under	18-1	Qz,Hy	over
L4-1I	Ol,Hy	sat	21-7	Qz,Hy	over
L4-1D	Ol	under	39-5	Qz,Hy	over
L4-1A	Ol,Ne	under	41-10	Qz,Hy	over
L1-13	Ol,Ne	under	84-7	Qz,Hy	over
L1-7	Ol,Ne	under	47-2	Qz,Hy	over
L5-1	Ol	under	85-4	Qz,Hy	over
L4-2	Ol	under	85-13B	Qz,Hy	over
Lower Jurassic gabbro/monzonite sills			86-18	Qz,Hy	over
86-26A	Qz,Hy	over	86-24	Qz,Hy	over
92-11	Qz,Hy	over	92-4	Qz	over
157-2	Qz,Hy	over	137-9	Qz,Hy	over
196-16	Ol,Hy	sat	144-3	Qz,Hy	over
198-2	Ol	under	137-3	Ol,Hy	sat
264-22	Qz,Hy	over	Nelson intrusions		
270-3	Qz,Hy	over	28-11	Qz,Hy	over
278-38	Qz,Hy	over	57-21	Qz,Hy	over
286-11	Qz	over	61-6B	Qz,Hy	over
301-8	Qz,Hy	over	64-9	Qz,Hy	over
324-14	Qz,Hy	over	65-2	Qz,Hy	over
Mammoth intrusions			62-8	Qz,Hy	over
91-6	Qz,Hy	over	72-4	Qz,Hy	over
91-14	Ol	under	72-8	Qz,Hy	over
93-5	Qz,Hy	over	72-10	Qz,Hy	over
99-8	Qz,Hy	over	74-6	Qz,Hy	over
Rossland monzonite			74-13	Qz,Hy	over
286-9	Qz,Hy	over	87-6	Qz,Hy	over
287-7	Qz,Hy	over	87-7	Qz,Hy	over
287-14	Qz,Hy	over	90-1A	Qz,Hy	over
320-14	Qz,Hy	over	91-15	Qz,Hy	over
323-3	Qz,Hy	over	69-5	Qz,Hy	over
324-22	Qz,Hy	over	85-13C	Qz,Hy	over
Silver King intrusions:			99-9	Qz,Hy	over
4-20	Qz,Hy	over	115-1	Qz,Hy	over
6-1	Qz	over	116-15	Qz,Hy	over
			117-13	Qz,Hy	over
			123-R	Qz,Hy	over
			135-2	Qz,Hy	over
			120-8	Qz,Hy	over
			213-5	Qz,Hy	over

oversaturated rocks only and, therefore, the dominantly silica undersaturated samples of the Eagle Creek intrusions are not plotted. On this plot, samples of the Rosslund monzonite range in composition from monzogabbro to quartz monzonite. Other small synvolcanic intrusions are monzogabbros, in agreement with the petrographic modal mineralogy described above.

On a quartz - alkali feldspar - plagioclase meso-normative plot (Le Maitre, 1989), sample nomenclatures closely match the petrographic names of Dunne and Höy (1992), Fyles (1984) and Little (1960). However, several mafic to ultramafic samples of the Eagle Creek complex do not plot on this figure probably because the mesonormative mafic minerals exceed 90 per cent and/or the mesonorm does not contain more than 10 per cent quartz, alkali feldspar plus plagioclase, a requirement for this plot.

These data are summarized in Table 6-4. In general, there is considerable agreement in names using the various plots and the modal mineralogies.

ALUMINOUS CHARACTER

The aluminous character of plutonic rocks may have important implications regarding mineralogy and petrogenesis as well as ore potential. Two diagrams are used to evaluate the aluminous character: Shand's index (Figure 6-7) and a more evolved version of the index by Debon and Le Fort (1983).

Shand's index (Shand, 1951) illustrates that Early Jurassic plutons have a metaluminous character, in contrast to the Middle Jurassic Silver King and Nelson which are both metaluminous and peraluminous (Figure 6-7). This has implications regarding tectonic setting, as described below.

Shand's index of $A=Al-(K+Na+2Ca)$ and the parameter $B=(Fe+Mg+Ti)$ of La Roche *et al.* (1980) are used to further define the aluminous character of these intrusions in Figure 6-8. The parameter B reflects the proportions by weight of dark minerals in common granitoid rocks (Debon and Le Fort, 1983). Early Jurassic plutons are dominantly metaluminous, usually characterized by minerals that are Al-poor and Ca-rich (*e.g.*, hornblende, augite, diopside, epidote, sphene, calcite). These are the dominant mineral phases of the Rosslund monzonite and the other small subvolcanic plutons. In contrast, peraluminous plutons are Al-rich and Ca-poor, with typically minerals such as biotite, muscovite, aluminosilicates, cordierite, tourmaline and topaz. These minerals are more common in the younger Middle Jurassic plutons of the Nelson-Rosslund area with, for example, the Silver King and Nelson intrusions commonly containing several per cent igneous biotite. Although use of Figure 6-8 can be justified from a descriptive point of view, it may not have genetic implications since magmatic associations commonly cross the metaluminous-peraluminous boundary (*cf.*, dashed lines in Figure 6-8).

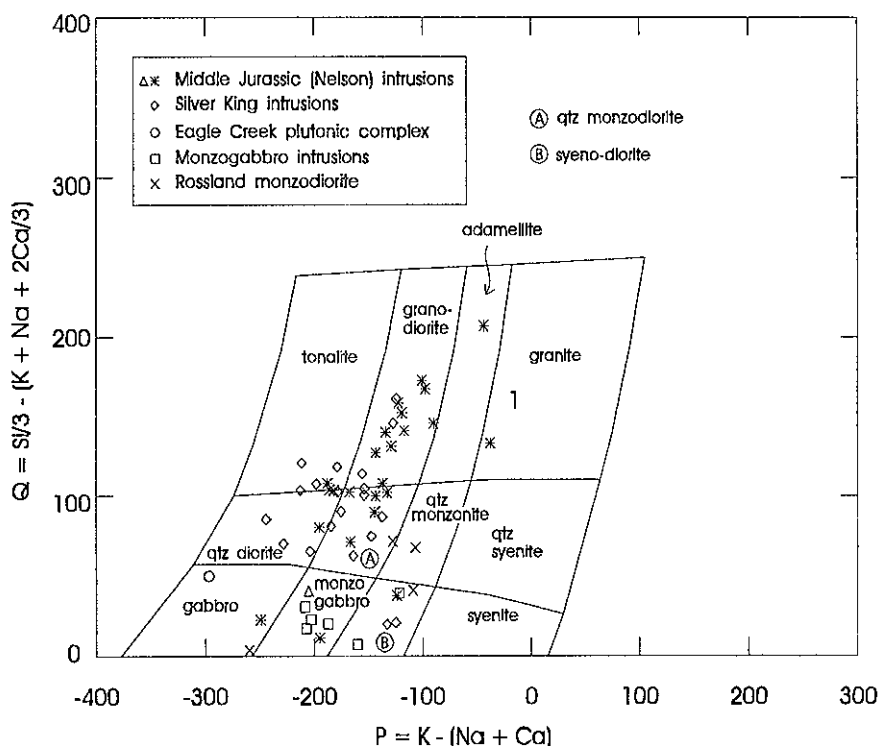


Figure 6-6. A Q-P plot of least altered Early Jurassic plutons, Tail map-area (from Debon and Le Fort, 1983).

FRACTIONAL CRYSTALLIZATION TRENDS

Before determining fractional crystallization trends, it is necessary to determine that suites of rocks are genetically related. Pearce element ratio (PER) diagrams (Pearce, 1968; Russell and Nicholls, 1988; Russell *et al.*, 1990) can be used to evaluate co-genesis by plotting incompatible element ratios for the sample suites involved. For example, a plot of P/Y versus Nb/Y of all sampled plutons (Figure 6-9) shows that P and Nb have virtually constant ratios, within analytical errors, in the Eagle Creek, Rosslund monzonite and monzogabbro intrusions. This supports a model that these plutons are co-genetic.

Approximate linear trends on Figure 6-10 are consistent with the fractionation of ferromagnesian minerals and plagioclase from parental basaltic magma. However, this trend is not evident between Al_2O_3 and SiO_2 . Relationships between some variables can be more clearly demonstrated by ratioing the variable with an element or parameter that remains constant. Applying PER's with yttrium as a denominator (Figure 6-11), a linear positive trend is apparent between Al_2O_3 and SiO_2 suggesting that aluminum is an important element in the crystal fractionation of these plutonic suites.

PER diagrams can also be used to evaluate a hypothesis of alkali feldspar crystal fractionation to explain the observed chemical diversity of these rocks. Variations between Pearce element ratios can be directly related to mineral formulae in order to explain mineralogical and chemical changes.

The effects of alkali feldspar fractionation are modelled on a PER diagram (Figure 6-12) with axes:

$$Y = Na + K/i$$

and $X = Al/i$, where i = a conserved element (yttrium in this case).

Rock compositions that are related through accumulation or loss of alkali feldspar define a trend with a slope of one on this diagram. Since the plutonic rock data define a positive slope of approximately 0.5, not 1.0, minerals other than the alkali feldspars are involved in the fractionation of Na and K.

TECTONIC IMPLICATIONS

Implicit in the tectonic interpretations of alkali-lime indices (Peacock, 1931; Shand, 1951) is the assumption that "calc-alkaline" granites are the products of volcanic arc magmatism, that "alkaline" and "per-alkaline" magmas are associated with within plate settings and that "peraluminous" granites result at continent-continent collisions (Pearce *et al.*, 1984). Although tectonic classification schemes based on these major elements are useful, they are limited as they do not use immobile trace elements.

In Figure 6-13, a limited number of data points with low yttrium and niobium values indicate that the Rosslund monzonite and monzogabbro intrusions plot in the volcanic arc or syn-collisional fields. Separation of these fields by inclusion of rubidium (Pearce *et al.*, 1984) supports the conclusion that the monzogabbro

Table 6-4: Summary of geochemical nomenclature for Rosslund-Nelson area plutonic rocks

Model (Paper)	Eagle Creek plutonic complex	Monzogabbro intrusions	Silver King intrusions	Rosslund monzonite
Streckeisen (1976)	syenite syeno-diorite gabbro	syeno-diorite granodiorite gabbro	syeno-diorite diorite granodiorite	syeno-diorite gabbro
Middlemost (1985)		monzodiorite/ monzogabbro	granodiorite qtz diorite qtz monzo- diorite/gabbro	qtz monzo- diorite/gabbro qtz monzonite monzonite
Debon and LeFort (1983)		monzodiorite/ monzogabbro	granodiorite qtz diorite qtz monzo- diorite/gabbro	monzodiorite/ monzogabbro qtz monzo- diorite/gabbro
Le Maitre (1989)	syenite monzonite	monzonite qtz diorite/ gabbro qtz monzo- diorite/gabbro	granodiorite qtz monzo- diorite/gabbro	monzonite qtz monzo- diorite

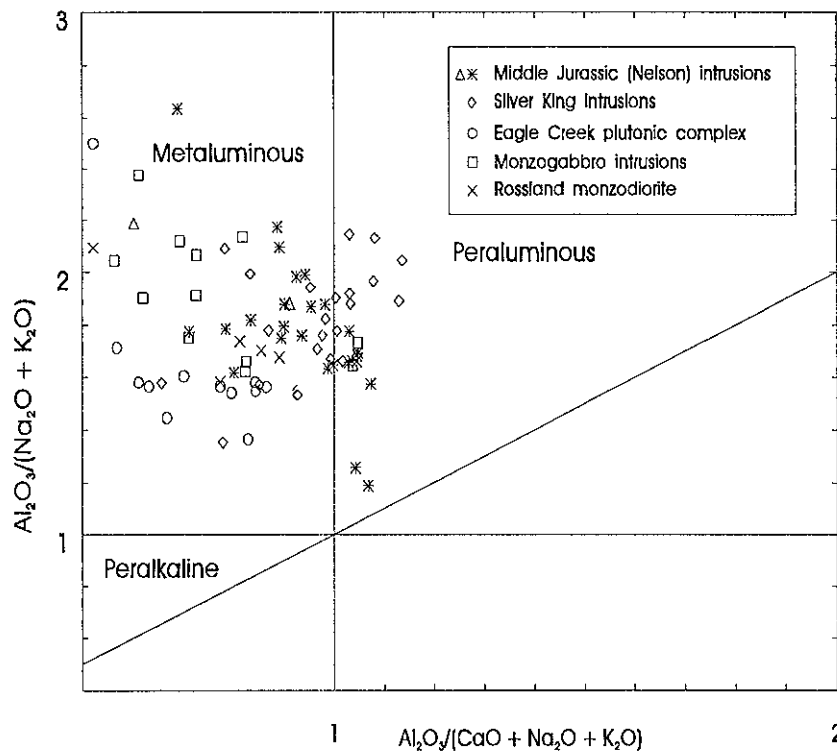


Figure 6-7. A plot of Shand's index: $Al_2O_3/(Na_2O + K_2O)$ versus $Al_2O_3/(CaO + Na_2O + K_2O)$ of least altered Early Jurassic plutons, Trail map-area (after Shand, 1951).

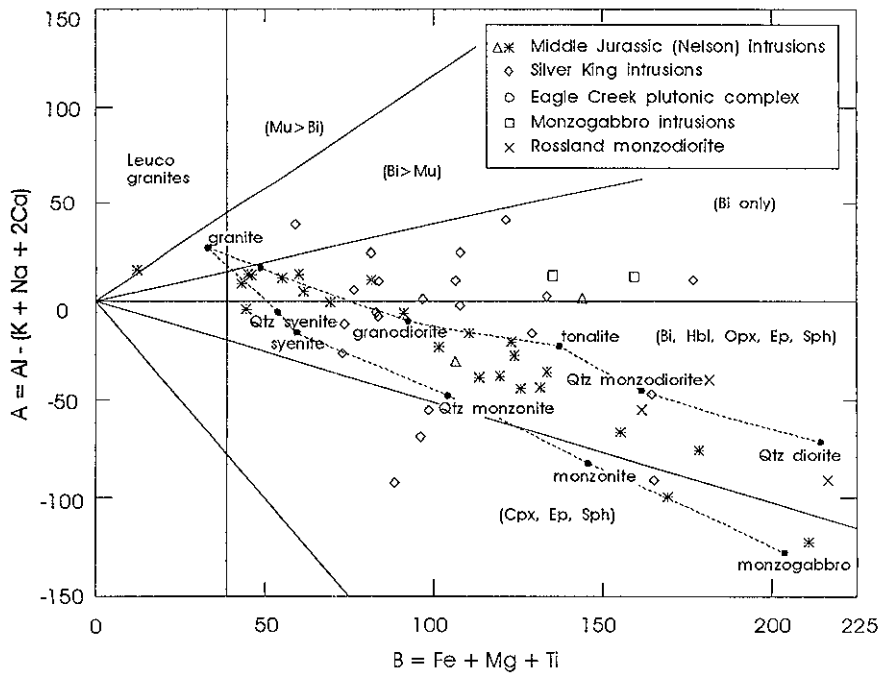


Figure 6-8. A plot of Shand's index: $A = Al - (K + Na + 2Ca)$ versus $B = Fe + Mg + Ti$ of Debon and Le Fort (1983) of least altered Early Jurassic plutons, illustrating their dominantly metaluminous character.

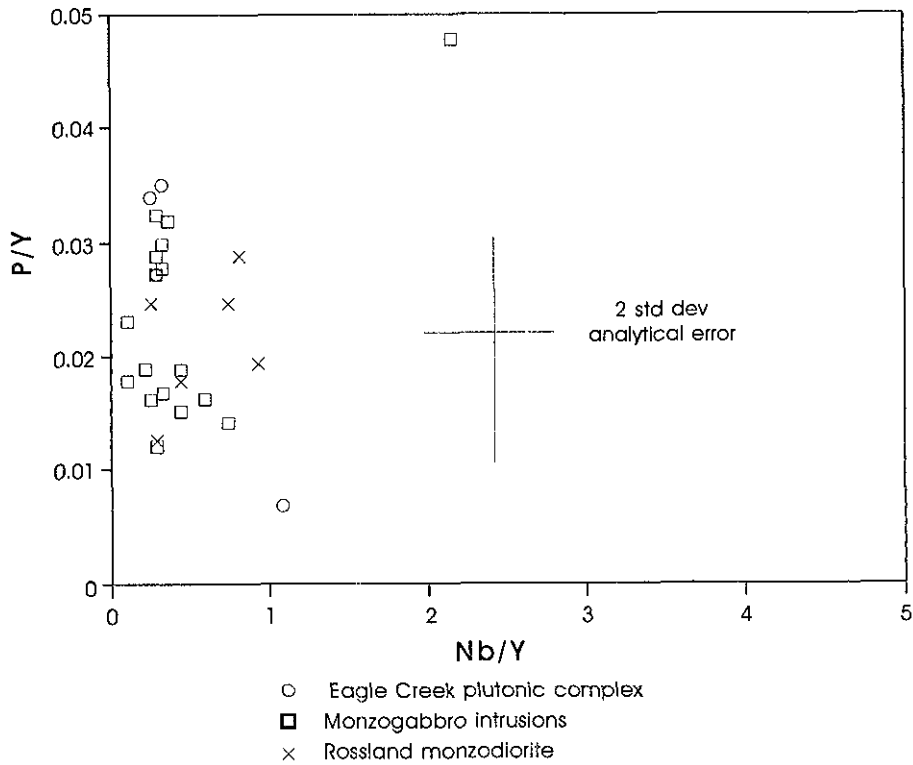


Figure 6-9. A Pearce element ratio plot of P/Y versus Nb/Y to test for cogenesis of least altered Early Jurassic plutons.

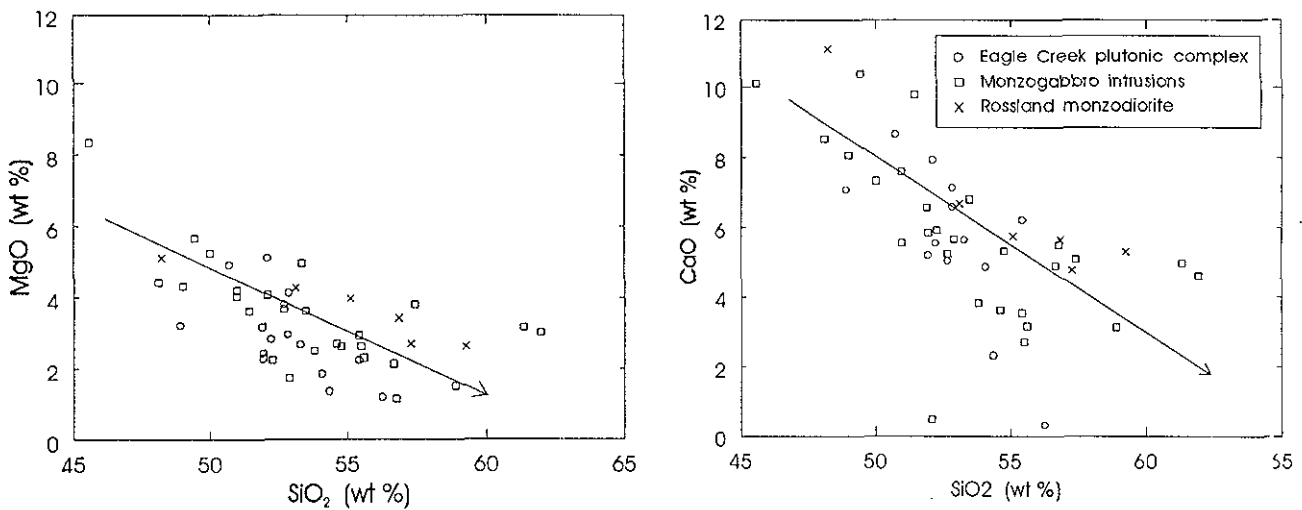


Figure 6-10. A plot of MgO versus SiO₂ (10a) and CaO versus SiO₂ (10b) of Early Jurassic plutons to illustrate fractionation trends.

intrusions are restricted to the volcanic arc field (Figure 6-14).

The Rossland monzonite and the Eagle Creek plutonic complex were both emplaced along major structures, and are both associated with mineralization: gold-copper veins in the Rossland area and dominantly alkali porphyry gold-copper in the Eagle Creek plutonic complex. The ubiquitous presence of both apatite and magnetite in these intrusions is common in Late Triassic to Early Jurassic arc complexes elsewhere in Quesnellia and Stikinia. These intrusive complexes

have phases that are typically calcalkaline as well as phases that resemble feldspar-bearing rocks found associated with Alaskan-type complexes in the Cordillera (Nixon and Hammack, 1991).

Small widely scattered monzogabbros are interpreted to be high-level synvolcanic intrusions. They are restricted to the Elise Formation, have diffuse, commonly brecciated margins, and may be associated with copper-gold-magnetite mineralization (eg., Katie and Shaft prospects).

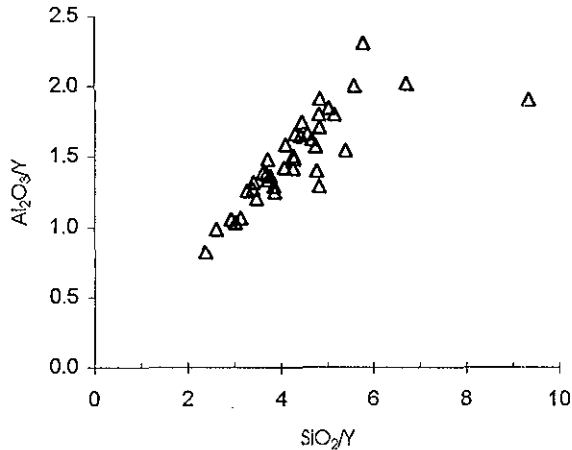


Figure 6-11. A Pearce element ratio plot of Al_2O_3/Y versus SiO_2/Y of least altered Early Jurassic plutons.

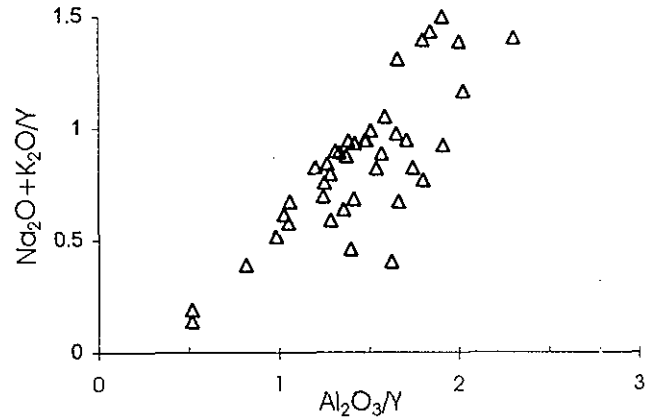


Figure 6-12. A Pearce element ratio plot of $Na+K/Y$ versus Al/Y of least altered Early Jurassic plutons to illustrate the effects of fractional crystallization of alkali feldspars.

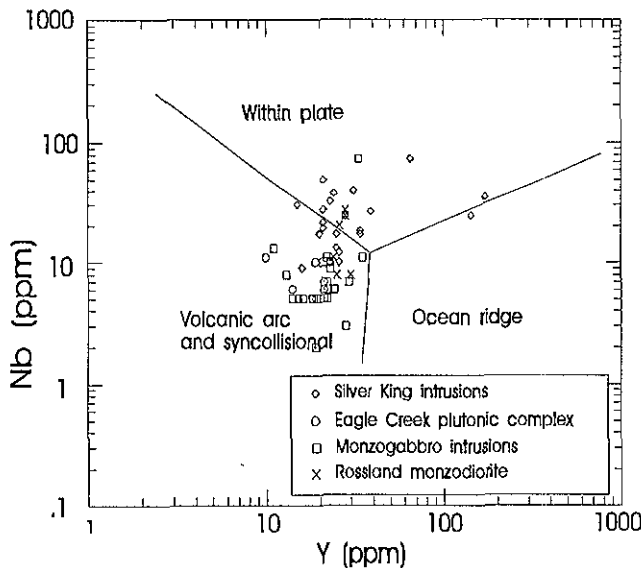


Figure 6-13. A tectonic discrimination plot of Nb versus Y of Early Jurassic plutons illustrating their volcanic arc or syn-collisional setting (after Pearce et al., 1984).

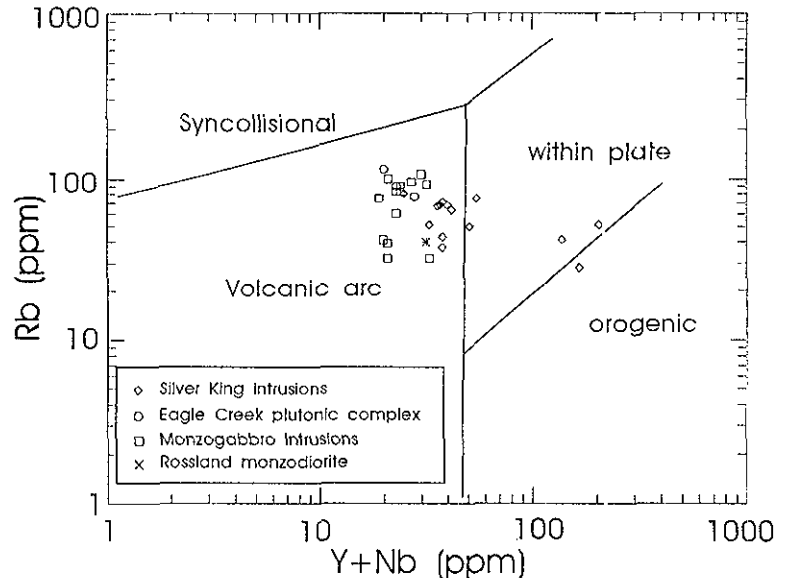


Figure 6-14. A tectonic discrimination plot of Rb versus $Y+Nb$ of Early Jurassic plutons illustrating their volcanic arc setting (after Pearce et al., 1984).

EARLY-MIDDLE JURASSIC PLUTONS

A number of generally highly deformed feldspar porphyries, referred to as the Silver King intrusions, occur within the Elise Formation south of Nelson. They have been dated as Aalenian to Toarcian and are interpreted to be collisional granitoids. Many are associated with copper, gold and silver mineralization.

DESCRIPTION

The main Silver King intrusive body can be traced southeast from Giveout Creek, 1 kilometre south of Nelson, to 5 kilometres south of Nelson (Figure 6-1). Several smaller lenses border this intrusion and others occur on the western slopes of Mount Elise (Andrew *et al.*, 1991).

Outcrops of Silver King intrusions are typically cream-coloured and form resistant ridges. Contacts with Rossland Group rocks are either sharp and discordant or intensely sheared. The Silver King pluton is sheared along its margins. Commonly, smaller lenses form sericite phyllites that resemble, and have been mapped as, foliated felsic volcanic rocks (*eg.*, Lectus). These contact relationships and the foliated to massive nature suggest that the Silver King intrusions are a pre to synkinematic suite.

PETROGRAPHY

Silver King plutonic rocks are porphyritic, characterised by 30 to 60 per cent euhedral to subhedral plagioclase (An₂₈₋₆₀) phenocrysts, 5-10 mm in size (Table 6-1) in a fine-grained greenish grey groundmass.

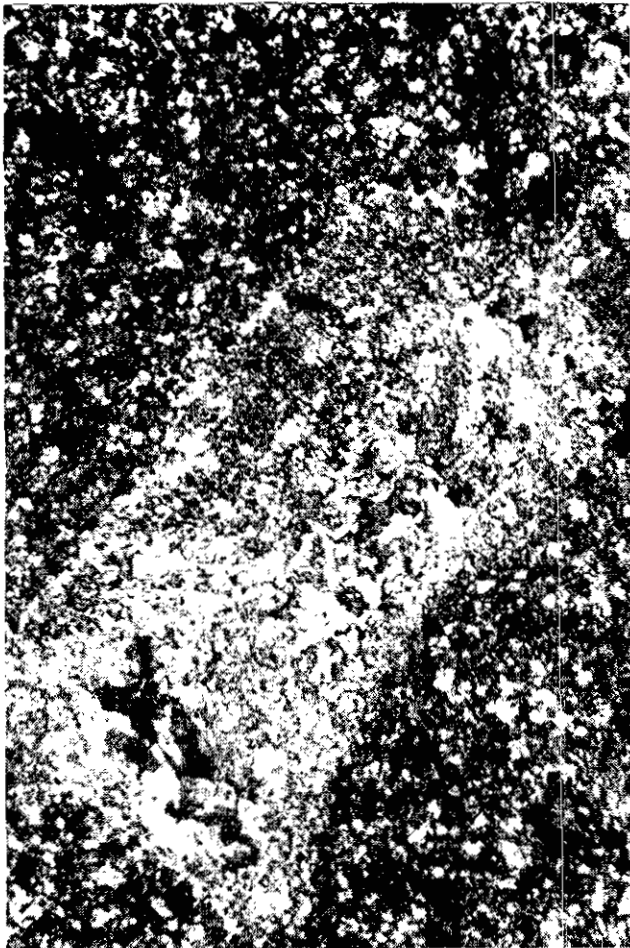


Plate 6-7: Intensely sausseritized plagioclase phenocrysts with inner zones replaced by clusters of sericite needles, in a fine-grained matrix of feldspar and secondary quartz, Silver King intrusion (field of view = 1.5 mm).



Plate 6-8: Cataclastic fabric in the Silver King intrusion; platy minerals rotated into parallelism and rounded feldspar boudins in a protomylonite (field of view = 1.5mm).

Quartz content ranges from 1 to 2 per cent; grains are commonly resorbed which may indicate a high-level of intrusion. Generally, primary mafic minerals are not preserved although acicular secondary hornblende needles are locally observed. Accessory sphene and ilmenite are common (Mulligan, 1951); apatite is rare.

The Silver King intrusion has been strongly altered and sheared. Plagioclase twinning is commonly obscured by intense saussuritization and the inner zones of the phenocrysts are replaced by clusters of sericite needles (Plate 6-7). Mafic minerals are almost totally replaced by chlorite and calcite. The groundmass comprises abundant secondary albite(?), epidote, carbonate and often 10 to 50 per cent interlocking aggregates of quartz grains and sericite "mats".

A cataclastic fabric is typically seen in thin section. This varies from shearing and parallelism of platy minerals to rotation of feldspar boudins in a protomylonite (Plate 6-8). At the Great Western (Lectus) mineral occurrence, a thin Silver King? lens is a quartz-sericite-carbonate schist. This outcrop is unusual because it contains 2 to 3 per cent scattered tourmaline crystals. It was originally mapped as rhyodacite, but based on U-Pb dating is tentatively interpreted as a Silver King intrusion.

Based on petrographic descriptions, the Silver King intrusion falls within the diorite/gabbro field on Streckeisen's (1973) quartz-alkali feldspar-plagioclase diagram (Figure 6-2). As the porphyry has few preserved mafic minerals and plagioclase is generally An < 50, it is classified as a leuco-diorite porphyry.

GEOCHEMISTRY

Major and trace element analyses of samples of Silver King intrusions are listed in Appendix 3. As described above for other Early Jurassic plutons, samples with obvious hydrothermal alteration, or with elevated K_2O values, have been eliminated from the major element plots.

Based on major element chemistry, Silver King intrusive samples are dominantly quartz monzodiorites and granodiorites on both the grid of Debon and LeFort (1983) and a quartz-alkali feldspar-anorthosite ternary diagram of Le Maitre (1989); (Figure 6-6). Some samples also plot in the tonalite and quartz diorite fields. This nomenclature contrasts with the leucodiorite classification based on petrography, probably due to the lack of complete identification of fine-grained matrix minerals as well as locally intense alteration.

Most Silver King samples plot in the calcalkaline field on a total alkali-silica plot (Figure 6-15), in contrast with high-K or alkaline character of many synvolcanic Early Jurassic plutons. It is possible that two samples that plot in the alkaline field have undergone some alteration.

Major element chemistry of these intrusions also suggests that they are "orogenic" granites (Maniar and Piccoli, 1989) with SiO_2 values generally less than 70 per cent and low MgO and FeO values.

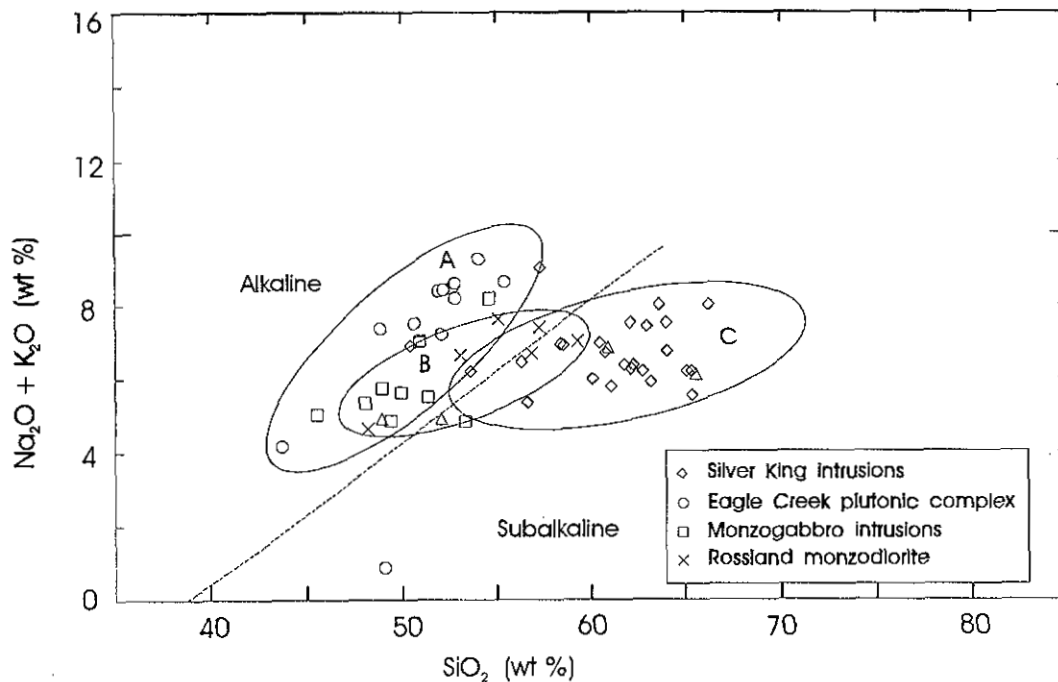


Figure 6-15. Alkali-silica plot of samples of "unaltered" Early Jurassic intrusions; note alkaline trend (A) of Eagle Creek and monzogabbro intrusions, "boundary" trend (B) of the Rosslund monzonite, and calcalkaline trend (C) of younger Silver King intrusions.

Trace element data are also compatible with these being orogenic granites. On a Y versus Nb plot, Silver King samples plot within the syncollisional or volcanic arc fields (Figure 6-13). However, low rubidium values (Figure 6-14) are more comparable to volcanic arc granites (Pearce *et al.*, 1984), perhaps reflecting contamination from the host Elise volcanic package.

AGE AND TECTONIC IMPLICATIONS

Uranium-lead zircon data from Silver King intrusions (Figure 6-1) are listed in Table 6-5 and plotted in Figures 6-16 and 6-17. Discordant data indicate that three of these plutons crystallized *ca.* 174-178 Ma. They are older than the Nelson batholith (*ca.* 165 Ma) and but perhaps similar in age to the Kuskanax batholith (> *ca.* 173 Ma; Parrish and Wheeler, 1983). A fourth intrusion, the intensely sheared Lectus "schist", is dated at *ca.* 185 Ma, similar to the Aylwyn Creek stock (*ca.* 184 Ma; Murphy *et al.* 1994) that hosts the Willa gold-copper-silver deposit near Slocan Lake (Heather, 1985; Wong and Spence, 1995) and the Cooper Creek stock (*ca.* 180 Ma; Klepacki, 1985) northwest of Kaslo, that has been interpreted to be a synorogenic intrusion (Klepacki, *op. cit.*). Many zircon fractions of the Silver King intrusions have clouded xenocrystic cores that record early Proterozoic inheritance.

The Silver King intrusions were interpreted to be a synkinematic plutonic suite (Dunne and Höy, 1992). Small intrusions and margins of large intrusions are penetratively foliated or intensely sheared; others are discordant, massive or only locally foliated. Younger (Nelson) intrusions are largely post intense deformation and metamorphism. The Silver King intrusions may record the first tectonism that affected Rossland Group rocks in southeastern British Columbia. The prominent Early Proterozoic inheritance in all sample suites contrasts with the limited inheritance recognized in Elise volcanic rocks. It is suggested, therefore, that the Silver King intrusions are a syncollisional intrusive suite that records the earliest onlap of the eastern margin of Quesnellia with North American crustal rocks.

MINERAL PROSPECTS

A genetic connection between some of the satellitic phases of the Silver King intrusions and a number of mineral deposits has been suggested by Drysdale (1915, p. 32). Deposit types spatially associated with the Silver King intrusions include shear-related copper-gold and copper-zinc-silver, and vein lead-zinc-silver-gold.

The California prospect is a vein deposit in the Elise Formation between the Silver King intrusion and the Nelson batholith. Quartz veins at the California deposit contain pyrite, galena, sphalerite and free gold. The Great Western and Kena occurrences and Silver King mine are examples of shear-related deposits.

The largest producer "associated with" the Silver King intrusions is the Silver King. The mine began production in 1896 and attracted wide attention to the Nelson area. The Silver King orebody comprises three main shear-controlled veins, with galena, chalcopyrite, pyrite and tetrahedrite and minor sphalerite, bornite and stromeyerite ((Ag,Cu)₂S; Baragar, 1950) within highly sheared Elise Formation mafic volcanic flows near the eastern contact of the Silver King intrusion. The gangue is quartz, carbonate and siderite in sericite schist, a highly sericitized and sheared Silver King intrusion. Although a spatial tie with the intrusion is evident, L. Addie (pers. comm., 1992) argues that the intrusion cuts both mineralization and associated alteration.

MIDDLE JURASSIC PLUTONS

Large plutons of Middle Jurassic age are common in the Intermontane and Omineca Belts, and less common in the Foreland Belt. Typically, these plutons are complex, with early alkaline plutonism followed by calcalkaline and finally, two mica granite. They include the Kuskanax, Nelson, Bonnington and Trail plutons (Figure 6-1), the Galena Bay stock, the Similkameen batholith, the Okanagan intrusions and a number of small stocks in the northern Selkirk Mountains. These have been studied in considerable detail by a number of workers and, hence, will only be described briefly here.

Based on U-Pb analyses of zircons, the age of these granites range from *ca.* 173 Ma to 160 Ma (Ghosh, 1995a; b). The Kuskanax batholith is dated at 173 Ma (Parrish and Wheeler, 1983) and an early phase on the eastern edge of the Nelson batholith is dated at 172.5 ± 5 Ma (Ghosh, *op. cit.*). A similar age has been determined for a feldspar porphyry unit that appears to be related to skarn and vein mineralization at the Second Relief deposit on Erie Creek. This data is summarized in Table 6-6 and plotted on Figure 6-18. Most phases of the Nelson batholith are dated *ca.* 167 Ma (*see* summary in Ghosh, *op. cit.*) with a young, coarse megacrystic phase dated at 161 ± 1 Ma (Ghosh, *op. cit.*) and an equigranular biotite granite dated at 158.9 ± 1 Ma (Sevigny and Parrish, 1993). The Bonnington pluton has a number of 167 Ma dates (Parrish and Wheeler, *op. cit.*; Ghosh, *op. cit.*) and the Trail pluton is dated at 169 ± 3 Ma (Carr *et al.*, 1987).

These Middle Jurassic intrusions are continental arc granitoids that have undergone considerable crustal contamination (Ghosh, 1995a). They record continued subduction of an ancestral Cache Creek ocean with obduction and onlap of the eastern edge of Quesnellia with the North American craton.

Many Middle Jurassic plutons have a variety of mineralized veins or skarns along their margins; the Slocan, Ainsworth, Ymir and Nelson mining camps all occur along the edges of the Nelson batholith, inferring a genetic link. Beaudoin *et al.* (1992) have argued, however, that the Slocan camp is related to Eocene extensional tectonics.

Table 6-5: U-Pb zircon data, Silver King intrusions; data are plotted in figures 6-16 and 6-17.

Fraction: 1,2	wt	U ³	Pb ³	208Pb	Pb	206Pb	Isotopic Ratios ($\pm 1\sigma$)			Isotopic Dates (Ma, $\pm 2\sigma$)	
	mg	ppm	ppm	% ⁴	pg ⁵	204Pb	206Pb/238U	207Pb/235U	207Pb/206Pb	206Pb/238U	207Pb/206Pb
H88R60-4 Silver King pluton, hornblende monzonite											
a N2,+b	0.700	310	9	6.1	104	3723	0.02867 (.12)	0.2111 (.15)	0.05339 (.07)	182.2 \pm 0.4	345.6 \pm 3.4
b N2,-b+d abr	0.300	259	7	6.5	31	4246	0.02809 (.07)	0.1978 (.13)	0.05108 (.09)	178.6 \pm 0.2	244.3 \pm 4.0
c M2,-d+e abr	0.200	374	11	7.0	480	310	0.03015 (.28)	0.2311 (.64)	0.05561 (.50)	191.5 \pm 1.1	436.8 \pm 2.2
d M1.5,-d abr	0.300	321	9	6.5	362	507	0.02956 (.18)	0.2273 (.49)	0.05576 (.40)	187.8 \pm 0.7	442.8 \pm 1.8
e M2,-d+e abr	0.400	441	12	7.1	47	6502	0.02853 (.12)	0.2154 (.15)	0.05475 (.06)	181.3 \pm 0.4	402.1 \pm 2.5
f M2,+d tips abr	0.162	320	9	6.1	22	4273	0.02959 (.08)	0.2315 (.13)	0.05674 (.08)	188.0 \pm 0.3	481.4 \pm 3.5
g M1.5,-d abr	0.085	378	12	7.2	13	4985	0.03212 (.12)	0.2601 (.21)	0.05873 (.12)	203.8 \pm 0.5	557.4 \pm 5.1
i N2,+d t abr	0.169	345	10	6.2	14	7163	0.02958 (.06)	0.2304 (.11)	0.05649 (.06)	187.9	471.5 \pm 2.7
j M2,-b+d t abr	0.042	286	7	5.9	15	1340	0.02730 (.13)	0.1867 (.35)	0.04961 (.28)	173.6	176.7 \pm 1.3
H88R70-1 Silver King pluton, hornblende monzonite											
a N2,-c+d abr	0.400	239	6	6.7	537	318	0.02745 (.59)	.1876 (.19)	0.04956 (1.7)	174.6 \pm 2.0	174 \pm 79
b N2,-d abr	0.900	337	9	5.2	147	3656	0.02930 (.13)	.2210 (.16)	0.05471 (.08)	186.1 \pm 0.5	400.4 \pm 4.0
c M1.5,-d+e abr	0.500	327	13	7.9	248	1651	0.04118 (.21)	.4646 (.27)	0.08183 (.14)	260.2 \pm 1.1	1241.4 \pm 5.5
d M1.5,-d abr	0.100	131	4	11.4	191	139	0.02926 (.24)	.2123 (2.1)	0.05261 (2.0)	185.9 \pm 0.7	312 \pm 92
e M2,-d+e abr	0.900	449	13	7.3	847	886	0.03017 (.18)	.2414 (.39)	0.05804 (.31)	191.6 \pm 0.4	531 \pm 13
f M2,-c+d abr	0.189	341	10	5.5	67	1807	0.0293 (.09)	.2230 (.25)	0.05458 (.17)	188.2 \pm 0.4	395.1 \pm 8.6
g M2,-d+e abr	0.121	374	11	6.6	55	1616	0.03124 (.10)	.2444 (.27)	0.05674 (.20)	198.3 \pm 0.4	481.3 \pm 8.9
H88R-47-2 Quartz monzonite											
a N2,+a abr	0.300	429	15	4.8	92	3037	0.03555 (.13)	0.3489 (.14)	0.07119 (.05)	225.2 \pm 0.6	963.0 \pm 1.9
b N2,-a+d abr	0.400	339	9	3.2	82	3016	0.02939 (.07)	0.2231 (.12)	0.05505 (.07)	186.8 \pm 0.3	414.2 \pm 3.3
c M2,-d+e abr	0.200	414	12	4.6	62	2576	0.03148 (.12)	0.2572 (.16)	0.05925 (.11)	199.8 \pm 0.5	576.3 \pm 4.6
d M1.5,-d+e abr	0.300	563	16	3.3	75	4137	0.03011 (.20)	0.2427 (.22)	0.05846 (.07)	191.3 \pm 0.8	546.9 \pm 3.1
f Ti 2	2.604	42	1	18.8	3649	71	0.02776 (1.0)	0.1910 (3.5)	0.04991 (2.9)	176.5 \pm	191 \pm 143
HR-Lectus Lectus intrusion?, sheared felsic unit											
a N2,+a abr	0.500	562	20	6.4	1665	382	0.0357 (.34)	.370 (.64)	0.07530 (.41)	226.0 \pm 1.5	1077 \pm 17
b N2,-a+d abr	0.150	629	19	3.6	420	455	0.0315 (.14)	.260 (.40)	0.05978 (.32)	199.9 \pm 0.5	596 \pm 14
c N2,-e abr	0.200	769	20	2.5	38	6761	0.0276 (.09)	.205 (.10)	0.05384 (.05)	175.6 \pm 0.3	364.5 \pm 2.4
d M2,-a+b abr	0.200	586	22	6.4	68	4029	0.0387 (.07)	.398 (.11)	0.07456 (.06)	244.8 \pm 0.3	1056.7 \pm 2.4
e M1.5,-d abr	0.400	655	20	3.6	73	6882	0.0316 (.18)	.266 (.20)	0.06111 (.05)	200.4 \pm 0.7	643.1 \pm 2.4
f M2,-d+e abr n	0.403	801	18	-6.3	1053	526	0.0268 (.32)	.223 (.51)	0.06034 (.33)	170.3 \pm 1.1	616 \pm 15
g N2,-a+d abr	0.113	449	9	-3.4	134	554	0.0227 (.15)	.143 (.80)	0.04553 (.75)	145.0	-27 \pm 37

Notes: Analyses and interpretation by J.E. Gabites, 1989 - 96, in the geochronology laboratory, Department of Geological Sciences, U.B.C. IUGS conventional decay constants (Steiger and Jäger, 1977) are: $^{238}\text{U}\lambda=1.55125\times 10^{-10}\text{a}^{-1}$, $^{235}\text{U}\lambda=9.8485\times 10^{-10}\text{a}^{-1}$, $^{238}\text{U}/^{235}\text{U}=137.88$ atom ratio.

1. Column one gives the label used in the figures.
2. Zircon fractions are labelled according to magnetic susceptibility and size. NM = non-magnetic at given amperes on magnetic separator, M = magnetic. Side slope is given in degrees. The - indicates zircons are smaller than, + larger than the stated mesh (μ). Abr = air abraded.
3. U and Pb concentrations in mineral are corrected for blank U and Pb. Isotopic composition of Pb blank is 206:207:208:204 = 17.299:15.22:35.673:1.00, based on ongoing analyses of total procedural blanks of 37 \pm 1 pg (Pb) and 6 \pm 0.5 pg (U) during the time of this study. Include sample weight error of ± 0.001 mg in concentration uncertainty.
4. Total common Pb in analysis
5. Radiogenic Pb
6. Initial common Pb is assumed to be Stacey and Kramers (1975) model Pb at the $^{207}\text{Pb}/^{206}\text{Pb}$ age for each fraction.

Size fractions are: a 149, b 134, c 104, d 74, e 44 μm . n = needles
 Magnetic fractions : N2 = NM2a/1 $^\circ$, M2 = M2a/1 $^\circ$, M1.5 = M1.5a/3 $^\circ$

Locations: H88R60-4: 49 $^\circ$ 25'35"N; 117 $^\circ$ 16'40"W H88R70-1: 49 $^\circ$ 27'12"N; 117 $^\circ$ 17'50"W
 H88R47-2: 49 $^\circ$ 18'20"N; 117 $^\circ$ 13'20"W H88-Lectus: 49 $^\circ$ 26'30"N; 117 $^\circ$ 18'45"W

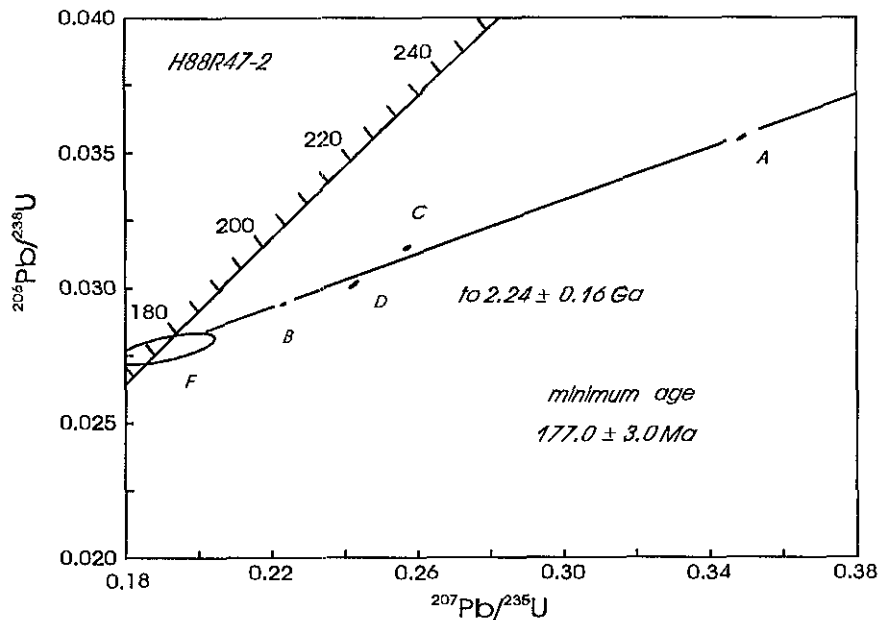


Figure 6-16a. Plot of U-Pb zircon data, sample H88R47-2, Silver King intrusion

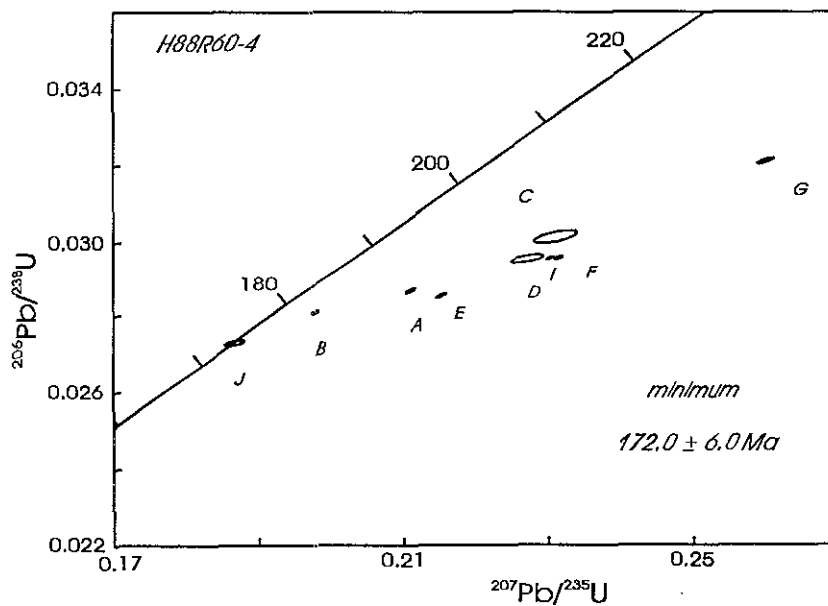


Figure 6-16b. Plot of U-Pb zircon data, sample H88R60-4, Silver King intrusion

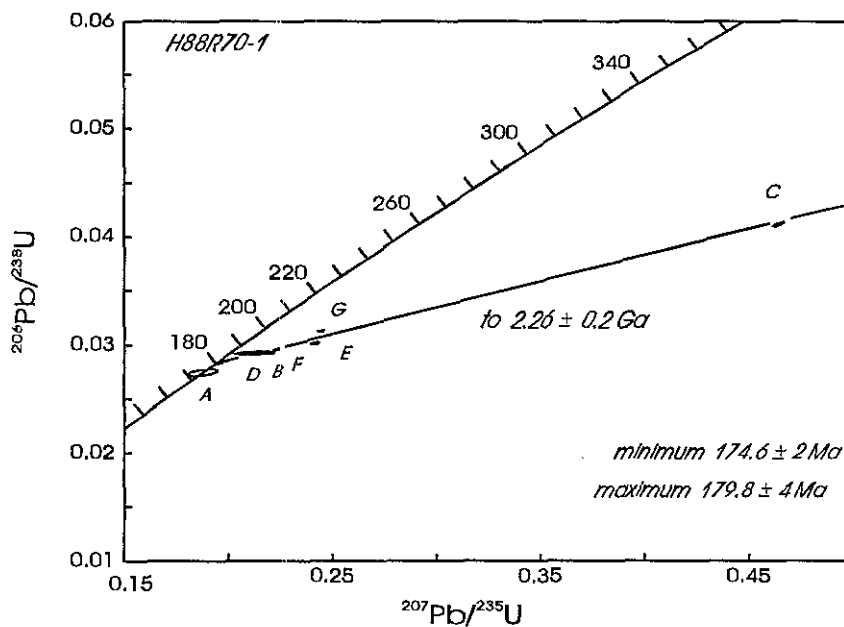


Figure 6-17a. Plot of U-Pb zircon data, sample H88R70-1, Silver King intrusion.

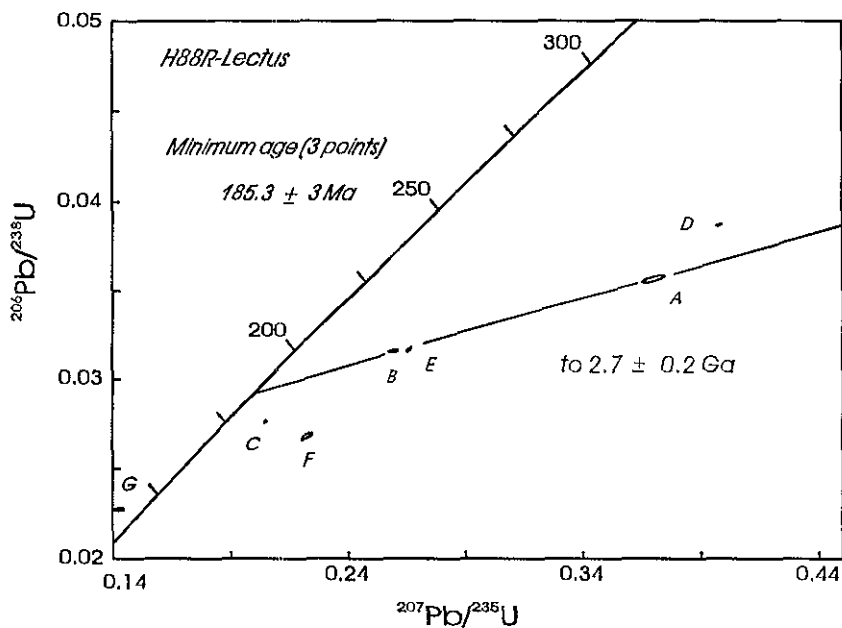


Figure 6-17b. Plot of U-Pb zircon data, sample H88R-Lectus, Silver King intrusion.

Table 6-6: U-Pb zircon data, sample H89R256-5B; data are plotted in Figure 6-18.

Fraction: 1,2	wt	U ³	Pb ³	208Pb	Pb	206Pb	Isotopic Ratios (±%1σ)			Isotopic Dates (Mε, ±2σ)		
	mg	ppm	ppm	% ⁴	pg ⁵	204Pb	206Pb/238U	207Pb/235U	207Pb/206Pb	206Pb/238U	207Pb/206Pb	
H89R256-5B		Nelson granodiorite										
a	N2,+a abr	0.500	390	10	6.7	81	3846	0.02629 (.26)	0.1792 (.32)	0.04944 (.17)	167.3±0.9	168.9±8
b	M2,-a+d abr	0.600	313	8	6.8	35	8562	0.02610 (.22)	0.1782 (.21)	0.04952 (.09)	166.1±0.7	172.6±4.2
c	M1.5,-e abr	0.200	472	12	7.2	38	3975	0.02615 (.15)	0.1795 (.16)	0.04979 (.10)	166.4±0.5	185.1±4.5
d	N2,+a abr	0.302	377	10	6.7	17	10851	0.02636 (.10)	0.1803 (.19)	0.04962 (.10)	167.7±0.5	177.3±4.6
e	M2,-d abr	0.195	408	10	6.8	14	8927	0.02634 (.11)	0.1805 (.20)	0.04970 (.10)	167.6±0.5	181.0±4.8
f	N2,+a abr	0.055	372	9	6.4	10	3208	0.02625 (.09)	0.1793 (.16)	0.04953 (.12)	167.0±0.5	172.9±5.6
g	N2,-b+d abr	0.051	424	12	8.5	1504	43	0.02795 (2.0)	0.2313 (6.0)	0.06000 (4.8)	177.7±0.5	604±225

Notes: Analyses and interpretation by J.E. Gabites, 1989 - 96, in the geochronology laboratory, Department of Geological Sciences, The University of British Columbia.

IUGS conventional decay constants (Steiger and Jäger, 1977) are: $^{238}\text{U}\lambda=1.55125\times 10^{-10}\text{a}^{-1}$, $^{235}\text{U}\lambda=9.8485\times 10^{-10}\text{a}^{-1}$, $^{238}\text{U}/^{235}\text{U}=137.88$ atom ratio.

1. Column one gives the label used in the figure.
2. Zircon fractions are labelled according to magnetic susceptibility and size. NM = non-magnetic at given amperes on magnetic separator, M = magnetic. Side slope is given in degrees. The - indicates zircons are smaller than, + larger than the stated mesh (μ). Abr = air abraded.
3. U and Pb concentrations in mineral are corrected for blank U and Pb. Isotopic composition of Pb blank is 206:207:208:204 = 17.299:15.22:35.673:1.00, based on ongoing analyses of total procedural blanks of 37 ± 1 pg (Pb) and 6 ± 0.5 pg (U) during the time of this study. Include sample weight error of ± 0.001 mg in concentration uncertainty.
4. Total Common Pb in analysis
5. Radiogenic Pb
6. Initial common Pb is assumed to be Stacey and Kramers (1975) model Pb at the $^{207}\text{Pb}/^{206}\text{Pb}$ age for each fraction.

Size fractions are: a 149, b 134, c 104, d 74, e 44 μm . n = needles

Magnetic fractions : N2 = NM2a/1°, M2 = M2a/1°, M1.5 = M1.5a/3°

Locations: H89R256-5B: 49°19'20"N; 117°23'45"W

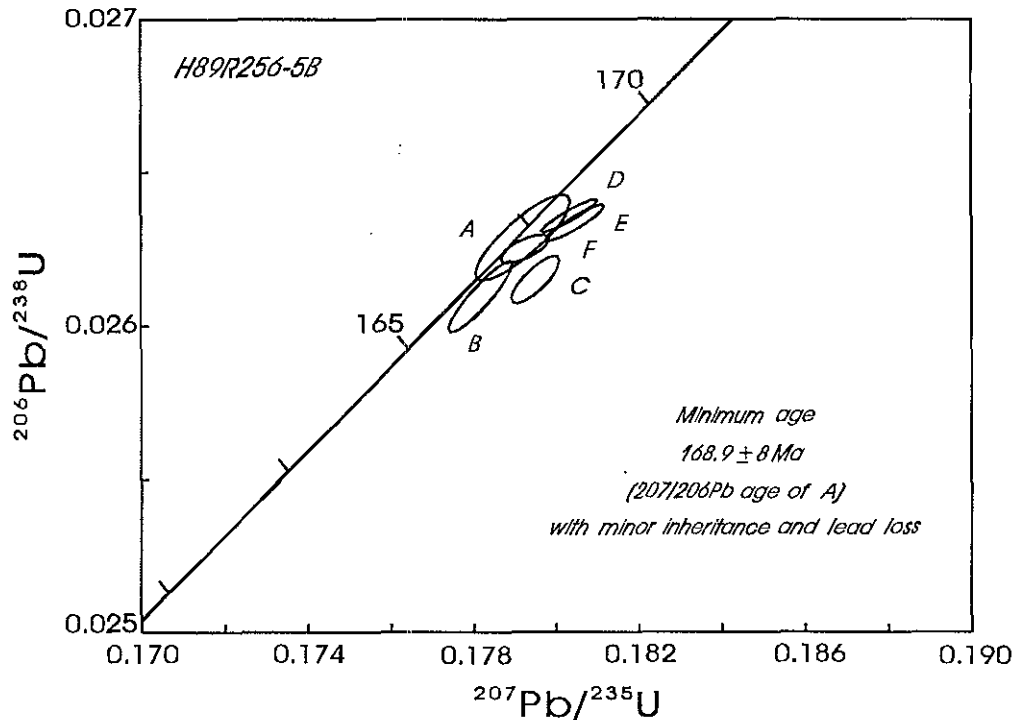


Figure 6-18. Plot of U-Pb zircon data, sample H89R256-5B.

CRETACEOUS PLUTONS

Early and Late Cretaceous granitic rocks also form an extensive plutonic suite in the Omineca belt of southeastern British Columbia. In contrast with the Middle Jurassic plutons, these are discordant, postdating Jurassic regional metamorphism and deformation. However, some are intensely foliated and sheared by Eocene extensional faults. The larger plutons include the Bayonne Batholith and the White Creek stock. Within the Rossland area, they include Castlegar orthogneisses (*ca.* 100-110 Ma) and pegmatites dated at *ca.* 70-80 Ma (Parrish, 1992). Cretaceous plutons, such as the Wallack Creek and Hidden Creek stocks near Salmo, are typically highly evolved S-type leucogranites and granodiorites. Many are associated with tungsten and minor copper, zinc mineralization; the Invincible, Dodger, Emerald and Feeney mines near Salmo are in skarn deposits along the contact of a small Cretaceous stock with Lower Cambrian limestone.

CENOZOIC PLUTONS

Cenozoic plutonic rocks are common north and west of Rossland. Their relationships to the complex Tertiary history of south central British Columbia has

been intensely investigated (*e.g.*, Parrish *et al.*, 1988; Carr, 1991). They are mainly late Paleocene to early Eocene in age, and range in composition from I-type quartz monzonites of the Ladybird suite to highly alkaline Coryell intrusions. Paleocene intrusions may be related to a final phase of compressional tectonics in the eastern Cordillera whereas Eocene magmatism, including both plutonic rocks and alkalic volcanics (Marron Formation), record regional extension associated with normal faulting and denudation of metamorphic core complexes.

SUMMARY

At least three suites of Early to Middle Jurassic intrusions are exposed in the Nelson-Rossland in-area. The Lower Jurassic (*ca.* 194-196 Ma?) Rossland monzonite, Eagle Creek plutonic complex, and small monzogabbros throughout the Elise Formation are interpreted to be coeval with the Rossland Group. They are subvolcanic oceanic arc granitoids related to arc volcanism of the Elise Formation. They are commonly associated with Au-Cu mineralization, including skarn, porphyry (*eg.*, Katie, Shaft), massive Au-pyrrhotite veins in the north and main veins of the Rossland camp, and Pb-Zn-Ag-Au veins to the south.

The Early/Middle Jurassic Silver King intrusions are interpreted to be synorogenic, related to collision

and initial onlap of the eastern margin of Quesnellia with North America. Overlap of U-Pb zircon data suggest crystallization of Silver King intrusions *ca.* 174-178 Ma. This contrasts with a *ca.* 185 Ma date on the Lectus quartz-sericite schist, which has been variously interpreted as an Elise rhyodacite (Höy and Andrew, 1989) or a sheared Silver King lens (Dunne and Höy, 1992). Further work is required to resolve the age and the origin of this unit. Mineralization spatially associated with Silver King intrusions includes shear-related Cu-Au and Cu-Zn-Ag, and vein Pb-Zn-Ag-Au.

Middle Jurassic (culminating *ca.* 166-169 Ma) Nelson granites are continental arc granitoids that have undergone considerable crustal contamination. They record a change from earlier subalkaline to calcalkaline magmatism in the Rossland-Nelson area. Many of the large precious and base metal vein camps, including the Ymir, Slocan and Nelson camps occur along the margins of the Nelson batholith.

CHAPTER 7: TECTONIC SYNTHESIS

TECTONIC SUMMARY

This chapter presents a model for the evolution of the Rossland-Nelson area, emphasising the tectono-stratigraphic evolution of the Rossland Group, its accretion to the western margin of North America and its subsequent structural and tectonic history.

Southeastern British Columbia records intermittent deformation from Late Devonian through Mesozoic time as arc and oceanic rocks were accreted or obducted on to the thinned continental margin of North America. The ages of these assemblages and the tectonic events are generally well constrained, and permit models for the accretion of the allochthonous terranes.

A summary model for the evolution of the Rossland-Nelson area in Late Triassic and Early Jurassic time is shown in Figure 7-1. The Rossland Group, built on deformed and possibly imbricated Permian arc-derived clastics, ophiolitic assemblages and associated sediments, is the youngest and most eastern of the arc rocks of Quesnellia. It is interpreted to have collided and obducted on to the western margin of North America in late Early Jurassic through Middle Jurassic time, and carried eastward with telescoping of the miogeoclinal prism through Paleocene time.

EARLY PALEOZOIC

Lardeau Group rocks of the Kootenay Terrane were deposited, at least in part, as distal sediments along the ancestral continental margin. Mafic volcanic rocks in the Lardeau, including those in the Index Formation in the northern Selkirk Mountains and in the Jowett Formation farther south, indicate periodic extension along the continental margin in early Paleozoic time. Tectonic activity to the west is inferred for deposition of grits of the Broadview Formation, probably from a crystalline source (Cecile and Norford, 1992). The total age span of the Lardeau is not known. However, orthogneiss that intruded the Lardeau Group east of Revelstoke has been dated at 366-422 Ma (Okulitch *et al.*, 1975) and feldspar porphyry clasts in the Cooper conglomerate in structurally overlying Slide Mountain terrane, presumably derived from the Lardeau Group, are dated at 418-431 Ma (Roback *et al.*, 1994). These dates suggest that the Lardeau Group may be restricted to pre Early Silurian.

LATE PALEOZOIC

The basement of the Rossland Group comprises dominantly clastic, carbonate and minor volcanic rocks of the Permian Mount Roberts Formation. These are within the Harper Ranch subterrane of Quesnellia and are derived, in part, from an active volcanic arc to the west (Smith, 1974; Okulitch and Peatfield, 1977). The facing direction of this arc is not known; it may have developed in response to eastward subduction of an ancestral Cache Creek ocean or the westward subduction of the oceanic Slide Mountain Terrane (*see p. 15*). In the former model, the Slide Mountain Terrane is inferred to have developed as a back-arc basin that initiated in Early Mississippian time (Nelson, 1993; Roback *et al.*, 1994; Ferri, 1997). Closure of the Slide Mountain basin occurred by either shortening and imbrication, a model preferred by Ferri (1997), or by westward subduction beneath the Harper Ranch subterrane (Souther, 1992).

Subduction of Slide Mountain Terrane, supported by presence of blueschist metamorphism in Slide Mountain rocks farther north (Erdmer and Armstrong, 1988), implies the presence of an accretionary complex along the western edge of Slide Mountain exposures. There is no documented evidence for this complex. However, it is possible that the imbricated succession of pre-Triassic rocks in the Greenwood area, including oceanic rocks of the Knob Hill and Attwood Formations, and their contact with slices of eastern facies of possible forearc sediments of the Harper Ranch in the Rossland area, may be the remnants of an accretionary wedge dominated by east-verging thrusts. Ultramafic clasts within the Middle Triassic Brooklyn Formation in the Greenwood area imply crustal-scale pre Middle Triassic faulting that exposed the Knob Hill and Attwood Formations (Fyles, 1995) and thrust faults in the Kaslo Group north of Nelson have been dated as Permian (Klepacki and Wheeler, 1985). As well, east-directed thrust faults within the Rossland area juxtapose ophiolitic serpentinites with arc-derived Mount Roberts Formation; these faults have documented Early Jurassic, early Middle Jurassic and Eocene movements (Fyles, 1984; Höy and Andrew, 1991a), and may as well be the loci for pre-Triassic faults.

The lack of an extensive accretionary prism does not necessarily mitigate against a wide ocean basin; some modern arcs have no accretionary prisms (Cas and Wright, 1987, p. 458). The age span of Slide Mountain rocks, approximately 100 million years, and lack of abundant terrigenous clastic rocks, favours a model for a Slide Mountain ocean rather than a marginal basin.

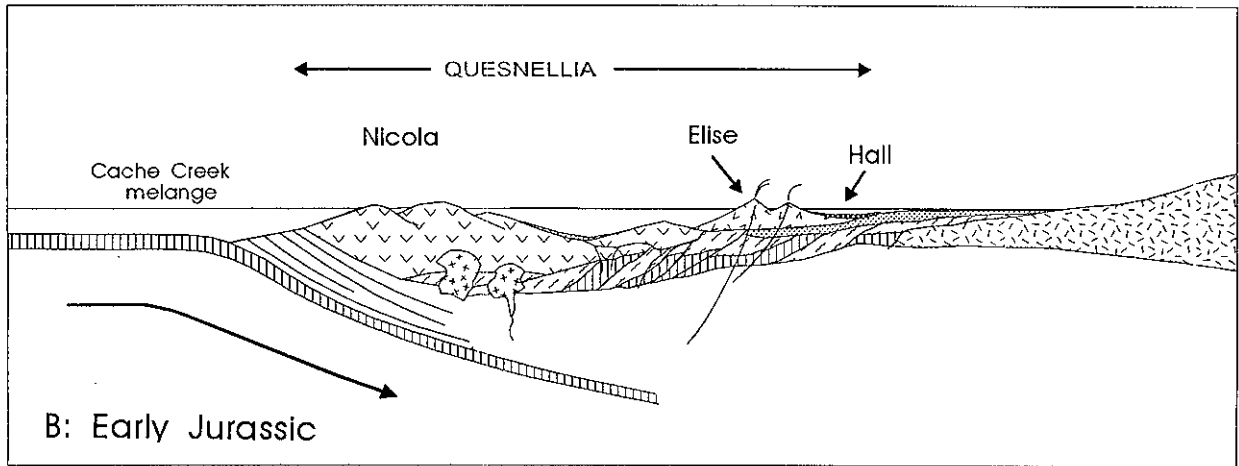
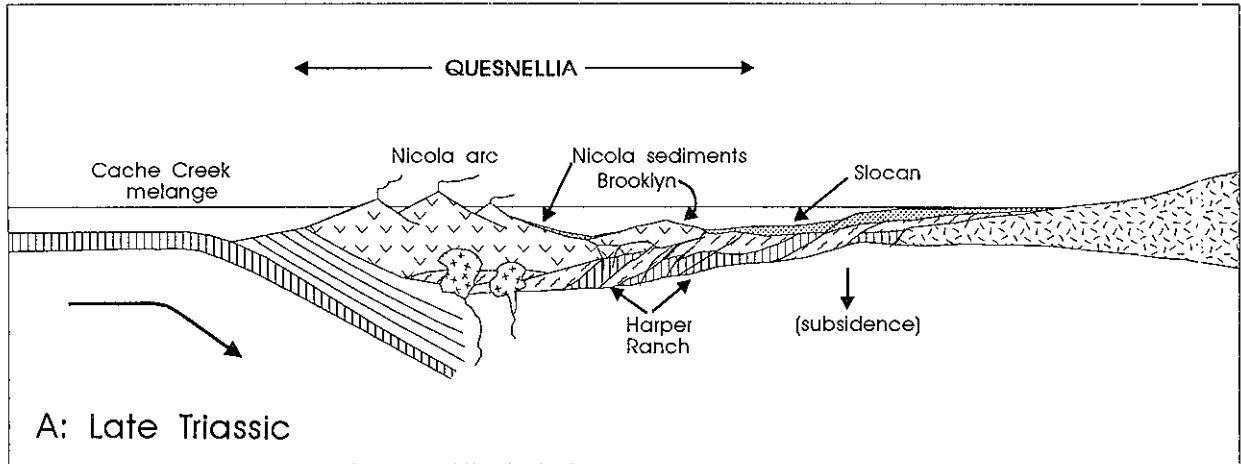


Figure 7-1: Evolution of the Rossland-Nelson area in southern British Columbia in (a) Late Triassic and (b) Early Jurassic time; see text for discussion and references.

EARLY TRIASSIC

A regional unconformity separates Permian rocks from overlying Mesozoic rocks in southern British Columbia. It extends across terrane boundaries, from the miogeoclinal rocks on the western edge of the craton to Quesnellia where, for example, arc rocks of the Rossland Group overlie the Mount Roberts Formation. The lack of any Early Triassic rocks in southern Quesnellia may be associated with a world wide drop in sea level or, alternatively, to more local uplift associated with arc reversal and initial collapse of the Slide Mountain ocean. However, there are no recorded west-derived sediments within Early Triassic miogeoclinal rocks of the Spray River Formation in the Rocky Mountains (Gibson, 1992) implying that an extensive basin or ocean separated an uplifted, eroding arc in the west from the craton.

MIDDLE AND LATE TRIASSIC

The first evidence of renewed volcanism occurred in Middle Triassic time with deposition of the Brooklyn Formation in the Greenwood area (Church, 1986; Fyles, 1990). The Late Triassic Nicola Group (Preto, 1979) represents a well defined west-facing volcanic arc with dominantly calcalkaline volcanism in the west and alkalic shoshonitic volcanism farther east (Mortimer, 1987). Comagmatic intrusive rocks, including the alkaline Iron Mask and Copper Mountain stocks and the calcalkaline Guichon Batholith, host many of the large porphyry deposits of the southern Cordillera.

To the east in the Nelson area, the Late Triassic Slocan Group and the correlative, unfossiliferous Ymir Group, both comprising thick accumulations of carbonates and fine clastic sediments and with inferred western source (Ghosh and St. Lambert, 1989), are remnants of the eastern edge of a basin that separated the Early Mesozoic Quesnel arcs from North America (Figure 7-1a). Distal tuffs within the upper part of the Slocan Group (Little, 1960) are the first indications of Late Triassic volcanism in southeastern Quesnellia.

EARLY JURASSIC (SINEMURIAN)

In Early Jurassic time, the locus of arc volcanism shifted to the east with deposition of the Rossland Group, in contrast to a normal oceanic advance of a magmatic arc caused, in part, by back-arc spreading. A simplistic explanation for this eastward shift in magmatism in the Quesnel arc is a decrease in the dip of the subducting oceanic plate, perhaps caused by an increased rate of convergence (Figure 7-1b). It coincided with development of the Bonanza arc in Wrangellia, suggesting a change in evolution of the oceanic Cache Creek terrane.

Early tectonism associated with arc development in the Rossland Group involves extension with uplift

and erosion in the west and deposition of coarse clastics of the Archibald Formation in a deepening structural basin to the east. This basin fill comprised dominantly sedimentary debris eroded from the underlying Mount Roberts Formation basement, as well as numerous intrusive clasts and occasional volcanic clasts. The intrusive clasts may be derived from Triassic subvolcanic intrusions or Permian intrusions that are exposed farther west (Church, 1986; Fyles, 1990). There are no recognized ultramafic clasts that would confirm imbrication and uplift of Slide Mountain lithologies prior to deposition of arc volcanics, as is demonstrated in the Greenwood area (Fyles, 1995). Farther east within the Archibald basin, lithologies become finer grained, dominated by turbidite deposition, and in western exposures of the correlative upper part of the Ymir Group, by argillaceous and carbonate muds.

Volcanism began in Late Sinemurian time with deposition of submarine shoshonitic flows above exposures of the Ymir Group and eastern exposures of the Archibald Formation and of mafic tuffs above shallower water to locally subaerial exposures of the Archibald in the Fruitvale area east of Rossland. The mafic, primitive character of this early Elise volcanism, dominated by augite phyric flows and tuffs, suggests minimal contamination by continental crustal rocks. As the volcanic arc evolved, it became dominated by stratovolcanoes; these were largely subaerial with only subaqueous deposition of debris flows and tuffs on their distal flanks. As well, plagioclase phyric volcanism began to dominate in upper Elise time, with deposition of thick accumulations of crystal tuffs. Chemical and U-Pb isotopic data indicates that these tuffs were contaminated by continental crustal rocks, suggesting that they may have formed on the distal, thin edge of the North American craton.

A number of comagmatic mafic intrusions, most notably the Rossland monzodiorite and perhaps the Eagle Creek intrusive complex west of Nelson, are associated with elevated copper and gold values, and formation of massive sulphide veins and associated skarns. Those in the Rossland camp have produced more than 84,000 kg of gold, 107,000 kg of silver and 54,295 tonnes of copper. Smaller diorite intrusions host copper-gold porphyry style mineralization at the Katie and Shaft prospects (Cathro *et al.*, 1993).

EARLY JURASSIC (TOARCIAN)

The overlying Hall Formation comprises marine clastic rocks that were deposited in a structural basin on an eroded Elise paleosurface. The disconformity between the Elise and the Hall formations, the inferred hiatus from Late Sinemurian to early Toarcian time, and the lack of any volcanism in the Hall indicates that it records essentially post-arc deposition in a marine basin. Although source areas appear to be local fault blocks to the north and east, and locally to the west, the

Hall may be part of a large marine onlap assemblage that extended westward to include clastic rocks of the Ashcroft Formation (Travers, 1982).

A suite of plagioclase porphyry intrusions, the Silver King suite, have been recognized in eastern exposures of the Rossland Group south of Nelson. These are Toarcian to early Middle Jurassic in age, interpreted to be syntectonic (Dunne and Höy, 1992), and may be syncollisional intrusions that record closure and overlap of the eastern margin of Quesnellia with the cratonic edge of North America. The suture is complex, with a number of overturned (due largely to rotation during Eocene extension) thrust faults, including the Waneta fault and farther west, the Tillicum Creek fault (Einarsen, 1991; 1995) that locally exposes slivers of ultramafic oceanic rocks. Intense compressional deformation, concentrated along the suture, decreased in intensity westward within the Rossland Group.

MIDDLE JURASSIC

Plutonic rocks of the Nelson batholith and the Bonnington and Trail plutons cut Rossland Group and older rocks in southeastern British Columbia. They are calcalkaline in composition, dominated by granodiorite, and were emplaced as a continental magmatic arc (Little, 1960) between 175 and 165 Ma (Parrish and Wheeler, 1983).

Contacts of these Early to Middle Jurassic plutons suggest largely post-tectonic intrusion. However, locally foliated and deformed margins of early phases indicate that Early Jurassic deformation continued intermittently until at least Middle Jurassic time. Southwest of Nelson, the Nelson batholith is cut by a large, west-dipping normal fault, the Mount Verde fault (the "Red Mountain fault" in Höy and Andrew, 1989b), implying that compressional deformation was not continuous in the southern Omineca, but rather was interrupted, at least locally, by extensional faulting.

Middle Jurassic plutons are contaminated by considerable crustal components and record an approximate 200 km eastward shift in the 0.704 Sr (Armstrong and Ghosh, 1990) and +6 Nd lines (Ghosh, 1991). Uplift associated with Middle Jurassic deformation is recorded in a change in depositional environment in the Foreland Belt, from marine sedimentation to nonmarine, foreland basin fill in Late Jurassic time. Nonmarine deposition continued through Early Cretaceous (Aptian and Albian) time in response to continued uplift and tectonic activity in the west. Within the Rossland-Nelson area, this continued activity is recorded by intrusion of small granitic plutons, such as the Wallack Creek Stock.

Nelson intrusive rocks host a number of porphyry molybdenite occurrences, including the Stewart deposit south of Nelson, and numerous polymetallic vein deposits. Contact rocks contain large silver-lead vein camps, such as the Slocan and Ymir camps in Late Triassic and Early Jurassic metasediments, and copper-

silver veins in Elise volcanic rocks south of Nelson. As well, the molybdenite breccia complex on Red Mountain at Rossland may be related to intrusion of a Nelson age stock, the Rainy Day pluton (Fyles, 1984). Thorpe (1967), however, argued that this mineralization is part of the zoned Mo-Cu-Au camp that includes the Rossland veins.

LATE CRETACEOUS

A marine transgression in the southern Cordillera in Late Cretaceous time deposited a blanket of marine sediments in the Foreland Belt. Although uplift continued in the west, presumably in the Rossland-Nelson area as well, deposition of coarse clastic rocks and argillite of the Sophie Mountain Formation may record regional extension and formation of structural basins. Alternatively, considering the generally exotic character of most clasts within the Sophie Mountain Formation, it may be the remnants of a shallow-water deltaic to fluvial complex that was marginal to the marine sediments farther east.

TERTIARY

Intense extensional faulting, uplift and tilting of structural blocks was synchronous with volcanism of the Marron Formation and intrusion of syenitic and granitic plutonic rocks in the Omineca Belt during the Eocene (Parrish *et al.*, 1988). Low-angle detachment faults have exposed Early Proterozoic metamorphic basement, the Monashee Complex, northwest of Nelson. Displacement on these faults changed markedly along strike, from tens of kilometres on the Slocan fault to zero displacement at its southern extension, at the south end of the Champion Lake fault east of Rossland.

Rotation of hangingwall blocks on these listric faults has resulted in large-scale tilting of extensive areas. The Rossland-Nelson area, in the hangingwall of the Slocan Lake and Kettle River faults, is tilted westward approximately 30° (Wingate, 1990) resulting in higher structural levels exposed farther west. This tilting affects pre-Tertiary intrusive rocks, including the Rossland monzodiorite, and may account for exposures of the abundant vein mineralization in the Rossland camp along the western edge of the pluton, in contrast to less mineralized and inferred deeper plutonic levels in eastern exposures of the intrusion.

SELECTED BIBLIOGRAPHY

- Alldrick, D.J. (1993): Geology and Metallogeny of the Stewart Mining Camp, Northwestern British Columbia; *B.C. Ministry of Energy, Mines and Petroleum Resources*, Bulletin 85, 105 pages.
- Anderson, R.N., Delong, S.E. and W.M. Schwarz (1980): Dehydration, Asthenospheric Convection and Seismicity in Subduction Zones; *Journal of Geology*, Volume 88, pages 445-451.
- Andrew, K.P.E. and Höy, T. (1988): Preliminary Geology and Mineral Deposits of the Rosslund Group between Nelson and Ymir, Southeastern British Columbia; *B.C. Ministry of Energy, Mines and Petroleum Resources*, Open File 1988-1.
- Andrew, K.P.E. and Höy, T. (1989): The Shaft Showing, Elise Formation, Rosslund Group; in Exploration in British Columbia 1988; *B.C. Ministry of Energy, Mines and Petroleum Resources*, pages B21-28.
- Andrew, K.P.E. and Höy, T. (1990): Geology and Exploration of the Rosslund Group in the Swift Creek area; in Exploration in British Columbia 1989; *B.C. Ministry of Energy, Mines and Petroleum Resources*, pages 73-80.
- Andrew, K.P.E. and Höy, T. (1991): Geology of the Erie Lake Area with Emphasis on Stratigraphy and Structure of the Hall Formation, Southeastern British Columbia; in Geological Fieldwork 1990, Newell, J.M. and Grant, B., Editors, *B.C. Ministry of Energy, Mines and Petroleum Resources*, Paper 1991-1, pages 9-20.
- Andrew, K.P.E., Höy, T., and Drobe, J. (1990a): Stratigraphy and Tectonic Setting of the Archibald and Elise Formations, Rosslund Group, Beaver Creek Area, Southeastern British Columbia; in Geological Fieldwork 1989, Newell, J.M. and Grant, B., Editors, *B.C. Ministry of Energy, Mines and Petroleum Resources*, Paper 1990-1, pages 19-27.
- Andrew, K.P.E., Höy, T., and Drobe, J. (1990b): Geology of the Rosslund Group, Beaver Creek Area, Southeastern British Columbia (82F/4E); *B.C. Ministry of Energy, Mines and Petroleum Resources*, Open File 1990-9.
- Andrew, K.P.E., Höy, T. and Simony, P. (1991): Geology of the Trail Map-area, Southeastern British Columbia; *B.C. Ministry of Energy, Mines and Petroleum Resources*, Open File 1991-16.
- Arculus, R.J. and Powell, R. (1986): Source Component Mixing in the Regions of Arc Magma Generation; *Journal of Geophysical Research*, Volume 91, pages 5913-5926.
- Armstrong, R.L. and Ghosh, D.K. (1990): Eastward Movement of the $^{87}\text{Sr}/^{86}\text{Sr}=0.704$ Line in Southern B.C. from Triassic to Eocene: Monitoring the Tectonic Overlap of Accreted Terranes on North America; Abstract, Project Lithoprobe Workshop, University of Calgary, March, 1990, pages 53-56.
- Ash, C.H., Macdonald, R.W.J. and Arksey, R.L. (1992): Towards a Deposit Model for Ophiolite Related Mesothermal Gold in British Columbia (82F/4); in Geological Fieldwork 1991, Newell, J.M. and Grant, B., editors, *B.C. Ministry of Energy, Mines and Petroleum Resources*, Paper 1992-1, pages 253-260.
- Ash, C.H., Macdonald, R.W.J. and Reynolds, P.R., (in press): Ophiolite-related Mesothermal Lode Gold in British Columbia: A Deposit Model; *B.C. Ministry of Energy, Mines and Petroleum Resources*, Bulletin
- Basaltic Volcanism Study Project (1981): Basaltic Volcanism on the Terrestrial Planets; New York, Pergamon Press, 1286 pages.
- Beddoe-Stephens, B. (1977): The Petrology and Geochemistry of the Rosslund Group Volcanic Rocks, Southern British Columbia; *University of Alberta*, Unpublished Ph.D. thesis, 390 pages.
- Beddoe-Stephens, B. and Lambert, R. St. J. (1981): Geochemical, Mineralogical and Isotopic Data Relating to the Origin and Tectonic Setting of the Rosslund Volcanic Rocks, Southeastern British Columbia; *Canadian Journal of Earth Sciences*, Volume 18, pages 858-868.
- Beaudoin, G., Roddick, J.C. and Sangster D.F. (1992): Eocene Age for Ag-Pb-Zn Vein and Replacement Deposits of the Kokanee Range, Southeastern British Columbia; *Canadian Journal of Earth Sciences*, Volume 29, pages 3-14.
- Bostock, H.S. (1940): Keremeos, British Columbia; *Geological Survey of Canada*, Map 341A.
- Bouma, A.H. (1962): Sedimentology of some Flysch Deposits; *Elsevier Publishing Co.*, Amsterdam, 168 pages.
- Bruce, E.L. (1917): Geology and Ore Deposits of Rosslund, British Columbia; *B.C. Ministry of Energy, Mines and Petroleum Resources*, Bulletin 4.
- Burrows, D.R., Wood, P.C. and Spooner, E.T.C. (1986): Carbon Isotope Evidence for a Magmatic Origin for Archean Gold-quartz Vein Ore Deposits; *Nature*, Volume 321, pages 851-854.
- Carr, S.D. (1984): Ductile Shearing and Brittle Faulting in Valhalla Gneiss Complex, Southeastern British Columbia; in Current Research, Part A, *Geological Survey of Canada*, Paper 85-1A, pages 89-96.
- Carr, S.D. (1986): The Valkyr Shear Zone and the Slocan Lake Fault Zone: Eocene Structures that Bound the Valhalla Gneiss Complex, Southeastern British Columbia, M.Sc. thesis, *Carleton University*, 106 pages.
- Carr, S.D. (1991): Three Crustal Zones in the Thor-Odin-Pinnacles Area, Southern Omineca Belt, British Columbia; *Canadian Journal of Earth Sciences*, Volume 28, pages 2003-2023.
- Carr, S.D., Parrish, R.R. and Brown, R.L. (1987): Eocene Structural Development of the Valhalla Complex, Southeastern British Columbia; *Tectonics*, Volume 6, pages 175-196.

- Cas, R.A.F. and Wright, J.V. (1987): Volcanic Successions, Modern and Ancient; *Allen and Unwyn Publishers Ltd*, London, United Kingdom, 528 pages.
- Cathro, M.S., Dunne, K.P.E. and Naciuk, T.M. (1993): Katie - An Alkaline Porphyry Copper-gold Deposit in the Rossland Group, Southeastern British Columbia; *B.C. Ministry of Energy, Mines and Petroleum Resources*, Geological Fieldwork 1992, Paper 1993-1, pages 233-247.
- Cecile, M.P. and Norford, B.S. (1992): Ordovician and Silurian Assemblages; in *Geology of the Cordilleran Orogen in Canada*, Gabrielse, H. and Yorath, C.J., Editors, *Geological Survey of Canada*, No. 4, pages 184-196.
- Church, B.N. (1973): Geology of the White Lake Basin; *B.C. Ministry of Energy, Mines and Petroleum Resources*, Bulletin 61, 120 pages.
- Church, B.N. (1986): Geological Setting and Mineralization in the Mount Attwood-Phoenix Area of the Greenwood Mining Camp (82E); *B.C. Ministry of Energy, Mines and Petroleum Resources*, Paper 1986-2.
- Church, B.N. (1992): The Lexington Porphyry, Greenwood Mining Camp, Southern British Columbia; *B.C. Ministry of Energy, Mines and Petroleum Resources*, Geological Fieldwork 1991, Paper 1992-1, pages 295-297.
- Cockfield, W.E., (1936): Lode Gold Deposits of Ymir- Nelson area, British Columbia; *Geological Survey of Canada*, Memoir 191, 78 pages.
- Colpron, M. and Price, R.A. (1992): Preliminary Results on the Stratigraphy and Structure of the Lardeau Group in the Illecillewaet Synclinorium, Western Selkirk Mountains, British Columbia; *Geological Survey of Canada*, Paper 92-1A, Current Research, Part A, pages 157-162.
- Colpron, M. and Price, R.A. (1995): Tectonic Significance of the Kootenay Terrane, Southeastern Canadian Cordillera: An Interactive Model; *Geology*, Volume 23, No. 1, pages 25-28.
- Colpron, M., Price, R.A. and Carmichael, C.M. (in press): Middle Jurassic Denudation and Uplift along the Western Flank of the Selkirk Fan Structure: Thermobarometric and Thermochronometric Constraints from the Illecillewaet Synclinorium, Southeastern British Columbia; *Canadian Journal of Earth Sciences*.
- Corbett, C.R. and Simony, P.S. (1984): The Champion Lake Fault in the Trail-Castlegar Area of Southeastern British Columbia; in *Current Research, Part A; Geological Survey of Canada*, Paper 84-1A, pages 103-104.
- Cox, K.G., Bell, J.D. and Pankhurst, R.J. (1979): The Interpretation of Igneous Rocks; London; *Allen and Unwin*, 450 pages.
- Crawford, M.L. and Hollister, L.S. (1986): Metamorphic Fluids: The Evidence from Fluid Inclusions; in *Fluid-Rock Interactions during Metamorphism*, *Advances in Physical Geochemistry* 5, Walther, J.V. and Wood, B.J., Editors, *Springer Verlag*, pages 1-35.
- Crowe, G.G. (1981): The Structural Evolution of the Mackie Plutonic Complex, Southern British Columbia; unpublished M.Sc. thesis, *University of Calgary*, Calgary, 154 pages.
- Daly, R.A. (1912): North American Cordillera, Forty-ninth Parallel; *Geological Survey of Canada*, Memoir 38, Parts 1, 2 and 3.
- Dawson, G.M. (1889): Report on a Portion of the West Kootenai District, British Columbia; *Geological Survey of Canada*, Annual Reports 1888-1889.
- Debon, F. and Le Fort, P. (1983): A Chemical-mineralogical Classification of Common Plutonic Rocks and Associations; *Transactions of the Royal Society of Edinburgh: Earth Sciences*, Volume 73, pages 135-139.
- de Rosen-Spence, A.F. (1976): Stratigraphy, Development and Petrogenesis of the Central Noranda Volcanic Pile, Noranda, Quebec, Unpublished Ph.D Thesis, *University of Toronto*.
- de Rosen Spence, A.F. (1985): Shoshonites and Associated Rocks of Central British Columbia; *B.C. Ministry of Energy, Mines and Petroleum Resources*, Geological Fieldwork 1984, Paper 1985-1, pages 426-442.
- Devlin, W.J. and Bond, G.C. (1987): The Initiation of the Early Paleozoic Cordilleran Miogeocline: Evidence from the Uppermost Proterozoic - Lower Cambrian Hamill Group of Southeastern British Columbia; *Canadian Journal of Earth Sciences*, Volume 25, pages 1-19.
- Devlin, W.J., Brueckner, H.K. and Bond, G.C. (1988): New Isotopic Data and a Preliminary Age for Volcanics near the Base of the Windermere Supergroup, Northeastern Washington, U.S.A.; *Canadian Journal of Earth Sciences*, Volume 25, pages 1906-1911.
- Drysdale, C.W. (1915): Geology and Ore Deposits of Rossland, British Columbia; *Geological Survey of Canada*, Memoir 77.
- Drysdale, C.W. (1917): Ymir Mining Camp, British Columbia; *Geological Survey of Canada*, Memoir 94.
- Dunne, K.P.E. and Höy, T. (1992): Petrology of Lower and Middle Jurassic Intrusions in the Rossland Group, Southeastern British Columbia; in *Geological Fieldwork 1991, Ministry of Energy, Mines and Petroleum Resources*, Paper 1992-1, pages 9-19.
- Dunne, K.P.E. and Höy, T. (in preparation): Geology of the Trail Map-area, Southeastern British Columbia; NTS 82F/SW, scale - 1:100 000; *B.C. Ministry of Employment and Investment*, Map.
- Einersen, J.M. (1994): Structural Geology of the Pend d'Oreille Area and Tectonic Evolution of the Southern Kootenay Arc; unpublished Ph.D. thesis, *The University of Calgary*, 172 pages.
- Erdmer, P. (1987): Blueschist and Eclogite in Mylonitic Allochthons, Ross River and Watson Lake Areas, Southern Yukon; *Canadian Journal of Earth Sciences*, Volume 24, pages 1439-1449.
- Ewart, A. (1982): The Mineralogy and Petrology of Tertiary-Recent Orogenic Volcanic Rocks: with Special Reference to the Andesitic-basaltic Compositional Range; in *Andesites:*

- Orogenic Andesites and Related Rocks, Thorpe, R.S., Editor, *Chichester, Wiley*, pages 26-87.
- Ferri, F. (1997): Nina Creek Group and Lay Range Assemblage, North-central British Columbia: Remnants of Late Paleozoic Ocean and Arc Terranes; *Canadian Journal of Earth Sciences*, Volume 34, Pages 854-874.
- Fisher, R.V. (1982): Pyroclastic Surges; in *Pyroclastic Volcanism and Deposits of Cenozoic Intermediate to Felsic Volcanic Islands with Implications for PreCambrian Greenstone Belts*; *Geological Association of Canada*, Short Course Notes, Volume 2, pages 71-110.
- Fisher, R.V. and Heiken, G. (1982): Mt. Pelee, Martinique: May 8 and 20, 1902, Pyroclastic Flows and Surges; *Journal of Volcanology and Geothermal Research*, Volume 13, pages 339-371.
- Fiske, R.S. and Matsuda, T. (1964): Submarine Equivalents of Ash Flows in the Tikwa Formation, Japan; *American Journal of Science*, Volume 262, pages 76-106.
- Fitzpatrick, M. (1985): The Geology of the Rosland Group in the Beaver Valley Area, Southeastern British Columbia; Unpublished M.Sc. thesis, *University of Calgary*, 150 pages.
- Frebold, H. (1959): Marine Jurassic Rocks in Nelson and Salmo Areas, Southeastern British Columbia; *Geological Survey of Canada*, Bulletin 49.
- Frebold, H. and Little, H.W. (1962): Paleontology, Stratigraphy, and Structure of the Jurassic Rocks in Salmo Map-area, British Columbia; *Geological Survey of Canada*, Bulletin 81.
- Frebold, H. and Tipper, H.W. (1970): Status of the Jurassic in the Canadian Cordillera of British Columbia, Alberta, and Southern Yukon; *Canadian Journal of Earth Sciences*, Volume 7, pages 1-20.
- Fyles, J.T. (1984): Geological Setting of the Rosland Mining Camp; *B.C. Ministry of Energy, Mines and Petroleum Resources*, Bulletin 74, 61 pages.
- Fyles, J.T. (1990): Geology of the Greenwood - Grand Forks Area, British Columbia (82E/1); *B.C. Ministry of Energy, Mines, and Petroleum Resources*, Open File 1990-25.
- Fyles, J.T. (1995): Day 3 (Morning): Knob Hill Group, Aitwood Group and Brooklyn Formation; in *Field Trip Guidebook B2*, *Geological Association of Canada*, Victoria, B.C., pages 40-49.
- Fyles, J.T. and Eastwood, G.P.E. (1962): Geology of the Ferguson area, Lardeau District, British Columbia; *B.C. Ministry of Energy, Mines, and Petroleum Resources*, Bulletin 45, 162 pages.
- Fyles, J.T. and Hewlett, C.G. (1959): Stratigraphy and Structure of the Salmo Lead-zinc Area; *British Columbia Department of Mines*, Bulletin 41, 162 pages.
- Ghosh, D. K. (1986): Geochemistry of the Nelson-Rosland Area, Southeastern British Columbia; Unpublished Ph.D. thesis, *University of Alberta*, Edmonton, Alberta, 310 pages.
- Ghosh, D.P. (1995a): Nd and Sr Isotopic Constraints on the Interactions of the Intermontane Superterrane with the Western Edge of North America in the Southern Canadian Cordillera; *Canadian Journal of Earth Sciences*, Volume 32, pages 1740-1758.
- Ghosh, D.P. (1995b): U-Pb Geochronology of Jurassic to Early Tertiary Granitic Intrusives from the Nelson-Castlegar area, Southeastern British Columbia; *Canadian Journal of Earth Sciences*, Volume 32, pages 1668-1680.
- Ghosh, D.P. and Lambert, R. St. J. (1989): Nd-Sr Isotopic Study of Proterozoic to Triassic Sediments from Southeastern British Columbia; *Earth and Planetary Science Letters*, Volume 94, pages 29-44.
- Gibson, D.W. (1992): Triassic Strata of the Foreland Belt; in *Upper Devonian to Middle Jurassic Assemblages*, Chapter 8 of *Geology of the Cordilleran Orogen in Canada*, Gabrielse, H. and Yorath, C.J., Editors, *Geological Survey of Canada*, No. 4, pages 265-276.
- Gilbert, G. (1948): Rosland Camp; in *Structural Geology of Canadian Ore Deposits*; *Canadian Institute of Mining and Metallurgy*, Jubilee Volume, pages 189-186.
- Gill, J.B. (1981): Orogenic Andesites and Plate Tectonics; *Springer Verlag*, Berlin, 389 pages.
- Goldfarb, R.J., Leach, D.L., Miller, M.L. and Pickthorn, W.J. (1986): Geology, Metamorphic Setting, and Genetic Constraints of Epigenetic Lode-gold Mineralization within the Cretaceous Valdez Group, South-central Alaska; in *Turbidite-hosted Gold Deposits*, Keppie, J.D., Boyle, R.W. and Haynes, S.J., Editors, *Geological Association of Canada*, Special Paper 32, pages 87-105.
- Green, T.H. (1980): Island Arc and Continent-building Models based on Experimental Petrology and Geochemistry; *Tectonophysics*, Volume 63, pages 367-385.
- Halwas, D.B. and Simony, P.S. (1986): The Castlegar Gneiss Complex, Southern British Columbia; in *Current Research, Part A*, *Geological Survey of Canada*, Paper 86-1A, pages 583-587.
- Hanson, G.N. (1978): The Application of Trace Elements to the Petrogenesis of Igneous Rocks of Granitic Composition; *Earth and Planetary Letters*, Volume 38, pages 26-43.
- Harker, A. (1909): *The Natural History of Igneous Rocks*; New York, *Macmillan*.
- Harms, T.A. (1986): Structural and Tectonic Analysis of the Sylvester Allochthon, Northern and Central British Columbia: Implications for Paleogeography and Accretion; Ph.D Thesis, *University of Arizona*, Tucson, Arizona.
- Hawkesworth, C.J. and Powell, M. (1980): Magma Genesis in the Lesser Antilles Island Arc; *Earth and Planetary Science Letters*, Volume 51, pages 297-308.
- Heather, K.B. (1985): The Alwin Creek Gold-Copper-Silver Deposit, Southeastern British Columbia; Unpublished M.Sc. Thesis, *Queen's University*, Kingston, Ontario, 253 pages.
- Heiken, G.H. (1972): Morphology and Petrology of Volcanic Ashes; *Geological Society of America*, Bulletin 83, pages 1961-1988.

- Hodgson, C.J., Chapman, R.S.G. and MacGeehan, P.J. (1982): Application of Exploration Criteria for Gold Deposits in the Superior Province of the Canadian Shield to Gold Exploration in the Cordillera; in *Precious Metals of the Northern Cordillera*, Levinson, A.A., Editor, *Association of Exploration Geochemists*, pages 173-206.
- Hole, M.J., Saunders, A.D., Marriner, G.F. and Tarney, J. (1984): Subduction of Pelagic Sediments: Implications for the Origin of Cenomanous Basalts from the Mariana Islands; *Journal of Geological Society of London*, Volume 141, pages 453-472.
- Höy, T. (1993): Geology of the Purcell Supergroup in the Fernie West-half Map Area, Southeastern British Columbia; *B.C. Ministry of Energy, Mines and Petroleum Resources*, Bulletin 84, 157 pages.
- Höy, T. and Andrew, K.P.E. (1988): Preliminary Geology and Geochemistry of the Elise Formation, Rossland Group, between Nelson and Ymir, Southeastern British Columbia; in *Geological Fieldwork 1987*, Newell, J.M. and Grant, B., Editors, *B.C. Ministry of Energy, Mines and Petroleum Resources*, Paper 1988-1, pages 19-30.
- Höy, T. and Andrew, K.P.E. (1989a): The Rossland Group, Nelson Map Area, Southeastern British Columbia; in *Geological Fieldwork 1988*, Newell, J.M. and Grant, B., Editors, *B.C. Ministry of Energy, Mines and Petroleum Resources*, Paper 1989-1, pages 33-43.
- Höy, T. and Andrew, K.P.E. (1989b): Geology of the Rossland Group, Nelson Map-area, Southeastern British Columbia; *B.C. Ministry of Energy, Mines and Petroleum Resources*, Open File Map 1989-1.
- Höy, T. and Andrew, K.P.E. (1989c): The Great Western Group, Elise Formation, Rossland Group; in *Exploration in British Columbia 1988*, *B.C. Ministry of Energy, Mines and Petroleum Resources*, pages B15-19.
- Höy, T. and Andrew, K.P.E. (1990a): Structure and Tectonics of the Rossland Group, Mount Kelly - Hellroaring Creek Area, Southeastern British Columbia; in *Geological Fieldwork 1989*, Newell, J.M. and Grant, B., Editors, *B.C. Ministry of Energy, Mines and Petroleum Resources*, Paper 1990-1, pages 11-17.
- Höy, T. and Andrew, K.P.E. (1990b): Geology of the Mount Kelly-Hellroaring Creek Map Area, Southeastern British Columbia; *B.C. Ministry of Energy, Mines and Petroleum Resources*, Open File Map 1990-8.
- Höy, T. and Andrew, K.P.E. (1991a): Geology of the Rossland Area, Southeastern British Columbia (82F/4E); in *Geological Fieldwork 1990*, Newell, J.M. and Grant, B., Editors, *B.C. Ministry of Energy, Mines and Petroleum Resources*, Paper 1991-1, pages 21-31.
- Höy, T. and Andrew, K.P.E., (1991b): Geology of the Rossland -Trail Area, Southeastern British Columbia (82F/4); *B.C. Ministry of Energy, Mines and Petroleum Resources*, Open File 1991-2.
- Höy, T. and Dunne, K.P.E. (in prep.): Metallogeny of the Rossland Group, Quesnellia, Southeastern British Columbia; *B.C. Ministry of Employment and Investment*.
- Höy, T., Dunne, K.P.E. and Wilton, P. (1993): Massive Sulphide and Precious Metal Deposits in Southeastern British Columbia; *Geological Association of Canada*, Field Trip Guide A-7, Edmonton, Alberta, 74 pages.
- Höy, T., Dunne, K.P.E. and Wehrle, D. (1992): Tectonic and Stratigraphic Controls of Gold-Copper Mineralization in the Rossland Camp, Southeastern British Columbia; in *Geological Fieldwork 1991*, Newell, J.M. and Grant, B., Editors, *B.C. Ministry of Energy, Mines and Petroleum Resources*, Paper 1992-1, pages 261-271.
- Irving, T.N. and Barager, W.R.A. (1971): A Guide to the Chemical Classification of the Common Rocks; *Canadian Journal of Earth Sciences*, Volume 8, pages 523-548.
- Joseph, N.L. (1990): Geologic Map of the Colville 1:100,000 Quadrangle, Washington-Idaho; *Washington Division of Geology and Earth Resources*, Open File 90-13, 78 pages.
- Kerrick, R. (1989): Geodynamic Setting and Hydraulic Regimes: Shear Zone Hosted Mesothermal Gold Deposits; in *Mineralization and Shear Zones*, Bursnall, J.T., Editor, *Geological Association of Canada*, Short Course Notes, Volume 6, pages 89-128.
- Klepachi, D.W. (1985): Stratigraphy and Structural Geology of the Goat Range Area, Southeastern British Columbia; unpublished Ph.D. thesis, *Massachusetts Institute of Technology*, 268 pages.
- Klepachi, D.W. and Wheeler, J.O. (1985): Stratigraphic and Structural Relations of the Milford, Kaslo and Slocan Groups, Lardeau and Nelson Map Areas, British Columbia; in *Current Research, Part A, Geological Survey of Canada*, Paper 85-1A, pages 277-286.
- Krogh, T.E. (1973): A Low Contamination Method for Hydrothermal Decomposition of Zircon and Extraction of U and Pb for Isotopic Age Determinations; *Geochimica et Cosmochimica Acta*, Volume 29, pages 485-494.
- Lambert, R. St. J. and Holland, J.G. (1974): Yttrium Geochemistry; *Geochimica et Cosmochimica Acta*, Volume 38, pages 1393-1414.
- La Roche, H., Le Terrier, J., Grandclaude, P. and Marchal, D. (1989): A Classification of Volcanic and Plutonic Rocks Using R1R2-Diagram and Major Element Analyses - its Relationships with Current Nomenclature; *Chemical Geology*, Volume 29, pages 183-210.
- LeBas, M.J., LeMaitre, R.W., Streckeisen, A. and Zanettin, B. (1986): A Chemical Classification of Volcanic Rocks Based on the Total Alkali-Silica Diagram; *Journal of Petrology*, Volume 27, Part 3, pages 745-750.
- LeClair, A.D. (1986): Geology, Midge Creek Area (82F/10); *Geological Survey of Canada*, Open File 1352.
- Lefebvre, D. V. (1976): Geology of the Nicola Group in the Fairweather Hills, British Columbia; unpublished M.Sc. thesis, *Queens University*, Kingston, Ontario, 178 pages.
- Le Maitre, R.W. (1989): A Classification of Igneous Rocks and Glossary of Terms; *Blackwell, Oxford Press*, 193 pages.
- Lindsay, D.D. (1991): Geology, Geochemistry and Petrography of the Moochie Cu-Au Occurrence, Nelson, British Columbia;

- unpublished B.Sc. thesis, Carleton University, 51 pages.
- Lis, M.G. and Price, R.A. (1976): Large-scale Block Faulting During Deposition of the Windermere Supergroup (Hadrynian) in Southeastern British Columbia; *Geological Survey of Canada*, Paper 1976-1A, pages 135-136.
- Little, H.W. (1950): Salmo Map-area, British Columbia; *Geological Survey of Canada*, Paper 50-19, 43 pages.
- Little, H.W. (1960): Nelson Map-area, West-half, British Columbia; *Geological Survey of Canada*, Memoir 308, 205 pages.
- Little, H.W. (1962): Trail Map-area, British Columbia; *Geological Survey of Canada*, Paper 62-5.
- Little, H.W. (1963): Rossland Map-area, British Columbia; *Geological Survey of Canada*, Paper 63-13.
- Little, H.W. (1964): Geology, Ymir Map-area, British Columbia; *Geological Survey of Canada*, Map 1144A.
- Little, H.W. (1965): Geology, Salmo Map Area, British Columbia; *Geological Survey of Canada*, Map 1145A.
- Little, H.W. (1982a): Geology, Bonnington Map Area, British Columbia; *Geological Survey of Canada*, Map 1571A.
- Little, H.W. (1982b): Geology, Rossland-Trail Map-area, British Columbia; *Geological Survey of Canada*, Paper 79-26, 38 pages.
- Little, H.W. (1985): Geological Notes, Nelson West-half (82F, W1/2) Map-area; *Geological Survey of Canada*, Open File 1199.
- Maniar, P.D. and Piccoli, P.M. (1989): Tectonic Discrimination of Grantoids; *Geological Society of America*, Bulletin, Volume 101, pages 635-643.
- McAllister, A.L. (1950): Geology of the Ymir Map-Area, British Columbia; unpublished Ph.D. thesis, *McGill University*, 160 pages.
- McAllister, A.L. (1951): The Geology of the Ymir Map-area, British Columbia; *Geological Survey of Canada*, Paper 51-4.
- McBirney, A.R. (1963): Factors Governing the Nature of Submarine Volcanism; *Bulletin of Volcanology*, Volume 26, pages 455-469.
- McConnell, R.G. and Brock, R.W. (1904): West Kootenay Sheet, British Columbia; *Geological Survey of Canada*, Map 792.
- McMillan, W.J. (1974): Stratigraphic Sections from the Jurassic Ashcroft Formation and Triassic Nicola Group Contiguous to the Guichon Creek Batholith; in *Geological Fieldwork, B.C. Ministry of Energy, Mines and Petroleum Resources*, pages 27-34.
- Middlemost, E.A.K. (1975): The Basaltic Clan; *Earth Science Review*, Volume 11, pages 337-364.
- Monger, J.W.H. and Berg, H.C. (1984): Lithotectonic Terrane Map of Western Canada and Southeastern Alaska; in *Lithotectonic Terrane Maps of the North America Cordillera*, Silberling, N.J. and Jones, D.L., Editors, *United States Geological Survey*, Open File Report 84-523.
- Monger, J.W.H., Wheeler, J.O., Tipper, H.W., Gabrielse, H., Harms, T., Struik, L.C., Campbell, R.B., Dodds, C.J., Gehrels, G.E. and O'Brien, J. (1991): Part B. Cordilleran Terranes; in *Upper Devonian to Middle Jurassic Assemblages*, Chapter 8 of *Geology of the Cordilleran Orogen in Canada*, Gabrielse, H. and Yorath, C.J., Editors, *Geological Survey of Canada*, No. 4, pages 281-327.
- Mortimer, N. (1986): Late Triassic Arc-related, Potassic Igneous Rocks in the North America Cordillera; *Geology*, Volume 14, pages 1035-1078.
- Mortimer, N. (1987): The Nicola Group: Late Triassic and Early Jurassic Subduction-related Volcanism in British Columbia; *Canadian Journal of Earth Sciences*, Volume 24, pages 2521-2536.
- Mulligan, R. (1951): The Geology of the Nelson (Bonnington) and Adjoining Part of Salmo Map Areas, British Columbia; unpublished Ph.D. thesis, *McGill University*, 202 pages.
- Mulligan, R. (1952): Bonnington Map Area, British Columbia; *Geological Survey of Canada*, Paper 52-13, 37 pages.
- Murphy, C.M., Gerasimoff, M., Van der Hedyden, P., Parrish, R.R., Klepacki, D.W., McMillan, W.J., Struik, L.C. and Gabites, J. (1994): New Geochronological Constraints on Jurassic Deformation on the Western Edge of North America, Southern Canadian Cordillera; in *Jurassic Magmatism and Tectonics of the North American Cordillera*, Miller, D.M. and Anderson, R.G., Editors, *Geological Society of America*, Special Paper 299, pages 159-171.
- Nelson, J.L. (1993): The Sylvester Allochthon: Upper Paleozoic Margin-basin and Island-arc Terranes in Northern British Columbia; *Canadian Journal of Earth Sciences*, Volume 30, pages 631-643.
- Nelson, J.L. and Bradford, J.A. (1993): Geology of the Midway-Cassiar Area, Northern British Columbia; *B.C. Ministry of Energy, Mines and Petroleum Resources*, Bulletin 83.
- Nesbitt, B.E. and Muehlenbachs, K. (1989): Geology, Geochemistry, and Genesis of Mesothermal Lode Gold Deposits of the Canadian Cordillera: Evidence for Ore Formation from Evolved Meteoric Water; *Economic Geology*, Monograph 6, pages 535-563.
- Nixon, G.T. (1990): Geology and Precious Metal Potential of Mafic - Ultramafic Rocks in British Columbia: Current Progress; in *Geological Fieldwork 1989, B.C. Ministry of Energy, Mines and Petroleum Resources*, Paper 1990-1, pages 353-358.
- Nixon, G.T. and Hammack, J.L. (1991): Metallogeny of Ultramafic-mafic Rocks in British Columbia with Emphasis on the Platinum Group Elements; in *Ore Deposits, Tectonics and Metallogeny in the Canadian Cordillera*, B. Grant and J.M. Newell, Editors, *B.C. Ministry of Energy, Mines and Petroleum Resources*, Paper 1991-4, pages 125-158.
- Okulitch, A.V. and Peatfield, G. R. (1977): Geologic History of the Late Paleozoic - Early Mesozoic Eugeocline in Southern British Columbia and Eastern Washington; Abstract,

- Geological Association of Canada*, Program with Abstracts, 1977 Annual Meeting, Vancouver, B.C., page 40.
- Okulitch, A.V., Wanless, R.K. and Loveridge, W.J. (1975): Devonian Plutonism in South-central British Columbia; *Canadian Journal of Earth Sciences*, Volume 12, pages 1760-1769.
- Panteleyev, A. (1992): Gold in the Canadian Cordillera - a Focus on Epithermal and Deeper Environments, in Ore Deposits, Tectonics and Metallogeny in the Canadian Cordillera, Grant, B. and Newell, J.M., Editors, *B.C. Ministry of Energy, Mines and Petroleum Resources*, Paper 1991-4, pages 163-212.
- Panteleyev, A. and Schroeter, T.G. (1986): Gold in British Columbia; *British Columbia Ministry of Energy, Mines and Petroleum Resources*, Preliminary Map 64.
- Parrish, R.R. (1984): Slocan Lake Fault: A Low Angle Fault Zone Bounding the Valhalla Gneiss Complex, Nelson Map-area, Southern British Columbia; in Current Research, Part A, *Geological Survey of Canada*, Paper 84-1A, pages 323-330.
- Parrish, R.R. (1992): U-Pb Ages of Jurassic-Eocene Plutonic Rocks in the Vicinity of the Valhalla Complex, Southeast British Columbia; in Radiogenic Age and Isotope Studies: Report 5, *Geological Survey of Canada*, Paper 91-2, pages 115-134.
- Parrish, R.R., Carr, S.D. and Parkinson, D.L. (1988): Eocene Extensional Tectonics and Geochronology of the Southern Omineca Belt, British Columbia and Washington; *Tectonics*, Volume 7, pages 181-212.
- Parrish, R.R. and Wheeler, J.O. (1983): A U-Pb Zircon Age from the Kuskanax Batholith, Southeastern British Columbia; *Canadian Journal of Earth Sciences*, Volume 20, pages 1751-1756.
- Parsons, I. (1978): Feldspars and Fluids in Cooling Plutons; *Mineralogical Magazine*, Volume 42, pages 1-17.
- Pearce, T.H. (1968): A Contribution to the Theory of Variation Diagrams; *Contributions to Mineralogy and Petrology*, Volume 19, pages 142-157.
- Pearce, J.A. (1982): Trace Element Characteristics of Lavas from Destructive Plate Boundaries; in Andesites: Orogenic Andesites and Related Rocks, Thorpe, R.S., Editor, *Wiley*, pages 525-548.
- Pearce, J.A. (1983): The Role of Sub-continental Lithosphere in Magma Genesis at Destructive Plate Margins; in Continental Basalts and Mantle Xenoliths; Hawkesworth, C.J. and Norry, M. J., Editors, Nantwich, *Shiva*, pages 230-249.
- Pearce, J.A., Harris, N.B.W. and Tindle, A.G. (1984): Trace Element Discrimination Diagrams for the Tectonic Interpretation of Granitic Rocks; *Journal of Petrology*, Volume 25, pages 956-983.
- Pearce, J.A. and Cann, J.R. (1973): Tectonic Setting of Basic Volcanic Rocks Determined Using Trace Element Analysis; *Earth and Planetary Science Letters*, Volume 19, pages 290-300.
- Pell, J. (1987): Alkaline Ultrabasic Rocks in British Columbia; *Ministry of Energy, Mines and Petroleum Resources*, Open File 1987-17, 109 pages.
- Pell, J. (1994): Carbonatites, Nepheline Syenites, Kimberlites and Related Rocks in B.C.; *Ministry of Energy, Mines and Petroleum Resources*, Bulletin 88.
- Powell, W.G. and Ghent, E.D. (1966): Low-pressure Metamorphism of the Mafic Volcanic Rocks of the Rossland Group, Southeastern British Columbia; *Canadian Journal of Earth Sciences*, Volume 33, pages 1402-1409.
- Preto, V.A. (1977): The Nicola Group: Mesozoic Volcanism Related to Rifting in Southern British Columbia; in Volcanic Regimes in Canada, Barager, W.R.A., Coleman, L.C. and Hall, J.M., Editors, *Geological Association of Canada*, Special Paper 16, pages 39-57.
- Preto, V.A. (1979): Geology of the Nicola Group between Merritt and Princeton; *B.C. Ministry of Energy, Mines and Petroleum Resources*, Bulletin 69.
- Ray, G.E. and Spence, A. (1986): The Potassium-rich Volcanic Rocks at Tillicum Mountain - Their Geochemistry, Origin, and Regional Significance; *British Columbia Ministry of Energy, Mines and Petroleum Resources*, Geological Fieldwork 1985, Paper 1986-1, pages 45-49.
- Ray, G.E. and Webster, I.C.L. (1997): Skarns in British Columbia; *B.C. Ministry of Employment and Investment*, Bulletin 101, 260 pages.
- Reesor, J.E. and Leclair, A.E. (1983): Nelson East-Half Map Area; *Geological Survey of Canada*, Open File 929.
- Roback, R.C. (1993): Late Paleozoic to Middle Mesozoic Tectonic Evolution of the Kootenay Arc; Unpublished Ph.D. Thesis, *University of Austin at Texas*, 192 pages.
- Roback, R.C., Sevigny, J.H. and Walker, N.W. (1994): Tectonic Setting of the Slide Mountain Terrane, Southern British Columbia; *Tectonics*, Volume 13, pages 1242-1258.
- Roback, R.C., Schiarizza, P., Nelson, J., Fyles, J., Ferri, F., Höy, T., Ash, C. and Danner, W.R. (1995): Late Paleozoic Arc and Oceanic Terranes and their External Relationships, Southern Quesnellia; in Field Trip Guidebook B2, *Geological Association of Canada*, Victoria, B.C., 79 pages.
- Roback, R.C. and Walker, N.W. (1995): Provenance, Detrital Zircon U-Pb Geochronometry, and Tectonic Significance of Permian to Lower Triassic Sandstone in Southeastern Quesnellia, British Columbia and Washington; *Geological Society of America*, Bulletin, Volume 107, pages 665-675.
- Robert, F. and Kelly, W.C. (1987): Ore-forming Fluids in Archean Gold-bearing Quartz Veins at the Sigma Mine, Abitibi Greenstone Belt, Quebec, Canada; *Economic Geology*, Volume 82, pages 1464-1482.
- Roedder, E. (1984): Fluid Inclusions; *Mineralogical Society of America*, Reviews in Mineralogy, Volume 12, pages.
- Ross, G.M., Bloch, J.D. and Krouse, H.R. (1995): Paleoproterozoic Strata of the Southern Cordillera and the Isotopic Evolution of

- Seawater Sulfate; *Precambrian Research*, Volume 73, pages 71-99.
- Russell, J.K. and Nicholls, J. (1988): Analyses of Petrologic Hypotheses with Pearce Element Ratios; *Contributions to Mineralogy and Petrology*, Volume 99, pages 25-35.
- Russell, J.K., Nicholls, J., Stanley, C.R. and Pearce, T.H. (1990): Pearce Element Ratios: a Paradigm for Testing Hypotheses; *EOS*, Volume 71, Number 5, pages 234-236; 246-247.
- Schiarizza, P. and Preto, V.A. (1987): Geology of the Adams Plateau - Clearwater - Vavenby Area; *B.C. Ministry of Energy, Mines and Petroleum Resources*, Paper 1987-2, 88 pages.
- Self, S. and Sparks, R.S.J. (1978): Characteristics of Widespread Pyroclastic Deposits Formed by the Interaction of Silicic Magma and Water; *Bulletin Volcanology*, Volume 41, pages 196-212.
- Sevigny, J.H. and Parrish, R.R. (1993): Age and Origin of Late Jurassic and Paleocene Granitoids, Nelson Batholith, Southern British Columbia; *Canadian Journal of Earth Sciences*, Volume 30, pages 2305-2314.
- Seraphin, R.H., Church, B.N. and Shearer, J.T. (1995): The Lexington-Lone Star Copper-gold Porphyry: an Early Jurassic Cratonic Linear System, Southern British Columbia; in Porphyry Deposits of the Northwestern Cordillera of North America, Schroeter, T.G., Editor, *Canadian Institute of Mining and Metallurgy*, Special Volume 46, pages 851-854.
- Shelton, K.L. and Orville, P.M. (1980): Formation of Synthetic Fluid Inclusions in Natural Quartz; *American Mineralogist*, Volume 65, pages 1233-1236.
- Simony, P.S. (1979): Pre-Carboniferous Basement near Trail, British Columbia; *Canadian Journal of Earth Sciences*, Volume 16, pages 1-11.
- Smith, A.D., Brandon, A.D. and Lambert, R.St.J. (1995): Nd-Sr Isotope Systematics of Nicola Group Volcanic Rocks, Quesnel Terrane; *Canadian Journal of Earth Sciences*, Volume 32, pages 437-446.
- Smith, D.L. and Evans, B. (1984): Diffusional Crack Healing in Quartz; *Journal of Geophysical Research*, Volume 89, pages 4125-4135.
- Smith, M.J. (1974): Geology of the Harper Ranch Group (Carboniferous-Permian) and Nicola Group (Upper Triassic), Northwest of Kamloops, British Columbia; Unpublished M.Sc. Thesis, *The University of British Columbia*, Vancouver, 211 pages.
- Smith, M.T. and Gehrels, G.E. (1992): Structural Geology of the Lardeau Group near Trout Lake, British Columbia: Implications for the Structural Evolution of the Kootenay Arc; *Canadian Journal of Earth Sciences*, Volume 29, pages 1305-1319.
- Smith, A.D., Brandon, A.D. and Lambert, R. St. J. (1995): Nd-Sr Isotopic Systematics of the Nicola Group Volcanic Rocks, Quesnel Terrane; *Canadian Journal of Earth Sciences*, Volume 32, pages 437-446.
- Souther, J.G. (1991): Volcanic Regimes; Chapter 14, *Geology of the Cordilleran Orogen in Canada*, Gabrielse, H. and Yorath, C.J., Editors, *Geological Survey of Canada*, No. 4, pages 457-490.
- Sparkles, R.S.J. and Huppert, H.E. (1984): Density Changes During Fractional Crystallization of Basaltic Magmas: Fluid Dynamic Implications; *Contributions to Mineralogy and Petrology*, Volume 85, pages 300-309.
- Steiger, R.H. and Jager, E. (1977): Subcommission on Geochronology: Convention on the Use of Decay Constants in Geo- and Cosmochronology; *Earth and Planetary Science Letters*, Volume 36, pages 359-362.
- Stoffel, K.L. (1990): Geological Map of the Republic 1:100,000 Quadrangle, Washington; *Washington Division of Geology and Earth Resources*, Open File Report 90-10, 62 pages.
- Streckeisen, A. (1976): To Each Plutonic Rock its Proper Name; *Earth Science Reviews*, Volume 12, pages 1-33.
- Sun, S.S. (1980): Lead Isotopic Study of Young Volcanic Rocks from Mid-ocean Ridges, Ocean Islands and Island Arcs; *Phil. Transactions of the Royal Society of London*, A297, pages 409-445.
- Thompson, R.N., Morrison, M.A., Hendry, G.L. and Parry, S.J. (1984): An Assessment of the Relative Roles of Crust and Mantle in Magma Genesis: an Elemental Approach; *Phil. Transactions of the Royal Society of London*, A310, pages 549-590.
- Thorpe, R.I. (1967): Mineralogy and Zoning of the Rosland Area; unpublished Ph.D. thesis, *University of Wisconsin*.
- Tipper, H.W. (1984): The Age of the Jurassic Rosland Group of Southeastern British Columbia; in *Current Research, Part A, Geological Survey of Canada*, Paper 84-1A, pages 631-632.
- Travers, W.B. (1982): Possible Large-scale Overthrusting near Ashcroft, British Columbia: Implications for Petroleum Prospecting; *Bulletin of Canadian Petroleum Geology*, Volume 30, pages 1-8.
- Turner, J. S. and Campbell, I.H. (1984): Convections and Mixing in Magma Chambers; *Earth Science Review*, Volume 23, pages 255-352.
- Walker, J.F. (1926): Geology and Mineral Deposits of Windermere Map-Area, British Columbia; *Geological Survey of Canada*, Memoir 148.
- Walker, J.F. (1934): Geology and Mineral Deposits of the Salmo Map-area, British Columbia; *Geological Survey of Canada*, Memoir 172, 102 pages.
- Walker, R.W. (1979): Facies Model 8. Turbidites and Associated Coarse Clastic Deposits; *Geoscience Canada*, Reprint Series 1, pages 91-104.
- Warren, M.J. (1996): Geology of the West-central Purcell Mountains, British Columbia; *B.C. Ministry of Employment and Investment*, Open File Map 1996-16.
- Waters, A.C. and Fisher, R.V. (1971): Base Surges and their Deposits: Capelinhos and Taal Volcanoes; *Journal of Geophysical Research*, Volume 76, pages 5596-5614.
- Webster, I.C.L., Ray, G.E. and Pettipas, A.R. (1992): Selected Mineralized Skarns in British Columbia; in *Geological Fieldwork 1991*,

- Newell, J.M. and Grant, B., Editors, *B.C. Ministry of Energy, Mines and Petroleum Resources*, Paper 1992-1, pages 235-252.
- Wheeler, J.O. and McFeely, P. (1991): Tectonic Assemblage Map of the Canadian Cordillera and Adjacent Parts of the United States; *Geological Survey of Canada*, Map 1712A, Scale 1:2,000,000.
- Wilson, M. (1989): Igneous Petrogenesis: a Global Tectonic Approach; *Unwin Hyman*, Boston, 466 pages.
- Wilson, M. and Davidson, J.P. (1984): Constraints Imposed by Experimental Petrology on Possible and Impossible Magma Sources and Products; *Phil. Transactions of the Royal Society of London*, A310, pages 439-456.
- Wingate, M.T.D. (1993): Extension in High-Grade Terranes of the Southern Omineca Belt: Evidence from Paleomagnetism; Unpublished M.Sc. Thesis, *University of Victoria*, 128 Pages.
- Wong, R.H. and Spence, C.D. (1996): Copper-gold Mineralization in the Willa Breccia Pipe, Southeastern British Columbia; in *Porphyry Deposits of the Northwestern Cordillera of North America*, Schroeter, T.G., Editor, *Canadian Institute of Mining, Metallurgy and Petroleum*, Special Volume 46, pages 401-409.
- Woodsworth, G.J., Anderson, R.G. and Armstrong, R.L. (1992): Plutonic Regimes, Chapter 15, in *Geology of the Cordilleran Orogen in Canada*, Gabrielse, H. and Yorath, C.J., Editors, *Geological Survey of Canada*, No. 4, pages 491-531.

APPENDICES

Appendix 1: Major, trace and minor element data, Elise Formation; (sample locations in Appendix 4)

Sample Unit	SiO ₂	TiO ₂	Al ₂ O ₃	Fe ₂ O ₃	MnO	MgO	CaO	Na ₂ O	K ₂ O	P ₂ O ₅	Total	Ni	Cr	Ba	Sr	Zr	Y	Nb	Ta	V	La
R3-01	Je7l	54.20	0.83	16.99	7.52	0.12	2.43	3.41	3.08	0.25	99.12	9	0	703	426	144	230	18	0	222	23
R3-5B	Je4	43.53	0.54	9.74	11.16	0.22	10.84	1.37	1.77	0.24	97.05	301	654	234	363	90	231	28	6	260	22
R3-5C	Je4	46.66	0.56	9.99	11.75	0.22	12.55	1.07	1.90	0.25	98.97	304	694	423	357	88	235	27	7	291	25
R4-03	Je4	47.12	0.76	14.01	11.57	0.21	6.69	11.02	2.10	0.95	98.61	23	46	377	1135	170	226	20	1	353	29
R4-09	Je8l	48.23	0.82	14.11	12.44	0.22	7.47	9.00	1.91	2.67	99.49	31	73	830	990	165	242	27	1	355	31
R4-10	Je8x	48.22	0.82	14.68	12.17	0.18	6.32	5.25	2.67	1.43	98.92	29	73	470	488	118	217	18	0	350	33
R4-15	Je8x	55.92	0.41	17.33	6.29	0.14	2.89	5.41	3.34	2.78	99.05	15	25	1028	1267	194	228	23	2	168	18
R6-12	Je8l	51.79	0.79	14.51	9.68	0.20	5.57	8.61	3.14	2.39	99.80	49	219	399	621	156	243	31	2	252	18
R6-14A	Je1	47.89	1.05	15.16	11.23	0.15	7.06	9.78	3.29	0.54	99.73	49	115	106	530	149	235	30	5	325	19
R7-08	Je7l	52.55	0.70	15.19	10.77	0.15	4.65	8.24	1.14	3.24	99.16	39	64	670	757	162	241	31	3	326	21
R10-6A	Je1	53.03	0.84	17.02	9.85	0.18	3.89	6.30	4.97	2.60	100.06	21	35	823	791	194	238	35	4	239	36
R10-6B	Je1	52.26	0.84	16.84	10.13	0.18	3.84	7.43	4.57	2.47	100.06	15	15	820	886	187	233	17	0	242	30
R11-1	Je4	48.64	0.65	11.83	11.74	0.26	11.05	9.53	1.89	2.04	100.40	153	455	515	523	114	241	29	4	283	22
R11-7	Je8l	48.30	0.90	16.27	10.67	0.20	3.79	6.96	3.07	1.90	98.27	23	32	412	967	165	224	15	0	303	35
R11-10	Je8l	53.27	0.84	15.10	12.33	0.17	4.18	4.99	3.32	1.09	99.27	17	24	350	801	157	236	27	6	294	24
R12-5	Je8x	55.94	0.40	17.78	5.94	0.08	1.83	3.96	4.36	3.84	98.91	6	9	1104	666	158	238	29	5	153	30
R13-4	Je8l	56.94	0.83	16.94	7.55	0.13	2.27	5.53	4.05	2.36	98.89	10	26	448	884	262	245	30	0	173	32
R15-5	Je8x	53.58	0.48	17.11	7.28	0.10	2.39	4.99	3.20	5.15	99.66	8	12	1207	687	161	259	38	3	189	30
R15-11	Je7l	45.84	0.98	17.42	9.40	0.15	3.90	8.07	2.07	3.25	98.94	19	11	637	564	143	234	24	2	339	21
R17-8	Je8l	48.60	0.83	16.32	11.36	0.21	4.63	8.89	2.44	2.78	99.03	13	10	857	1020	170	234	16	0	308	29
R12-1	Je8x	58.27	0.38	17.47	3.03	0.04	1.78	3.27	3.23	7.56	99.01	5	17	1130	559	151	243	32	5	184	34
R18-13	Je7f	48.72	0.77	15.07	11.18	0.18	4.57	7.78	3.52	3.36	98.87	19	9	1248	587	130	234	27	0	311	13
R21-5	Je4	48.30	0.54	9.68	11.28	0.24	11.80	11.46	1.31	1.42	98.92	252	633	488	580	962	221	15	0	278	21
R22-2C	Je8l	45.53	0.89	15.83	8.62	0.16	6.97	11.26	3.08	1.15	98.25	71	182	1423	1974	360	231	149	3	212	195
R31-6	Je8l	49.21	0.84	16.19	8.61	0.15	3.06	10.88	2.03	1.75	99.42	20	15	782	627	123	218	15	0	319	13
R31-9	Je4	49.64	0.77	14.79	10.98	0.22	6.71	8.39	3.11	2.26	99.15	32	100	699	757	145	235	26	4	298	23
R33-13	Je4	46.60	0.52	9.78	11.34	0.19	11.39	11.71	1.53	2.22	98.99	167	528	448	413	86	221	17	0	264	18
R34-3	Je4	44.71	0.70	14.10	10.55	0.16	7.40	6.91	3.76	1.24	98.24	43	62	504	495	109	213	24	0	296	16
R34-14	Je8x	56.18	0.69	14.04	9.26	0.03	3.41	2.87	4.24	2.39	98.29	17	74	426	344	128	227	29	0	242	32
R37-13	Je1	47.40	0.68	13.62	10.59	0.18	7.50	11.41	2.04	2.27	98.60	76	238	643	1078	167	244	29	0	277	17
R19-4	Je10	47.81	0.76	15.70	10.77	0.16	4.98	7.69	2.21	2.25	99.61	61	61	933	341	81	21	5			
R4-1	Je4	47.64	0.78	14.51	12.38	0.20	6.75	9.87	1.33	1.09	100.12	66	66	299	1083	63	17	4			

Sample Unit	SiO ₂	TiO ₂	Al ₂ O ₃	Fe ₂ O ₃	MnO	MgO	CaO	Na ₂ O	K ₂ O	P ₂ O ₅	Total	Ni	Cr	Ba	Sr	Zr	Y	Nb	Ta	V	La	
R22-1C	Je5	48.60	0.64	16.50	9.33	3.18	9.76	3.09	2.52	0.31	99.80	29	538	875	84	20	4					
R20-1	Je8x	52.38	0.68	16.96	8.50	2.78	5.87	3.55	2.27	0.29	99.47	21	652	514	84	23	4					
R30-14	Je10	49.70	0.75	18.53	9.33	3.75	7.87	2.19	2.59	0.37	99.39	25	869	949	100	25	4					
R33-11	Je8l	46.83	0.97	17.14	11.52	2.59	9.33	1.95	2.62	0.32	100.37	18	549	591	87	29	4					
R37-23	Je4	48.23	0.76	15.85	10.85	5.11	8.62	2.66	3.08	0.27	99.36	17	22	760	727	132	231	17	0	307	16	
R8-6	Je1	49.53	0.71	13.79	11.08	7.31	11.45	2.19	1.81	0.32	99.76	114	216	657	1033	181	250	39	4	297	8	
R8-13	Je8l	53.94	0.80	17.33	8.36	3.45	8.10	3.39	1.96	0.29	100.07	15	50	407	1143	249	248	33	5	211	27	
R9-2	Je4	62.08	0.42	16.83	4.32	1.34	3.34	2.78	3.72	0.16	99.57	11	17	1270	214	231	247	45	4	72	361	
R9-3	Je4	62.34	0.42	16.87	4.26	1.33	3.27	2.84	3.78	0.15	100.41	14	12	1252	199	213	238	34	0	77	29	
R9-4A	Je8l	54.52	0.76	17.11	8.27	2.70	5.16	4.01	2.01	0.23	99.22	6	12	880	346	169	237	33	1	199	36	
R9-4B	Je8l	60.16	0.57	17.42	6.56	4.38	1.19	1.85	3.34	0.23	99.31	7	19	808	342	186	246	39	5	148	32	
R9-6B	Je8l	49.92	0.93	21.44	13.27	3.25	1.80	1.92	1.76	0.30	99.38	11	0	755	524	129	238	25	1	289	27	
R9-7	Je8l	47.17	1.41	13.03	10.13	9.87	8.57	3.19	1.75	1.61	100.23	176	422	1765	1649	398	253	163	13	235	187	
R11-14	Je8l	50.35	0.72	16.23	8.97	3.20	8.39	3.13	3.18	0.39	100.12	31	21	734	767	181	245	32	4	242	22	
R36-8	Je7f	47.74	0.73	13.40	9.92	5.50	8.25	1.84	1.69	0.22	98.91	84	337	826	328	106	234	30	0	271	374	
R38-6A	Je4	45.90	1.00	14.25	11.52	6.25	12.91	1.92	1.08	0.23	99.19	101	268	417	978	79	21	7	5	372	20	
R38-6B	Je4	45.36	1.01	14.42	12.71	6.41	11.50	2.08	1.41	0.26	99.53	105	262	412	857	82	23	6	7	329	19	
R39-2	Je8l	48.24	1.05	16.53	10.60	3.18	8.47	3.97	1.37	0.31	99.82	17	12	411	857	105	30	10	5	286	15	
R41-1	Je11a	49.57	0.66	12.29	11.11	7.32	8.98	3.54	1.93	0.30	99.27	99	430	849	401	58	18	14	5	280	16	
R42-4	Je11a	54.40	0.84	16.93	8.92	3.65	5.41	4.02	3.79	0.28	99.51	13	12	1055	645	112	34	15	6	242	15	
R43-4	Je11a	55.20	0.65	14.78	7.24	2.10	12.65	0.97	3.76	0.28	100.52	14	35	967	553	91	23	14	5	239	27	
R53-5	Je1	48.94	0.73	10.44	10.02	12.41	9.91	2.23	0.74	0.16	99.45	267	680	258	268	50	17	9	5	240	15	
R54-6	Je8l	53.73	0.69	17.23	8.73	2.70	3.49	3.49	3.92	0.33	98.60	8	10	1581	591	90	23	10	5	242	21	
R55-4	Je1	44.91	1.17	16.15	14.06	8.44	7.46	2.53	0.86	0.22	98.86	95	182	390	516	91	28	7	7	339	19	
R57-19	Je1	48.56	0.79	13.78	11.14	10.91	7.62	2.66	1.12	0.20	99.54	187	386	109	376	54	17	7	5	55	15	
R64-4	Je	54.74	0.96	16.57	8.91	3.62	6.41	3.77	3.43	0.34	99.99	19	28	994	713	122	26	7	5	248	15	
R72-19	Je	60.54	0.61	15.39	5.16	1.56	5.10	2.73	3.21	0.18	100.22	5	10	796	460	142	17	13	5	69	24	
R73-7	Je	52.57	0.64	18.12	8.32	3.23	5.41	3.47	4.57	0.48	99.64	19	16	994	981	84	19	5	5	216	19	
R73-9	Je	49.05	0.54	9.38	10.04	14.89	8.08	0.75	3.28	0.18	99.45	417	1028	549	142	44	13	7	7	225	15	
R73-11	Je	52.07	0.74	15.84	8.97	4.90	0.96	3.84	1.36	0.50	99.76	37	85	548	870	90	20	9	5	243	24	
R74-19	Je	44.90	1.32	12.30	9.20	8.83	11.27	0.62	4.69	1.66	98.22	164	541	4626	1818	269	31	215	17	228	234	
R68-5	Je	52.03	0.81	15.20	11.28	5.48	9.20	2.44	1.88	0.33	99.72	22	43	805	1033	86	21	5	8	314	21	
R69-2	Je1	47.29	0.76	13.60	11.99	5.61	8.88	2.69	3.20	0.37	99.34	27	42	861	804	74	20	6	6	335	24	
R72-14	Je	50.64	0.65	11.84	9.98	9.46	11.55	2.29	1.70	0.22	99.46	148	438	435	401	51	20	9	11	307	15	

Sample	Unit	SiO2	TiO2	Al2O3	Fe2O3	MnO	MgO	CaO	Na2O	K2O	P2O5	Total	Ni	Cr	Ba	Sr	Zr	Y	Nb	Ta	V	La
R72-15b	Je	50.59	0.59	10.75	10.25	0.19	10.89	14.30	1.20	0.94	0.24	100.12	120	564	459	464	38	16	7	6	277	18
R83-4	Je4	47.77	0.69	12.35	11.97	0.20	7.82	9.72	3.33	1.12	0.29	99.31	80	269	372	684	54	17	8	5	295	15
R83-5	Je7l	49.75	1.00	17.16	10.34	0.13	4.29	3.68	0.25	4.47	0.28	98.14	23	15	768	151	82	27	14	5	309	15
R83-6	Je4	57.91	0.81	13.64	11.07	0.40	4.25	2.23	0.27	2.98	0.20	99.63	159	299	651	68	60	14	9	5	303	15
R83-8	Je1	50.84	0.71	15.93	10.45	0.18	5.16	4.10	3.76	3.37	0.44	99.53	33	68	739	785	87	25	15	6	279	15
R84-6	Je1	48.23	0.71	11.74	11.28	0.19	6.25	12.67	2.30	1.34	0.24	98.44	58	188	669	717	68	21	9	7	297	18
R85-7	Je	47.79	1.05	14.47	11.40	0.23	6.19	10.74	2.75	1.12	0.23	99.57	46	85	514	607	58	21	8	6	369	15
R85-9	Je	57.53	0.51	14.55	6.87	0.15	3.49	5.82	4.23	2.18	0.21	100.18	64	195	768	496	78	17	12	7	206	15
R86-16	Je7l	53.54	0.52	17.63	7.29	0.15	2.25	5.44	5.24	2.60	0.31	99.44	12	13	1276	721	84	23	20	5	272	15
R87-3	Je2	47.71	0.59	10.83	12.36	0.18	9.43	12.51	1.53	2.04	0.27	99.23	199	487	459	707	49	18	7	9	306	16
R88-1	Je	49.43	0.61	10.59	11.84	0.21	10.96	10.49	2.12	1.85	0.26	99.67	164	442	470	588	47	14	6	5	293	15
R88-6	Je4	46.01	0.62	11.14	12.77	0.28	0.84	12.91	1.33	2.06	0.29	99.48	181	482	456	901	49	17	5	8	329	25
R93-13	Je3	54.69	0.73	17.32	8.70	0.16	2.49	7.40	4.28	2.58	0.35	100.52	12	12	651	745	106	24	5	9	214	17
R94-5	Je3	52.89	0.72	15.09	10.26	0.22	5.27	10.14	2.42	1.96	0.33	99.99	31	77	1231	881	71	22	5	8	293	15
R95-5	Je3	49.68	0.88	14.84	10.64	0.15	6.20	10.71	1.88	1.18	0.22	100.06	65	148	406	537	77	23	7	9	286	15
R95-17	Je2	51.36	0.58	10.97	8.97	0.22	6.34	13.42	1.32	3.17	0.22	100.01	87	271	1033	569	59	21	9	5	242	17
R95-20	Je2	51.94	0.89	13.72	10.41	0.18	8.25	10.21	2.02	0.63	0.22	100.07	51	210	337	457	75	26	11	7	319	15
R85-7	Je	48.31	1.06	14.55	11.55	0.23	6.23	10.68	2.76	1.14	0.23	99.84	46	90	524	617	60	23	7	8	364	15
R62-1	Je1l	52.12	0.77	12.26	9.85	0.22	7.56	9.85	2.47	2.01	0.29	99.55	71	290	981	564	69	21	7	9	317	15
R71-6	Je1	50.91	0.69	14.90	8.33	0.20	3.75	5.20	2.87	4.77	0.30	99.17	24	80	822	413	68	20	6	6	282	15
R71-5	Je1	45.52	0.42	11.54	4.89	0.34	5.05	10.14	4.23	3.15	0.26	99.20	6	10	363	436	70	19	11	7	128	15
R73-6	Je	59.03	0.37	19.93	4.60	0.04	0.89	0.46	2.67	9.43	0.20	99.36	4	10	3455	587	123	17	10	5	112	17
R78-1	Je4	47.80	0.92	15.76	10.28	0.18	4.67	9.22	2.80	1.17	0.23	99.03	15	13	415	656	96	30	11	5	299	17
R78-19	Je8x	41.82	0.83	15.70	5.80	0.17	1.66	13.65	2.00	4.72	0.26	99.44	15	25	1010	843	74	24	5	5	274	16
R78-21	Je7l	47.85	0.86	15.62	7.27	0.14	2.29	7.84	1.04	7.33	0.25	99.90	17	21	1413	358	76	24	8	5	294	15
R78-23	Je8x	50.39	0.94	16.31	9.26	0.10	2.15	5.20	1.52	7.45	0.25	99.41	22	20	1586	349	77	20	5	6	299	15
R78-23e	Je8x	49.96	0.84	15.34	8.07	0.14	1.63	6.64	0.87	7.63	0.23	99.55	18	17	1392	384	67	21	6	7	249	15
R78-24	Je4	46.72	0.77	15.75	8.63	0.11	3.82	7.08	1.77	5.17	0.27	99.34	21	47	733	358	72	19	7	7	294	15
R79-2	Je4	49.77	0.70	13.18	10.75	0.25	7.22	11.04	1.66	2.30	0.29	99.54	66	298	577	702	66	19	8	8	289	18
R79-4	Je8x	53.43	0.60	17.49	7.73	0.24	2.51	4.41	2.71	5.89	0.31	99.73	4	10	844	396	101	18	7	5	175	15
R79-15	Je7l	51.24	0.59	15.96	8.32	0.30	2.62	6.47	2.79	4.80	0.30	99.74	4	10	884	370	95	22	6	10	223	18
R80-4	Je4	48.21	0.79	15.86	11.17	0.26	4.79	5.42	3.37	3.98	0.34	99.59	7	10	720	42	62	19	5	10	294	20
R80-5	Je4	50.36	0.75	15.15	9.66	0.22	3.19	6.84	3.21	4.02	0.33	99.01	8	20	1330	447	58	18	5	5	295	15
R80-9	Je	50.72	0.73	14.98	10.32	0.19	3.58	6.55	3.26	4.26	0.33	98.97	80	10	696	817	63	19	5	5	309	20

Sample	Unit	SiO ₂	TiO ₂	Al ₂ O ₃	Fe ₂ O ₃	MnO	MgO	CaO	Na ₂ O	K ₂ O	P ₂ O ₅	Total	Ni	Cr	Ba	Sr	Zr	Y	Nb	Ta	V	La
R80-17	Je	48.88	0.74	15.00	10.43	0.21	5.06	8.71	3.13	3.04	0.35	99.32	12	16	632	1045	70	19	5	5	311	16
R80-21	Je	44.62	0.72	14.19	9.35	0.29	4.05	6.70	1.58	4.32	0.30	99.14	8	12	830	301	52	16	5	5	279	15
R80-24	Je71	47.84	0.76	14.65	11.17	0.19	5.51	6.45	3.09	3.51	0.33	99.09	19	47	651	507	63	17	5	7	328	23
R80-26	Je	45.14	0.68	14.45	9.02	0.34	3.02	10.28	2.72	3.83	0.32	99.33	5	11	841	542	58	18	6	5	219	16
R81-1	Je	56.01	0.58	18.18	6.91	0.10	2.63	1.66	3.87	6.26	0.37	99.18	4	15	1134	590	87	22	11	7	279	15
R82-7	Je	51.96	0.71	12.78	10.34	0.24	7.31	3.58	2.46	5.30	0.27	99.48	50	271	625	355	57	19	7	9	343	16
R82-10a	Je	61.65	0.55	14.77	5.97	0.00	1.08	0.02	0.03	1.11	0.12	100.13	4	14	2333	405	80	11	5	12	169	15
R78-11	Je7	48.00	0.75	14.46	11.15	0.19	5.69	8.35	1.83	2.62	0.27	99.68	29	43	424	707	64	19	7	11	310	15
R110-14	Je	41.16	0.34	7.58	27.90	0.20	4.30	0.30	0.00	2.10	0.10	97.28	49	10	811	38	20	10	5		151	15
R110-3	Je	52.09	0.61	13.85	11.22	0.22	2.80	8.50	2.41	2.50	0.27	99.59	26	97	1219	701	79	16	5	5	285	14
R111-2	Je	51.36	0.75	15.31	9.69	0.20	4.93	10.92	2.72	1.49	0.37	99.67	53	68	422	814	102	19	9	5	280	23
R129-2	Je8x	60.50	0.65	15.30	7.68	0.14	4.03	3.43	4.74	1.95	0.15	99.64	10	14	1595	446	149	37	43	5	161	15
R133-4	Je	58.21	0.63	17.13	7.63	0.15	2.82	4.76	3.67	2.57	0.23	99.83	17	19	1892	705	216	55	57	5	302	15
R98-6	Je	51.08	0.74	14.00	12.12	0.20	6.62	6.64	2.89	3.15	0.32	99.89	37	93	1043	694	69	18	5	5	329	20
R99-3	Je2	52.63	0.78	13.22	9.63	0.16	8.00	10.92	3.35	0.41	0.19	100.17	119	344	165	250	60	18	11	5	296	15
R100-13	Je2	50.19	0.83	17.11	10.55	0.19	4.72	10.85	2.14	2.04	0.27	99.78	24	39	816	670	75	20	6	5	334	15
R102-2	Je3	50.62	0.69	16.75	10.02	0.14	6.26	9.51	2.77	1.65	0.18	99.82	31	58	631	682	91	30	26	5	288	15
R103-2	Je3	50.30	0.88	15.98	10.96	0.18	6.26	10.63	2.33	0.78	0.20	100.05	24	111	309	570	96	30	17	5	324	15
R123-19	Je81	54.84	0.85	16.93	10.38	0.19	4.12	3.72	4.28	2.24	0.25	99.50	11	10	1119	436	154	52	55	5	309	15
R124-10	Je71	52.58	0.70	15.25	10.07	0.18	4.65	7.79	3.57	2.81	0.35	99.29	25	72	869	762	101	24	16	5	269	15
R125-11	Je1	49.39	0.80	15.29	12.21	0.24	5.50	10.00	2.97	0.76	0.32	99.76	29	68	172	419	79	30	22	5	392	15
R132-7	Je7	49.04	0.82	14.92	10.23	0.35	6.00	5.96	3.66	0.74	0.26	99.70	25	50	286	470	119	45	51	5	609	15
R134-6	Je8x	47.81	0.85	16.24	12.18	0.21	7.82	5.87	1.44	1.51	0.14	99.66	25	97	512	251	55	17	10	5	269	15
R134-7	Je8x	57.34	0.68	16.55	7.95	0.13	3.15	8.09	2.40	1.20	0.19	100.09	42	40	580	741	180	46	49	5	304	15
R136-12	Je1	50.52	0.57	10.31	11.60	0.21	9.84	12.33	1.73	1.06	0.31	99.59	116	448	441	639	65	20	15	5	310	18
R110-5	Je	46.39	0.31	9.32	7.55	0.62	2.78	28.62	0.00	0.02	0.44	100.26	14	128	37	93						
R173-2	Je4	49.28	1.06	15.29	11.98	0.17	6.53	12.22	1.31	0.65	0.22	99.85	33	100	283	460	57	22	5	15	331	23
R170-7	Je1	49.23	1.23	15.35	12.03	0.17	6.03	11.28	2.37	0.55	0.25	99.24	52	199	253	611	81	24	2	15	299	17
R163-2	Je2	46.50	1.25	16.41	9.10	0.15	5.06	7.21	3.06	2.82	1.15	99.16	29	52	2108	1348	194	29	96	15	176	161
R155-3	Je2	49.42	0.78	14.35	11.59	0.18	6.12	6.73	3.10	1.59	0.32	99.08	22	76	1306	800	60	15	6	15	303	23
R187-10	Je4	47.62	0.79	13.73	12.42	0.22	7.62	12.14	2.16	1.66	0.27	99.39	31	94	599	723	43	16	1	15	343	27
R200-8	Je1	49.61	0.64	17.96	8.59	0.14	2.60	8.19	4.40	2.26	0.39	99.01	2	16	432	563	63	18	3	15	190	14
R204-24	Je2	47.34	0.96	14.81	11.31	0.21	5.54	8.41	3.17	1.73	0.46	99.28	16	83	755	440	62	23	1	15	332	22
R217-6	Je81	50.63	0.77	13.94	11.52	0.22	6.19	8.85	2.95	1.70	0.35	99.60	20	64	641	628	62	12	5	15	222	12

Sample	Unit	SiO ₂	TiO ₂	Al ₂ O ₃	Fe ₂ O ₃	MnO	MgO	CaO	Na ₂ O	K ₂ O	P ₂ O ₅	Total	Ni	Cr	Ba	Sr	Zr	Y	Nb	Ta	V	La
R218-2	Je1,2	60.55	0.61	15.71	7.18	0.12	2.92	3.32	3.88	3.26	0.16	99.22	5	16	1441	475	104	18	6	15	132	19
R219-10	Je1	48.38	0.74	15.26	10.83	0.17	4.66	9.40	3.17	2.21	0.34	99.11	14	34	816	891	54	20	2	15	306	20
R226-2	Je8x	48.85	0.80	15.03	11.98	0.18	6.88	8.70	1.65	1.67	0.33	99.27	18	45	1072	811	58	18	3	15	324	27
R233-8	Je8x	53.67	0.85	15.33	10.30	0.18	4.77	7.68	2.89	0.39	0.23	99.61	22	69	209	615	74	25	2	15	267	13
R241-2	Je2	46.31	0.73	13.57	10.79	0.23	6.72	8.76	3.59	1.27	0.26	99.56	41	154	564	294	45	17	1	15	275	22
R241-7	Je7l	49.48	0.73	15.90	10.76	0.22	4.93	9.26	2.73	2.53	0.23	99.20	7	20	687	937	66	20	6	15	323	21
R249-4	Je4	45.72	0.72	16.31	9.44	0.19	6.45	7.22	2.58	3.71	0.27	99.03	31	67	1054	679	50	16	2	15	280	20
R253-7	Je2	50.60	0.81	15.30	10.93	0.28	6.60	6.37	3.80	1.97	0.29	99.26	42	105	586	676	51	18	1	15	301	16
R256-4b	Je8x	60.93	0.54	12.51	14.76	0.10	0.94	0.35	0.32	2.95	0.14	99.05	18									
R256-4c	Je8x	62.97	0.55	13.73	6.27	0.56	0.99	7.38	0.19	5.43	0.16	99.77	20									
R256-4d	Je8x	59.17	0.68	14.90	7.98	0.13	5.24	2.62	4.34	0.78	0.18	99.52	19									
R256-4di	Je8x	60.35	0.67	15.23	7.99	0.13	4.80	2.78	4.95	0.62	0.17	99.88	19									
R256-4e	Je8x	59.27	0.64	15.63	7.62	0.16	4.05	4.34	3.68	1.78	0.17	99.09	22									
R256-4f	Je8x	61.31	0.66	15.36	7.33	0.12	2.38	4.44	4.07	2.50	0.18	100.00	20									
R256-6	Je8x	55.61	0.77	18.59	8.50	0.18	2.40	4.09	6.05	1.70	0.22	99.21	2									
R159-13	Je1	65.61	0.82	14.56	5.18	0.21	2.53	2.16	3.41	1.97	0.11	99.47	1									
R257-15	Je7l	48.55	0.80	13.82	8.49	0.17	5.88	12.89	3.53	0.59	0.22	99.92	72	240	152	438	54	17	5			
R258-11	Je7x	52.34	0.85	13.92	10.43	0.18	5.55	9.62	2.32	0.08	0.20	99.36	43	120	53	522	65	21	5			
R262-3	Je7x	49.09	0.95	12.59	11.16	0.16	7.70	10.03	3.92	0.14	0.20	99.26	68	239	109	356	57	21	5			
R262-14	Je4	50.41	0.75	14.95	11.27	0.19	5.09	7.91	3.43	2.38	0.38	99.27	19	63	806	839	66	22	5			
R266-1	Je7l	47.29	0.88	15.96	10.72	0.24	5.76	10.16	2.21	1.29	0.26	99.20	28	36	480	479	59	17	5	15	287	21
R266-2	Je7l	49.01	0.82	12.94	11.65	0.20	7.67	10.10	2.35	0.81	0.22	99.03	53	136	295	491	47	17	5	15	300	15
R265-6	Je4	49.84	0.65	13.83	10.13	0.17	5.83	10.30	2.57	2.97	0.40	99.29	30	124	886	912	62	16	5	15	281	29
R279-9	Je4	48.80	0.67	14.59	0.15	0.16	5.07	8.56	3.58	2.60	0.39	98.92	31	113	917	607	57	16	5	15	250	17
R281-21	Je7l	48.81	0.79	16.81	10.19	0.19	5.62	9.38	2.36	2.01	0.19	99.38	24	40	621	495	52	20	5			
R284-16	Je7x	50.17	1.00	15.21	11.87	0.18	5.88	9.93	2.81	0.67	0.22	99.60	24	34	257	376	70	23	5			
R286-5	Je8l	60.05	0.67	15.41	7.60	0.12	3.08	5.97	3.81	1.36	0.21	99.10	4	13	750	570	78	26	5			
R293-4	Je7x	53.75	0.85	14.13	10.80	0.15	4.92	8.68	2.86	0.60	0.22	99.45										
R294-7	Je8l	48.63	0.63	13.63	9.63	0.18	5.43	11.00	2.29	3.46	0.40	98.86										
R296-11	Je1	46.15	1.00	16.50	11.79	0.21	7.75	7.80	2.77	2.73	0.29	98.97										
R297-11	Je4	47.12	0.75	13.61	12.00	0.22	6.85	10.43	2.46	1.92	0.29	99.14										
R302-9	Je4	49.59	0.74	14.91	11.11	0.20	5.25	8.68	3.01	2.28	0.38	99.10										
R308-9	Je4	49.61	0.91	17.17	11.45	0.22	4.65	8.11	3.62	2.14	0.33	99.25										
R312-9	Je7x	49.53	0.65	13.70	10.41	0.19	6.70	9.90	2.59	2.66	0.40	98.93										

Sample	Unit	SiO ₂	TiO ₂	Al ₂ O ₃	Fe ₂ O ₃	MnO	MgO	CaO	Na ₂ O	K ₂ O	P ₂ O ₅	Total	Ni	Cr	Ba	Sr	Zr	Y	Nb	Ta	V	La
R314-1	Je7x	53.80	0.86	16.83	8.70	0.19	3.81	8.35	2.96	2.37	0.34	99.55					97	25	7	15	237	
R329-13	Je7l	61.77	0.75	15.91	5.68	0.07	2.32	3.39	3.89	2.60	0.19	99.34					87	16	5	15	213	
R337-9	Je8x	48.90	0.78	14.15	10.59	0.19	10.14	8.52	2.83	1.54	0.17	99.35	145	308	410	389	53	18	5	15	156	15
R339-3	Je4	55.55	1.18	14.76	8.55	0.16	4.74	6.96	2.49	3.36	0.37	99.14	22	127	1664	822	235	28	15	15	194	55
R340-5	Je3	49.95	0.97	14.28	12.14	0.19	6.19	8.61	2.28	3.21	0.34	99.13	25	71	1250	698	60	17	5	15	387	26
R343-5	Je7x	49.03	0.84	15.92	10.57	0.18	5.00	10.90	2.75	0.58	0.25	99.12	25	36	427	510	53	19	5	15	323	19
R344-3a	Je8l	55.63	0.62	18.41	7.80	0.21	2.43	7.34	3.15	1.68	0.22	99.13	1	10	867	935	72	18	5	15	144	16
R344-3b	Je8l	59.26	0.61	17.38	7.24	0.28	2.06	4.93	0.15	4.06	0.20	99.79	1	10	1203	195	65	20	5	15	131	15
R344-4g	Je7l	65.55	0.43	16.49	3.93	0.15	1.32	5.29	0.27	3.92	0.15	99.64	13	10	996	214	109	18	9	15	66	15
R344-4h	Je7l	64.99	0.43	16.58	5.19	0.29	1.26	4.28	0.30	3.71	0.15	99.58	4	13	875	158	110	20	9	15	61	15
R344-4k	Jr7l	54.20	0.65	19.99	7.44	0.25	2.50	6.23	0.26	4.46	0.23	99.40	2	10	1760	236	80	25	5	15	156	17
R344-4l	Je7l	56.67	0.62	18.32	7.83	0.17	1.74	7.23	2.76	2.14	0.23	99.13	4	10	1034	592	80	22	5	15	142	15
R344-4m	Je8l	55.86	0.63	18.16	7.68	0.22	2.08	9.27	2.27	1.40	0.21	99.59	4	10	636	652	73	23	5	15	147	21
R349-1a	Je8l	56.58	0.73	18.59	7.71	0.20	2.28	6.08	2.50	2.36	0.21	99.31	2	10	750	372	71	20	5	15	228	15
R349-2f	Je8x	59.49	0.65	15.25	7.93	0.23	3.61	3.26	3.15	1.88	0.17	99.52	18	55	873	294	94	21	5	15	151	16
R349-2g	Je8x	53.18	0.75	16.67	8.82	0.29	4.77	6.14	3.64	1.67	0.19	99.31	23	81	847	513	103	23	5	15	178	15
R349-3a	Je8l	62.37	0.61	16.66	6.05	0.17	2.68	4.75	0.96	2.78	0.22	99.60	20	73	650	226	130	18	13	15	100	29
R349-3e	Je8l	65.06	0.45	17.23	4.17	0.11	1.45	4.57	1.68	3.49	0.16	99.60	4	10	773	241	107	16	6	15	70	15
R349-3g	Je8l	61.26	0.62	15.54	5.97	0.18	1.31	8.83	0.51	3.21	0.17	99.78	17	60	799	163	97	18	5	15	157	17
R349-3h	Je8l	60.18	0.65	14.37	8.93	0.14	0.54	4.25	0.52	4.45	0.16	99.41	24	67	928	138	90	16	5	15	187	15
R344-5a	Je8x	64.24	0.58	16.51	5.16	0.13	1.94	4.31	3.16	2.06	0.22	99.57	5	25	833	843	133	19	9	15	82	17
R344-5c	Je8l	56.10	0.63	18.66	7.42	0.18	3.06	5.13	4.71	1.15	0.24	99.15	3	10	713	671	87	29	5	15	145	15
R344-6b	Je8x	64.76	0.58	14.20	6.49	0.09	2.14	4.54	5.23	0.69	0.15	99.30	12	69	1086	549	87	19	5	15	121	15
R344-2a	Je	60.66	0.64	14.52	7.47	0.17	4.43	3.58	4.52	0.95	0.17	99.24	20	63	695	335	94	19	5	15	155	15
R271-1	Je2	51.29	0.94	14.80	10.66	0.14	5.37	8.85	3.49	1.51	0.27	99.18	37	77	890	635	73	25	5			
R93-13	Je3	54.69	0.73	17.32	8.70	0.16	2.49	7.40	4.28	2.58	0.35	100.52	12	12	651	745	106	24	5	9	214	17
R59-1	Je8l	49.71	1.08	16.28	11.95	0.06	4.95	4.15	3.37	2.69	0.50	99.63	14	17	627	673	75	22	7	8	392	21
R60-11A	Je8l	46.87	0.59	12.90	10.76	0.19	3.25	6.57	2.27	3.30	0.25	98.97	14	19	791	372	52	18	8	6	193	15
R60-11B	Je8l	54.97	0.53	16.77	6.13	0.16	1.95	5.20	5.04	3.70	0.28	98.68	3	10	837	853	110	19	12	5	190	16
R60-11C	Je8l	52.26	0.61	17.83	7.40	0.35	2.67	3.91	2.43	6.63	0.33	98.34	5	10	1324	554	109	19	6	7	230	18
R60-12A	Je8l	60.12	0.49	17.52	4.78	0.09	1.53	4.13	3.51	3.82	0.19	99.45	6	30	715	682	135	24	16	6	99	15
R60-12C	Je8l	52.53	0.68	16.61	8.22	0.11	3.98	2.57	2.93	5.92	0.34	98.88	10	22	1026	391	104	22	6	5	246	19

Appendix 2: Minor, trace and rare earth element data, Elise Formation (in ppm).

Field No.	Unit	Cr	Ni	Sc	V	Pb	Zn	Bi	Mo	Rb	Cs	Ba	Sr	Tl	Li	Ta	Nb	Hf	Zr	Y	Th	U	La	Ce
R-3	Je4	67		29	354	8	116	0.03	0.69	31.0	1.8	300	1105	0.04	21.5	0.29	0.7	1.0	27	15	2.8	1.1	13.5	28.4
R-4	Je4	68		29	323	9	114	0.06	0.9	43.0	1.7	987	954	0.04	14.9	0.22	0.9	1.2	30	16	2.9	1.2	27.3	51.2
R-6	Je8x	14		16	212	12	95	0.04	0.6	43.0	1.1	673	525	0.04	18.8	0.25	3.5	0.9	22	13	2.7	0.8	14.9	28.55
R7-8	Je7l	64		26	326	8.5		0.19	0.8	63.3	3.0	656	741	0.16	29.1	1.17	6.3	1.6	42	13	3.1	1.1	8.7	18.9
R8-6	Je1	216		25	318	8.1		0.07	1.0	45.1	3.5	690	976	0.13	18.1	0.62	5.6	0.6	19	13	1.5	0.7	9.4	19.4
R8-13	Je8l	50		28	297	10.3		0.14	1.3	56.6	1.3	392	1092	0.15	26.4	1.08	9.5	2.1	77	22	3.5	1.0	13.3	29.0
R11-14	Je8l	21		24	242	9.6		0.04	0.9	69.5	0.8	754	778	0.11	17.7	0.80	5.7	1.8	62	17	3.6	1.1	13.7	28.4
R16-3	Jsk	12		5	60	10.1		0.08	0.8	75.6	2.1	748	914	0.53	11.6	0.89	11.9	1.5	33	17	3.6	1.5	14.8	30.3
R18-1	Jsk	44		17	183	9.2		0.08	0.9	28.2	0.4	335	844	0.11	25.6	0.99	13.9	1.7	54	24	5.2	1.5	19.7	41.5
R21-5	Je4	633		33	278	2.2		0.06	0.9	42.5	1.5	497	619	0.39	23.4	0.53	1.9	0.5	21	10	1.3	0.6	6.2	13.2
R31-6	Je8l	15		26	319	3.8		0.05	0.7	39.7	1.0	795	641	0.22	11.9	0.40	2.8	0.9	22	15	1.2	0.5	6.5	14.5
R31-9	Je4	100		25	298	6.3		0.03	0.9	47.0	1.6	673	801	0.05	18.3	0.44	2.8	0.7	25	15	2.6	1.1	12.7	27.3
R129-2	Je8x	67	17		161	3.8		0.05	0.7	52.2	2.7	1488	394	0.15	17.4	0.42	4.4	1.1	29	14	3.4	1.0	11.2	23.9
R99-3	Je2	344	119		296	4.7		0.04	1.2	7.3	0.1	155	252	0.04	4.8	0.37	2.5	0.7	19	16	1.4	0.6	6.9	15.1
R100-13	Je2	39	24		334	5.5		0.04	1	35.3	0.8	800	657	0.13	12.1	0.45	3.1	0.5	16	16	1.7	0.9	8.1	17.7
R134-17	Je8x	23	42	21	192	7.9	70	0.12	1.3	33.9	1.6	525	662	0.08	17.1	0.38	4.6	2.0	52	15	4.8	2.3	13.6	29.1
R173-2	Je4	100	33		331	5.6		0.06	1.1	16.9	1.3	274	460	0.11	14.1	0.36	2.7	0.6	18	16	1.5	1.1	7.5	17.5
R170-7	Je1	199	52		299	4.6		0.07	1.1	10.4	0.3	250	631	0.09	8.5	0.32	2.7	0.7	16	20	1.8	0.7	8.2	19.7
R219-10	Je1	34	14		306	5.3		0.06	1.3	44.9	1.4	805	880	0.17	15.1	0.22	2.8	1.7	47	13	3.1	1.3	14.5	30.0
R296-11	Je1				394	5.9		0.40	0.9	72.9	6.5	948	445	0.54	24.3	0.27	2.7	0.6	23	13	2.4	1.2	11.4	26.4
R302-9	Je4				265	4.4		0.03	1.2	46.2	1.8	830	601	0.24	12.4	0.28	3.5	1.7	58	15	3.5	1.5	15.6	33.1
R308-9	Je4				323	25.2		0.16	0.9	67.0	2.8	455	936	0.38	29.0	0.21	2.7	2.0	31	17	3.5	1.7	15.7	35.1
R257-15	Je7l	240	72		0	4.1		0.17	1.6	11.0	0.5	150	448	0.12	7.8	0.18	2.3	1.2	43	15	1.5	0.8	7.5	16.6
R265-6	Je4	124	30		0	6.8		0.09	1.2	75.1	2.0	885	896	0.17	7.2	0.23	3.2	1.3	53	14	3.5	1.6	15.2	31.1
R281-21	Je7l	40	24		0	4.1		0.09	0.9	50.0	1.415	585	490	0.27	18.1	0.17	2.1	2.4	47	15	1.1	0.5	5.5	12.3
R270-3	Jm	10	7		281	12.4		0.08	1.1	50.0	1.936	1186	1118	0.24	12.8	0.20	3.1	1.4	52	16	3.1	1.3	14.8	31.6
R337-9	Je8x	308	145		256	6.1		0.13	0.8	39.0	3.235	390	403	0.20	19.8	0.16	2.0	0.7	22	15	1.1	0.5	5.3	12.5
R339-3	Je4	127	22		194	13.4		0.14	0.8	98.8	4.319	1565	832	0.90	14.1	0.89	18.8	3.5	138	21	9.4	1.9	47.5	96.4

Field No.	Pr	Nd	Sm	Eu	Gd	Tb	Dy	Ho	Er	Tm	Yb	Lu
R-3	3.7	16.3	3.9	1.26	3.9	0.53	3.19	0.63	1.72	0.24	1.5	0.2
R-4	5.7	22.1	4.5	1.42	4.8	0.56	3.35	0.65	1.84	0.24	1.6	0.21
R-6	3.5	14.9	3.5	1.10	3.8	0.5	2.97	0.55	1.50	0.21	1.33	0.21
R7-8	2.5	11.4	2.8	0.92	3.7	0.48	3.04	0.60	1.70	0.24	1.56	0.22
R8-6	2.6	12.0	2.8	0.93	4.0	0.46	2.86	0.58	1.69	0.22	1.42	0.18
R8-13	3.7	16.1	4.0	1.23	4.8	0.72	4.61	0.94	2.67	0.4	2.78	0.38
R11-14	3.6	16.1	3.9	1.24	4.8	0.58	3.74	0.70	2.14	0.31	1.96	0.28
R16-3	3.6	14.6	3.1	0.98	3.7	0.51	3.25	0.69	2.11	0.30	2.14	0.33
R18-1	5.1	21.9	4.9	1.51	5.7	0.76	4.94	0.95	3.00	0.42	2.60	0.37
R21-5	1.8	8.2	2.1	0.70	3.0	0.34	2.15	0.44	1.25	0.17	1.09	0.17
R31-6	2.1	9.9	2.7	1.01	4.0	0.51	3.35	0.70	1.92	0.28	1.74	0.24
R31-9	3.5	16.4	4.1	1.29	4.8	0.56	3.26	0.66	1.91	0.26	1.63	0.23
R129-2	3.1	12.7	2.9	0.83	3.6	0.47	3.01	0.58	1.74	0.23	1.60	0.21
R99-3	2.1	10.0	2.7	0.96	3.4	0.53	3.24	0.67	2.02	0.28	1.83	0.25
R100-13	2.4	11.1	3.0	1.02	4.3	0.53	3.36	0.68	1.96	0.28	1.77	0.28
R134-17	3.6	15.2	3.4	1.00	3.8	0.48	3.15	0.66	1.91	0.27	1.58	0.26
R173-2	2.5	11.6	3.3	1.19	4.0	0.56	3.59	0.76	2.07	0.30	1.89	0.25
R170-7	2.8	13.5	3.9	1.34	4.9	0.68	4.41	0.89	2.59	0.37	2.25	0.35
R219-10	3.9	17.4	4.2	1.49	5.7	0.59	3.03	0.60	1.71	0.24	1.65	0.23
R296-II	3.5	16.2	3.8	1.44	5.5	0.57	2.95	0.60	1.75	0.23	1.44	0.20
R302-9	4.2	18.7	4.2	1.48	6.1	0.61	3.30	0.65	1.81	0.28	1.86	0.28
R308-9	4.5	20.4	4.6	1.57	4.8	0.61	3.69	0.71	2.06	0.26	1.89	0.27
R257-15	2.4	11.5	2.8	0.99	3.6	0.48	3.26	0.67	1.83	0.26	1.74	0.25
R265-6	4.0	17.6	4.0	1.19	4.8	0.46	2.79	0.58	1.58	0.23	1.67	0.25
R281-21	1.7	8.3	2.4	0.89	3.5	0.47	3.14	0.65	1.88	0.26	1.85	0.25
R270-3	4.2	19.7	4.4	1.38	5.5	0.56	3.36	0.69	1.91	0.26	1.72	0.25
R337-9	1.8	8.7	2.4	0.91	3.5	0.46	3.04	0.60	1.68	0.24	1.42	0.21
R339-3	11.0	43.5	7.8	1.89	8.2	0.82	4.81	0.85	2.52	0.33	1.90	0.28

Comments (Appendices 1, 2 and 3):

1. Lithological Units, Elise Formation, Rossland Group (Table 4-2).

Lower Elise flow units	
Je1	augite plagioclase phyric flows, flow breccias
Lower and upper Elise (Midday Peak)	
Je2	mafic lapilli tuff, pyroclastic breccia, with augite plagioclase bearing clasts
Je3	mafic to intermediate lapilli, crystal and fine tuff, commonly well bedded, locally crossbedded (surge deposits)
Upper Elise flow units	
Je4	augite - plagioclase mafic flows, flow breccia
Je5	plagioclase - amphibole andesite flow
Je6	rhyolite, dacite
Pyroclastic units	
Je7	mafic tuff, fine tuff
Je8	andesitic lapilli tuff, minor mafic tuff
	Je8l - lapilli tuff
	Je8x - crystal-vitric tuff
Epiclastic units	
Je10	tuffaceous siltstone, sandstone
	Je10a - argillaceous siltstone
Je11	tuffaceous conglomerate
	Je11c - intermediate to felsic and intrusive clasts
volcanic	
	Je11b - mixed mafic to felsic clasts
	Je11a - predominantly mafic clasts

2. Analytical methods: summary.

Major oxides (SiO_2 , TiO_2 , Al_2O_3 , Fe_2O_3 , MnO , MgO , CaO , Na_2O , K_2O , P_2O_5) were determined by X-ray fluorescence using a fused disc and a Philips 1404 spectrometer. Minor and trace elements (Ni, Cr, Ba, Sr, Zr, Y, Nb, Ta, V, La) were determined by X-ray fluorescence using both pressed pellets and fused discs. The X-ray fluorescence were carried out by the Geological Survey Branch analytical laboratory.

A number of minor and trace elements (including rare earths) were determined by neutron activation and atomic absorption methods by Beceral Laboratories, Ontario.

3. Rossland-Trail area intrusions: map units

Ja (sill)	Archibald Formation sill	KTr	Tertiary? "rhyolite" dike
Jh (sill)	Hall Formation sill	Kum	"ultramafic"
Jn	Nelson intrusion	IJec	Eagle Creek complex
Jn1	Nelson intrusion	IJecu	Eagle Creek "ultramafic"
mJp	Middle Jurassic pluton	IJm	Early Jurassic "monzogabbro"
Es	Eocene Sheppard intrusion	IJmm	Mammoth intrusion
Kg	Cretaceous "granite"	IJrm	Rossland monzonite
KTd	Tertiary? "diorite" dike	IJsk	Silver King intrusion
KTg	Tertiary? "granitic" dike	mEc	Coryell intrusion
KTi	Tertiary dike	mRc	Coryell (Velvet deposit)
KTl	Tertiary? lamprophyre	Pmr	intrusion in Mount Roberts Fm

Appendix 3: Major and trace element data, Rossland-Trail area intrusions

Field No.	Unit	SiO ₂ %	TiO ₂ %	Al ₂ O ₃ %	Fe ₂ O ₃ %	MnO %	MgO %	CaO %	Na ₂ O %	K ₂ O %	P ₂ O ₅ %	Total %
R119-10	Ja(sill)	52.78	0.79	14.49	10.01	0.21	7.97	6.83	3.60	1.29	0.22	99.94
R117-7	Ja(sill)	51.29	0.74	14.22	11.71	0.22	6.04	9.58	3.07	1.71	0.38	99.92
R127-4	Ja(sill)	48.05	0.71	13.21	13.11	0.21	8.86	1.38	1.08	1.08	0.32	89.16
R117-7-D	Ja(sill)	51.57	0.73	14.32	11.59	0.22	6.01	9.63	3.15	1.74	0.38	100.15
R185-3a	Ja(sill)	48.81	0.76	14.47	11.48	0.22	6.58	10.53	1.58	2.43	0.38	99.73
R269-5a	Ja(sill)	50.97	0.71	17.91	7.82	0.12	2.98	9.18	4.15	1.89	0.19	99.16
R66-5	Jh(sill)	46.03	1.36	14.01	9.74	0.17	5.77	9.26	2.97	2.93	1.59	99.27
R276-13	Jh(sill)	50.38	0.74	16.47	10.81	0.19	5.23	8.10	3.06	2.56	0.35	99.32
R23-2	Jn	68.55	0.38	15.72	2.70	0.06	0.84	2.56	3.34	4.15	0.10	99.05
R28-11	Jn	61.13	0.60	17.60	5.67	0.15	1.92	6.26	3.88	1.87	0.21	100.38
R50-2B	Jn	60.79	0.63	16.50	7.22	0.13	2.51	3.70	4.06	2.41	0.23	100.10
R41-10	Jn	60.47	0.61	17.05	5.27	0.13	1.38	3.82	4.76	2.20	0.20	99.90
R114-5	Jn	64.96	0.65	17.22	5.05	0.11	1.31	4.05	3.14	1.91	0.24	99.51
R115-1	Jn	59.98	0.65	15.56	7.92	0.12	2.87	5.39	4.46	2.11	0.17	99.74
R123-r	Jn	60.91	0.59	17.25	5.53	0.15	1.91	5.47	3.73	2.37	0.21	99.81
R120-8	Jn	68.64	0.30	16.15	3.30	0.13	0.66	3.74	3.62	2.89	0.12	100.01
R213-5	Jn	76.72	0.09	12.77	0.79	0.08	0.05	0.66	3.76	4.22	0.01	99.61
R305-6	Jn	62.43	0.64	15.33	5.38	0.07	2.04	4.41	3.06	4.24	0.23	99.22
R91-15	Jn	62.09	0.59	16.68	5.84	0.13	2.14	5.29	3.36	3.10	0.24	100.15
R340-3	Jn/Es	75.44	0.15	13.46	1.07	0.03	0.10	0.40	3.87	4.62	0.02	99.72
R116-15	Jn1	67.88	0.34	15.94	3.66	0.13	0.78	3.45	3.38	3.81	0.11	99.80
R99-9	Jn1	58.97	0.69	17.05	7.25	0.19	2.25	6.09	3.75	2.96	0.30	99.95
R117-13	Jn1	52.86	0.66	15.44	8.98	0.18	3.63	7.13	2.59	4.11	0.40	99.49
R135-2	Jn1	69.84	0.34	15.24	2.38	0.04	0.85	1.37	3.89	5.29	0.11	99.85
R246-8	Kg	75.90	0.14	13.38	0.65	0.00	0.12	0.28	3.75	4.28	0.04	99.23
R30-3	KTd	47.85	1.13	12.44	13.53	0.23	8.61	11.04	1.44	1.18	0.21	99.30
R22-2C	KTd	45.53	0.89	15.83	8.62	0.16	6.97	11.26	3.08	1.15	1.34	98.25
R24-2	KTd	52.74	0.74	17.73	7.93	0.18	2.30	6.36	4.53	3.52	0.34	98.39
R28-1	KTd	46.22	0.83	12.45	8.56	0.17	9.24	11.77	2.25	1.69	1.38	98.52
R34-3	KTd	44.71	0.70	14.10	10.55	0.16	7.40	6.91	3.76	1.24	0.25	98.24
R30-14	KTd	45.85	1.08	16.00	9.17	0.16	7.92	10.62	2.75	1.42	1.29	99.41
R30-11	KTd	68.68	0.56	10.85	5.42	0.01	1.11	0.31	0.84	2.16	0.17	100.55
R33-16B	KTd	28.79	1.09	8.97	8.24	0.20	8.27	14.25	0.51	2.62	2.15	97.83
R65-2A	KTd	46.28	1.71	15.96	10.31	0.19	5.53	8.46	3.18	2.60	1.23	98.90
R77-10	KTd	53.91	0.76	15.78	9.84	0.18	4.19	7.34	3.95	2.18	0.30	99.96
R91-9	KTd	45.85	1.57	14.72	9.45	0.16	7.06	9.14	2.48	2.34	1.14	98.87
R107-14	KTd	62.78	0.57	16.62	5.17	0.16	1.18	4.38	3.71	2.69	0.22	99.93
R113-2	KTd	65.87	0.63	17.79	4.79	0.15	0.46	0.56	3.59	3.46	0.25	100.08
R169-7	KTd	52.25	1.18	15.81	8.60	0.15	5.20	6.74	4.02	2.64	0.98	99.06
R207-5	KTd	50.32	0.84	16.79	9.30	0.21	3.56	6.43	3.87	1.13	0.37	99.25
R91-9	KTd	45.85	1.57	14.72	9.45	0.16	7.06	9.14	2.48	2.34	1.14	98.87
R109-7	KTg	53.37	0.81	16.89	9.04	0.20	3.51	8.44	3.62	2.86	0.40	100.23
R109-13	KTg	55.01	0.83	14.79	7.14	0.13	5.26	7.00	2.43	5.58	0.81	99.32
R73-3A	KTg	53.13	0.60	18.62	7.41	0.16	2.70	5.56	3.55	5.18	0.46	99.75
R77-1A	KTg	60.51	0.51	15.40	4.74	0.09	1.65	4.20	3.69	2.47	0.19	99.59
R77-13	KTg	65.81	0.31	16.48	3.48	0.12	0.54	2.64	4.21	2.87	0.11	100.04
R74-18	KTg	53.64	0.54	16.30	6.97	0.09	4.83	4.89	3.97	3.41	0.42	99.54
R219-7	KTi	54.40	0.73	15.41	7.76	0.13	5.18	6.94	2.79	5.18	0.62	99.33
R61-3	KTi	50.76	1.31	13.70	9.32	0.17	6.78	7.27	3.26	4.00	1.05	98.81
R123-1	KTi	47.78	1.23	10.03	9.82	0.19	11.09	10.47	2.24	4.53	1.11	99.08
R42-5	KTr	75.64	0.03	13.13	1.21	0.09	0.12	1.09	3.01	4.02	0.00	100.29
R45-5	KTr	76.05	0.02	13.35	1.37	0.14	0.22	0.65	1.15	5.12	0.01	100.19
R49-13	KTr	57.86	0.61	14.63	7.94	0.16	1.22	3.60	1.64	3.95	0.25	99.94
R40-9	KTr	76.43	0.03	13.36	1.37	0.04	0.00	0.03	3.31	4.80	0.00	100.24
R62-5	KTr	76.32	0.03	13.46	1.32	0.04	0.02	0.02	3.24	4.41	0.01	99.82
R67-13	KTr	65.21	0.45	15.08	4.33	0.12	1.90	2.85	3.64	4.19	0.51	99.77

Field No.	Ni ppm	Cr ppm	Ba ppm	Sr ppm	Zr ppm	Y ppm	Nb ppm	Ta ppm	V ppm	La ppm
R119-10	17	63	898	599	86	22	13	5	266	15
R117-7	33	147	541	581	90	29	20	5	324	30
R127-4	103	375	1333	1119	93	29	26	5	457	15
R117-7-D	32	161	572	577	90	27	21	5	329	27
R185-3a	27									
R269-5a	11	10	758	574	87	16	5			
R66-5	63	112	2427	1914	304	39	122	5	199	209
R276-13	12	33	860	1010	60	17	5			
R23-2	0	22	0	510	208	255	46	8	0	0
R28-11	0	26	0	723	235	239	34	5	0	0
R50-2B	19	46	424	649	137	24	15	6	148	15
R41-10	9	16	587	716	190	34	17	5	81	20
R114-5	9	10	1343	1700	297	33	39	5	98	56
R115-1	6	10	1777	471	152	41	37	5	244	15
R123-r	100	241	623	826	160	30	23	5	127	15
R120-8	2	20	875	948						
R213-5	2									
R305-6					147	22	13	15	107	
R91-15	9	21	962	727	141	22	12	7	120	26
R340-3	2	10	893	82	118	18	36	15	6	38
R116-15	23	83	1271	845	130	18	11	5	72	22
R99-9	5	10	782	701	140	30	16	5	151	40
R117-13	5	10	1043	1122	112	21	8	5	271	15
R135-2	15	40	1589	836	557	87	226	5	73	88
R246-8	3									
R30-3	0	204	0	527	127	236	20	0	0	0
R22-2C	0	182	0	1974	360	231	149	3	0	0
R24-2	0	19	0	1099	201	248	31	2	0	0
R28-1	0	538	0	1677	348	244	169	9	0	0
R34-3	0	62	0	495	109	213	24	0	0	0
R30-14	0	0	0	1802	190	28	120	0	0	0
R30-11	0	163	0	73	152	259	42	3	0	0
R33-16B	0	460	0	1675	369	229	171	14	0	0
R65-2A	44	40	2917	1758	213	34	103	6	227	157
R77-10	25	35	706	774	99	22	12	5	290	16
R91-9	122	250	2055	1528	239	37	74	12	217	129
R107-14	5	10	1215	1377	325	47	55	5	97	62
R113-2	40	120	888	572	327	52	63	5	100	140
R169-7	65									
R207-5	7									
R91-9	122	250	2055	1528	239	37	74	12	217	129
R109-7	15	27	801	899	139	35	23	5	265	21
R109-13	26	97	1965	1110	215	22	12	5	190	7
R73-3A	16	13	1342	1151	85	18	5	6	197	20
R77-1A	9	31	895	577	123	15	12	6	91	15
R77-13	5	10	1074	626	201	29	36	5	37	15
R74-18	35	70	1813	776	78	22	9	6	204	16
R219-7	29									
R61-3	102	197	2900	2004	300	30	66	5	186	122
R123-1	176	656	1922	1550	282	30	66	5	229	88
R42-5	5	10	123	90	106	33	269	18	6	15
R45-5	5	10	649	100	87	25	207	17	5	15
R49-13	15	19	889	270	78	21	9	5	211	15
R40-9	5	15	76	70	91	17	197	20	5	15
R62-5	5	10	243	84	135	40	255	6	7	15
R67-13	13	20	2117	937	195	19	159	5	68	123

Field No.	Unit	SiO ₂ %	TiO ₂ %	Al ₂ O ₃ %	Fe ₂ O ₃ %	MnO %	MgO %	CaO %	Na ₂ O %	K ₂ O %	P ₂ O ₅ %	Total %
R66-17	KTr	76.79	0.02	13.36	0.93	0.01	0.02	0.02	3.55	4.57	0.00	99.89
R66-17	KTr	76.91	0.02	13.17	0.98	0.01	0.02	0.02	3.55	4.69	0.00	100.01
R141-13	KTr	71.74	0.10	15.88	1.31	0.10	0.20	1.63	3.99	2.58	0.02	99.36
ARL-A	KTr	72.96	0.04	15.14	1.99	0.00	0.07	0.66	3.94	2.18	0.20	99.27
ARL-B	KTr	74.55	0.04	15.13	1.05	0.00	0.03	0.46	4.10	2.03	0.02	99.15
ARL-C	KTr	77.20	0.04	13.25	0.87	0.00	0.04	0.33	3.89	1.61	0.02	98.72
R319-10	Kum	33.07	0.01	0.24	10.58	0.14	39.92	0.45	0.00	0.01	0.01	99.17
R324-27	Kum	39.88	0.02	0.38	10.13	0.11	41.52	0.55	0.00	0.01	0.00	100.03
R73-3	IJec	52.67	0.65	17.79	8.28	0.18	3.82	5.04	4.00	4.44	0.47	100.14
R75-1	IJec	52.09	0.66	15.30	9.82	0.19	5.12	7.93	3.51	3.70	0.50	99.95
R75-2	IJec	52.84	0.54	16.07	8.02	0.16	4.14	7.14	4.03	4.14	0.41	99.49
R75-4	IJecu	47.28	0.57	4.46	12.50	0.21	15.91	15.20	0.26	0.71	0.12	99.77
R75-4	IJecu	49.10	0.28	2.98	8.23	0.15	16.74	16.94	0.25	0.63	0.06	99.88
R86-26A	IJm	58.90	0.45	15.06	7.36	0.11	1.51	3.13	2.29	4.55	0.17	98.59
R92-11	IJm	54.61	0.57	18.51	6.81	0.08	2.70	3.63	4.30	3.86	0.32	99.84
R79-1	IJm	52.90	0.54	16.71	7.71	0.20	1.73	5.67	2.91	5.79	0.28	99.05
R79-3	IJm	54.77	0.61	17.32	7.62	0.18	2.62	5.32	3.56	4.76	0.59	99.67
R79-10	IJm	50.97	0.79	16.55	10.67	0.25	4.20	5.55	3.72	3.56	0.37	99.21
R79-17	IJm	51.94	0.55	15.57	8.32	0.27	2.29	5.85	2.60	5.48	0.29	99.63
R79-18	IJm	53.80	0.59	17.47	7.59	0.21	2.49	3.83	3.90	5.07	0.30	99.66
R79-21	IJm	55.50	0.62	18.08	7.99	0.22	2.62	2.71	4.62	4.39	0.31	99.51
R80-1a	IJm	51.88	0.66	15.16	9.83	0.20	3.18	6.57	4.03	3.49	0.34	99.07
R80-1b	IJm	55.60	0.57	17.15	7.32	0.12	2.30	3.16	4.87	5.07	0.33	99.38
R80-6	IJm	54.29	0.57	16.91	7.44	0.14	2.45	3.91	4.52	5.27	0.32	99.22
R82-3	IJm	52.67	0.82	16.07	10.17	0.24	3.68	5.24	4.49	3.09	0.31	99.46
R82-8	IJm	52.07	0.72	16.50	9.67	0.05	4.08	0.49	1.90	8.92	0.31	99.18
R82-9	IJm	69.33	0.46	12.02	5.94	0.00	0.39	0.08	0.05	8.65	0.18	100.13
R79-17	IJm	52.27	0.55	15.46	8.18	0.27	2.24	5.93	2.56	5.49	0.29	99.25
R125-9	IJm	55.65	0.96	16.52	8.94	0.11	3.18	6.76	3.43	1.28	0.22	100.21
R159-5	IJm	45.50	1.17	15.29	11.37	0.17	5.49	10.44	1.90	0.77	0.25	99.09
R196-16	IJm	50.95	1.11	16.51	9.69	0.18	4.04	7.60	3.25	3.77	0.41	99.14
R198-2	IJm	45.55	1.54	14.29	10.39	0.19	8.35	10.11	2.74	2.29	1.30	99.12
R264-22	IJm	48.09	0.75	16.00	11.17	0.21	4.42	8.55	3.14	2.20	0.36	98.77
R270-3	IJm	48.99	0.74	16.42	11.06	0.24	4.31	8.07	3.09	2.65	0.37	98.77
R281-21	IJm	48.81	0.79	16.81	10.19	0.19	5.62	9.38	2.36	2.01	0.19	99.38
R324-14	IJm	51.41	1.11	16.37	9.42	0.17	3.63	9.80	4.70	0.81	0.40	99.25
R341-5	IJm	49.51	0.75	16.22	11.61	0.22	5.59	9.07	2.55	2.18	0.39	99.30
R349-1c	IJm	56.67	0.73	17.98	8.02	0.18	2.13	4.90	5.40	1.60	0.21	98.99
R349-1d	IJm	55.41	0.75	18.19	8.27	0.18	2.93	3.55	6.00	2.05	0.22	99.11
R349-1k	IJm	56.78	0.67	16.75	9.96	0.19	1.16	5.50	0.38	3.26	0.20	99.17
R349-2c	IJm	61.97	0.61	14.01	6.88	0.21	3.01	4.61	4.92	0.50	0.15	99.48
R349-2d	IJm	53.46	0.71	16.39	8.65	0.40	3.63	6.80	3.60	1.62	0.19	99.98
R344-6c	IJm	61.35	0.61	15.21	7.38	0.40	3.17	4.97	1.81	1.86	0.15	99.28
R344-2b	IJm	57.42	0.67	15.71	7.80	0.23	3.82	5.08	4.46	1.32	0.17	99.19
R92-11	IJm	54.61	0.57	18.51	6.81	0.08	2.70	3.63	4.30	3.86	0.32	99.84
R91-6	IJmm	60.88	0.60	17.11	6.23	0.11	2.36	4.06	3.99	2.85	0.24	99.69
R91-14	IJmm	48.97	0.66	13.81	10.99	0.20	6.22	12.24	2.39	2.52	0.40	99.55
R93-5	IJmm	52.10	0.74	14.76	10.72	0.19	5.33	9.78	2.52	2.40	0.27	100.13
R99-8	IJmm	65.53	0.56	15.92	4.16	0.08	1.91	4.95	3.29	2.82	0.21	100.05
R91-6	IJmm	60.88	0.60	17.11	6.23	0.11	2.36	4.06	3.99	2.85	0.24	99.69
R91-14	IJmm	48.97	0.66	13.81	10.99	0.20	6.22	12.24	2.39	2.52	0.40	99.55
R93-5	IJmm	52.10	0.74	14.76	10.72	0.19	5.33	9.78	2.52	2.40	0.27	100.13
R286-9	IJrm	53.11	0.83	16.03	10.16	0.20	4.27	6.68	3.45	3.19	0.66	99.51
R287-7	IJrm	56.86	0.75	15.67	8.41	0.17	3.43	5.64	3.16	3.53	0.37	99.19
R287-14	IJrm	59.28	0.75	16.59	6.97	0.15	2.62	5.30	3.84	3.17	0.26	99.17
R313-4	IJrm	53.51	0.98	16.31	9.53	0.18	4.26	6.62	3.10	3.54	0.42	99.18
R318-3	IJrm	52.14	0.57	15.67	7.03	0.13	6.99	8.09	2.76	3.83	0.45	98.78
R320-14	IJrm	48.24	1.37	14.06	12.69	0.25	5.11	11.12	2.99	1.66	0.61	98.70
R323-3	IJrm	55.11	0.85	15.84	8.56	0.16	3.98	5.75	3.14	4.48	0.52	99.05

Field No.	Ni ppm	Cr ppm	Ba ppm	Sr ppm	Zr ppm	Y ppm	Nb ppm	Ta ppm	V ppm	La ppm
R66-17	5	24	141	78	96	22	221	9	7	15
R66-17	7	11	132	84	135	41	280	35	9	15
R141-13	5	10	1144	451	126	30	40	5	12	15
ARL-A	9	13	1112	350	111	10	6	15	5	15
ARL-B	8	10	1101	325	106	10	5	15	5	15
ARL-C	8	10	918	299	88	10	5	15	5	15
R319-10					20	10	5	15	20	
R324-27					20	10	5	15	33	
R73-3	22	33	1186	983	84	21	7	5	233	16
R75-1	49	111	1032	1074	60	18	5	9	283	29
R75-2	31	82	1049	1133	61	14	6	5	232	20
R75-4	238	885	200	178	52	15	20	5	268	20
R75-4	190	1130	141	129	21	10	11	5	128	21
R86-26A	15	19	1674	244	77	13	8	5	226	18
R92-11	12	10	1068	746	96	14	5	8	270	15
R79-1	4	10	989	531	103	23	9	7	181	15
R79-3	4	20	1245	967	113	22	5	7	196	22
R79-10	11	21	768	660	97	23	9	6	290	22
R79-17	4	10	1106	344	90	18	5	6	209	15
R79-18	4	10	1032	911	126	22	7	12	185	19
R79-21	4	10	925	731	123	24	6	8	192	19
R80-1a	6	20	646	711	80	22	11	5	233	16
R80-1b	4	10	916	440	97	18	5	5	178	15
R80-6	4	10	891	724	96	16	5	5	226	15
R82-3	13	48	436	1060	85	21	5	10	290	15
R82-8	9	23	1977	395	76	16	5	13	270	20
R82-9	4	13	1865	328	72	11	13	9	162	15
R79-17	4	10	1097	341	90	19	5	8	204	15
R125-9	10	61	455	431	80	16	6		273	15
R159-5	10									
R196-16	14									
R198-2	108									
R264-22	12	10	849	974	55	16	5			
R270-3	7	10	1247	1106	54	15	5			
R281-21										
R324-14					111	29	7	15	277	
R341-5	13	35	986	731	56	17	5	15	293	23
R349-1c	2	10	645	465	71	19	5	15	149	15
R349-1d	2	10	580	259	72	20	5	15	171	15
R349-1k	2	10	1570	142	66	18	5	15	152	22
R349-2c	18	62	552	413	87	19	5	15	137	15
R349-2d	22	76	1150	533	110	21	5	15	183	17
R344-6c	17	52	815	328	92	19	5	15	155	15
R344-2b	22	73	901	552	98	22	6	15	160	15
R92-11	12	10	1068	746	96	14	5	8	270	15
R91-6	8	12	1266	1272	116	19	9	7	152	15
R91-14	61	202	1061	947	60	17	5	9	306	22
R93-5	28	82	775	581	68	20	7	8	296	15
R99-8	5	28	1220	811	137	18	14	5	92	27
R91-6	8	12	1266	1272	116	19	9	7	152	15
R91-14	61	202	1061	947	60	17	5	9	306	22
R93-5	28	82	775	581	68	20	7	8	296	15
R286-9										
R287-7										
R287-14										
R313-4					196	27	20	15	197	
R318-3					120	16	13	15	140	
R320-14					82	30	8	15	424	
R323-3					209	26	20	15	162	

Field No.	Unit	SiO2 %	TiO2 %	Al2O3 %	Fe2O3 %	MnO %	MgO %	CaO %	Na2O %	K2O %	P2O5 %	Total %
R324-22	IJrm	57.29	0.74	16.53	8.42	0.17	2.70	4.77	3.33	4.06	0.44	99.30
RR39-5	IJsk	60.10	0.59	17.00	5.76	0.14	2.00	4.99	4.04	1.95	0.21	100.14
R50-20	IJsk	63.60	0.42	17.31	3.46	0.06	0.79	4.05	4.70	3.30	0.12	100.27
R84-7	IJsk	65.31	0.47	17.05	4.21	0.10	0.92	3.92	3.52	2.67	0.17	100.03
R47-2	IJsk	62.22	0.54	17.28	4.87	0.14	1.17	4.47	3.94	2.41	0.18	100.21
R85-4	IJsk	63.99	0.43	17.81	4.03	0.12	0.83	3.73	4.61	2.90	0.13	100.27
R85-13B	IJsk	65.33	0.57	16.54	4.98	0.08	1.55	4.14	3.14	2.40	0.20	100.31
R86-11	IJsk	56.33	0.74	16.01	7.11	0.13	2.67	5.17	3.59	2.86	0.26	99.78
R86-18	IJsk	64.01	0.42	17.46	3.89	0.13	0.79	4.30	5.21	1.53	0.12	99.96
R86-24	IJsk	60.75	0.58	18.31	5.54	0.10	1.81	3.58	4.34	2.36	0.22	99.92
R78-2	IJsk	65.05	0.38	16.48	2.31	0.08	1.02	3.54	2.41	3.78	0.15	98.99
R92-4	IJsk	57.32	0.37	16.52	4.34	0.06	1.19	4.95	4.40	4.60	0.21	99.10
R92-5	IJsk	54.94	0.37	16.05	4.58	0.06	2.13	4.52	4.67	5.16	0.21	99.09
R92-10	IJsk	55.38	0.48	17.38	3.97	0.04	1.56	4.35	4.71	5.78	0.32	99.04
R137-9	IJsk	62.72	0.54	17.31	5.24	0.11	1.38	4.15	4.42	1.79	0.20	99.97
R144-3	IJsk	62.12	0.46	17.18	4.09	0.14	1.05	4.42	4.71	1.55	0.16	100.09
R150-16	IJsk	43.56	0.55	11.12	9.30	0.25	5.34	9.62	1.30	3.45	0.35	99.40
R150-17	IJsk	47.15	0.68	12.93	11.55	9.58	0.46	0.96	0.08	7.31	0.42	97.59
R150-18	IJsk	42.61	0.54	10.77	9.21	0.29	7.24	9.32	0.94	3.76	0.34	99.36
R150-20	IJsk	43.18	0.57	12.39	8.50	1.12	3.05	10.97	1.17	4.34	0.38	99.47
R150-21	IJsk	62.96	0.61	17.71	6.11	0.23	0.91	0.96	2.33	5.08	0.22	100.05
R92-5	IJsk	54.94	0.37	16.05	4.58	0.06	2.13	4.52	4.67	5.16	0.21	99.09
R92-10	IJsk	55.38	0.48	17.38	3.97	0.04	1.56	4.35	4.71	5.78	0.32	99.04
R50-21	IJsk	66.21	0.52	18.13	0.51	0.03	0.16	3.07	5.62	2.37	0.00	99.78
R286-6	mEc	54.33	1.18	15.37	7.94	0.15	4.30	5.81	3.84	4.40	0.77	99.07
R325-16	mEc	57.48	0.79	14.97	6.23	0.12	4.26	3.90	4.35	4.83	0.49	99.22
R347-3	mEc	53.39	0.85	14.40	7.84	0.15	6.17	7.31	3.00	4.49	0.59	99.06
R45-11	mEc	45.25	1.97	12.51	10.86	0.20	7.14	9.10	2.20	4.54	2.08	97.87
R62-3	mEc	53.18	0.99	15.21	7.85	0.16	4.71	5.78	2.34	6.81	0.88	99.15
R76-1	mEc	52.20	0.76	12.31	7.70	0.13	9.46	7.22	1.98	5.68	0.69	99.08
R286-2	mEc	56.02	1.08	16.22	7.62	0.13	3.40	5.51	3.42	4.26	0.54	98.87
R286-3	mEc	56.80	1.01	18.29	5.10	0.08	2.29	4.02	3.78	6.53	0.47	98.82
R50-4	mJp	65.42	0.62	16.08	4.81	0.08	1.47	2.04	2.75	4.61	0.16	99.88
R50-2	mJp	61.79	0.58	17.40	5.44	0.12	1.62	3.30	5.79	2.36	0.21	99.92
R56-1A	mJp	69.89	0.25	15.12	2.38	0.04	0.76	2.08	3.71	4.44	0.16	99.41
R56-1B	mJp	66.84	0.30	16.60	3.51	0.09	0.71	4.15	3.80	3.19	0.12	99.78
R57-21	mJp	68.49	0.34	16.27	2.95	0.07	0.76	3.25	3.88	3.02	0.12	99.80
R61-6B	mJp	65.62	0.46	16.72	3.97	0.09	1.05	3.35	4.35	2.68	0.19	99.92
R64-9	mJp	68.61	0.25	16.39	2.39	0.08	0.46	3.61	3.86	3.40	0.07	99.67
R65-2	mJp	54.01	0.70	18.41	8.22	0.21	2.32	7.24	4.15	3.22	0.35	99.71
M1068-4	mJp	55.47	1.03	14.10	9.47	0.19	5.92	8.07	1.91	2.02	0.30	99.84
R62-8	mJp	68.57	0.23	16.86	2.36	0.13	0.43	3.41	4.23	2.98	0.07	99.71
R72-4	mJp	70.51	0.24	15.69	2.10	0.05	0.63	3.13	3.51	3.24	0.08	99.64
R72-8	mJp	70.28	0.25	15.79	2.12	0.05	0.66	3.07	3.55	3.39	0.08	99.75
R72-10	mJp	65.13	0.45	16.95	4.29	0.10	1.28	4.52	3.53	2.98	0.15	100.25
R74-6	mJp	62.20	0.53	17.47	5.12	0.15	1.60	4.92	4.30	2.11	0.20	99.90
R74-13	mJp	60.73	0.62	17.43	5.85	0.15	2.04	6.40	3.55	2.01	0.22	100.12
R87-6	mJp	62.89	0.51	16.73	5.58	0.15	1.50	5.01	3.58	3.40	0.22	99.95
R90-1A	mJp	61.92	0.59	17.45	5.59	0.15	1.84	5.35	4.10	1.88	0.20	100.26
R91-15	mJp	62.09	0.59	16.68	5.84	0.13	2.14	5.29	3.36	3.10	0.24	100.15
R69-5	mJp	62.98	0.54	17.32	4.82	0.10	1.39	4.76	3.90	3.17	0.22	99.95
R85-13c	mJp	49.69	1.00	17.52	10.87	0.17	4.22	10.32	3.03	1.54	0.29	100.03
R98-1	mJp	56.27	0.35	19.20	8.16	0.06	1.20	0.32	0.50	11.90	0.25	99.90
R98-3a	mJp	76.69	0.27	9.51	1.74	0.00	0.24	0.10	0.00	5.64	0.22	98.72
R98-5	mJp	54.35	0.50	19.22	6.84	0.09	1.37	2.32	3.48	7.70	0.39	99.05
R98-12	mJp	53.28	0.44	15.98	2.33	0.15	2.67	5.64	1.21	10.26	0.35	98.19
R87-7	mJp?	61.75	0.52	17.40	5.88	0.16	1.59	5.29	3.72	3.31	0.25	100.38
R325-22	mRc	70.87	0.20	14.73	1.84	0.01	0.25	0.13	4.29	5.50	0.04	98.82
R286-1	Pmr	53.06	0.86	16.03	7.34	0.13	3.86	6.43	2.61	5.46	0.68	98.87

Field No.	Ni ppm	Cr ppm	Ba ppm	Sr ppm	Zr ppm	Y ppm	Nb ppm	Ta ppm	V ppm	La ppm
R324-22					271	28	27	15	157	
RR39-5	11	15	728	916	163	26	12	5	108	19
R50-20	5	10	614	1003	176	25	17	5	68	15
R84-7	7	10	1213	972	202	20	17	8	65	26
R47-2	7	10	685	820	201	34	18	5	85	16
R85-4	11	10	823	969	173	26	12	7	74	15
R85-13B	10	14	996	885	220	21	27	6	82	29
R86-11	16	30	521	586	129	26	10	5	166	15
R86-18	7	10	591	1003	168	25	13	6	72	15
R86-24	10	12	666	758	138	23	10	5	121	15
R78-2	4	10	1554	503	175	15	30	8	53	34
R92-4	4	10	744	632	88	16	9	8	148	15
R92-5	4	15	869	614	89	18	10	10	145	15
R92-10	4	14	714	424	69	14	5	7	164	15
R137-9	5	10	618	975	208	39	26	5	100	15
R144-3	5	10	826	713	288	65	74	5	114	15
R150-16	141	525	718	538						
R150-17	151	614	2356	338						
R150-18	143	470	566	393						
R150-20	140	494	1334	223						
R150-21	8	36	743	190						
R92-5	4	15	869	614	89	18	10	10	145	15
R92-10	4	14	714	424	69	14	5	7	164	15
R50-21	3	10	140	288	174	28	24	5	28	8
R286-6										
R325-16	0				325	26	68	15	110	
R347-3	65	244	2135	1301	139	21	37	15	164	66
R45-11	103	157	5523	2779	364	44	166	9	248	267
R62-3	44	128	2562	1296	268	23	12	5	231	38
R76-1	156	648	1794	1128	219	18	14	5	193	39
R286-2	21	64	2096	1303	232	27	41			
R286-3	19	37	2797	1394	181	21	25			
R50-4	6	13	2665	1191	201	28	22	8	63	39
R50-2	5	10	525	854	169	29	18	5	126	15
R56-1A	5	30	1926	721	259	38	186	12	36	79
R56-1B	5	10	1118	998	127	18	15	5	64	16
R57-21	5	10	1180	834	164	15	22	5	43	20
R61-6B	5	10	1512	1095	225	25	34	5	58	31
R64-9	5	10	1432	997	156	26	33	5	50	15
R65-2	5	10	842	1318	96	23	10	5	216	15
M1068-4	33	301	711	619	130	36	25	5	227	33
R62-8	5	10	1192	874	131	14	9	5	45	18
R72-4	5	12	1133	912	175	27	44	5	37	15
R72-8	5	10	1090	894	158	24	45	5	36	15
R72-10	5	10	1130	854	162	19	19	5	66	16
R74-6	14	13	716	852	177	28	18	6	108	15
R74-13	11	10	585	744	175	32	23	5	122	15
R87-6	7	10	1009	741	136	23	11	8	109	20
R90-1A	13	15	688	774	146	23	8	11	116	15
R91-15	9	21	962	727	141	22	12	7	120	26
R69-5	7	27	1163	1064	207	23	22	5	87	38
R85-13c	23	39	465	781	70	24	10	5	393	19
R98-1	2	10	930	242	110	23	10	0	112	15
R98-3a	3	12	708	102	25	20			93	15
R98-5	3	10	1210	593	85	19	10		157	15
R98-12	6	15	1626	567	74	21	6		187	15
R87-7	6	10	1074	837	137	25	15	6	116	19
R325-22					387	21	53	15	11	
R286-1	9	50	3415	3233	236	27	41			

Appendix 4: Location of samples

Lab No.	Field No.	Easting	Northing
22708	R31-6	483399	5469284
31833	R19-4	483995	5470600
31834	R19-4	483995	5470600
31835	R4-1	483310	5470392
31836	R4-1	483310	5470392
31837	R22-1C	482182	5468092
31838	R20-1	482144	5467705
31839	R30-14	482406	5465152
31840	R30-14	482406	5465152
31841	R33-11	482287	5463381
31842	R33-11	482287	5463381
33567	R3-01	482674	5469799
33568	R3-5B	482523	5470034
33569	R3-5C	482523	5470034
33570	R4-03	483283	5470531
33571	R4-09	483216	5471072
33572	R4-10	483112	5471238
33573	R4-15	483244	5471597
33574	R4-20	483543	5471947
33575	R6-01	484017	5470769
33576	R6-04	483647	5470717
33577	R6-08	483908	5471328
33578	R6-11	483673	5471610
33579	R6-12	483814	5471719
33580	R6-14A	484051	5471828
33581	R7-08	482593	5470884
33582	R8-6	484400	5472021
33583	R8-13	483686	5472160
33584	R9-2	472037	5474613
33585	R9-3	472037	5474613
33586	R9-4A	471803	5473922
33587	R9-4B	471803	5473922
33588	R9-6B	471600	5474707
33589	R9-7	471600	5474613
33590	R10-6A	484400	5472021
33591	R10-6B	484400	5472021
33592	R11-1	482223	5469118
33593	R11-7	481823	5469147
33594	R11-10	481806	5469629
33595	R11-14	481580	5469742
33596	R12-5	482154	5472678
33597	R13-4	483047	5472670
33598	R15-5	482317	5472467
33599	R15-11	482308	5471724
33600	R17-8	484774	5469321
33693	R16-3	481471	5472640
33694	R21-7	483313	5467509
33695	R23-2	486500	5469787
33696	R27-7	483468	5466149
33697	R28-11	481087	5467800
33698	R30-3	484569	5459190
33699	R30-11	482129	5466193
33700	R33-15	483114	5462105
33701	R12-1	482472	5472701
33702	R18-1	484870	5469916
33703	R18-13	485231	5468444
33704	R21-5	483058	5467695
33705	R22-2C	482162	5467878
33706	R24-2	482352	5466419
33707	R28-1	482058	5467096
33709	R31-9	483810	5469248
33710	R33-13	482797	5462492
33711	R33-16B	483426	5461613
33712	R34-3	482232	5474168
33713	R34-14	482229	5473210
33714	R36-8	485940	5465788
33715	R37-13	486783	5467792
33716	R37-23	485566	5467895
36225	R38-6A	483438	5455076
36226	R38-6B	483438	5455076
36227	R39-2	482290	5474261
36228	R41-1	482878	5462811
36229	R42-4	482945	5460015
36230	R42-5	482926	5459875
36231	R43-4	482944	5455328
36232	R45-5	481411	5455561
36233	R49-13	480178	5475120
36234	R50-2B	480809	5476056
36235	R53-5	481129	5474911
36236	R54-6	480058	5475778
36237	R55-4	482761	5475624
36238	R57-19	482496	5479606
36239	R64-4	477445	5458236
36240	R39-5	482221	5473959
36241	R40-9	482684	5460554
36242	R41-10	483428	5463618
36243	R45-11	481232	5456278
36244	R50-4	480668	5476258
36245	R50-20	478716	5477323
36246	R50-2	480809	5476056
36247	R56-1A	472057	5457921
36248	R56-1B	472057	5457921
36249	R57-21	480399	5481923
36250	R61-3	480737	5480798

Lab No.	Field No.	Easting	Northing	Lab No.	Field No.	Easting	Northing
36251	R61-6B	480933	5480220	36430	R91-15	478573	5467215
36252	R64-9	477669	5457989	36431	R92-11	481720	5473400
36253	R65-2	475568	5458869	36432	R93-5	476053	5462189
36254	R65-2A	475568	5458869	36433	R66-17	482342	5458792
36255	M1068-4	486668	5459707	36434	68-5	480703	5455957
36275	78-24	477275	5476241	36435	69-2	480407	5477675
36388	R62-3	482562	5456667	36436	69-5	479992	5478365
36389	R62-5	482178	5456882	36437	69-12	479971	5482190
36390	R62-8	482289	5457461	36438	72-14	475627	5479820
36391	R67-13	481937	5454949	36439	72-15b	475346	5479500
36392	R66-5	481695	5459815	36440	83-4	477394	5476032
36393	R66-17	482342	5458792	36441	83-5	477337	5475994
36394	R72-4	477645	5479065	36442	83-6	477278	5475732
36395	R72-8	476522	5479492	36443	83-8	476999	5475459
36396	R72-10	475812	5479911	36444	84-6	481699	5477543
36397	R72-19	475627	5479065	36445	74-18	478167	5463975
36398	R73-3	473968	5478175	36446	85-7	477325	5478229
36399	R73-3A	473968	5478175	36447	85-9	477209	5478208
36400	R73-7	474524	5477783	36448	85-13c	477243	5478336
36401	R73-9	474655	5477985	36449	86-16	481327	5473545
36402	R73-11	474787	5478217	36450	87-3	477626	5464691
36403	R74-6	480916	5464041	36451	88-1	477232	5464632
36404	R74-13	478791	5464271	36452	88-6	477443	5464131
36405	R74-19	478109	5464001	36453	88-6	477443	5464131
36406	R75-1	470190	5481927	36454	93-13	477232	5462189
36407	R75-2	469663	5481538	36455	94-5	476544	5464131
36408	R75-4	471700	5481005	36456	95-5	475454	5461563
36409	R75-4	471700	5481005	36457	95-17	474407	5460816
36410	R76-1	481607	5461260	36458	95-20	474171	5460185
36411	R77-1A	482321	5463262	36459	85-7	477325	5478229
36412	R77-10	482573	5461933	36460	62-1	483114	5456948
36413	R77-13	482315	5461492	36461	66-7	481561	5459558
36414	R83-2	478006	5477625	36462	71-6	474899	5476376
36415	R84-7	481570	5477571	36463	71-6	474899	5476376
36416	R47-2	483880	5461150	36464	71-5	474530	5476480
36417	R85-4	477622	5478018	36465	73-6	474098	5477677
36418	R85-13B	477243	5478336	36466	76-6	480444	5459151
36419	R86-9	482058	5473304	36467	78-2	477274	5476245
36420	R86-11	481421	5473498	36468	78-1	477274	5476247
36421	R86-18	481222	5473589	36469	78-19	477276	5476240
36422	R86-24	481471	5473446	36470	78-21	477275	5476240
36423	R86-26A	481699	5473538	36471	78-23	477275	5476241
36424	R87-6	476053	5465383	36472	78-23e	477275	5476241
36425	R87-7	473533	5465650	36473	78-24	477275	5476241
36426	R90-1A	479049	5464296	36475	79-1	479706	5475849
36427	R91-6	479825	5467065	36476	79-2	479706	5475849
36428	R91-9	479482	5467128	36477	79-3	479706	5475849
36429	R91-14	478923	5467215	36478	79-4	479706	5475849

Lab No.	Field No.	Easting	Northing	Lab No.	Field No.	Easting	Northing
36479	79-10	479706	5475849	36981	133-4	473018	5472871
36480	79-15	479706	5475850	36982	134-4	473018	5472871
36481	79-17	479706	5475850	36983	135-2	471505	5473558
36482	79-18	479706	5475850	36984	137-9	478469	5473764
36483	79-21	479706	5475850	36985	144-3	467253	5473055
36484	80-1a	479714	5475852	36986	98-6	474230	5476580
36485	80-1b	479714	5475852	36987	99-3	474971	5463950
36486	80-4	479714	5475849	36988	100-13	475400	5464556
36487	80-5	479712	5475849	36989	102-2	474649	5463190
36488	80-6	479712	5475849	36990	102-8	473442	5463002
36489	80-9	479712	5475848	36991	103-2	473954	5462189
36490	80-17	479712	5475847	36992	117-7	472342	5456284
36491	80-21	479712	5475848	36993	123-1	474148	5471702
36492	80-24	479712	5475847	36994	123-19	472928	5471083
36493	80-26	479712	5475845	36995	124-10	476211	5473077
36494	81-1	479711	5475844	36996	125-11	475205	5474157
36495	82-3	480854	5474376	36997	127-4	473805	5469203
36496	82-7	480854	5474376	36998	132-7	478895	5474805
36497	82-8	480854	5474376	36999	134-6	473044	5473022
36498	82-9	480855	5474376	37000	134-7	472982	5473145
36499	82-10a	480854	5474375	37001	136-12	477297	5472891
36500	78-11	477264	5476243	37002	137-3	478293	5474123
36501	92-4	481699	5473620	37003	141-13	471820	5474180
36502	92-5	481790	5473538	37004	117-7-D	472342	5456284
36503	92-10	481920	5473316	37700	110-5	475771	5455947
36504	79-17	479706	5475850	37701	150-16	478158	5474091
36950	98-1	473890	5476970	37702	150-17	478154	5474086
36951	98-3a	474025	5477260	37703	150-18	478153	5474083
36952	98-5	473800	5477645	37704	150-20	478153	5474083
36953	98-8	474510	5476615	37705	150-21	478153	5474083
36954	98-12	473570	5477250	37706	120-8	467376	5461770
36955	110-14	475014	5456245	38997	185-3a	462278	5442782
36956	125-9	475532	5473562	38998	177-1	460320	5445885
36966	99-8	474270	5464310	38999	173-2	459758	5448686
36967	99-9	474270	5464556	39000	170-7	455478	5449412
36968	107-14	487638	5464043	39001	169-7	453308	5444027
36969	109-7	479445	5458383	39002	163-2	459725	5443763
36970	109-13	478872	5458500	39003	159-5	456977	5447822
36971	110-3	475917	5456018	39004	157-2	460700	5443914
36972	111-2	476000	5456000	39005	155-13	460453	5442367
36973	113-2	487429	5463550	39006	155-3	461399	5441962
36974	114-5	489000	5467800	39007	196-16	456209	5437833
36975	115-1	470748	5461893	39008	187-10	464071	5449527
36976	116-15	470763	5460862	39009	198-2	456800	5434101
36977	117-13	472834	5457030	39010	198-2a	456800	5434101
36978	119-10	472123	5461648	39011	155-3	461399	5441962
36979	123-r	475016	5471837	39012	198-8	456803	5434826
36980	129-2	471961	5470712	39013	200-8	469326	5444443

Lab No.	Field No.	Easting	Northing
39014	202-19	470739	5440710
39015	204-24	467335	5446638
39016	207-5	467377	5445726
39017	213-5	477054	5447832
39018	217-6	475287	5444711
39019	218-2	471623	5445554
39020	219-7	469489	5441430
39021	219-10	469307	5440541
39022	226-2	466497	5444093
39023	233-8	467387	5439679
39024	241-2	475002	5441862
39025	241-7	475627	5441872
39026	246-8	477471	5440302
39027	249-4	477688	5445459
39028	253-7	460768	5437729
39093	256-4a	471267	5463143
39094	256-4b	471267	5463143
39095	256-4c	471267	5463143
39096	256-4d	471267	5463143
39097	256-4di	471267	5463143
39098	256-4e	471267	5463143
39099	256-4f	471267	5463143
39100	256-6	471267	5463143
39101	159-13	457172	5448519
41668	293-4	445247	5432671
41669	294-7	444479	5430732
41670	296-11	452523	5429317
41672	297-11	441437	5429914
41673	301-8	447631	5431074
41674	302-9	446267	5430863
41675	305-1	439531	5438209
41676	305-6	439445	5437574
41677	305-10	439574	5437136
41678	308-9	453202	5430997
41679	312-9	443134	5430715
41680	313-4	444525	5434725
41682	314-1	445603	5432216
41683	319-10	438727	5435325
41684	318-3	473053	5469640
41685	320-14	442518	5435585
41686	323-3	441502	5437130
41687	324-14	438788	5433959
41688	324-22	439334	5434692
41689	324-27	438875	5434800
41690	325-10	433292	5429158
41692	325-16	433062	5428897
41693	325-22	432914	5428141
41694	329-13	446937	5436167

Lab No.	Field No.	Easting	Northing
41995	257-15	443716	5429731
41996	258-11	441835	5431832
41997	262-3	440088	5430293
41998	262-14	440492	5429005
41999	265-6	440109	542979
42000	281-21	442986	5432572
42002	284-16	436845	543179
42003	286-5	440083	5441068
42004	286-6	440428	5440545
42005	286-9	441303	5437555
42006	286-11	440699	5436298
42007	287-7	444280	5436443
42008	287-14	443629	5435053
42068	264-22	440778	5429512
42069	266-1	441907	5431614
42070	266-2	441970	5431697
42072	269-5a	439452	5428430
42073	270-3	441409	5429400
42074	278-38	442779	5431418
42075	279-9	444273	5431284
42379	331-5	477945	5449478
42380	337-9	474353	5454664
42381	339-3	448444	5431159
42383	340-3	478925	5451010
42384	340-5	478677	5450890
42385	341-5	469663	5449616
42386	343-5	477267	5450199
42387	347-3	443333	5436585

